01 Dec 1991

Part 1 of the McMaster University Laboratory Test Program on Brick Veneer/Steel Stud Wall Systems

Robert G. Drysdale

Normand Breton

PART 1 OF THE McMASTER UNIVERSITY LABORATORY TEST PROGRAM ON BRICK VENEER/STEEL STUD WALL SYSTEMS

A

REPORT ON

STRENGTH AND STIFFNESS CHARACTERISTICS OF STEEL STUD BACKUP WALLS DESIGNED TO SUPPORT BRICK VENEER

Prepared for

PROJECT IMPLEMENTATION DIVISION
CANADA MORTGAGE AND HOUSING CORPORATION

by

Robert G. Drysdale, P.Eng.
Professor

and

Normand Breton
Graduate Student

Department of Civil Engineering and Engineering Mechanics
McMaster University
Hamilton, Ontario, Canada
L8S 4L7

December 1991

RGD-89

ACKNOWLEDGEMENTS

This research was funded by Canada Mortgage and Housing Corporation. The contributions by Bailey Metal Products Limited for donations of steel stud components and by Westrock for donations of gypsum board sheathing are recognized. The assistance of Mr. T. Trestain, P.Eng., who reviewed and provided advice on the test program, and of Dr. S. Sivakumaran who provided assistance as co-supervisor for Mr. Breton's M.Eng. thesis are gratefully acknowledged. Mr. Breton's M.Eng. thesis, "Investigations of the Strength and Stiffness Characteristics of Steel Stud Backup Wall Panels", McMaster University, 1989, was used as the basis for this report.

DISCLAIMER

This study was conducted by McMaster University in collaboration with Suter Keller Inc for Canada Mortgage and Housing Corporation under Part V of the National Housing Act. The analysis, interpretations and recommendations are those of the consultants and do not necessarily reflect the views of Canada Mortgage and Housing Corporation or those divisions of the Corporation that assisted in the study and its publication.

While all possible care was taken to ensure that tests were properly carried out and reported, that the information is accurate and that recommendations represent the best advice possible, the authors do not warrant or assume liability for the suitability of the material for any general or particular use.

C.M.H.C. STATEMENT

Canada Mortgage and Housing Corporation, the Federal Government's housing agency, is responsible for administering the National Housing Act.

This legislation is designed to aid in the improvement of housing and living in Canada. As a result, the Corporation has interests in all aspects of housing and urban growth and development.

Under Part V of this Act, the Government of Canada provides funds to C.M.H.C. to conduct research into the social, economic and technical aspects of housing and related fields, and to undertake the publishing and distribution of the results of this research. C.M.H.C. therefore has a statutory responsibility to make widely available information which may be useful in the improvement of housing and living conditions.

This publication is one of the many items of information published by C.M.H.C. with the assistance of federal funds.

ABSTRACT

The behaviour of steel stud backup wall panels subjected to lateral loads was investigated experimentally and analytically. In addition, various steel stud to track connections were investigated experimentally.

The experimental work consisted of the fabrication and testing of 109 steel stud to track connections. Thirty-two full size steel stud backup wall panels were also tested. Some of the panels were braced with various types of commonly used steel bridging while others were braced with gypsum board sheathing or Styrofoam SM insulation. Twelve beam tests were also performed in order to establish the flexural bending capacity of the steel studs tested.

The analytical study consisted of an evaluation of the results of the test program. A one-dimensional elastic Finite Element program was developed to investigate the distribution of torsional stresses in steel studs as part of the analysis. The model had the limitation of ignoring the effects of web perforations.

Based on analysis of the test and analytical results, several recommendations were made for design and construction of steel stud backup walls.

ABRÉGÉ

Le comportement des murs de fond à ossature d'acier soumis à des surcharges latérales font l'objet d'expérimentations et d'analyses. Diverses pièces d'acier servant à fixer les poteaux aux rails sont également étudiées.

Pour la partie expérimentale du travail, il a fallu réaliser et mettre à l'essai 109 assemblages de poteaux d'acier et de rails. Trente-deux murs de fond à ossature d'acier ont aussi fait l'objet d'essais. Certains murs sont contreventés par divers types d'entretoises courantes en acier, tandis que d'autres le sont au moyen de plaques de plâtre ou d'isolant Styrofoam SM. Douze essais de poutre ont été réalisés afin d'établir la capacité de flexion des poteaux d'acier mis à l'essai.

La partie analytique évalue les résultats du programme d'essai. Un logiciel de calcul des éléments finis unidimensionnels élastiques a été conçu pour évaluer, dans le cadre de la même analyse, la répartition des contraintes de torsion des poteaux d'acier. Cependant, ce modèle ne prend pas en compte les effets des perforations de l'âme.

L'analyse des essais et les résultats analytiques permettent de formuler plusieurs recommandations en vue de la conception et de la construction des murs de fond à ossature d'acier.

CMHC SCHL

Helping to house Canadians

Question habitation, comptez sur nous

National Office

700 Montreal Road
Ottawa, Ontario
K1A 0P7

Bureau National

700 chemin Montréal
Ottawa (Ontario)
K1A 0P7

Puisqu'on prévoit une demande restreinte pour ce document de recherche, seul le sommaire a été traduit.

La SCHL fera traduire le document si la demande le justifie.

Pour nous aider à déterminer si la demande justifie que ce rapport soit traduit en français, veuillez remplir la partie ci-dessous et la retourner à l'adresse suivante :

Le Centre canadien de documentation sur l'habitation
La Société canadienne d'hypothèques et de logement
700, chemin de Montréal, bureau C1-200
Ottawa (Ontario)
K1A 0P7

TITRE DU RAPPORT : _____

_____

Je préférerais que ce rapport soit disponible en français.

NOM _____

ADRESSE _____
rue *app.*

_____
ville *province* *code postal*

No de téléphone ( ) _____

TEL: (613) 748-2000
Canada Mortgage and Housing Corporation Société canadienne d'hypothèques et de logement

Canada

TABLE OF CONTENTS

TABLE OF CONTENTS (continued)

TABLE OF CONTENTS (continued)

TABLE OF CONTENTS (continued)

TABLE OF CONTENTS (continued)

CHAPTER 1

INTRODUCTION

1.1 GENERAL

This report contains research information on the strength and stiffness behaviour of steel stud walls constructed to act as the backup for brick veneer facing on buildings. The research reported comprises Part 1 of a five part laboratory test program at McMaster University sponsored by the Project Implementation Division of Canada Mortgage and Housing Corporation. While information in this report is relevant for other uses of steel stud construction, the primary objective of this investigation was to focus on those aspects directly relating to the performance of the combined brick veneer/steel stud (BV/SS) wall system.

1.2 BACKGROUND

Since its introduction in the United States in the 1960's and somewhat later in Canada, the development of steel stud construction as a sound backup for brick veneer has been hampered by several factors which, in hindsight, are now readily identified.

Briefly, the main factors were:

- Formal education of designers did not and in most cases still does not incorporate any instruction in either masonry or cold formed steel construction. Therefore the general level of design competance either for the individual components or as a combined system was quite low.
- Even though it is wind bearing, the BV/SS form of construction normally was not considered to be part of the structure and therefore was not included as part of the structural designers area of responsibility. Designs were usually based on simple to use manufacturers' catalogues or design aids.
- Building Science as a recognized subject area was in its infancy. Although the Division of Building Research at the National Research Council of Canada had

already become an excellent source of information and support for designers, it has taken nearly two decades for the importance of the interactions of thermal differences, air pressure differences, vapour pressure differences, and rain penetration to be widely recognized by designers. Therefore both design and construction practices often lacked proper attention to these considerations.

- No design criteria existed for the combined BV/SS system and no widely recognized standard of good practice had been established in the construction industry. As a result, design and construction decisions tended to be more heavily influenced by economic factors than would be the case where requirements for proper performance were better understood.

In some cases, the apparent cost saving and reduction in construction time resulted in SS backup being used in situations where inherently low quality construction was found regardless of the construction materials.

Simply put, the use of the BV/SS wall system preceeded adequate research and development of well established standards of good practice. Buildings where problems with the BV/SS walls have received attention in the press and at technical meetings have helped draw attention to this topic area. While in many cases these buildings represent extremes of poor construction quality and therefore should not be taken as representative of the existing quality of construction, the close examination which has followed has helped to identify problem areas and has documented the existence of vastly differing design criteria, details, and construction practices. For BV/SS construction to continue as a viable and reliable form of wall construction, it was apparent that research was required and that the results of this research be used to help define appropriate design requirements and standards for construction.

1.3 SCOPE AND ORGANIZATION OF THE CMHC RESEARCH PROJECT

Although useful information on BV/SS construction has been recently published, limitations on scope and/or some controversy regarding interpretation of the results meant that the need for a comprehensive research effort remained. In early 1986, Canada Mortgage and Housing Corporation sponsored a project to provide an independent investigation of the BV/SS wall system. The project was divided into the following three activities:

A. Production of an Advisory Document on design and construction aspects.

B. Organization of a Canada wide survey of BV/SS design and construction practices.

C. Laboratory testing of the BV/SS system and components.

SUTER KELLER INC. in collaboration with R.G. Drysdale of McMaster University were asked to undertake this research. The Advisory Document written by R.G. Drysdale and G.T. Suter has been prepared and H. Keller reported the findings of the Canada wide survey.

The Laboratory Test Program was conducted at McMaster University under the direction of R.G. Drysdale. It was composed of the following five parts:

Part 1: Fabrication and Testing of Components of Steel Stud Backup Walls.

Part 2: Fabrication and Testing of Brick Masonry Assemblages for Leakage.

Part 3: Fabrication of a Small Wall Test Facility and Tests of Small Walls for Air, Water Vapour and Heat Flow.

Part 4: Tests of Ties and Interactions of Ties with Other Wall Components.

Part 5: Fabrication and Tests of Full Scale Walls.

In addition to a CMHC Advisory Committee which reviewed the original proposal and attended a mid term meeting at McMaster University to monitor progress, an open door policy was adopted which resulted in significant interaction with interested parties who arranged intermittent visits to the laboratory.

This report contains the results of the investigation of the components of the steel stud wall identified as Part 1 of the McMaster BV/SS Laboratory Test Program.

1.4 RECENT BV/SS RESEARCH PROJECTS

The aim of this section is to give a brief synopsis of the most recent laboratory research projects. Its primary focus will be on parts of the research which dealt directly with the behaviour of the backup wall assembly. A more comprehensive review regarding all aspects of the BV/SS wall system was given in Reference 5.

1) Clemson Study[1]

This study was co-sponsored by the Brick Institute of America (B.I.A.) and the Metal Lath/Steel Stud Framing Association and was conducted at Clemson University under the direction of R.H. Brown. A first phase provided documentation of the performance of two different types of metal ties used to fasten brick veneer to steel studs. In a second phase, six BV/SS wall panels were tested under lateral load. Three walls were tested under positive lateral load and three under negative lateral load. Two 3-5/8 inch (92 mm) deep, 20 gauge cold formed channel sections, spaced 24 inches (600 mm) apart were used for each backup wall panel. One line of 16 gauge bridging was inserted into a web cutout hole at midspan of the steel stud. This row of bridging was fastened to each stud with clip angles and screws. All panels were identically sheathed on the interior and exterior with 0.5 inch (12.5 mm) thick gypsum board. The sheathing was jointed horizontally at mid height of the wall and was fastened with Number 6-DG screws. Some of the key conclusions reached were:

1. Flexural cracking of brick veneer was improbable under twice the design lateral wind load for an L/360 design criteria for deflection.
2. Composite action between the steel stud and the gypsum board sheathing, although present, was not significant.
3. Tie forces were not uniform.
4. Allowable stress in metal studs should not be exceeded.

2) University of Alberta Study[16]

This study was conducted in 1985 at the University of Alberta under the direction of M.A. Hatzinikolas et al., and was co-sponsored by Dow Chemical Canada Incorporated and the Prairie Masonry Research Institute. The thirty-two BV/SS wall specimens were approximately 1200 mm wide and the steel studs spanned 3 metres while the brick veneer was 3.2 metres in height.

Nine steel stud wall panels were also built and tested. Eight of the test panels had the compressive face of the steel studs sheathed with either gypsum board or Styrofoam S.M. insulation. The tension face of all eight panels were sheathed with gypsum board. The panels were additionally braced with two lines of channel bridging welded to the studs at the web cutout holes. The last panel was not provided with any type of exterior sheathing. All panels were tested under third point loading. It is interesting to note that this effectively placed each point load at approximately the same location as each line of bridging.

Some of the more important findings and conclusions included the following:

1. Brick veneer cracking will result if design practice allows the midspan deflection of the steel studs to be L/360.
2. Gypsum board provides more lateral bracing than polystyrene insulation

3) Murden, J.A. (M.Eng. Thesis)[24]

An experimental investigation into the out-of-plane stiffness of steel stud backup walls subjected to cyclic loading was carried out at Clemson University under the guidance of R.H. Brown.

The experimental program included cyclic testing of eleven backup panels in which seven were fabricated with 20 gauge studs and track and four with 16 gauge studs and track. All the studs were 3-5/8 inches in depth and were approximately 7 feet 10 inches long. Each panel was sheathed with 0.5 inch thick exterior and interior gypsum board. The sheathing was installed in a continuous fashion or with a butt joint at midspan. The sheathing was

attached to the flanges of the studs with 1 inch long Number 8 drywall screws. The panels were loaded in an alternating manner with a single midspan load which caused a midspan panel deflection of slightly less than L/360 in each direction. Each panel underwent 5000 loading cycle. Some important findings were:

1. The composite action between the gypsum board and the steel studs was dependent on the spacing of the drywall fasteners and the facing orientation of the drywall sheaths on the steel studs. The amount of composite action was also quite variable and very sensitive to the care taken during installation of the sheathing.
2. Cyclic loading decreased the amount of composite action very rapidly.

1.5 CURRENT DESIGN CRITERIA

In Canada there are no specific codes governing the overall design, construction and inspection of a BV/SS curtain wall systems. However, CAN3-S304-M84[22] governs the design of masonry structures and CAN3-S136-M84[6] covers the design of cold form steel structural members. In the masonry code, brick veneer is defined as a non-load bearing facing which is attached to a structural backing and is not relied on to act with the structural backing to resist any lateral load. For the more traditional brick veneer and masonry block backup, this assumption is reasonable since the stiffer backup wall resists the majority of the load. However, when a brick veneer with a steel stud backup wall is used, the brick veneer is much stiffer than the backup and will resist a much greater portion of the lateral load, at least until it cracks. If the brick veneer is assumed to be a structural element, then Table 3 of the masonry code limits the allowable tensile stresses normal to the mortar bed joint to 0.25 MPa for Type S mortar. However BIA Technical Note 28B 4 states that the brick veneer/steel stud wall system should not be designed using the allowable flexural tensile stresses as contained in the structural design standards for masonry. It suggests that the design of the wall system be empirically based on past observations and experience. This has led the B.I.A. to

recommned a maximum deflection limitation of L/600 to L/720 when the steel stud backup alone is considered to resist the full unfactored lateral design load. It was concluded that this will ensure the necessary stiffness for satisfactory performance. An additional requirement was that the steel studs must be securely sheathed on both sides. Also, only Type S mortar was recommended for use in brick veneer walls at locations where wind loads are expected to exceed 1.2 KN/m^2.

Others[23] contend that the L/360 deflection limitation for the steel stud backup acting alone, is acceptable. However, they also stated that the L/360 design critieria should be limited to the parameters of the Clemson test assembly and that for other applications, some judgement by the designer is required.

Based on the above, steel stud manufacturers have developed wind load design tables for their products. These tables are usually based on an L/360 or L/600 deflection criteria under unfactored design wind loads. Regarding strength requirements for the steel studs, these tables are usually based on the assumption that adequate stud bracing is provided. It is then left to the designer to decide what bracing is required. However the current cold formed design standard[6] does not have any specific guidance for perforated studs.

1.6 GOALS AND OBJECTIVES

An experimental research program was undertaken to document and evaluate the strength and stiffness characteristics of various components of the steel stud backup wall assembly. To accomplish this, the laboratory test program was planned with the objective of achieving the following goals:

1. Documentation of the bending, torsional and web crippling strengths as well as the deformational behaviour of steel studs.
2. Provision of data on strength, stiffness and construction features for steel stud to track, top and bottom connection details.

3. Evaluation of the effectiveness of various currently used types of bridging and bridging connections.
4. Determination of the bracing capacity of gypsum board as well as other sheathing materials.
5. Observation of effects of cyclic loading and wetted gypsum board on the stiffness of the backup wall.

CHAPTER 2

TESTS OF STEEL STUD TO TRACK CONNECTIONS

2.1 INTRODUCTION

The experimental test program was divided into two distinct phases. Testing of steel stud to track connections is included in this chapter. In Chapter 3, test results for full scale backup wall panels are presented.

This chapter deals with the design, detailing and fabrication of the test specimens and experimental set-ups used in the steel stud to track connection tests. A description and discussion on the test conditions, instrumentation, tests procedures, and the results obtained in this phase of the test program are presented.

2.2 COLD FORMED STEEL STUD TO TRACK CONNECTION TESTS

2.2.1 Design And Set-Up Of Experiments

A simple test set-up was devised to investigate and document the strength and behaviour of various steel stud to track connection details. The horizontal translation of the steel stud end was expected to be due mainly to the transfer of lateral load from the end of the steel stud to the supporting steel track. In order to simulate this type of action, an experiment was designed which isolated the transfer of lateral load. To accomplish this, a short section of steel stud was fastened to a length of track, as shown in Figure 2.1, using a specified fastening detail. (A complete description of the fabrication details is provided in Section 2.2.2.) The track was fastened to a concrete beam which was used to simulate a typical floor slab. In order to minimize the influence of the flexural deflection of the steel stud, the free end of the short length was supported by a load cell. Use of the load cell made the specimen statically determinate and provided a means of obtaining the lateral force at the track. The test apparatus was designed to fit into an hydraulic test machine as shown in Figure 2.2. This

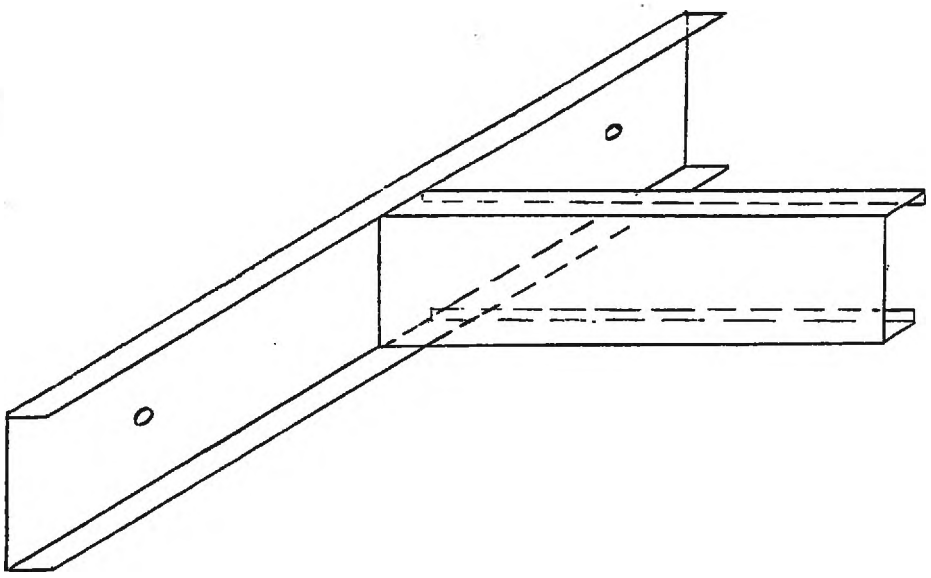

Figure 2.1 Steel Stud to Track Connection Specimen

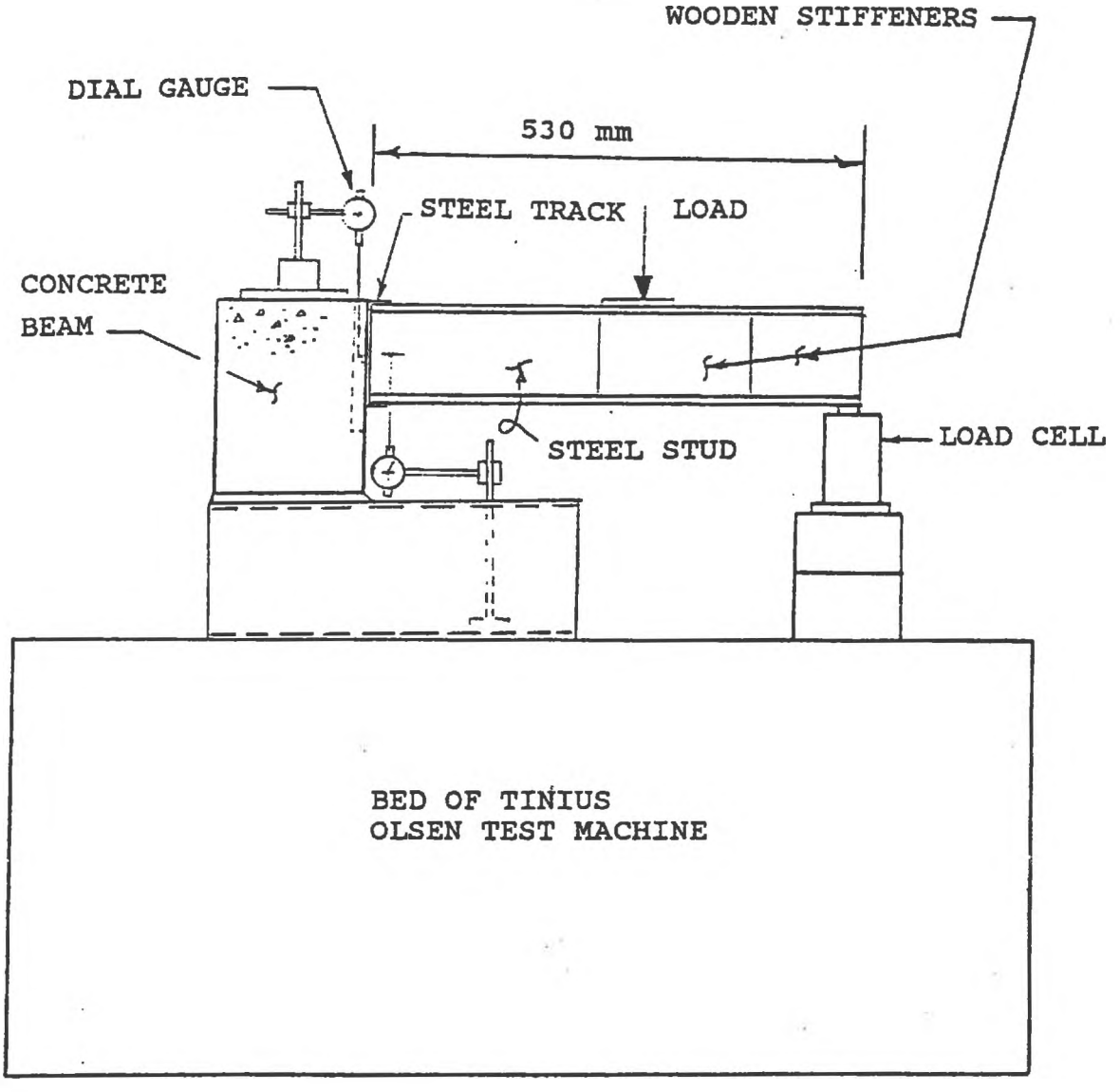

Figure 2.2 Experimental Set Up Used for Steel Stud to Track Connection Tests

facilitated the application of the total lateral load to the steel stud. A complete description of the test procedure is provided in Section 2.2.3.

The above experiment has the advantage of isolating the effect of shear transfer of one stud on a short section of track. However, in a typical steel stud backup wall, steel studs are usually spaced 300 mm to 400mm on center. Therefore, it is possible that nearby studs might influence the translational characteristics of the stud to track connection under observation. This was investigated by fastening two short lengths of steel stud to the track, and loading both studs simultaneously. Comparison of these results with those for single studs will indicate whether the translational characteristics of a particular connection is local in nature or if it is significantly influenced by the action of nearby studs.

Preliminary investigation showed that the rotational restraint of the track at the stud to track connection was not significant and therefore no tests were done to provide moment-rotation relationships.

To investigate the connection strength at the bearing end of a cold formed steel stud at the stud track interface, the experiment was designed to allow failure to occur at the connection and not prematurely under the load applied to the top flange of the steel stud. This was accomplished by stiffening the steel stud with wooden blocks at locations other than at the stud to track connection. This will be discussed in more detail later.

Various types of track anchors were also investigated. In the majority of tests, each track was fastened to the concrete beam using drilled in expansion anchors. However, in practice nail anchors are generally used. Each nail anchor is fired from a specially designed gun which uses an explosive charge as the driving force to drive the nail through the steel track and into the supporting concrete slab or support member. For the strength characteristics of this type of anchor be investigated, the last eleven tests in this phase used nail anchors to fasten the steel tracks to the concrete beam.

2.2.2 Preparation And Fabrication Of Test Specimens

The test specimens were fabricated from cold formed track and channel shaped members. Typical cross-sections used are listed in Table 2.1 with manufacturer's published dimensions. The 0.53 meter long steel stud specimens were cut from 2.59 meter long cold formed steel members using a band saw. The tracks were similarly cut into 1.22 metre lengths from 3.048 metre long sections. Only sections of steel stud and track free from visible damage were used to fabricate the test specimens. Each short length of steel stud was attached at the center of a steel track specimen.

Various connection details were used to attach the steel stud to a track. Each type of connection tested is described in the next section. In order to fasten the track quickly to the concrete beam in the test rig, two 10 mm diameter holes were drilled into the web of the track at locations shown in Figure 2.4. This allowed the track to be fastened to the concrete beam using two 8 mm diameter threaded rods. The rods had been previously screwed into expansion type anchors which had been set in holes drilled in the concrete beam. This provided a reasonable method of attachment were no damage or displacement occurred in either the concrete beam or the anchor bolts through many test repetitions.

For the test specimens that used screws to connect the end of the stud to the track, an electric screw gun was used to drive number 6 pan head self-drilling screws. The steel stud was first aligned in the track and secured in this position with locking pliers. The gun was then used to drive the self-tapping screws through the connecting pieces.

2.2.2.1 Description of the Types of Stud to Track Connections Tested

1) Series D1 - Minimum Gap, 2 Screw Connection

In this series the stud was inserted into the track as shown in Figure 2.4. The inside corner radius at the track web to flange junction did not permit contact between the stud end and the inside face of the track. This resulted in a gap of 1.5 mm to 2 mm between the end of the stud and the inside face of the track . The stud was then fastened to the track with two

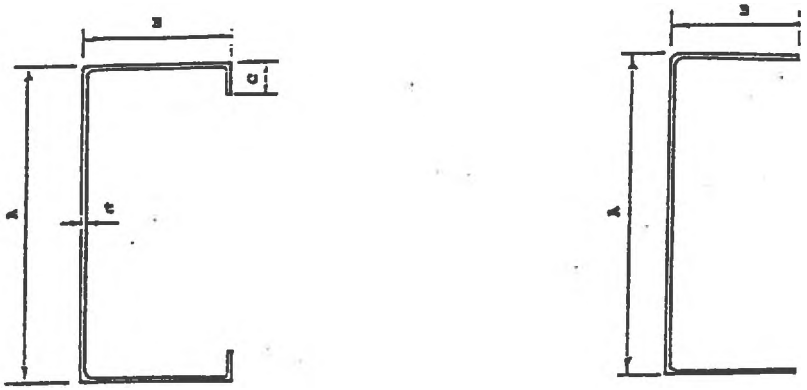

FIGURE 2.3 TYPICAL CROSS SECTIONS USED IN TEST PROGRAM

TABLE 2.1

STEEL STUD AND TRACK STECTION GEOMETRIC PROPERTIES

Stud	Dimensions (mm)			Thickness
Type	A	B	C	t (mm)
20 ga.	92.08	34.93	9.53	0.91
20 ga.	152.40	34.93	9.53	0.91
18 ga.	92.08	41.28	12.7	1.22
18 ga.	152.40	41.28	12.7	1.22

Track	Dimensions (mm)			Thickness
Type	A	B	C	t (mm)
20 ga.	92.58	33.35	–	0.91
20 ga.	152.90	33.35	–	0.91
18 ga.	92.58	33.35	–	1.22
18 ga.	152.58	33.35	–	1.22
14 ga.	92.58	33.35	–	1.90
20 ga.	92.58	63.50	–	0.91
20 ga.	152.58	63.50	–	0.91

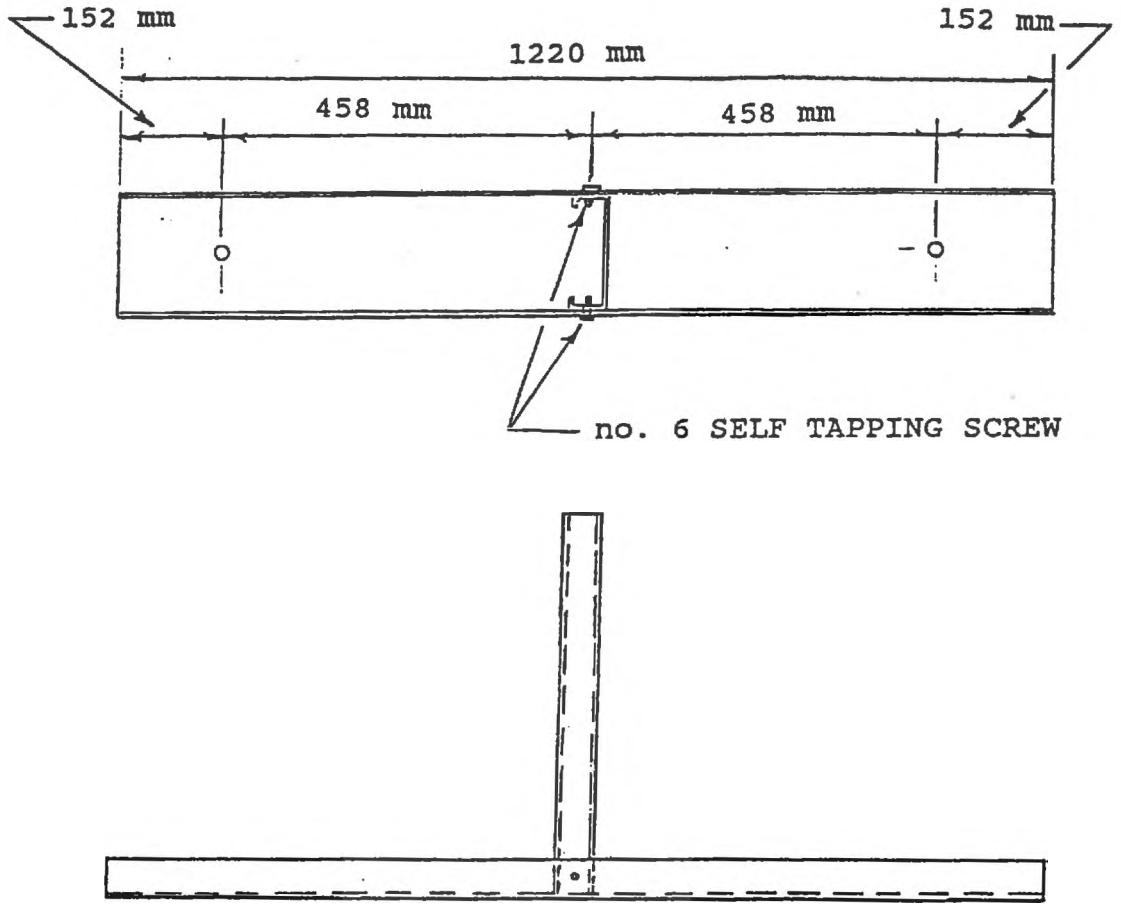

Figure 2.4 Typical Specimen Used for Series D1

Number 6 pan head self-drilling screws. The screws were located approximately 15 ± 1 mm from the lip of the track flange.

2) **Series D2 - 12 mm Gap, 2 Screw Connection**

The fabrication process for this series followed the procedure for Series D1 except that a 12 mm gap was left between the end of the stud and the bottom of the track .

3) **Series D3 - Minimum Gap, 1 Screw Connection**

This series was identical to series D1 except that the stud was fastened to the track with only one screw. This screw was used to fasten the tension flange of the stud to the track.

4) **Series D4 - Minimum Gap, 1 Screw Connection**

This series was also identical to series D1 except that only the compression flange of the stud was fastened to the track with a screw.

5) **Series D5 - 12 mm Gap, 1 Screw Connection**

In this series a 12 mm gap was used. In addition, only the tension flange of the stud was fastened to the track with one screw. This screw was located 15 ± 1 mm from the lip of the track flange.

6) **Series D6 - Minimum Gap, 2 Screw Track End Test**

In this series the stud was attached to the track in the same manner as in Series D1. The only difference between this Series and D1 is that the stud was located at the end of the track as shown in Figure 2.5.

7) **Series D7 - Clip Angle Connection**

A clip angle such as shown in Figure 2.6 was used to fasten the stud to the track. This is a technique which provides a movement joint in the steel stud wall assembly. The stud end was first drilled to allow the use of two screws to fasten the clip angle to the stud. As shown in the figure the other leg of the clip angle was then fastened to the track and concrete beam by means of fired nail anchors.

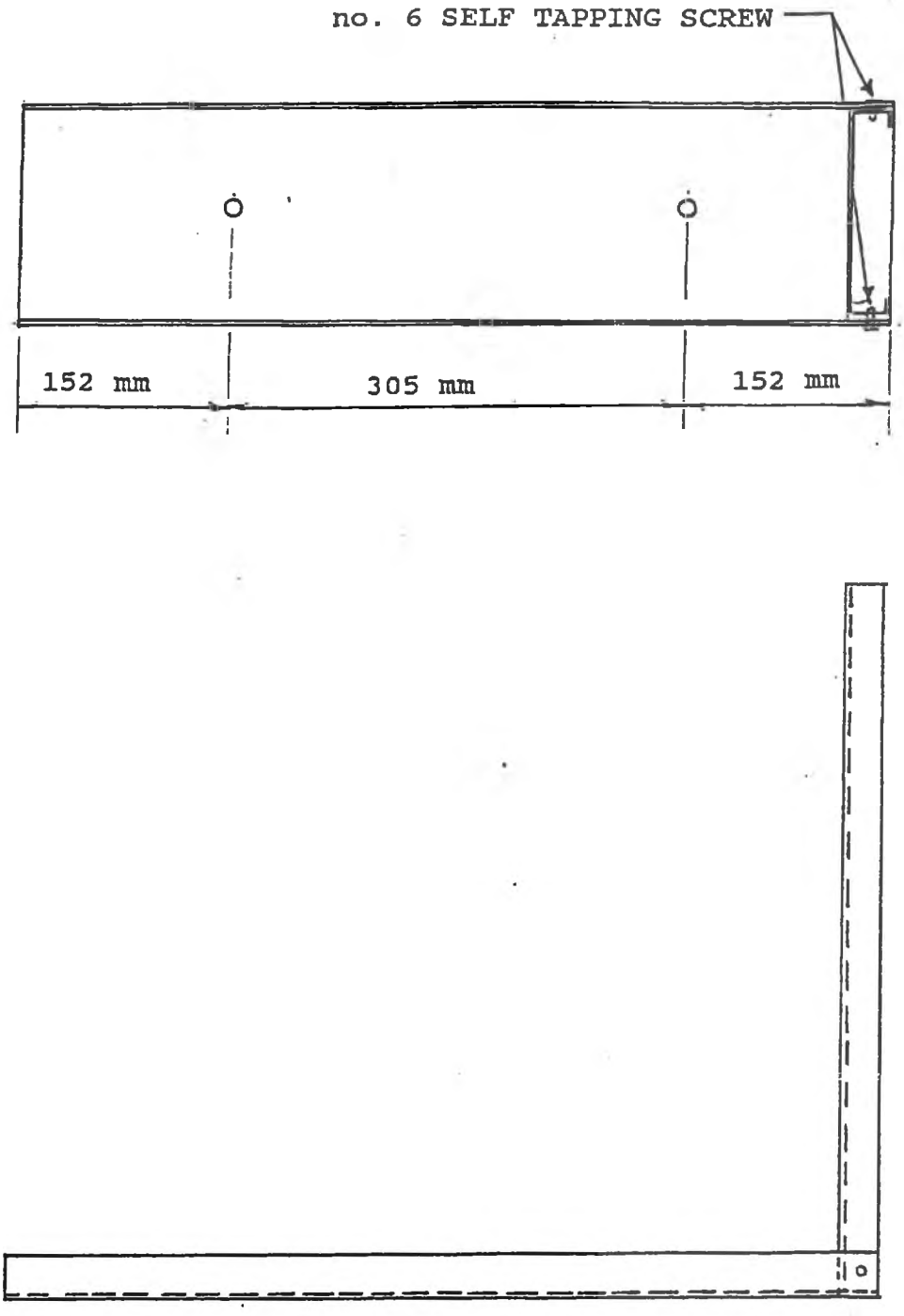

Figure 2.5 Typical Specimen Used for Series D6

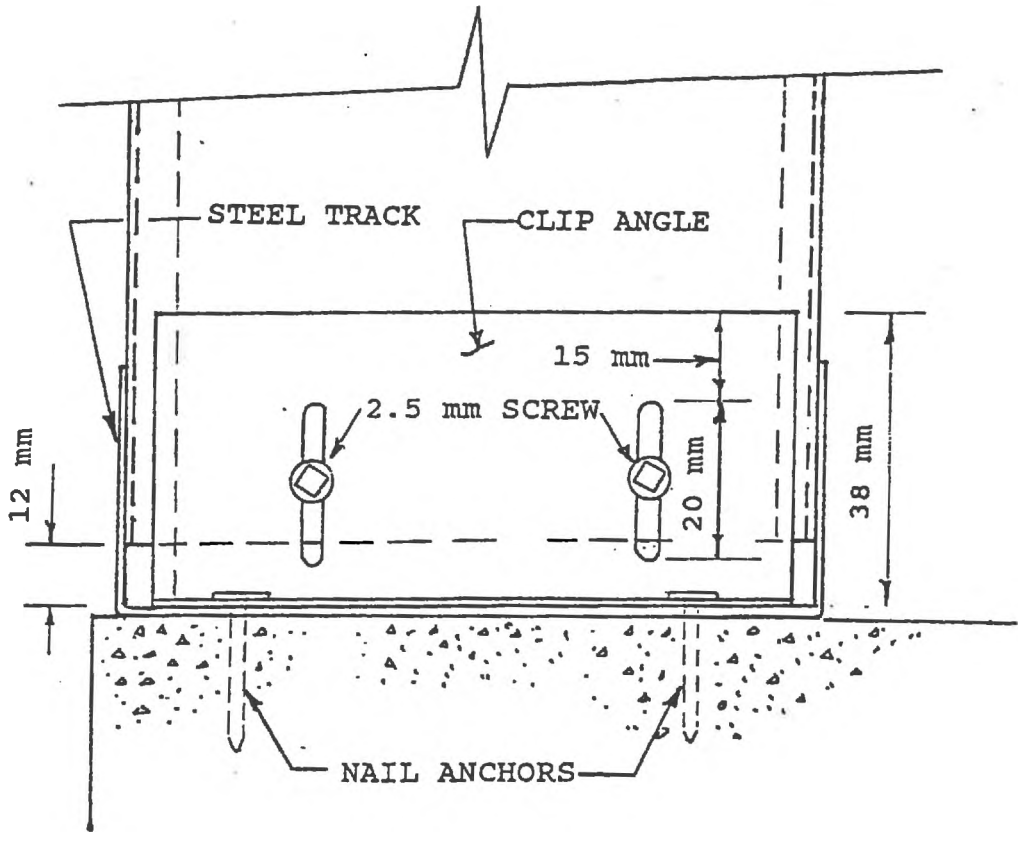

Figure 2.6 Typical Clip Angle Connection Detail Used for Series D7

8) **Series D8 - Flexible Clip Movement Joint Connection**

In this series the flexible clip angle shown in Figure 2.7 was used to attach the stud to the track and concrete beam. The clip angle was first fastened to the stud end by means of two Number 6 Tek self-drilling screws. The other end of the flexible clip was then attached to the track and concrete beam by two nail anchors that were fired through the clip and track web, and into the concrete beam. This type of connection allows a 12 mm movement gap as the end of the steel stud can move along a slight arc.

9) **Series D9 - Box Track Movement Joint Connection**

The box track arrangement shown in Figure 2.8 , was used in this test. This type of detail also allowed a 12 mm movement gap between the end of the stud and the inside face of the track. The steel stud was not fastened to the track in this test series.

10) **Series D10 - Minimum Gap, 2 Screw Connection**

This series was the same as Series D1 except that a 20 gauge stud was attached to a 14 gauge track, in order to investigate the influence of a thicker track on the connection behaviour.

11) **Series D11 - Minimum Gap, 2 Screw Connection**

In this series a 20 gauge stud was fastened to an 18 gauge track for the same reasons discussed in Series D10. The stud was also connected in an identical manner as in Series D1.

12) **Series D12 - Nested Track Connection**

A nested top track detail was tested in this series. This type of connection is commonly used to accommodate movement at the top of the backup wall. For these tests a 12 mm gap was provided between the inside tracks as shown in Figure 2.9 . The stud was fastened to the inside track with two Number 6 self tapping screws, one for each stud flange. The screws were located approximately 25 mm from the lip of the inside track.

13) **Series D13 - Minimum Gap Welded Connection**

The connection detail in this series consisted of welding the stud to the track as shown in Figure 2.10 where the top represents the interior face of the stud for welded in place

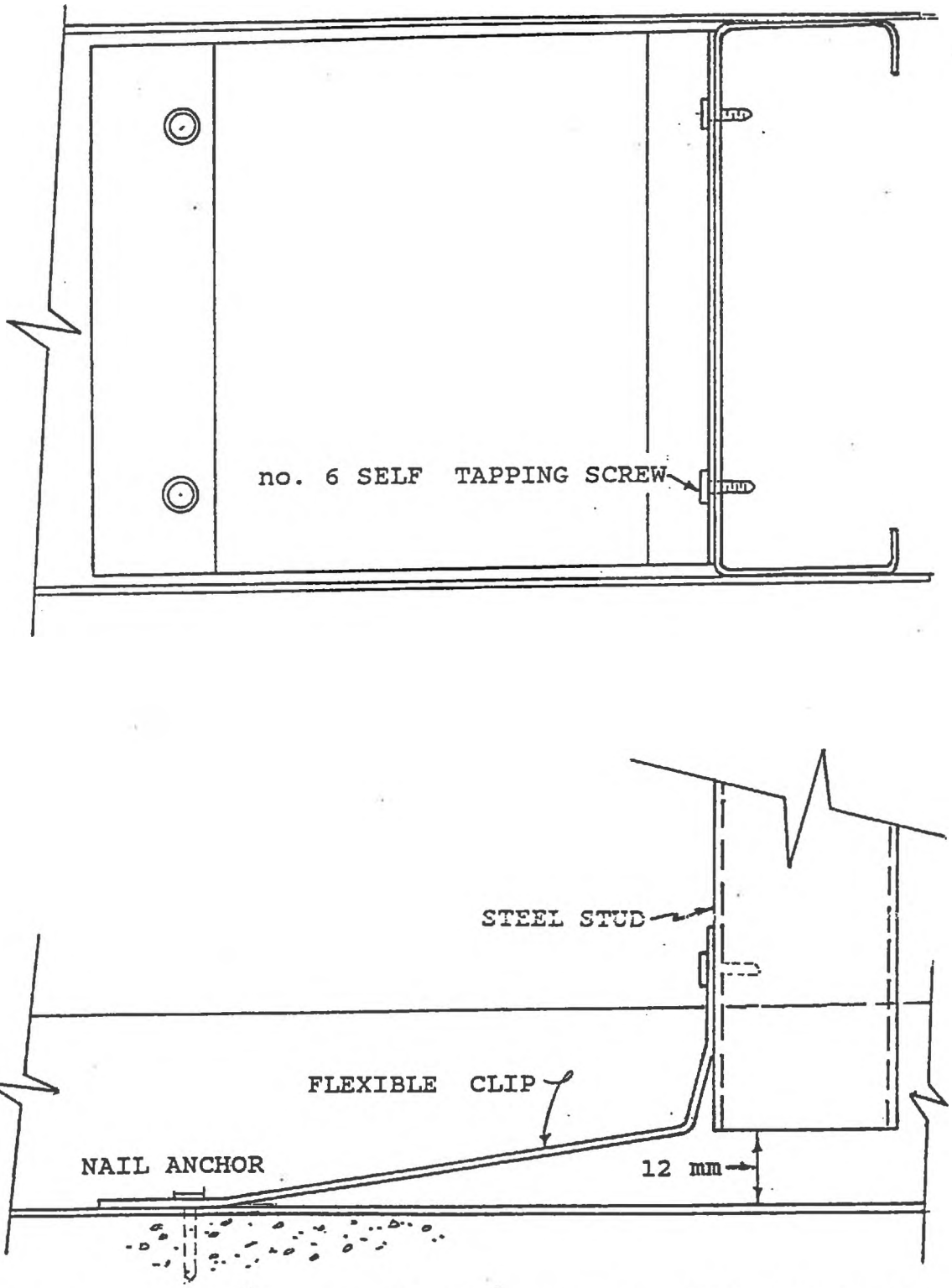

Figure 2.7 Typical Flexible Clip Connection Detail Used for Series D8

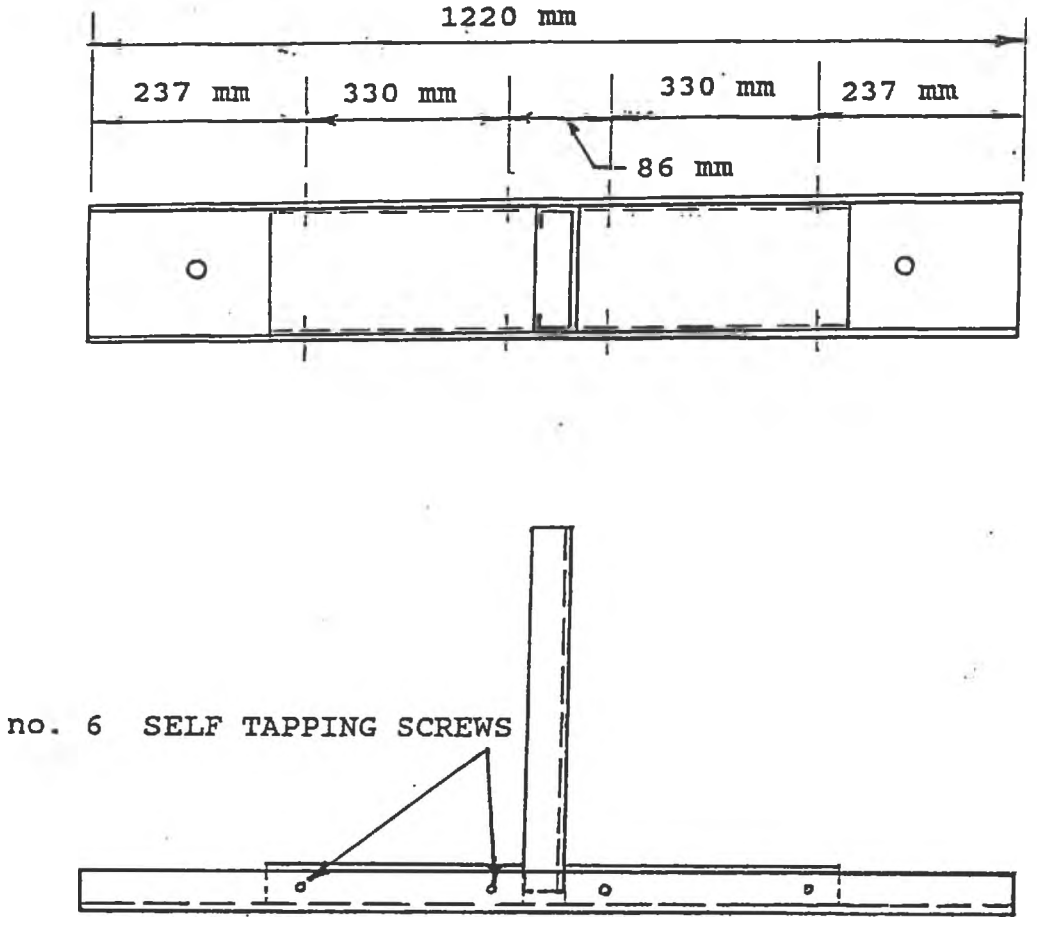

Figure 2.8 Typical Box Track Detail Used for Series D9

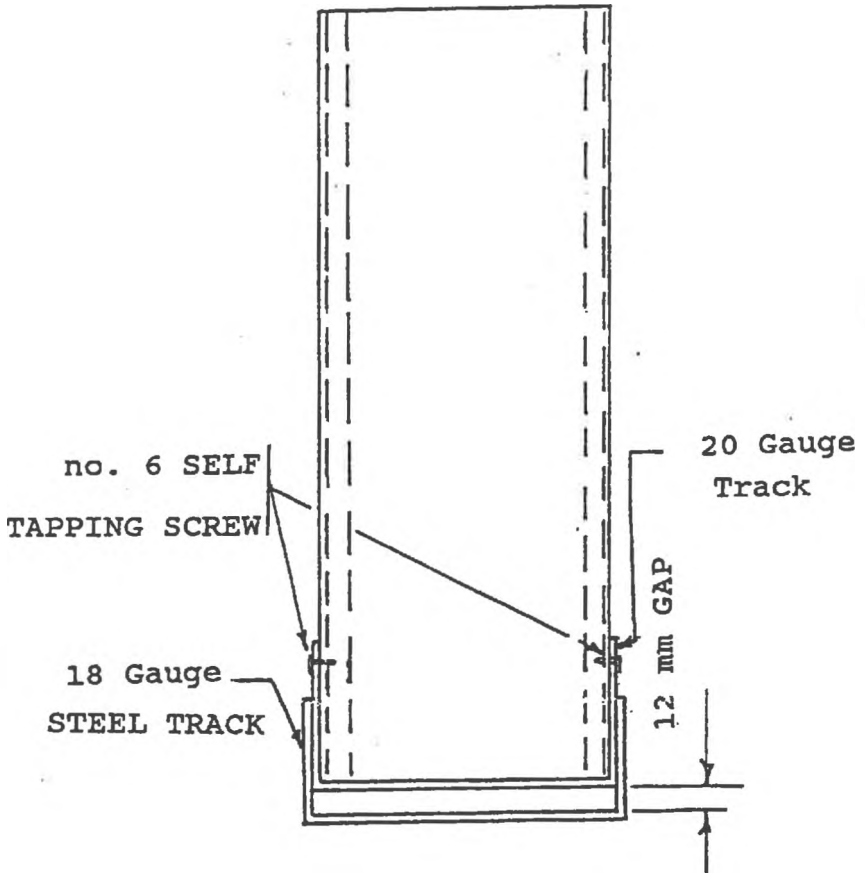

Figure 2.9 Typical Nested Track Detail Used for Series D12

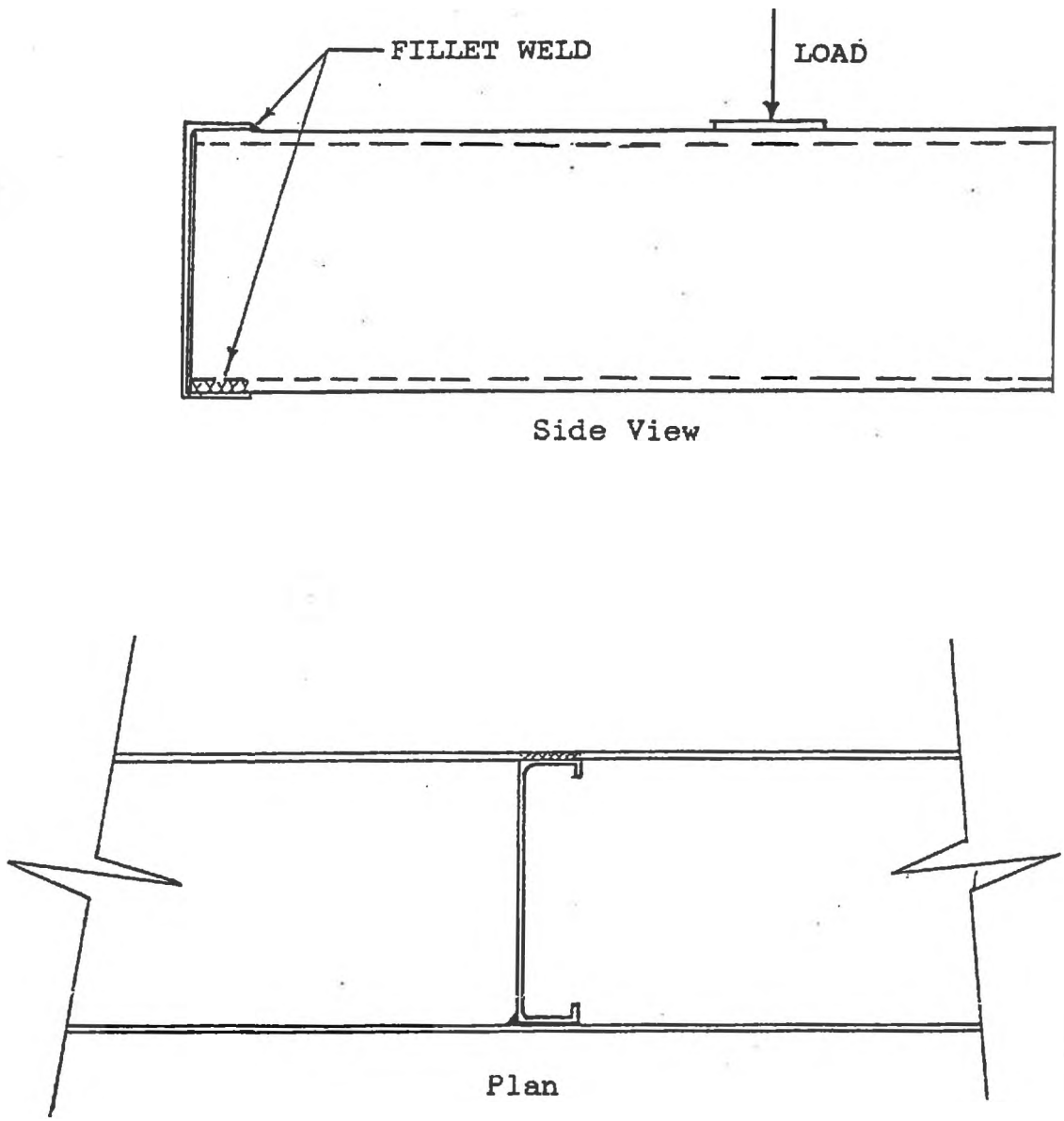

Figure 2.10 Typical Welded Stud to Track Connection Detail Used for Series D13

construction. Only 18 gauge specimens were used in this series. Since a stud can be loaded in either direction, it was decided that this type of connection should be tested in each direction because of the nonsymmetry of the welding. Three 90 mm, 18 gauge specimens were tested with the load applied as shown in Figure 2.10 and three were tested with the connection detail inverted. Three 150 mm, 18 gauge specimens were also tested under the loading orientation shown in Fig. 2.10.

14) **Series D14 - Two Stud Connection Tests**

Each specimen in this Series consisted of two steel studs attached to the track using the standard two screw connection detail. A typical fabricated specimen is shown in Figure 2.11.

2.2.3 Testing Apparatus and Methodology

Once the stud and track pieces were assembled to form a test specimen, it was attached to a 200 mm deep by 150 mm wide by 1830 mm long concrete beam. The concrete beam had been cast previously in the lab, and contained two 15 M top and bottom bars enclosed in 6.35 mm wire stirrups spaced 300 mm on center. The concrete beam was also drilled to allow for the insertion of expansion type anchors. The beam was leveled in the test machine and was supported by two, 152.4 mm square by 6.35 mm by 400 mm long, thick hollow steel sections, which sat firmly on the bed of a Tinius Olsen testing machine and prevented any rotation.

The web of the track, with its pre-drilled 10 mm diameter holes, was secured to the beam using 8 mm diameter expansion anchors and threaded rods . Once the threaded rods, anchored to the concrete beam, had been fitted into the holes provided in the track web, a nut and washer were used to tightly clamp the track to the beam at each of the two anchor locations. The free end of the steel stud was then leveled on top of the load cell. Wooden stiffeners were inserted inside the steel studs at locations shown in Figure 2.2. A 75 mm load plate was placed on the top flange of the steel stud.

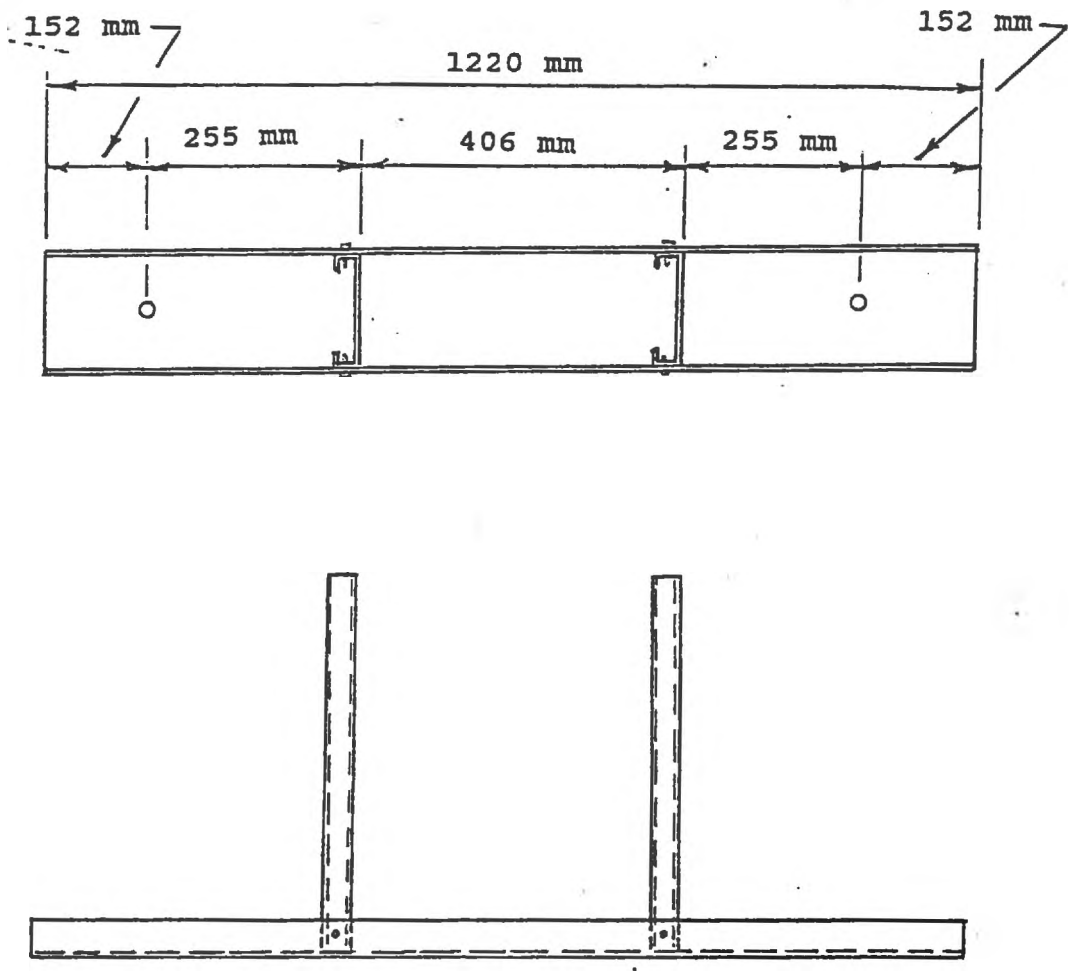

Figure 2.11 Two Stud Specimen Used for Series D14

Metric dial gauges were used to measure the vertical displacement of the stud end and track midspan. Two dial gauges were also used to measure any potential track movement at each track anchor location. The locations of the dial gauges and method of attachment are shown in Figure 2.2. As can be seen inthis figure, the stud end deflection was recorded at the elastic centreline of the steel stud. This was done since preliminary testing had revealed that the displacement reading at the top flange of the stud was not accurate over the full range of displacements since local flange deformations distorted the readings.

In order to attach the dial gauges, each gauge was modified to allow a thin steel wire to be attached to the tip. The other end of the wire was attached to the steel stud or track at locations noted previously. To attach the wire to the steel stud or track, 3 mm diameter holes had been drilled at the locations of attachment. The end of the wire was wrapped around a small threaded screw. A nut was then used to tighten the screw and subsequently hold the wire firmly at each location where deflection readings were required.

Figure 2.12 is a photograph of a typical test set-up for a 90 mm, 20 gauge, Series D1 specimen. Normally each specimen was loaded in 500 newton increments, but in some tests, 250 newton increments were used. The load head was lowered at a rate of 0.15 inches per minute. This was increased to approximately 0.20 inches per minute as the loading approached the ultimate value. At the end of each load increment, deflection readings were recorded. Failure was defined at the point where the load dropped off significantly with increased displacement.

2.3 RESULTS OF STEEL STUD TO TRACK CONNECTION TESTS

2.3.1 General

The results obtained from this phase of the test program are presented in the following sections. These results are presented in summarized form in order that attention be focused on the most important findings. Complete listings of all the results are reproduced in Appendix B.

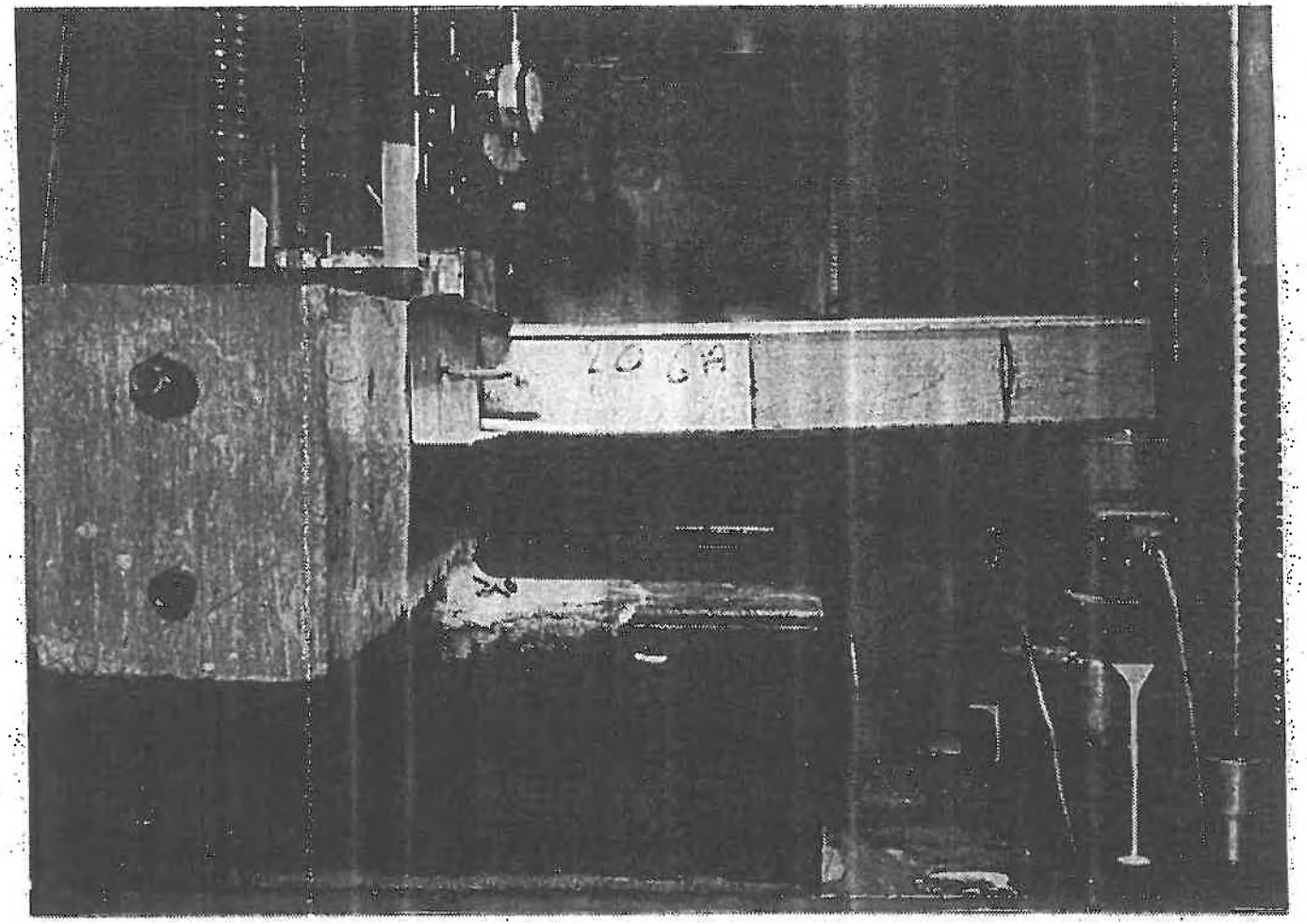

Figure 2.12 Photograph of 20 Gauge, 90 mm Stud to Track Test Set Up - Series D1

2.3.2 Load-Displacements Relationships

In all the tests series, some stud end displacement was recorded. Each test series consisted of three or more repetitions. The load-displacement relationships for all the tests are reproduced in Figures B1 to B24 in Appendix B. In most test series it was noted that the load-displacement relationships were linear for loads up to approximately 75 to 80 percent of ultimate. Since the expected steel stud end reaction under working load, will normally be well within this range, it was decided that a linear regression analysis could be used to fit the data. These results are shown in Figures 2.13 to 2.16. The series designation is explained in Table 2.2. Since the stud end translation should usually be limited to a value no greater than 2 mm, the regression analysis only included data points which were within this range. Since these curves represent the best fit of the data in each test series, they provide the best estimate of the slope of the load-displacement relationships. From examination of Figure 2.13 to 2.16 and those in Appendix B, it is evident that the type of fastening detail used greatly affected the stiffness of the connection.

2.3.3 Failure Loads

The maximum lateral load recorded for each test at the track to stud connection prior to unloading, is listed in column two of Table 2.3. Lateral load values were obtained by subtracting the value recorded by the load cell which supported the free end of the stud from the total lateral load applied to the top flange by the Tinius Olsen Machine. Column three is the mean yield load for each individual test series. This value basically defines the load level that marks the beginning of large permanent deformations at the stud to track connection and as such is a useful limit. The mean yield value for each test group was obtained from the load-displacement graphs reproduced in Appendix B.

TABLE 2.2

STUD TO TRACK CONNECTION TEST SERIES DESIGNATION LEGEND

18 A	–	D1	–	1

18A = 18 Gauge , 90 mm Stud

18B = 18 Gauge , 150 mm Stud

20 A = 20 GAUGE , 90 mm STUD

20 B = 20 GAUGE , 150 mm STUD

Specimen number in each Series

D1 TO D14 is designation for the type of connection detail used (See Section 2.2.2.1)

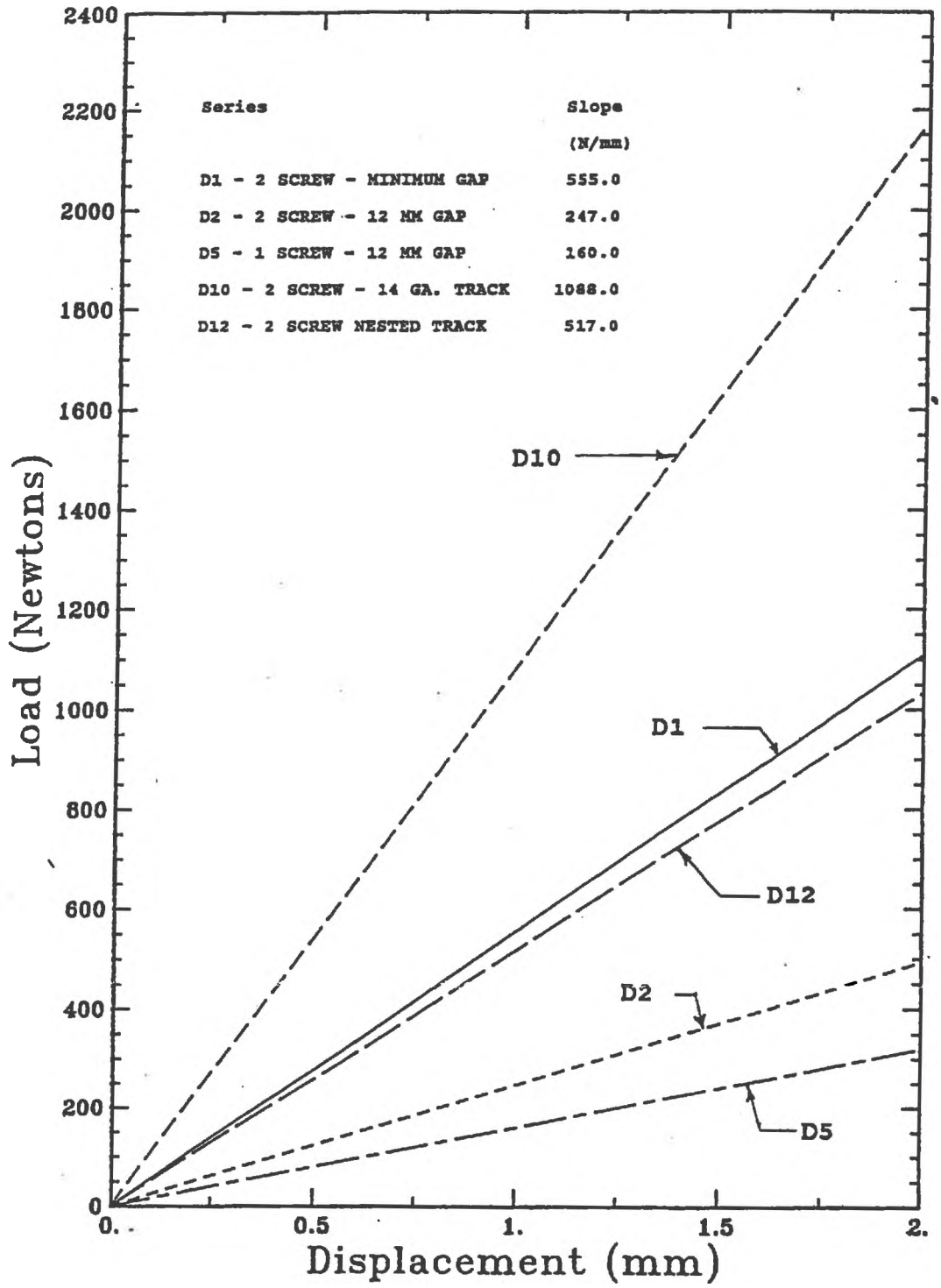

Figure 2.13 Load Versus Displacement Summary 20 Gauge, 90 mm Deep Steel Stud to Track Connection Tests

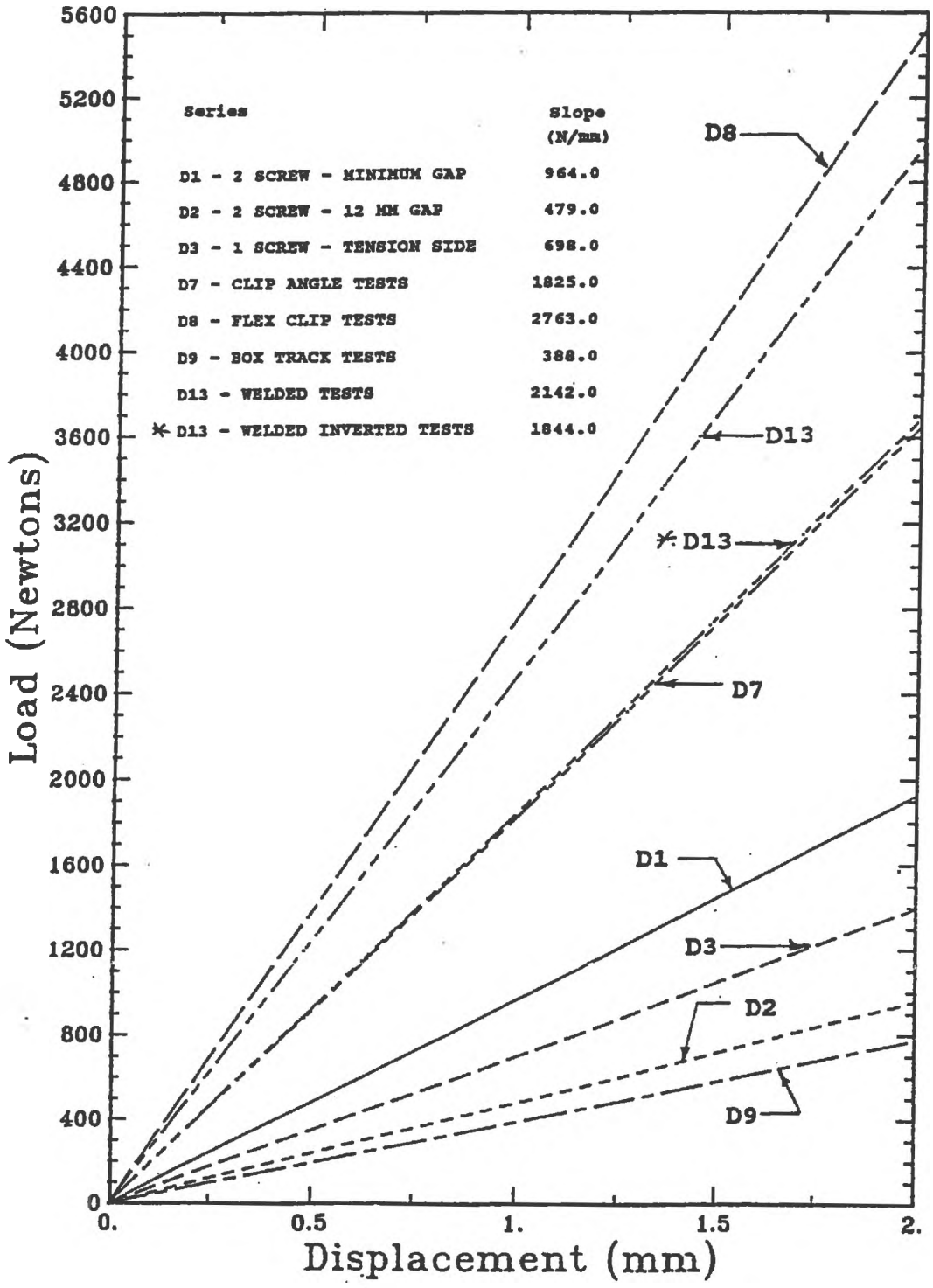

Figure 2.14 Load Versus Displacement Summary 18 Gauge, 90 mm Deep Steel Stud to Track Connection Tests

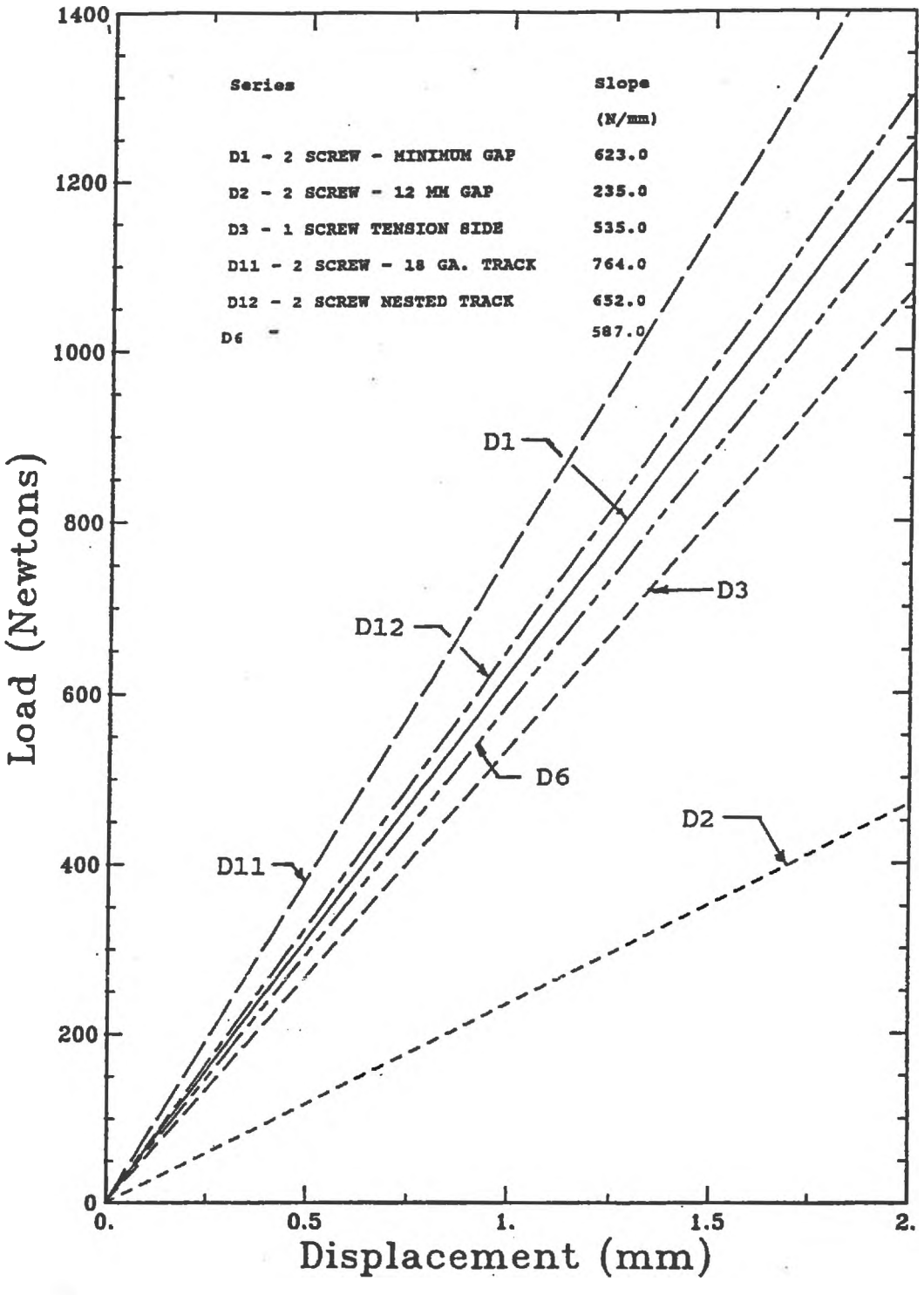

Figure 2.15 Load Versus Displacement Summary 20 Gauge, 150 mm Deep Steel Stud to Track Connection Tests

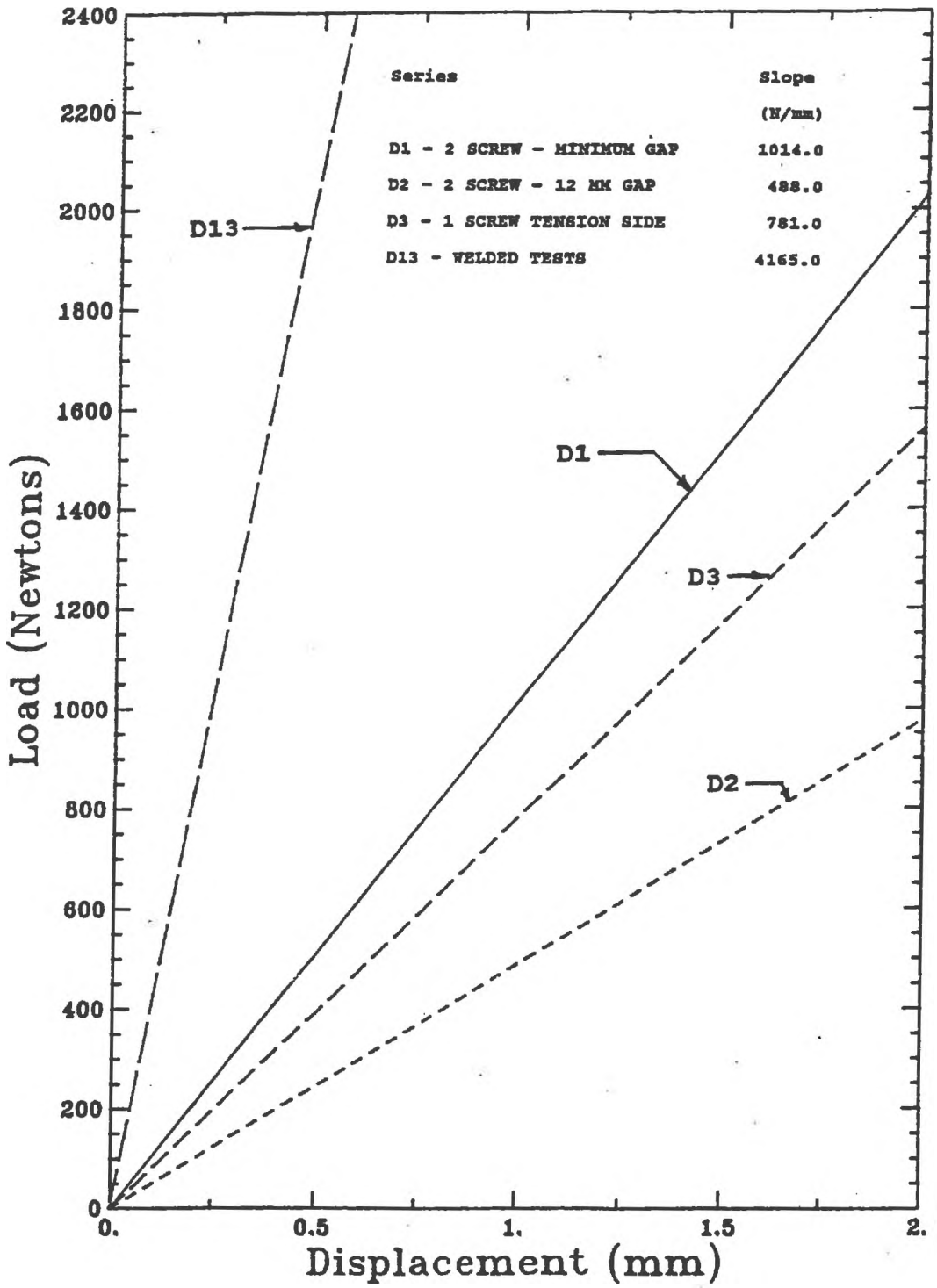

Figure 2.16 Load Versus Displacement Summary 18 Gauge, 150 mm Deep Steel Stud to Track Connection Tests

TABLE 2.3

SUMMARY OF STEEL STUD TO RACK CONNECTION FAILURE LOADS

Specimen Number	Ultimate Load (KN)	Yield Load (KN)	Load at 2 mm Displ. (KN)
20A-D1-1	3.00		
20A-D1-2	2.68		
20A-D1-3	3.01		
20A-D1-4	2.66	2.00	1.11
20A-D1-5	3.04		
20A-D1-6	2.89		
20A-D1-7	2.60		
20A-D1-8	2.55		
20A-D1-9.	2.99		
18A-D1-1	4.97		
18A-D1-2	4.57		
18A-D1-3	4.95	3.70	1.93
18A-D1-4	4.47		
18A-D1-5	4.55		
20B-D1-1	2.48		
20B-D1-2	2.63		
20B-D1-3	2.84	1.90	1.25
20B-D1-4	2.47		
20B-D1-5	2.80		
20B-D1-6	2.67		
18B-D1-1	4.30		
18B-D1-2	4.74		
18B-D1-3	4.55		
18B-D1-4	4.29	3.30	2.03
18B-D1-5	4.62		
18B-D1-6	4.08		
20A-D2-1	2.59		
20A-D2-2	2.90		
20A-D2-3	2.77	*	0.49
20A-D2-4	2.98		
20B-D2-1	2.41		
20B-D2-2	2.65		
20B-D2-3	2.41	*	0.47
20B-D2-4	2.52		

* - no specific yield point

Table 2.3 (continued)

Specimen Number	Ultimate Load (KN)	Yield Load (KN)	Load at 2 mm Displ. (KN)
18A-D2-1	4.82		
18A-D2-2	4.76		
18A-D2-3	4.57	2.80	0.96
18A-D2-4	4.46		
18B-D2-1	4.27		
18B-D2-2	4.10	3.40	0.98
18B-D2-3	3.90		
20A-D3-1	2.42		
20A-D3-2	2.84	na.	na.
20A-D3-3	2.62		
18A-D3-1	4.39		
18A-D3-2	4.42		
18A-D3-3	4.54	2.90	1.40
18A-D3-4	4.11		
20B-D3-1	2.34		
20B-D3-2	2.27	1.90	1.07
20A-D3-3	2.28		
18B-D3-1	4.16		
18B-D3-2	3.73	3.00	1.56
18B-D3-3	3.97		
18A-D4-1	3.81		
18A-D4-2	4.60	3.30	1.80
18A-D4-3	4.48		
18A-D4-4	4.64		
20A-D5-1	2.28		
20A-D5-2	2.05		
20A-D5-3	2.56	na.	na.
20A-D5-4	2.52		
20B-D6-1	2.22	1.90	1.17
20B-D6-2	2.56		
18A-D7-1	4.33		
18A-D7-2	4.82	3.00	3.65
18A-D7-3	UNRELIABLE		

Table 2.3 (continued)

Specimen Number	Ultimate Load (KN)	Yield Load (KN)	Load at 2 mm Displ. (KN)
18A-D8-1	5.18		
18A-D8-2	4.44	3.00	5.53
18A-D8-3	4.84		
18A-D9-1	4.38		
18A-D9-2	4.15	2.90	0.78
18A-D9-3	UNRELIABLE		
20A-D10-1	3.13		
20A-D10-2	3.06	2.50	2.18
20A-D10-3	3.02		
20B-D11-1	3.09		
20B-D11-2	3.06	1.90	1.53
20B-D11-3	3.36		
20A-D12-1	2.90		
20A-D12-2	2.83	1.90	1.03
20A-D12-3	3.06		
20B-D12-1	2.36		
20B-D12-2	2.69	*	1.34
20B-D12-3	2.45		
18B-D13-1	4.58		
18B-D13-2	5.02	*	8.33
18B-D13-3	5.79		
18A-D13-1	5.70		
18A-D13-2	4.94		
18A-D13-3	4.82	*	4.28
18A1-D13-4	4.79 **		
18A1-D13-5	4.78 **	*	3.69
18A1-D13-6	4.85 **		

* - no definite yield point
** - inverted welded connection

The point at which the slope of the curves changed significantly was chosen as the mean yield value for the test series. This value was obtained graphically and is only approximate since a different observer might select a slightly different value. Column four of Table 2.3 is the mean load at a displacement of 2 mm. This value was obtained by multiplying the slope of the linear regression analysis performed for each test series by 2 mm.

2.3.4 Qualitative Description Of Stud To Track Connection Failures

1) Series D1 – Minimum Gap, 2 Screw Connection

For the 18 and 20 gauge, 90 mm deep specimens, web crippling of the stud end was initiated at the web and tension flange intersection. The maximum out-of-plane deformation occurred approximately at 0.2 times the depth of the stud (0.2D) from the tension flange. Figure 2.17 is a photograph of a typical bearing failure of a 90 mm, 20 gauge specimen. It should be noted that in this test, the top screw pulled out of the compression flange of the stud. The large permanent deformation shown in this figure is typical for all specimens tested in this series. However, this gross type of deformation, only occurred very near the ultimate load. Initiation of web crippling (bearing failure) was observed to start at load levels between 55 % to 80% of ultimate load. This corresponded closely to the load at which the top (compression) flange screw pulled free from the stud.

For the 150 mm deep studs, web crippling failure was again initiated at the web and tension flange intersection. The maximum out-of-plane deformation occurred at approximately 0.1D from the tension flange of the stud.

The length of the crippled zone, along the length of the stud, varied from 60 mm to 80 mm for 20 gauge, 90 mm studs and 30 mm to 50 mm for 18 gauge, 90 mm studs. For 20 gauge, 150 mm deep studs, the crippled zone varied from 60 mm up to 85 mm in length. The crippled zone of the 18 gauge, 150 mm studs, varied from 60 mm to 75 mm in length.

In all tests, the track flanges sustained permanent deformation. The amount of top track flange deformation depended on whether the screw which fastened the compression

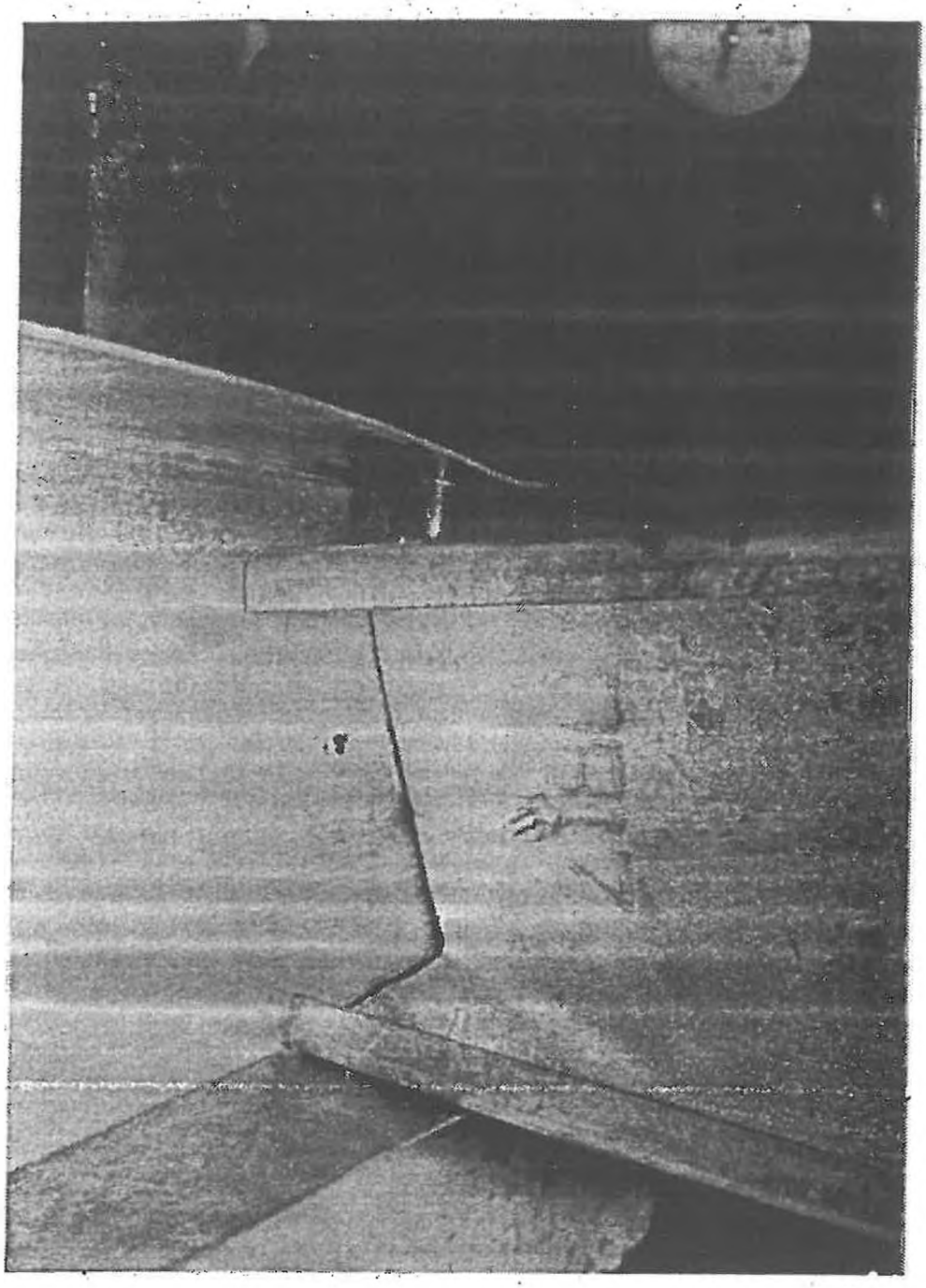

Figure 2.17 **Photograph of Typical Failure for 20 Gauge, 90 mm Deep Specimen - D1**

flange of the stud to the track flange, pulled free at an early stage or whether it did not completely let go. It was observed that when the top screw did not pull out, the top flange of the track received more permanent damage. In all cases the deformation was local in nature.

2) **Series D2 – 12 mm Gap, 2 Screw Connection**

The failure pattern observed in this series is similar to Series D1, except large permanent deformations occurred at levels 5 to 10 % lower than in Series D1. The photograph in Figure 2.18 shows a typical 150 mm stud after failure.

For the 90 mm deep, 20 gauge specimens, the failure zone along the stud length varied from 60 mm to 100 mm in length while the 18 gauge, 90 mm failure zone varied from 30 mm to 60 mm in length. The 150 mm deep stud failure zone was similar to that of Series D1.

3) **Series D3 – Minimum Gap, 1 Screw Connection (Tension Flange)**

In Series D3 the steel stud compression flange (top) was not attached to a track flange. During the test it was observed that the stud end translation was significantly greater than the displacements observed in Series D1 for a given load level. The mode of failure in this series was also by web crippling. The maximum out-of-plane deformations for the 90 mm deep, 18 and 20 gauge studs occurred at 0.1D from the tension flange (bottom). The length of the crippled zone for the 90 mm, 20 gauge studs was approximately 90 mm in length. For the 18 gauge, 90 mm deep studs, this zone was approximately 35 mm in length.

For 150 mm deep, 18 and 20 gauge specimens, the location of maximum out-of-plane deformations ranged from 0.1D to 0.25D. For the 20 gauge specimens, the web crippling zone along the length of the stud was found to be approximately 40 mm. For the 18 gauge specimens, the crippled zone ranged from 75 mm up to 100 mm in length. Figure 2.19 is a photograph showing an 18 gauge specimen at failure. As shown, the unattached track flange did not sustain any permanent deformation. The flange attached to the tension flange of the stud did sustain permanent deformation similar to that of Series D1.

Figure 2.18 Photograph of Typical Failure for 18 Gauge, 150 mm Deep Specimen - D2

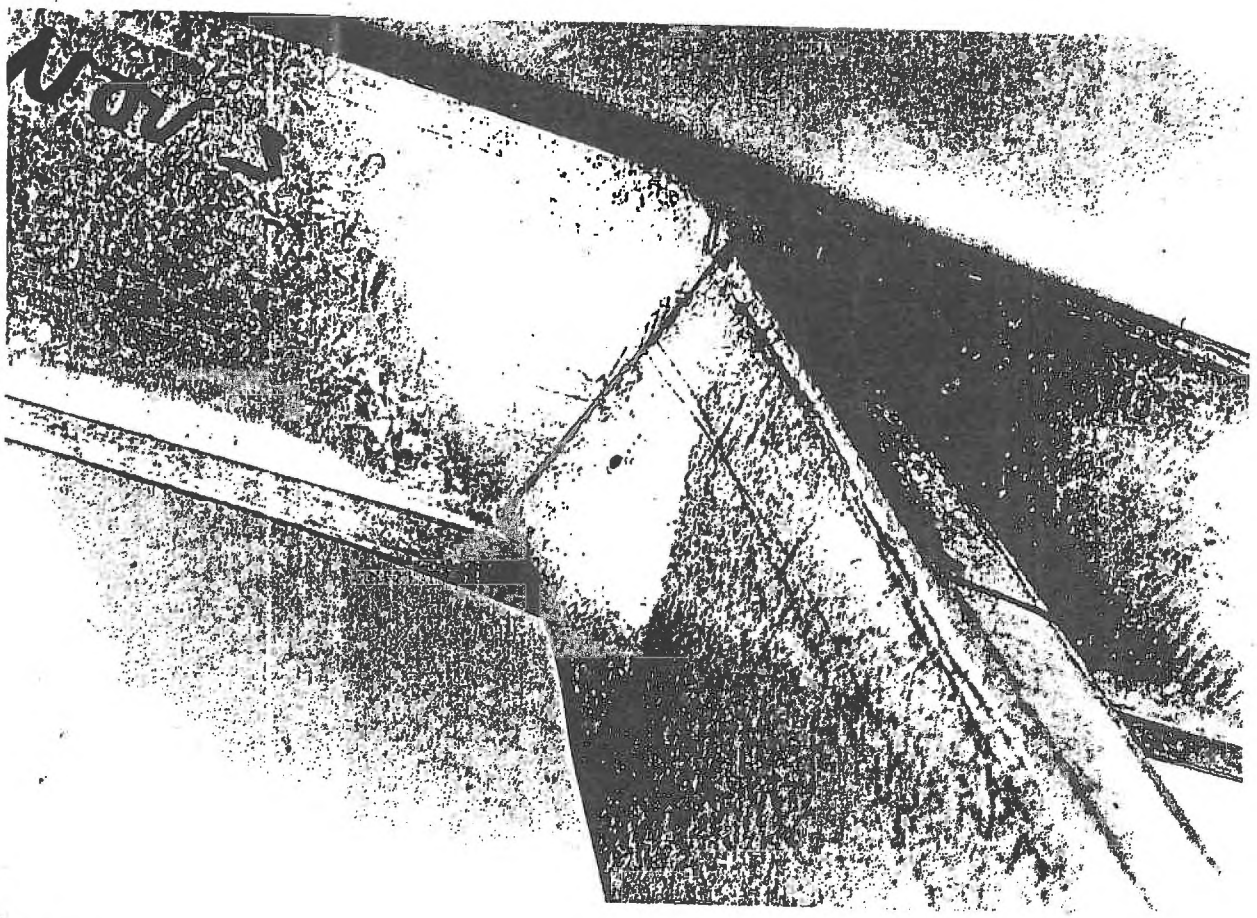

Figure 2.19 **Photograph of Typical Failure for 18 Gauge, 150 mm Deep Specimen - D3**

4) **Series D4 – Minimum Gap, 1 Screw Connection (Compression Flange)**

In this series only the top compression stud flange was attached to the track. During the test it was observed that the deformation behaviour was similar to Series D1 up to the point where the top screw pulled out of the compression flange of the stud. After pullout, the stud end translation increased significantly. Failure in this series was again by web crippling of the stud. The crippled zone was observed to be similar to that of Series D3. Both track flanges were observed to be permanently deformed.

5) **Series D5 – 12 mm Gap, 1 Screw Connection (Tension Flange)**

In this series, the track flanges were observed to be deformed at an earlier stage than in all the previous series. Web crippling was also the mode of failure in this series.

6) **Series D6 – Minimum Gap, 2 Screw Track End Test**

The mode of failure for the specimens tested was also by web crippling. The stud deformations were similar to those of Series D1. Typical failure is shown in Figure 2.20.

7) **Series D7 – Clip Angle Connection**

For the clip angle connection tests, failure was due to the shear failure of one of the two bolts connecting the clip angle to the stud and/or by pulling out of the nail anchors from the concrete beam. A typical failure is shown in Figure 2.21. During loading, it was observed that very little movement could be seen prior to failure. The mode of failure was sudden, once the pullout of the anchors or shearing of the bolts occurred. Up to this point, no track flange deformation occurred and no visible sign of web crippling was observed.

8) **Series D8 – Flexible Clip Movement Joint Connection**

The flexible clip angle connection, like Series D7, did not show any sign of web crippling failure. Failure was initiated by twisting of the flexible clip angle and/or by pulling out of one of the nail anchors. Up to this point, this connection was observed to allow very little stud end translation. As in Series D7, the connection failure was sudden. Permanent track flange deformations were minimal.

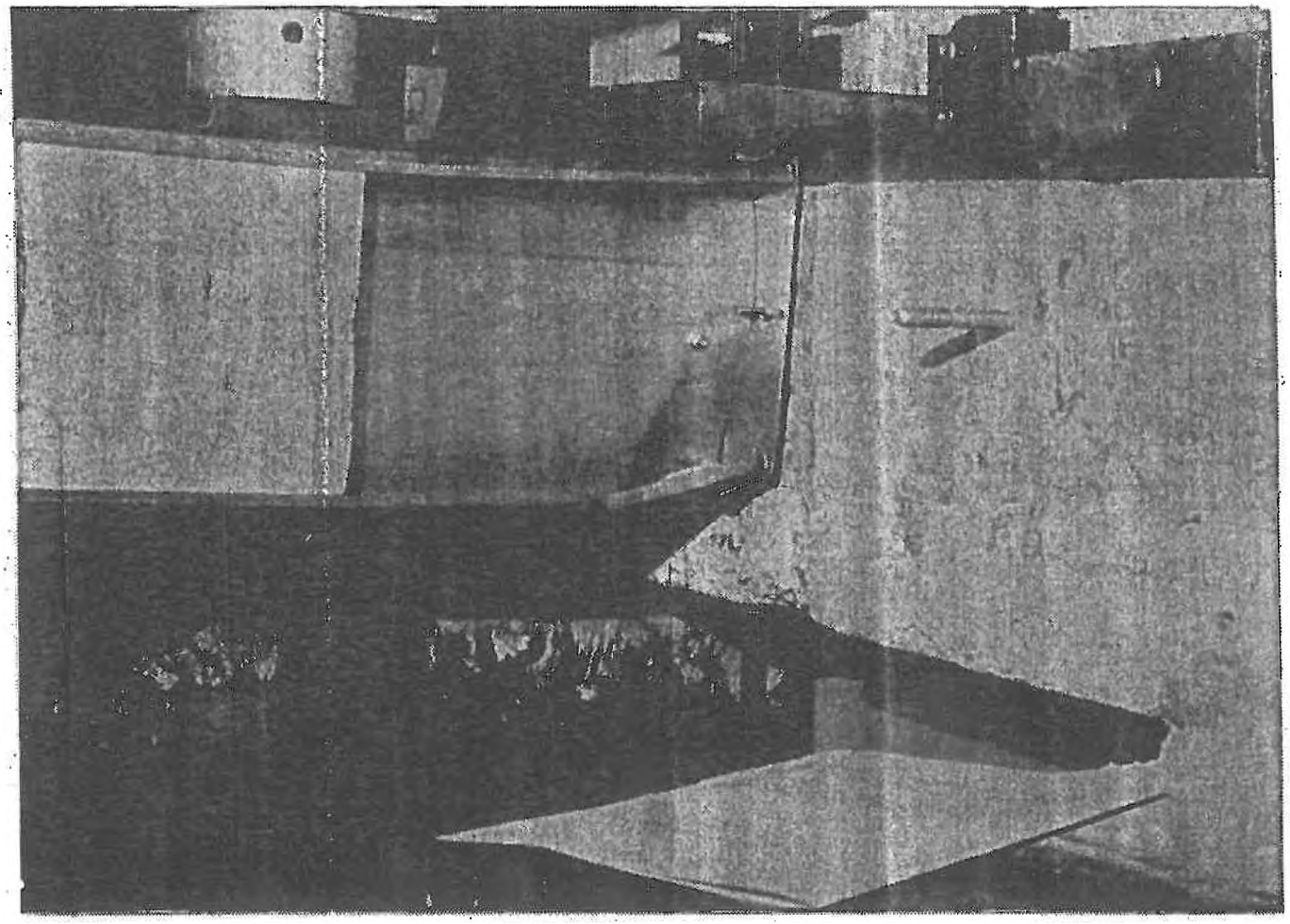

Figure 2.20 Photograph of Typical Failure for 20 Gauge, 150 mm Deep Specimen - D6

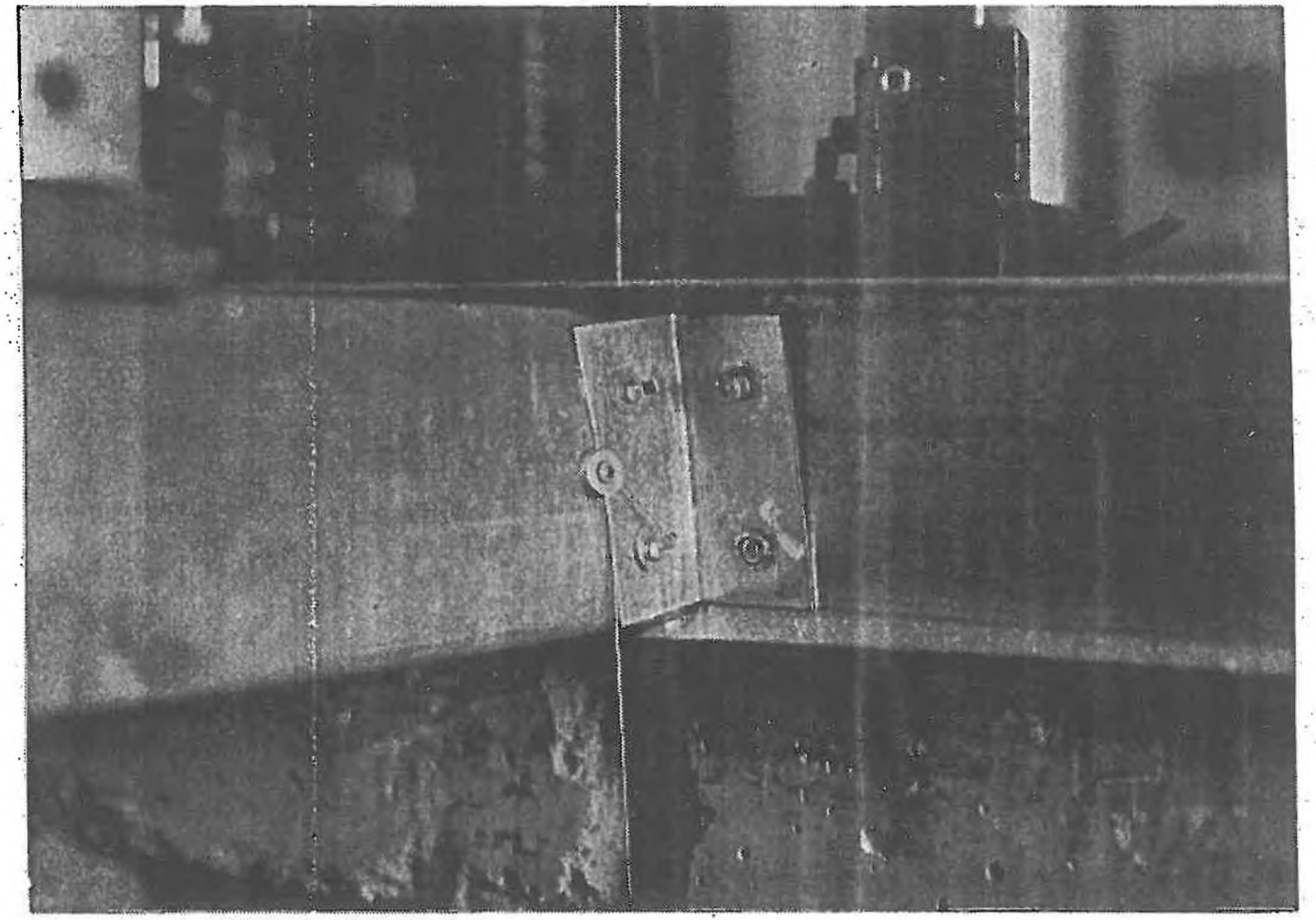

Figure 2.21 Photograph of Typical Failure of Clip Angle Connection Tests Specimen - D7

9) **Series D9 – Box Track Movement Joint Connection**

The box track movement connection failed by web crippling. A typical connection failure is shown in Figure 2.22. It should be noted that the additional screws used to fasten the two interior pieces of studs to track flanges did little to stiffening the connection. This is due to the fact that the track flange deformation zone, on the tension side of the stud, was local in nature and the additional screws were not effective.

10) **Series D10 – Minimum Gap, 2 Screw Connection**

In this series, a 20 gauge stud was fastened to a 14 gauge track with two screws. The stiffer track was observed to stiffen the connection significantly compared to a stud and track of the same gauge. Failure was again due to web crippling and the stud deformations were similar to that of Series D1.

11) **Series D11 – Minimum Gap, 2 Screw Connection**

Failure of the specimens tested in this series was by web crippling. Since a 20 gauge stud had been fastened to an 18 gauge track with 2 screws, this connection also proved to be stiffer than a comparable stud to track connection using the same gauge. The failure pattern was similar to that of Series D1.

12) **Series 12 – Nested Track Connection**

The nested track connection detail failed when the stud failed by web crippling. Like Series D1, the web crippling was initiated at the stud web to tension flange junction. For the 90 mm and 150 mm deep specimens, the crippled zone was approximately 75 mm in length. An example of the permanent deformation sustained by a 150 mm specimen at failure is shown in Figure 2.23..

13) **Series D13 – Minimum Gap Welded Connection**

In the case of the 18 gauge, 90 mm deep specimens, no web crippling occurred at the welded stud to track connection. Instead, web crippling occurred under the top load plate due to the total lateral load applied by the loading head of the test machine to the steel stud. It should be noted however, that web crippling at the connection would have already have been

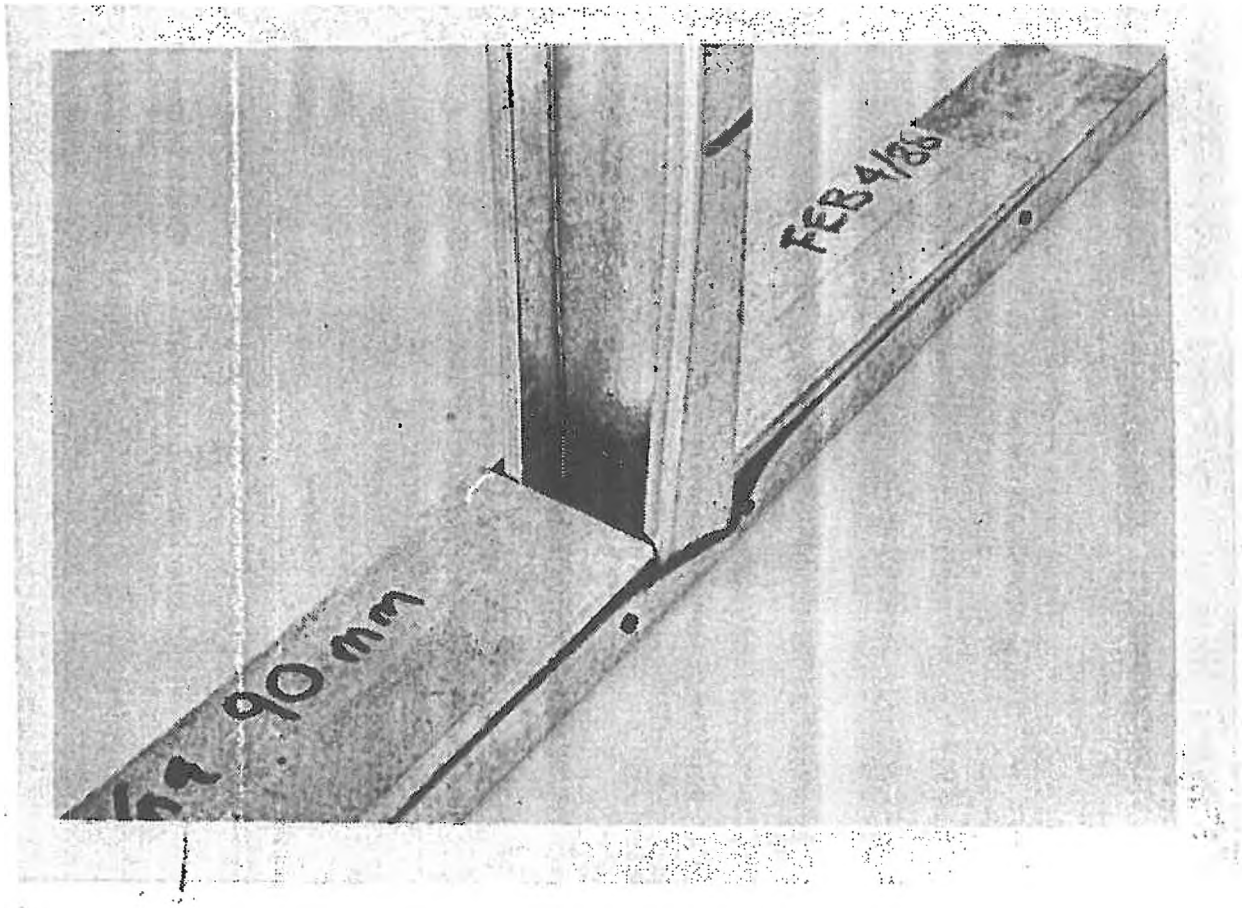

Figure 2.22 Photograph of Box Track Connection Specimen After Failure - Series D9

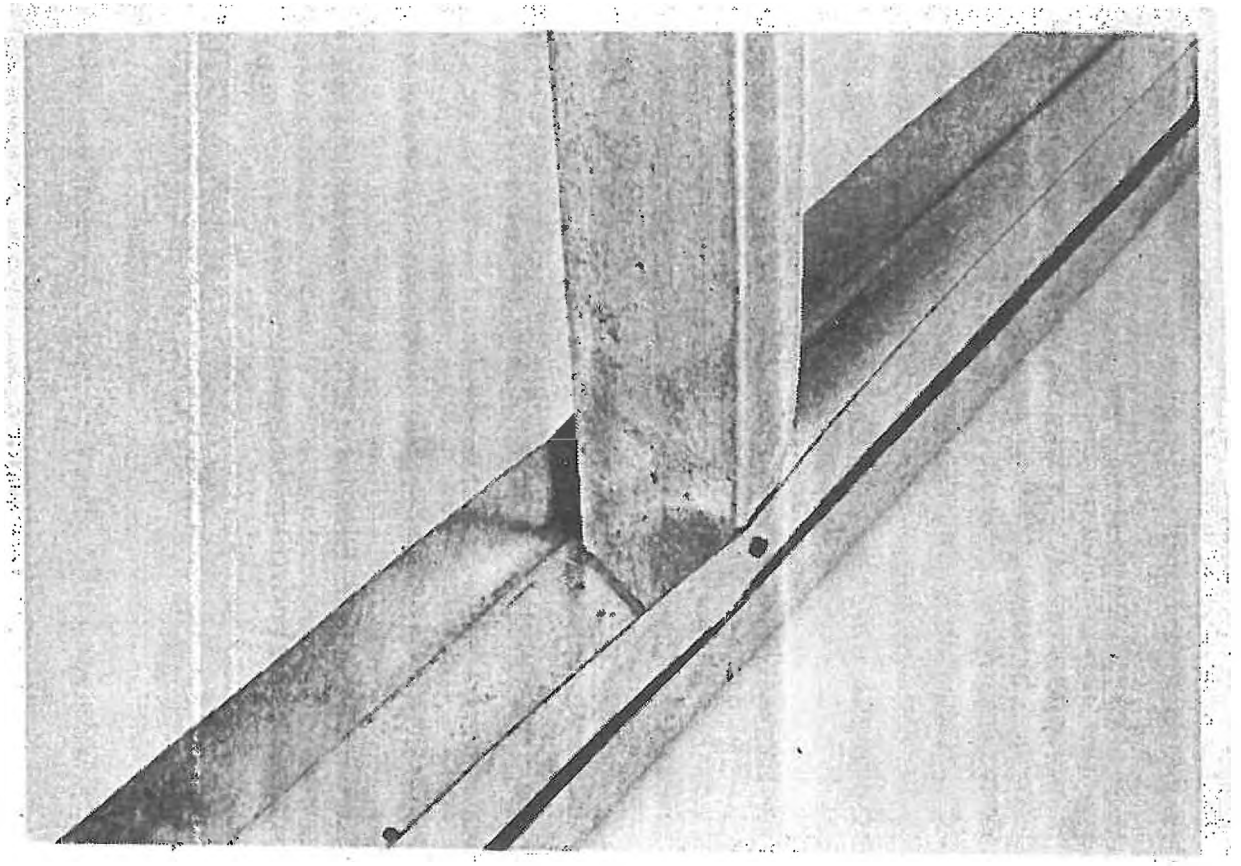

Figure 2.23 Photograph of Typical Failure of 20 Gauge, 90 mm Nested Track Connection Specimen - Series D12

in progress when failure occurred, were it not for the added strength provided by the welding. For the inverted 90 mm stud welded connection test, failure was also by web crippling under the top load plate.

For the 150 mm deep, 18 gauge test specimens, web crippling did occur at the stud to track connection as shown in Figure 2.24. The maximum out-of-plane stud web deformation occurred 30 mm from the tension flange and the length of this crippled zone was approximately 100 mm.

2.4 NAIL ANCHOR TESTS

2.4.1 Test Procedure

As discussed in Section 2.2.1, nail anchors were also tested. For these tests, 18 gauge, 90 mm stud and track sections were used. These were assembled to form specimens similar to Series D1. Each specimen was placed against the concrete beam used in the other tests and on each side of the stud, a nail anchor was fired through the track and into the concrete beam. Each anchor was located approximately 380 mm from the stud. Once the track was fastened, the inside of the stud was stiffened with wooden blocks at all locations so that no premature stud failure could take place before failure of one or both nail anchors occurred. The test procedure from this point on followed essentially that given in Section 2.2.3.

2.4.2 Results Of Tests

The load needed to cause failure of a nail anchor was recorded after each test. The test data for the eleven tests are presented in Table 2.4. In this table, the ultimate load required to cause failure of one of the anchors was calculated by dividing the ultimate failure load for the track assembly by two, since it was assumed that each anchor resisted half of the load applied to the track.

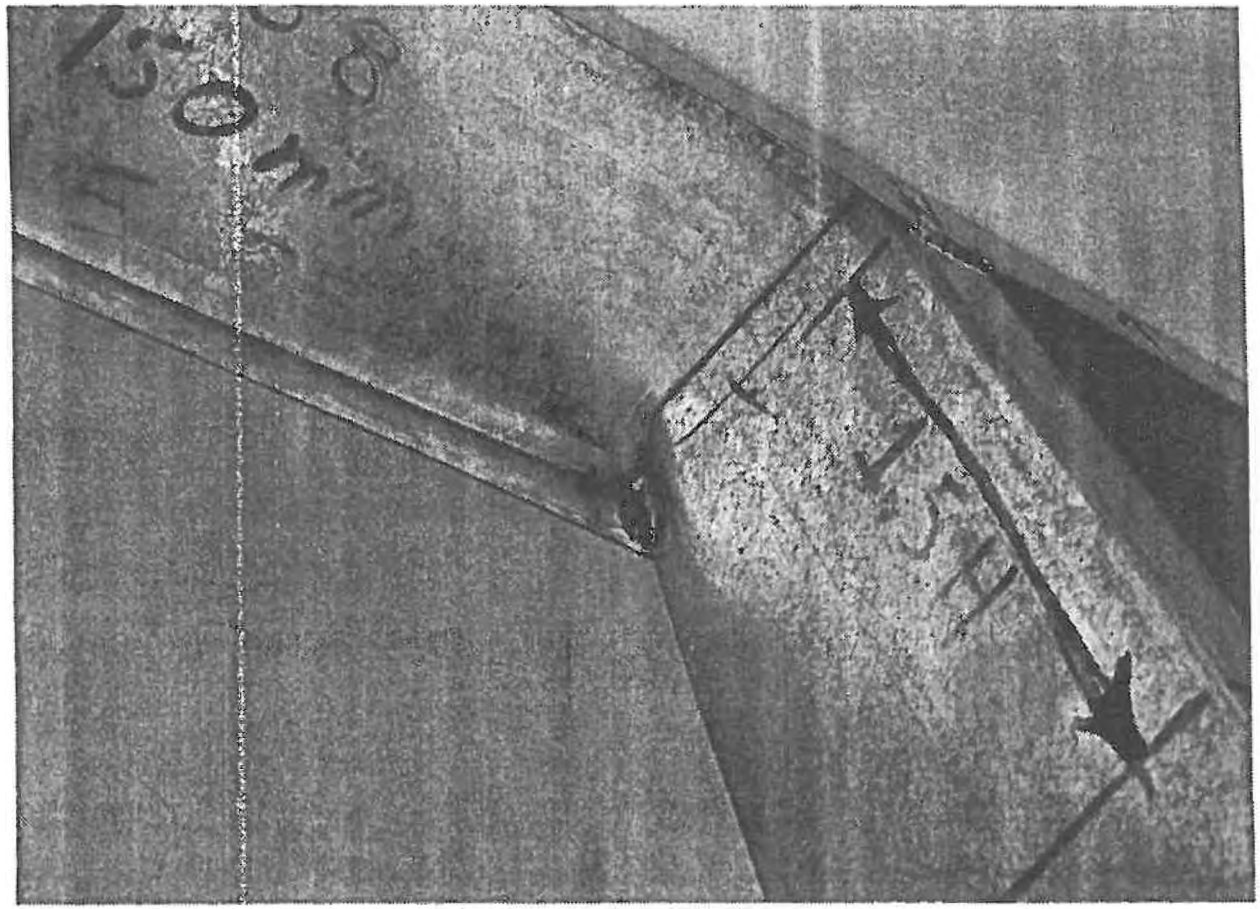

Figure 2.24 **Photograph of Typical Failure of 18 Gauge, 150 mm Deep Welded Connection Specimen - Series 13**

TABLE 2.4

FAILURE LOADS FOR FIRED NAIL ANCHORS TESTS

Specimen Number	Anchor Failure Load (KN)
H-1	2.2
H-2	2.2
H-3	1.4 *
H-5	0.9 *
H-6	2.3
H-7	2.7
H-8	3.0
H-9	3.2
H-10	1.0 *
H-11	3.0

* - Improper installation or nail penetration not complete.

2.4.3 Description of Failures

Failure of the nail track fastener occurred by pullout or bending or a combination of both. When failure occurred it was usually noted that a cone of concrete surrounding the anchor was removed with the fastener. The photograph in Figure 2.24 illustrates the condition of a nail anchor after failure. In the case of improperly installed anchors, it was noted that the anchor was either bent by a stone upon entry into the concrete or adequate depth of penetration was not fully achieved. In this situation failure was by pullout of the anchor at a much lower load than in the other tests. (Note: The 30 MPa concrete (minimum) was made with 20mm maximum size crushed limestone aggregate.)

2.5 DISCUSSION AND CONCLUSIONS

In nearly all of the steel stud to track connection tests, the track anchors were spaced approximately 900 mm on centre . For this anchor spacing , the track sections and expansion type anchors used were found to perform adequately. However in some preliminary tests the track anchors were spaced at 1500 mm on centre and it was found that a greater track deflection occurred and in some cases the top flange of the track buckled before the stud failed by web crippling . Since the installation of the track anchors is a field operation and proper track anchorage is required to control the out of plane deflections of the steel stud backup wall assembly it was concluded that until other data is available an anchor spacing of 800 mm on centre or less would be good practice regardless of the type of anchors used:

When the results of the tests of the two stud specimens, Series D14 shown in Figure B24, were compared to the results of Series D1 , Figure B1 , it was concluded that the out-of-plane deformations of each stud was not significantly influenced by the actions of nearby studs. This is due to the fact that the deformations at the track to stud connections are mainly local in nature .

The test results indicated that the two screw steel stud to track connection detail provided a much stiffer connection detail than the one screw connection . However the welded

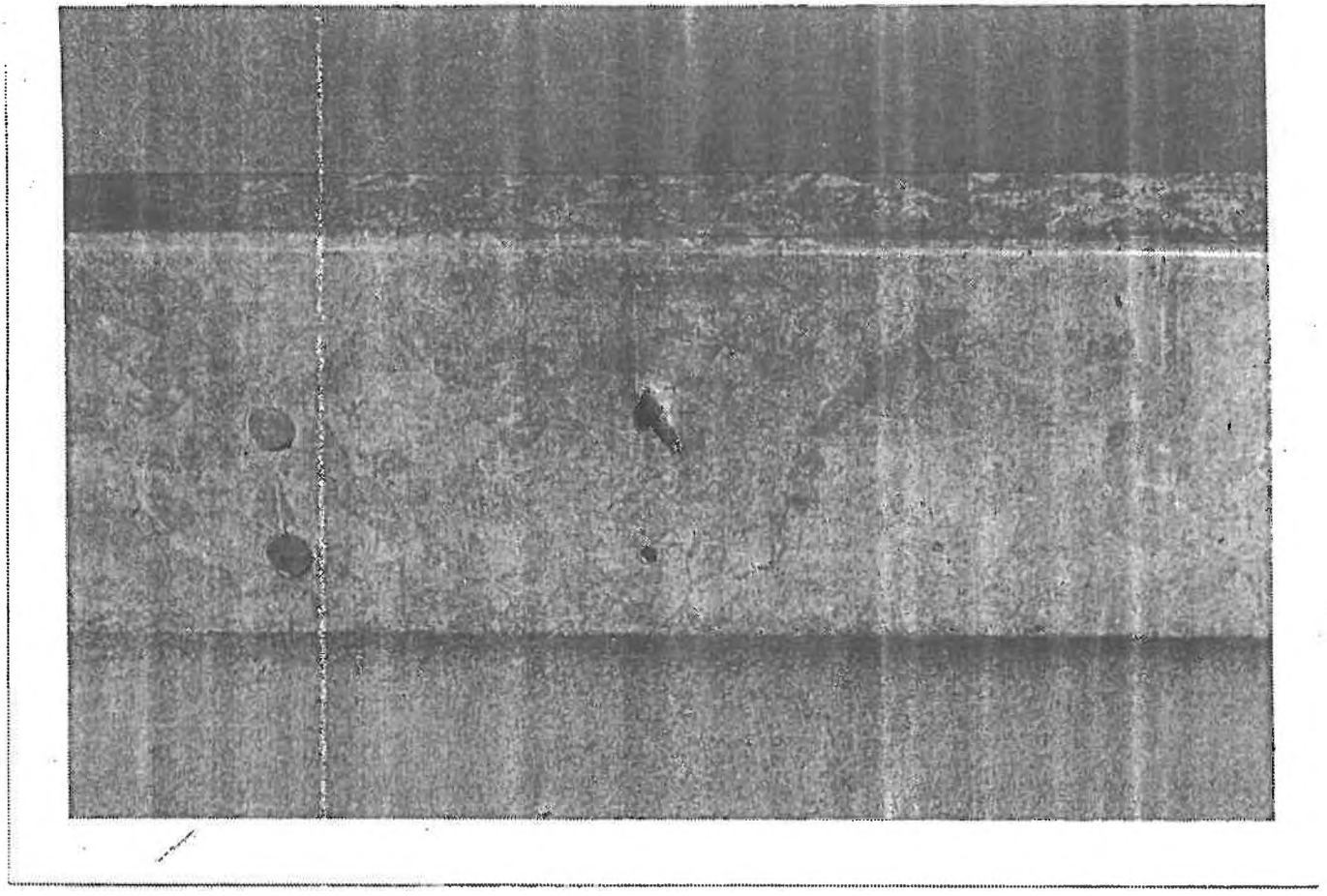

Figure 2.25 Photograph of Typical Nail Anchor After Failure

and the clip angle type of connection details were found to provide the stiffest type of connection detail . The strength of connections will be discussed again in Chapter 4.

CHAPTER 3

TESTS OF STEEL STUD BACKUP WALL PANELS

3.1 INTRODUCTION

Steel stud wall panels were tested to assess the effects of various design or construction practices on the behaviour of steel stud backup wall systems intended to support brick veneer. Separate tests of steel stud wall assemblies were designed to investigate specific aspects. Selection of test conditions, design of test specimens, design and fabrication of the test apparatus, test procedure and the test results are included in this chapter. In addition general observations and conclusions arising from these tests results are provided. More detailed discussion of the results in terms of analytical models and building code provisions are included in Chapter 4.

3.2 DESIGN OF THE EXPERIMENTAL PROGRAM

3.2.1 General

The objective of this part of the experimental research program was to document the influence of various factors on the strength and stiffness of the complete steel stud backup wall assembly. Therefore it was necessary to design a test program which would include information on:

- influence of realistic support conditions
- effectiveness of internal (through the web) versus surface bridging to prevent premature torsional-flexural buckling
- influence of connection conditions and spacing of bridging
- interaction of gauge of steel stud with other factors
- effectiveness of sheathing to provide composite action and/or torsional bracing
- effect of repeated loading
- influence of the type and method of connection of sheathing.

3.2.2 Design Of The Test Specimens

The experiment had to be designed to provide full information while not over complicating either the fabrication or the the test procedures. To accomplish this and still have a realistic experimental model, consideration was given to the following:

1) In plane height of backup wall assembly,
2) Spacing and number of studs used,
3) Type and number of loads on each stud,
4) Continuity of stud bracing,
5) Support track anchor spacing, and
6) Type of wall studs.

The in-plane height of the backup wall assembly was chosen to be 2.59 metres which is in the range commonly used for residential construction. The wall studs consisted of 92 mm deep lipped channels which are normally used for this range of backup wall heights. In all the tests, the commonly specified stud spacing of 406 mm on centre was used.

Each steel stud in the backup wall panel was symmetrically loaded with two equal concentrated loads located approximately at the quarter points of the span. This type of loading was chosen since the maximum moment between the loads was approximately equal to the maximum moment for uniformly distributed load. Also, two point loading on the compression flanges of the studs was used to simulate the most severe concentrated loading condition for lateral wind load on the backup wall. In general the transfer of lateral loads to the backup wall through brick ties or by direct air pressure represents a less severe loading condition for the stud.

Continuity of the stud bracing and the support track anchor spacing will be discussed in the following sections. Since testing of a large number of full length backup wall assemblies was not practical it was decided that specimens should be fabricated either with four studs or with two studs.

3.2.2.1 Four Stud Specimens

The use of four stud backup wall panels were required to investigate the strength and deformation characteristics of backup walls braced at discrete locations or with studs braced with sheathing and discrete bracing. This length was necessary to allow the continuity of bracing to be reasonably well modelled for the interior studs. Therefore this test was designed to allow the two interior studs to fail first. This was accomplished by providing additional lines of bracing for the exterior studs. (These details are discussed in Section 3.4.3.) The discrete bracing consisted of various types of steel bridging and the location and number of rows of bridging were varied in the test program.

As noted earlier each steel stud in a backup wall panel was symmetrically loaded with two equal concentrated loads. These loads were applied as shown in Figure 3.1 where the point loads on both exterior studs were applied over the plane of the web while the point loads on the interior studs were applied a distance 'b' from the outside face of the web. The load was transferred to the exterior studs as near as possible to the shear centre to minimize the torsional moments on the exterior studs and hence to allow failure to occur first at one or both of the interior studs. Equal loading of the four studs allowed each stud to deflect approximately the same amount. Equal loading represents the most conservative or severe loading condition since overloaded studs cannot redistribute load to less highly loaded neighbouring studs.

The loading arrangement used in the four stud backup wall tests was designed to allow independent rotation of each stud. This minimized the potential for unintentional lateral bracing at the load points which might otherwise have been provided by the loading arrangement. A more complete description of the loading system is given in Section 3.4.3.1.

In a long steel stud backup wall panel, the steel studs located near the centre of the panel are expected to deflect approximately the same amount when subjected to wind load. Consequently, the steel bridging in this area was also expected to be displaced by

Figure 3.1 Cross-Section Showing the Location of Loads on the Top Flange of 4 Stud Test Specimen

approximately the same amount. In order to accommodate this uniform displacement in the experiments, one end of each row of steel bridging was fastened to a bridging displacement control rig such as shown in Figure 3.2.

The steel stud backup wall panels were incrementally loaded to permit the deflections of each steel stud to be recorded at the location of the line of bridging and the out-of-plane displacements were subsequently determined. The bridging displacement rig was then used to lower the end of the steel bridging by the same amount as the out-of-plane displacement of the exterior steel stud located nearest to the rig. This was repeated for each load increment. The bridging was thus prevented from having differential lateral translation. [Note: when an end of the bridging is anchored to a building column or wall or if the last stud is adequately anchored to the building frame differential displacement of the bridging would occur. However this would have very little effect near the centre of the wall.] To allow approximately equal deflection of the studs, the top and bottom tracks were fastened to the concrete floor beams every 760 mm on center. This prevented the ends of the two interior studs from deflecting more than the ends of the two exterior studs.

3.2.2.2 Two Stud Specimens

The two stud test specimens were used to test steel studs with gypsum board sheathing on both the interior and exterior faces of the wall. The use of two stud wall panels was sufficient since it was expected that the sheathing would prevent buckling of the studs. For these tests, the continuity of bridging was not considered. Each panel was cyclically loaded in order to investigate whether any additional stiffness of the backup wall panel achieved through composite action would be sustained after repeated cycles of loading. Two stud backup wall panels were also used for unbraced stud tests. The loading arrangements for these tests are discussed in Section 3.4.3.2.

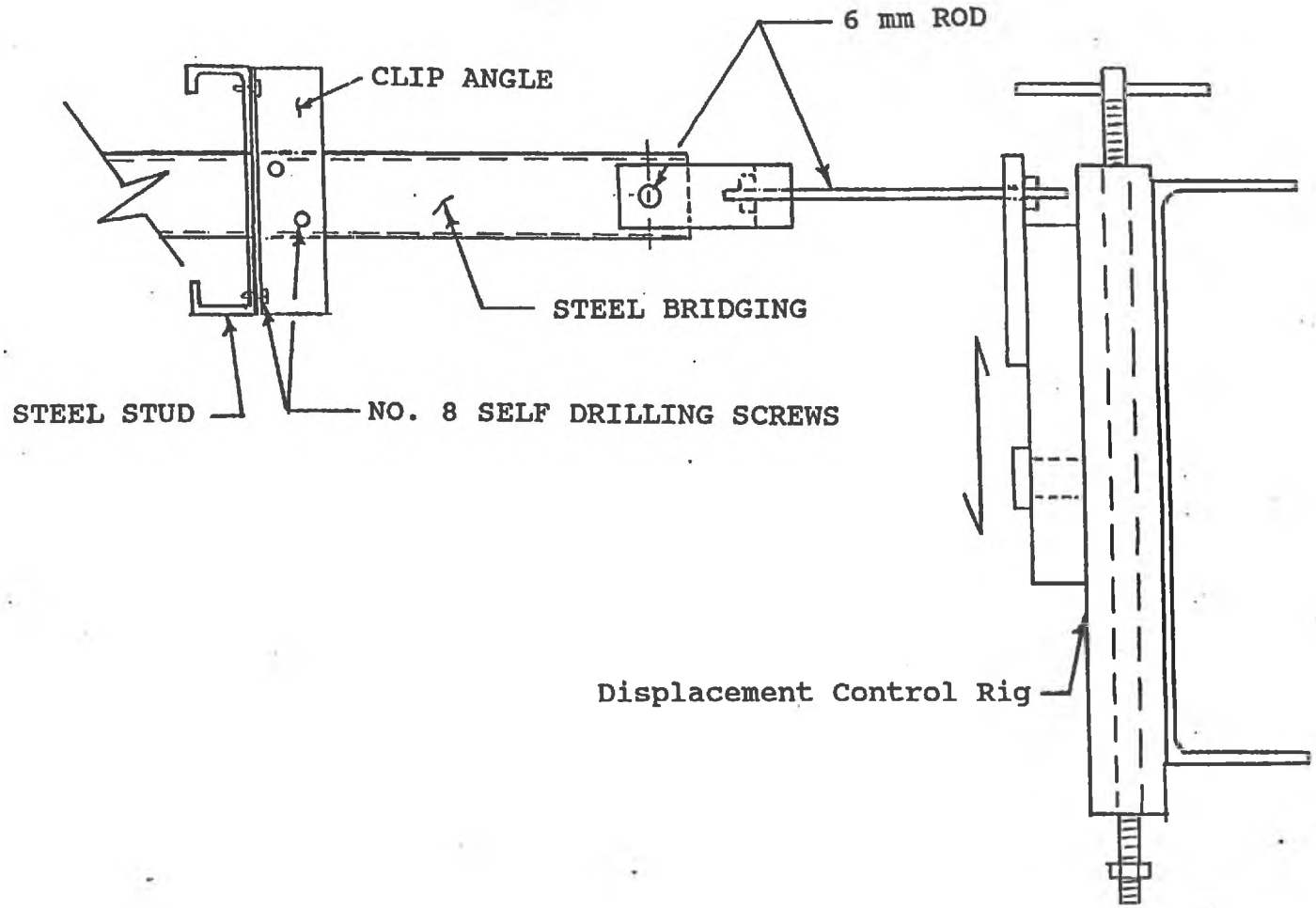

Figure 3.2 **Displacement Control Rig Used in 4 Stud Tests**

In addition to tests of backup wall panels, beam tests were performed on specimens fabricated with two studs. These tests were done to determine the flexural capacity of studs for test conditions when torsional loads were minimized.

3.3 SPECIMEN FABRICATION

Forty-four steel stud wall panel specimens were fabricated and tested. These tests were divided into seven tests series. For simplicity, all steel stud backup wall panels were fabricated in a horizontal position. Typical types of studs used in the fabrication are shown in Figure 3.3. These steel studs had prepunched 102 mm by 38 mm web cutout holes located as shown. In some tests, steel bridging was inserted through some of these holes to provide bracing of the steel studs at these locations.

In general, one end of each stud was inserted into a bottom track while the other end was inserted into the inner top track of a nested top track connection. An exception to this was for the beam test specimens which were simply supported. The studs were spaced at 406 mm on centre and were aligned parallel to each other. Each stud end was in turn temporarily fixed in position inside a track with locking pliers. Two Number 6 Tek Panhead self-tapping screws were used to attach each end to its supporting track. One screw was used to fasten the inside track flange to the interior flange of the stud, while the other screw was used to attach the outside track flange to the exterior flange of the stud. Once a stud was fastened, the locking pliers were removed and the process was repeated until all the studs were attached. Bridging and sheathing details as well as any other special test conditions for each individual test series are described in Section 3.5.

3.4 TEST APPARATUS, INSTRUMENTATION AND TEST METHODOLOGY

3.4.1 General Description

The steel stud backup wall specimens were tested in the test frame illustrated in Figure 3.4 . The top and bottom of the frame, representing the floors of a building, consisted of

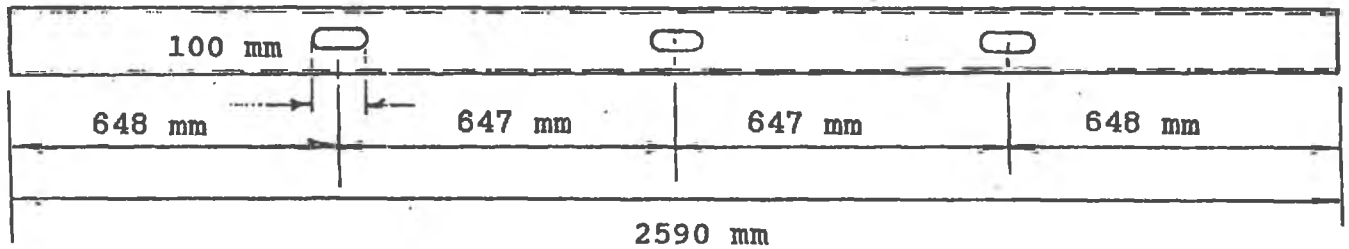

Figure 3.3A 20 Gauge

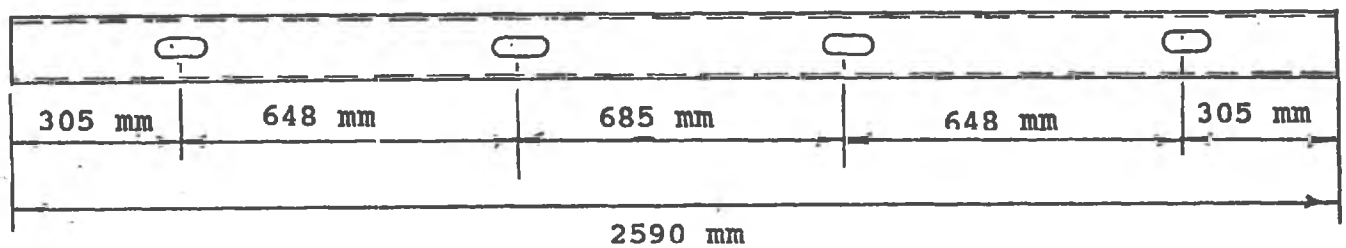

Figure 3.3B 18 Gauge

Figure 3.3 Typical Types of Steel Stud Used in Test Program

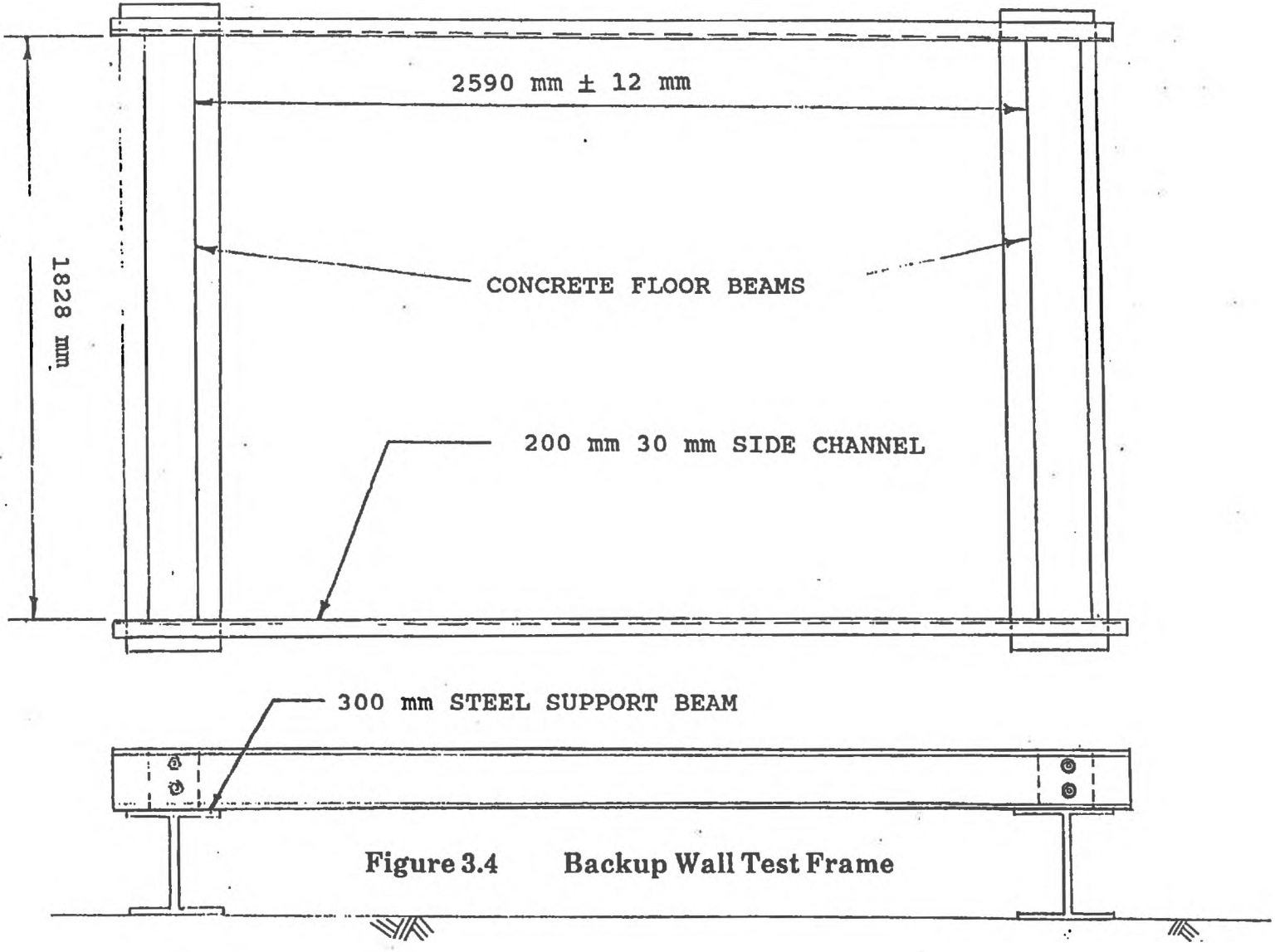

Figure 3.4 Backup Wall Test Frame

200 mm deep by 150 mm wide by 1.83 metres long reinforced concrete beam. The reinforcement used in these beams was identical to that used in the beam for the stud-track connection test program. Two 22 mm diameter threaded rods, approximately 300 mm long, were inserted into each end of the beams prior to pouring of the concrete. The rod ends protruded 50 mm from the end faces of the beams. Each side of the frame consisted of a 200 mm by 30 mm steel channel, approximately 3 metres long. The channels were drilled and fastened to the threaded rods protruding from the ends of the top and bottom floor beams. The clear distance between the top and bottom beam was 2.59 meters.

The frame was designed to allow an adjustment of $\pm$ 12 mm to the span. This was accomplished by slotting the holes of one of the ends of each side channel. The beam faces were drilled at regular intervals so that expansion type anchors could be set into the drill holes and used later to attach the top and bottom backup wall tracks. The frame was squared and levelled horizontally on two 300 mm deep steel beams. This was done to facilitate placing of instrumentation underneath the test specimens.

Once the test frame was in position, a loading frame was placed over it as shown in Figure 3.5 . The loading frame consisted of two steel columns and a steel beam. The base plates of the columns were prestressed to the laboratory floor. A horizontal beam was then used to span between the vertical columns. A hydraulic jack was attached to the beam with a sliding plate arrangement. The jack and sliding plate were positioned directly over the midspan of the test specimen. The plate was then tightened and the jack shimmed to a vertical position. The process was repeated until the jack was both vertical and stationed directly over the mid-point of the test specimen. A load cell was attached to the end of the hydraulic jack.

3.4.2 Instrumentation and Data Acquisition

3.4.2.1 Test Series No. 1

During the backup wall tests, metric dial gauges and linear potentiometric displacement transducers (L.P.D.T.) were used to measure the out-of-plane deflections. For wall panels

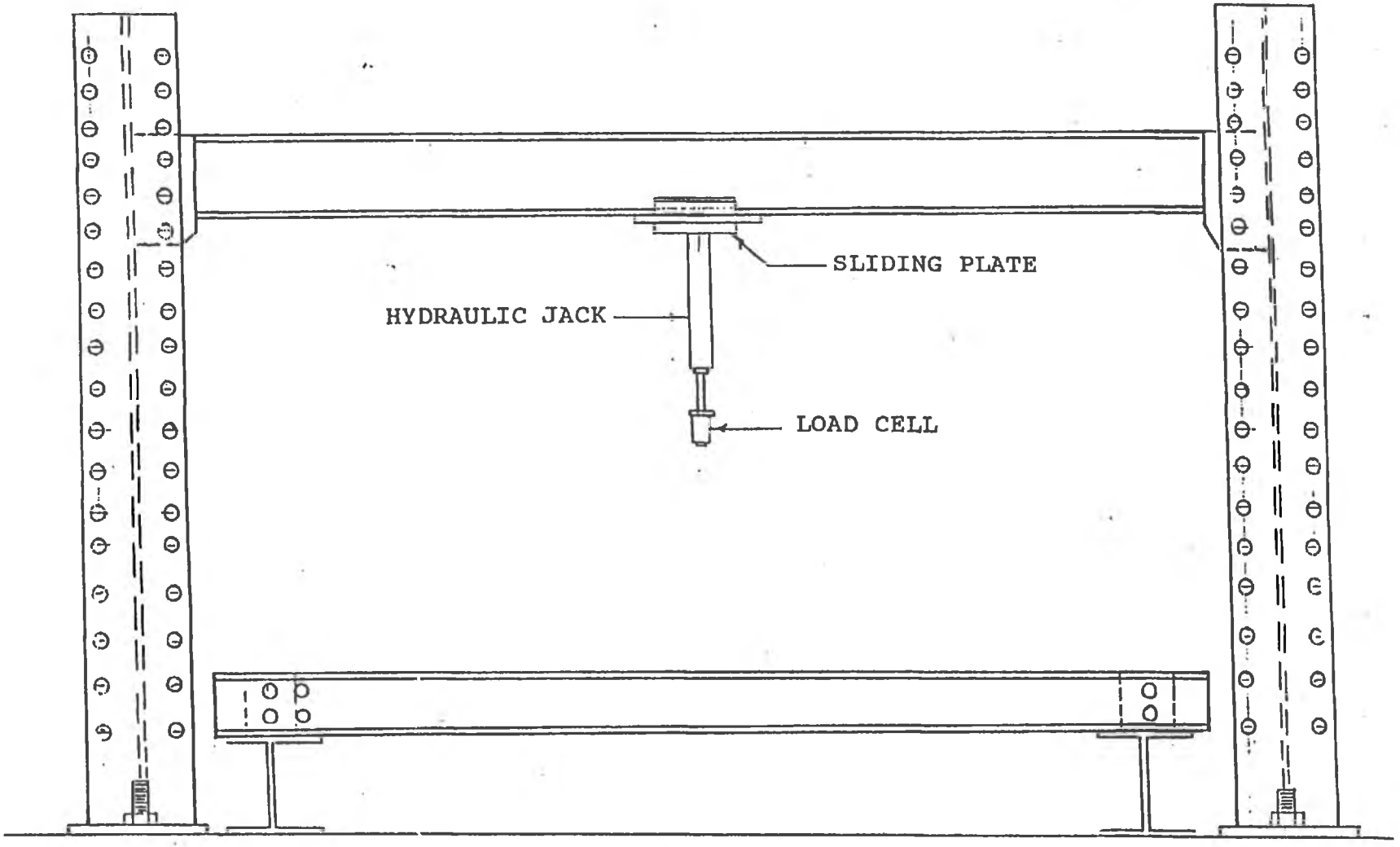

Figure 3.5 **Backup Wall Test Frame with Loading Frame in Position**

1-BW-1 to 1-BW-6, the locations of the dial gauges and potentiometers are shown in Figure 3.6. Dial gauges 1 to 4 were located at midspan of the wall studs and measured the displacement of the bottom flange directly beneath the web. Dial gauge 5 was used to adjust one end of the bridging as described in Section 3.3.2. Eight L.P.D.T.s were used to measure the translations at the out-of-plane ends of the studs. These L.P.D.T.s were located as shown in Figure 3.6. The deflection readings obtained from these devices were automatically recorded by the Optilog data acquisition device which was interfaced with a Texas Instrument microcomputer.

For test specimens 1-BW-7 and 1-BW-8, the locations of the dial gauges and L.P.D.T.s are shown in Figure 3.7. This setup is similar to that described above except additional dial gauges were required at locations 4 through 7. Dial gauges 4 and 6 were used to measure the deflections of stud A, at the locations of the two lines of bridging. Dial gauges 5 and 7 were subsequently used to adjust the end of the bridging at the bridging displacement control rig location, as described in Section 3.3.2. Finally, for specimens 1-BW-9 and 1-BW-10, the midspan deflection of the two interior studs were measured with dial gauges while the stud end translations were measured with the L.P.D.T.s.

3.4.2.2 Test Series No. 2

The location and type of instrumentation for backup wall panel 2-BW-1 to 2-BW-3, was the same as shown in Figure 3.6 for wall panels 1-BW-1 to 1-BW-6. For wall panels 2-BW-4 and 2-BW-5, the instrumentation was located as shown in Figure 3.7.

3.4.2.3 Test Series No. 3 and 4

For test Series 3, the dial gauges and potentiometers were located as shown in Figure 3.6 . In Series 4, deflections at midspan of the interior studs were measured with dial gauges. The deflections at the ends of these two studs were also measured with linear potentiometers as in the previous series.

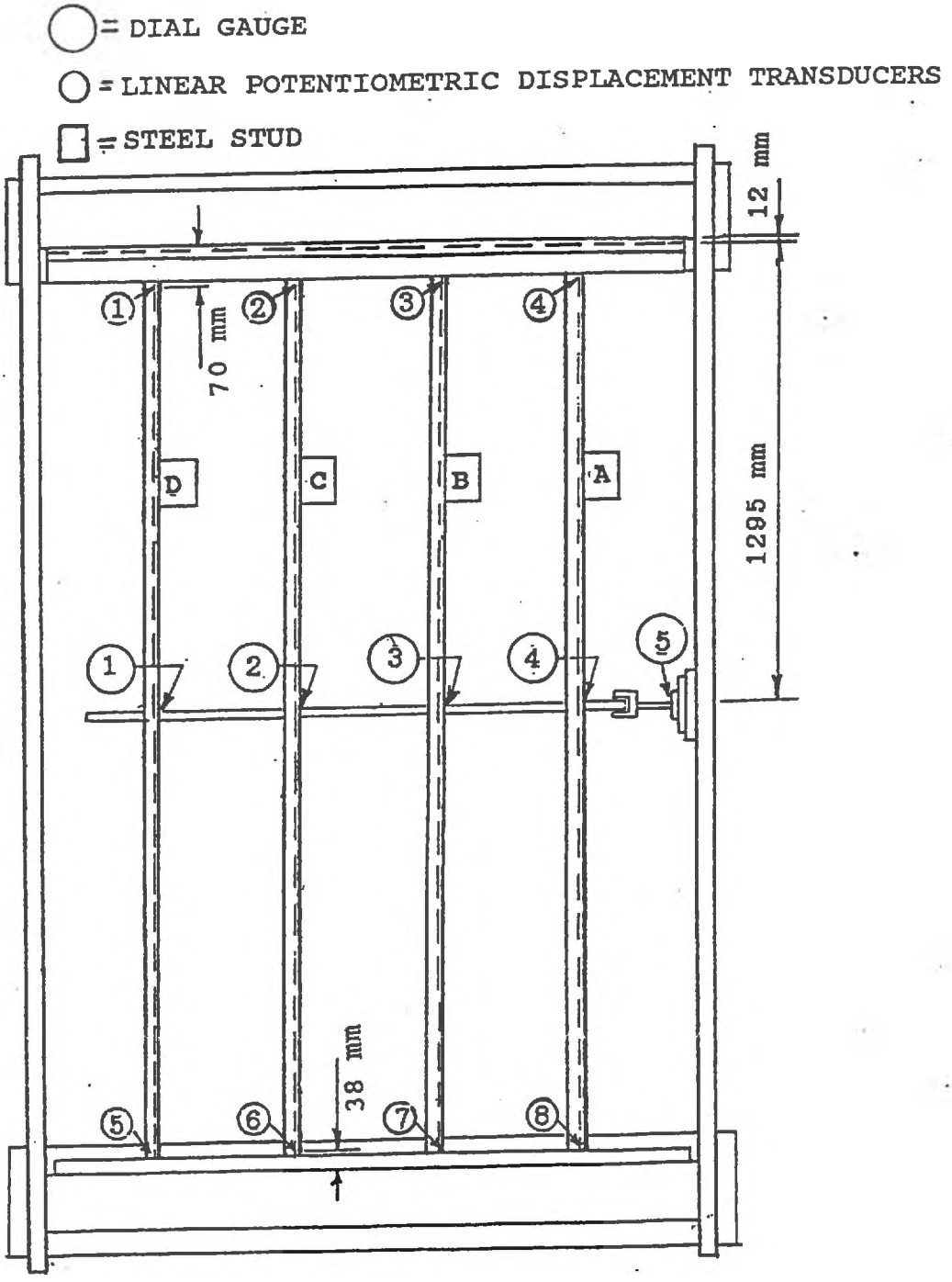

Figure 3.6 Location of Displacement Recording Devices for 4 Stud Specimens with One Line of Bridging

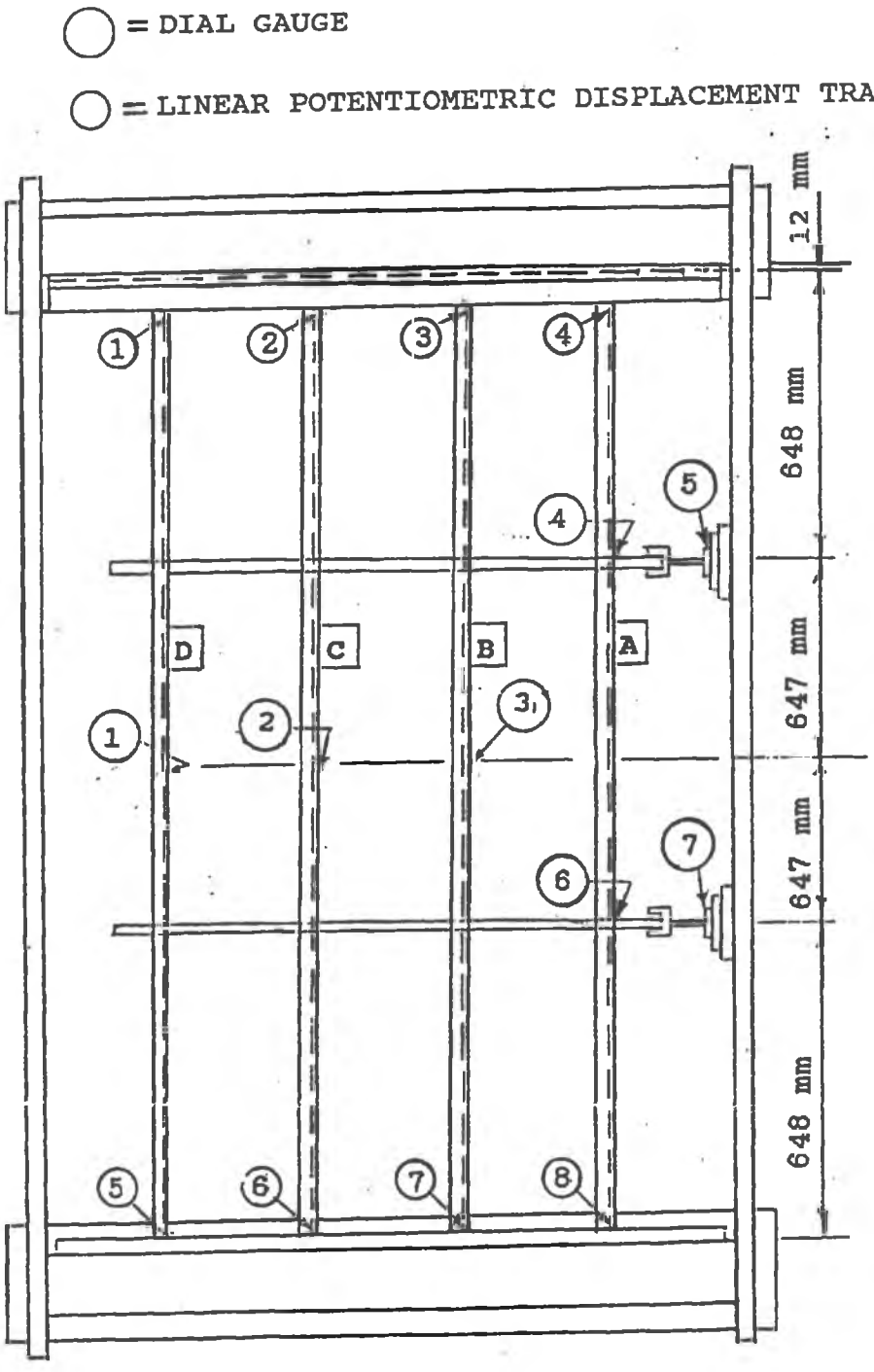

Figure 3.7 Location of Displacement Recording Devices for 4 Stud Specimens with Two Lines of Bridging

3.4.2.4 Test Series No. 5

In this series the stud rotations at midspan were measured by protractors mounted on a bracket attached to the web of each stud. Details are provided in Section 3.4.2.6.

3.4.2.5 Test Series No. 6 and 7

In Series 6, the midspan deflections were measured with dial gauges. In the seventh and final series , the midspan deflection of the panel was recorded by dial gauges at both stud locations. The end translations of the studs were measured with potentiometers.

3.4.2.6 Stud Rotation Measurements

Rotation measurements were taken in Series 1 through 3 at the locations shown in Figure 3.8 . To measure the rotations of the stud, a small hole was drilled into the web at the locations shown in the figure. A protractor mounted on a bracket was then attached to the stud with a small nut and bolt as shown in Figure 3.9. The protractor had been drilled to allow a thin wire, with a weight attached, to hang freely as a plumbline. The wire acted as a pointer on the protractor and any change in orientation of the web could be read directly, to within one half of one degree, as the wire remained in its vertical position while the protractor rotated with the stud.

3.4.3 Test Setup and Procedures

3.4.3.1 Four Stud Test Specimens

Each test specimen was lowered into the test frame. The inside top track, of the nested top track connection, was slipped into the outside top track which had been previously fastened to the top concrete floor beam. The holes in the predrilled bottom track were then aligned with the holes drilled into the bottom floor beam. Threaded 8 mm diameter rods were inserted in these holes and screwed into the threaded expansion anchors which had been set

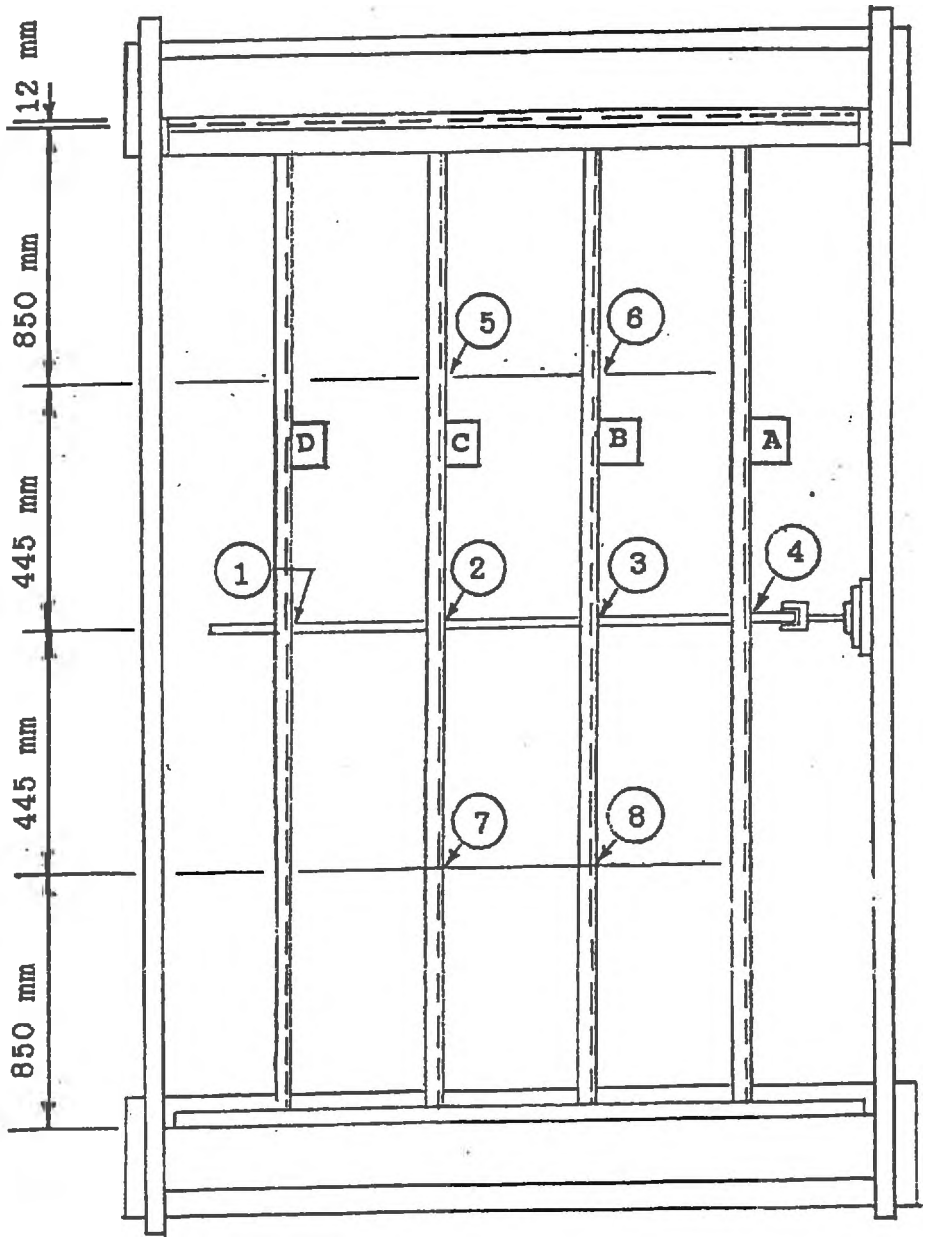

Figure 3.8 Location of Rotation Reading Devices -

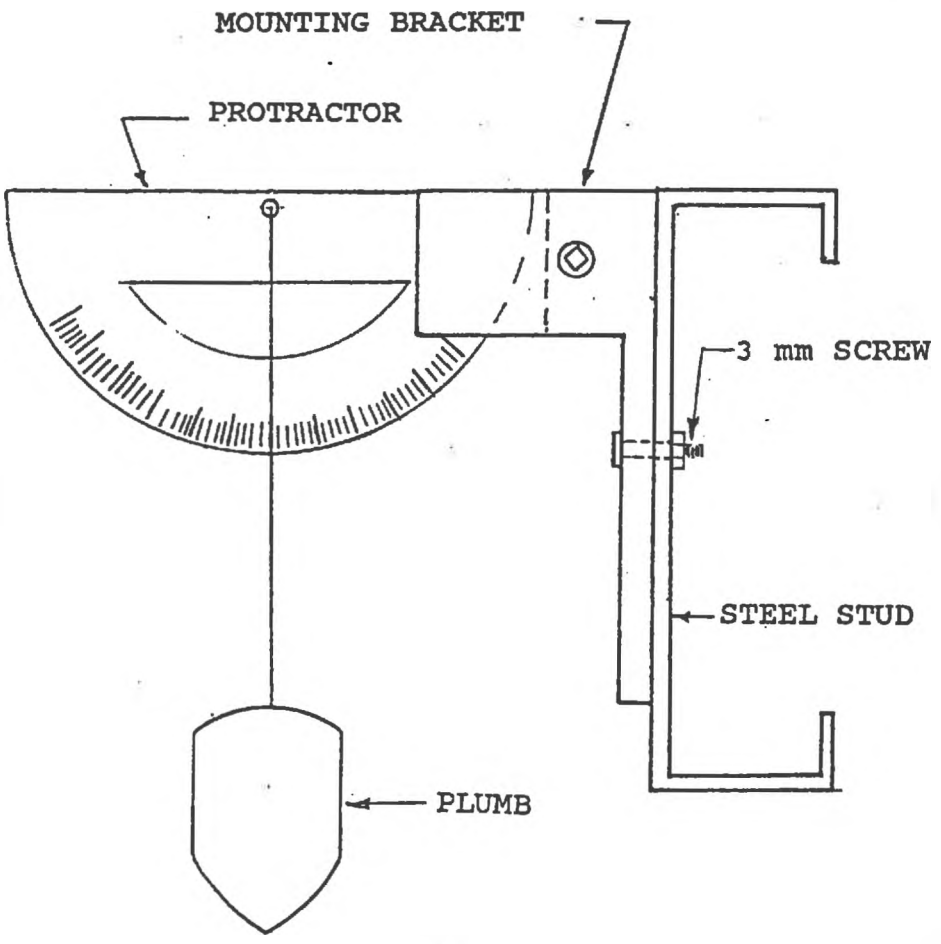

Figure 3.9 Rotation Reading Device

in the concrete. Nuts and washers were then used at fasten the track securely to the three points spaced 760 mm on centre. The outside top track was attached to the concrete floor beam in a similar manner.

Prior to fastening a 4 stud wall specimen into the test frame, additional bracing was attached to the two exterior studs. For the specimens fabricated with one line of steel bridging, the additional bracing was provided at the locations shown in Figure 3.10 . This bracing was used to prevent the premature failure of the two exterior studs before one or both interior studs failed. For test specimens with a line of steel bridging located at each quarter point, only one line of additional bracing was used to brace the exterior studs at midspan. Since it had been anticipated that the additional bracing could interfere with the two interior studs, it was decided to provide 16 mm thick spacer plates at the locations shown in Figure 3.11. These plates allowed enough clearance for the interior studs to rotate without any interference from these additional braces.

Wrap around brick ties were fastened to the webs of the interior studs at the load points. Two small holes were drilled into the top flange of the exterior studs so that the bottom hinge plates of the loading beams shown in Figure 3.12 could be fastened to the flanges at the locations shown. This was repeated at each loading point on the exterior studs . At the other end of loading beam A1, a stiffened plate was used to transfer the load from the loading beams to the top of the brick tie. The hinge on the exterior studs accommodated rotation of the interior studs without either restraining the rotation with the loading beam or magnifying the rotation due to application of nonperpendicular forces. Since the exterior studs had additional bracking, some inclination of the hinged load transfer mechanism due to rotation of an interior stud would not be critical for the exterior stud.

Beams A2 were used to span between beam A1 and were placed parallel to each other. Beam A3 was placed perpendicular to beams A2. At the end of beams A3 and A2, a pin and roller set was used to transfer the load. All beams and supports were aligned and adjusted to allow equal loading of the studs. A 25 mm diameter steel bar, 500 mm long, was used to

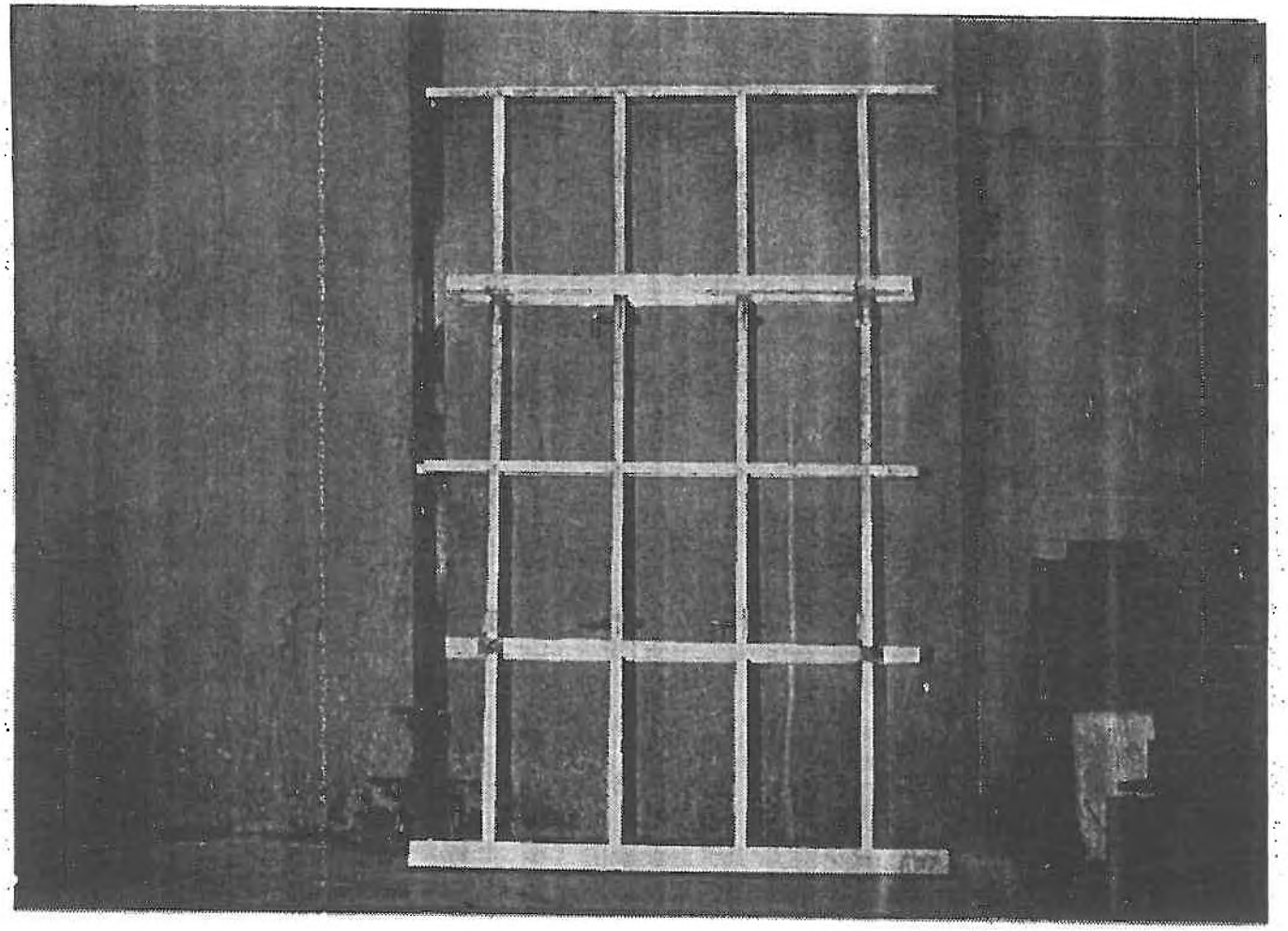

Figure 3.10 Photograph of a 4 Stud Wall Specimen Showing Additional Lines of Bracing for Exterior Studs

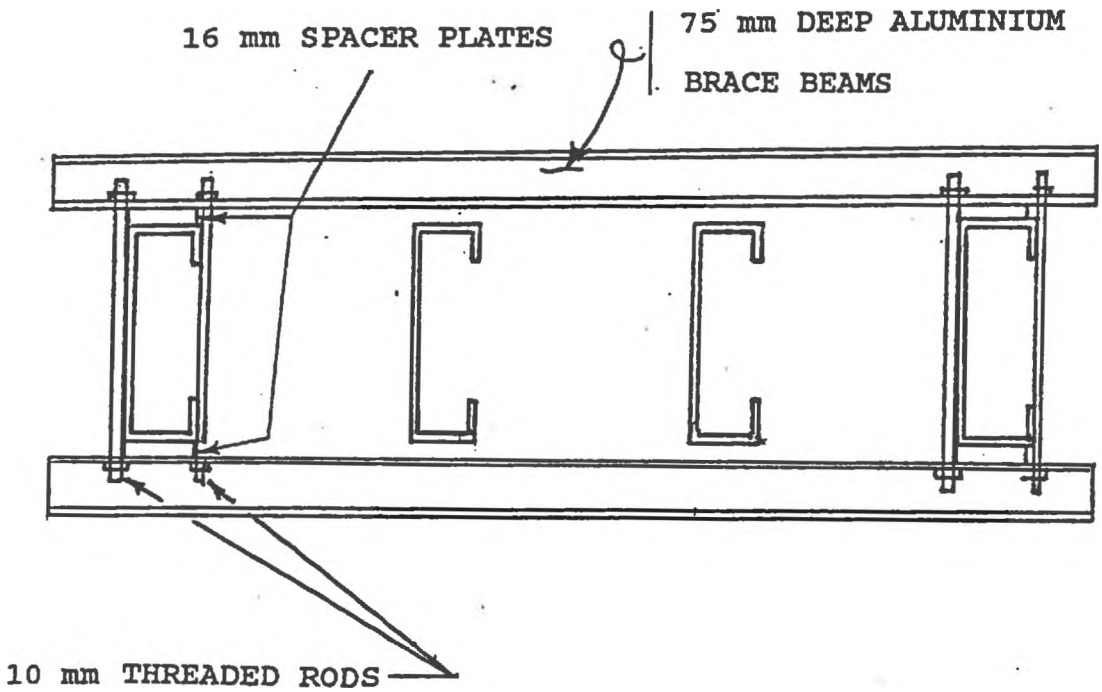

Figure 3.11 **Cross-Section of 4 Stud Specimen Showing Exterior Wall Stud Bracing**

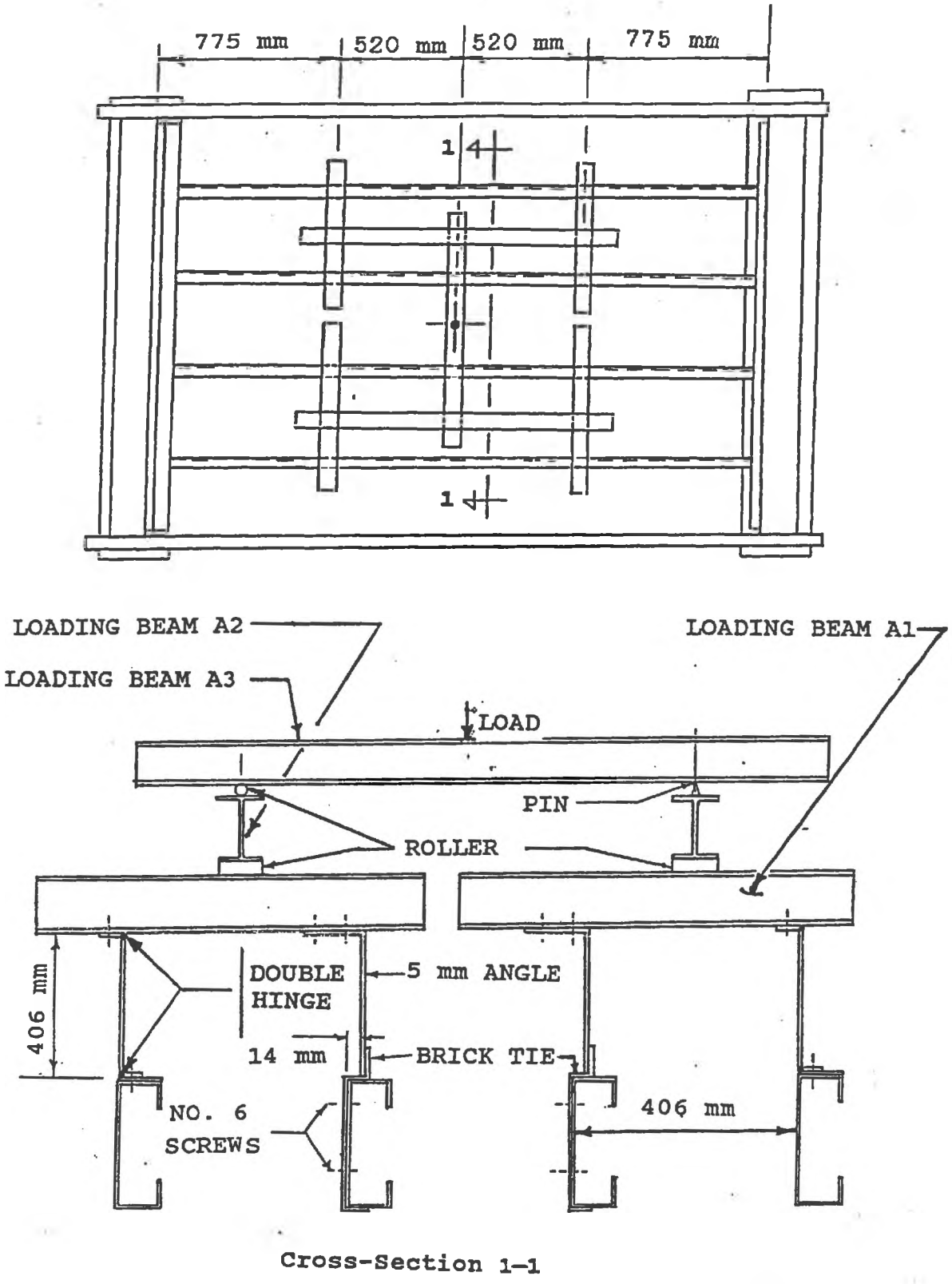

Figure 3.12 Test Setup for 4 Stud Backup Wall Specimen

transfer the load fron the head of the load cell to beam A3. This bar was centred and aligned vertically under the load cell.

One predrilled end of each line of bridging was fastened to the bridging displacement control rig. The small threaded rod that connected the end of the bridging to the sliding support was tightened snugly using the nuts shown in Figure 3.2. This effectively restrained the steel bridging from translating in the plane of the backup wall. The end of the bridging attached to the rig was however free to rotate since the bridging was effectively pinned at this attachment location. The final preparation step was to install the instrumentation used to measure the backup wall deflections and rotations.

The load cell was lowered by means of the hydraulic jack until light contact was made with the top of the vertical loading bar. The bar was aligned and plumbed vertically. The hydraulic jack was then used to apply load to the loading bar. This load was transformed into equal two point loading on each stud by the system of loading beams. At each load increment, the deflections of stud A, at the locations of the lines of bridging, were measured the ends of the lines of steel bridging fastened to the bridging displacement control rig were lowered by the same amount. Deflections and rotations were subsequently measured and recorded at all other locations either manually or by the data aquisition system. The load cell reading was also recorded. The backup wall was loaded until the load cell reading dropped and no further increase in load was achieved. The ultimate load was taken as the highest load recorded from the load cell prior to the load dropping off.

3.4.3.2 Two Stud Test Specimens

Two drilled 8 mm diameter expansion anchors spaced 455 mm on either side of the support track centreline were used to securely attach the top and bottom track to the test frame floor beams. The anchoring procedure was the same as for the four stud test. Brick ties were fastened to the studs at the loading points. Since large stud rotations were anticipated for

some of these tests, the loading system used in the four stud tests was considered unstable. The loading arrangement shown in Figure 3.13 was used.

The load cell was lowered by the hydraulic jack until light contact was made with the top of the loading bar. Next, the bar was aligned vertically. The hydraulic jack was used to apply load and at the end of each load increment, the loading bar was checked for shifts from its vertical position. Any shifting of the bar was due to the rotations by the studs causing the bottom of the loading bar to be displaced. Since the hydraulic jack was fastened to a sliding plate, the plate was adjusted. This moved the hydraulic jack and the top of the loading bar in the same direction as the displaced bottom of the bar. The plate was adjusted until the loading bar was vertical again. The next load increment was then applied. This procedure was repeated until failure occurred. At the end of each load increment, the midspan rotation of each stud was recorded.

3.5 TESTS OF STEEL STUD WALL PANELS

3.5.1 General Discussion

The particular details and special test conditions for each of the seven steel stud panel tests series are described in this section. A summary of the test results is also presented. In general, it was observed that the failure of a steel stud backup wall panel was initiated when one or more studs started to twist significantly. Failure of a stud was always observed to occur in the region around one or more web cutout holes. Visual examination of the panels immediately after testing indicated that no significant track flange deformation and/or stud web crippling occurred at the stud to track connections.

The failure loads for Series 1 through 7 are listed in Table 3.1. Each steel stud in a backup wall panel was loaded with two equal concentrated loads. For each test the value listed in Table 3.1 is the total load on one steel stud at failure. For comparison purposes, the results of each series the failure loads obtained for the 20 gauge backup wall specimens were divided

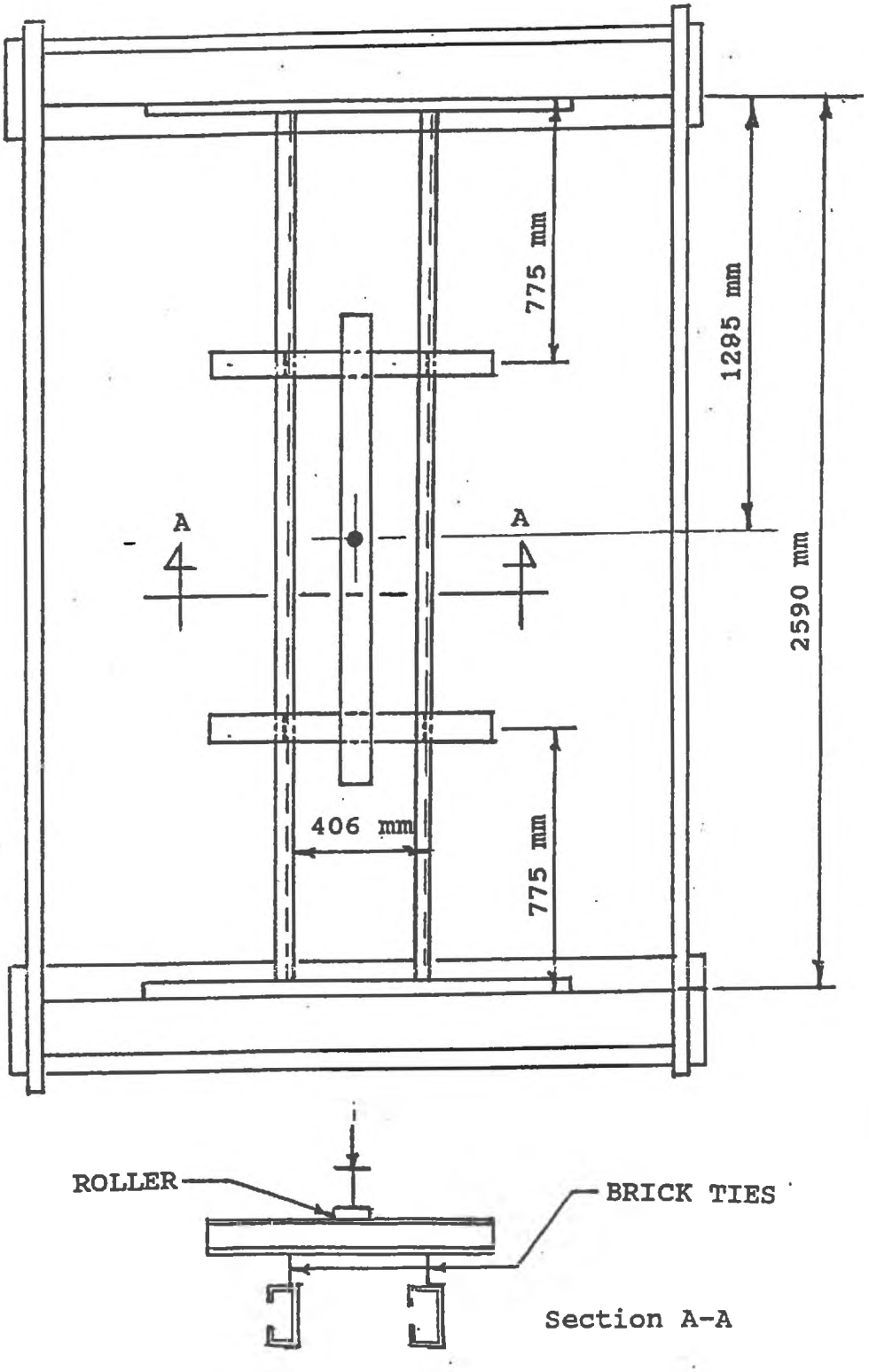

Figure 3.13 Test Setup for 2 Stud Backup Wall Specimen

TABLE 3.1 SUMMARY OF FAILURE LOADS PER STUD FOR WALL PANEL TESTS

Specimen No.	Failure Load P_{tot} (N)	P_{tot}/P_{avg}	Specimen No.	Failure Load P_{tot} (N)	P_{tot}/P_{avg}
1-BW-1	1796	0.64	6-BW-1	3428 *	
1-BW-2	1734	0.62	6-BW-2	3248 *	
1-BW-3	1718	0.61	6-BW-3	3376 *	
1-BW-4	1734	0.62	6-BW-4	5356 *	
1-BW-5	1734	0.62	6-BW-5	5616 *	
1-BW-6	1478	0.53	6-BW-6	5460 *	
1-BW-7	2352	0.84	6-BW-7	2708	0.97
1-BW-8	2400	0.86	6-BW-8	2970	1.06
1-BW-9	2050	0.73	6-BW-9	2708	0.97
1-BW-10	1920	0.69	6-BW-10	4370	0.96
2-BW-1	3770	0.83	6-BW-11	4644	1.02
2-BW-2	3730	0.82	6-BW-12	4604	1.01
2-BW-3	3778	0.83			
2-BW-4	4100	0.90	7-BW-1	3080	1.10
2-BW-5	3724	0.82	7-BW-2	2922	1.05
			7-BW-3	3350	1.19
3-BW-1	3628	0.80	7-BW-4	3112	1.11
3-BW-2	3590	0.79	7-BW-5	2276 **	0.81
			7-BW-6	4084	0.90
4-BW-1	2700	0.96	7-BW-7	4834	1.06
4-BW-2	3962	0.87			
5-BW-1	1196	0.26			
5-BW-2	1230	0.26			
5-BW-3	1196	0.28			
5-BW-4	1462	0.32			
5-BW-5	1456	0.32			
5-BW-6	1512	0.33			

* 4 Point Load Beam Tests

** Wetted Exterior Drywall Test

by the average failure load obtained from the results of the 20 gauge beam tests 6B-BW-7 to 6B-BW-9. The failure loads for the 18 gauge backup wall specimens were treated in a similar manner using the results of beam tests 6B-BW-10 to 6B-BW-12. The results are shown in Table 3.1. Results are not shown for tests 6A-BW-1 to 6A-BW-6 since in these tests the steel studs were loaded with four concentrated loads and a direct comparison could not be made using the above procedure. A more detailed analysis of the failure loads is presented in Chapter 4.

3.5.2 Series No. 1

3.5.2.1 Details Of Panels

In this series, ten 4 stud wide wall panels were fabricated with 20 gauge studs. The first five panels, specimens 1-BW-1 to 1-BW-5, were braced at midspan with 38.1mm x 12.7mm x 1.14mm interior type steel bridging channels. As shown in Figure 3.14, the bridging was inserted through the midspan stud web cutout hole and fastened to the web of each stud with a 16 gauge clip angle and four number 8 self drilling screws. Specimen 1-BW-6 was identical to the first five except that only two screws were used in the connection. For specimens 1-BW-7 and 1-BW-8, two lines of interior steel bridging were used. Each line of bridging was inserted into the cutout holes at the quarter points and then attached to the studs in a manner similar to the first five tests specimens. The last two specimens (1-BW-9 and 1-BW-10) were fabricated identically to the first five specimens except that 12 mm thick interior gypsum board sheathing was also attached to the studs as shown in Figure 3.15.

3.5.2.2 Special Test Conditions

For this series the test procedure outlined in Section 3.4.3.1 was followed.

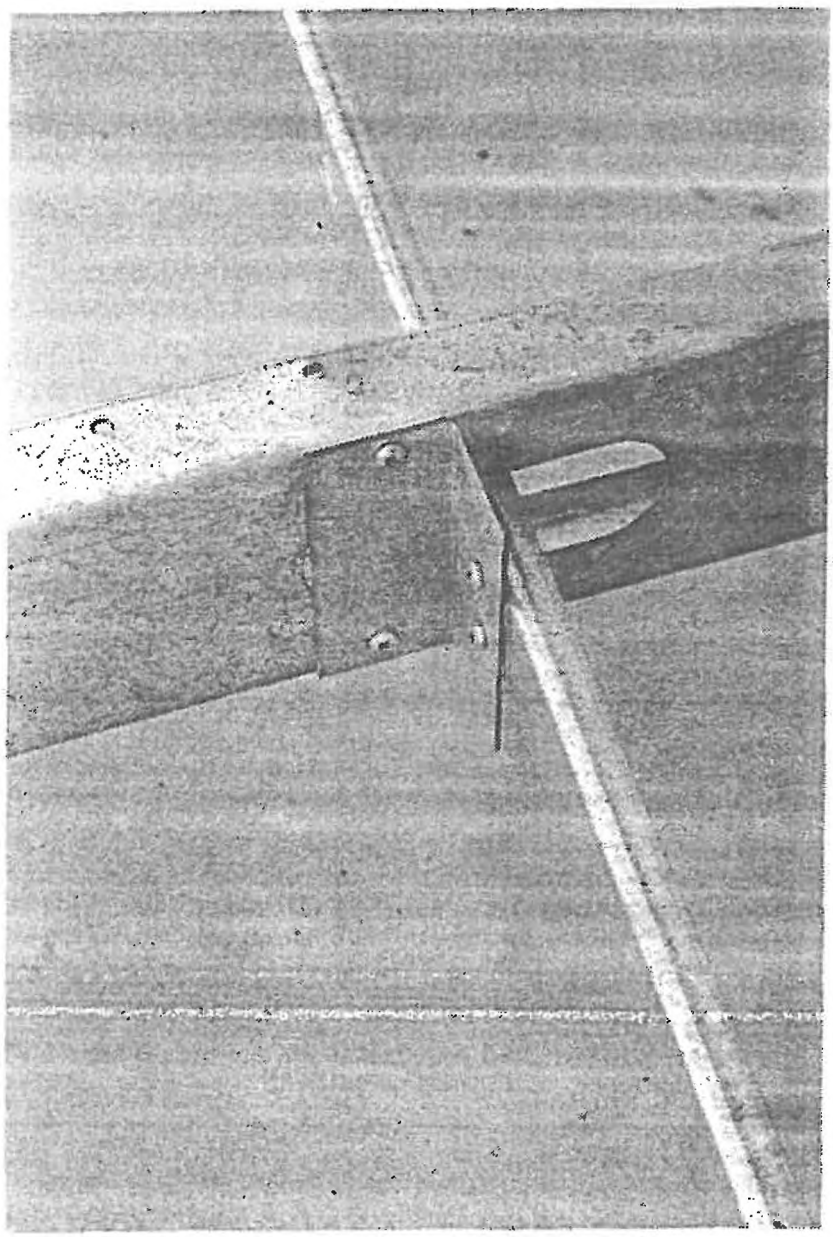

Figure 3.14 Photograph of Typical Clip Angle Bridging Connection Used in Test Program

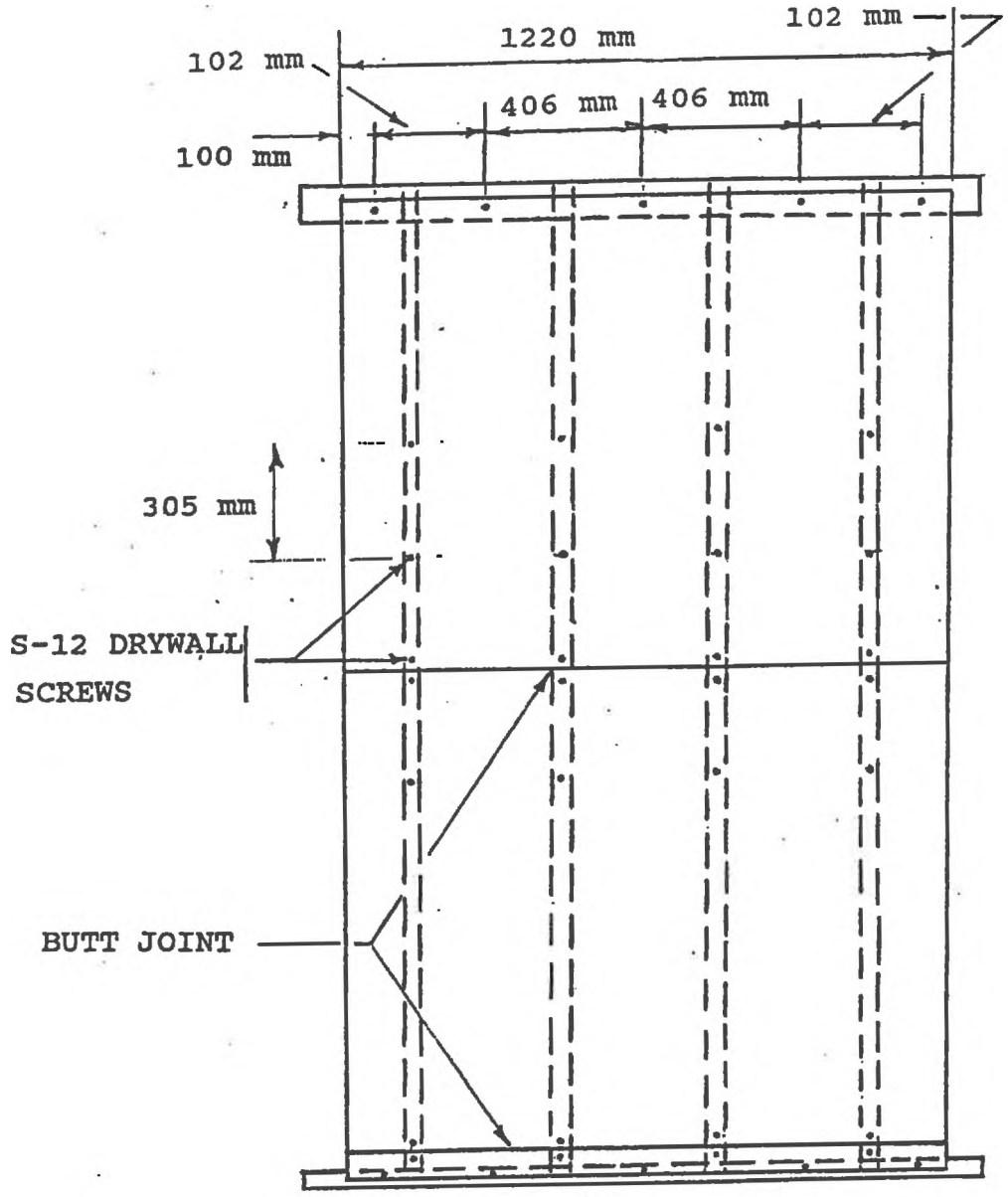

Figure 3.15 Typical 4 Stud Panel Showing Screw Locations for Interior Drywall Sheathing

3.5.2.3 Results Of Tests

Plots of Load versus Displacements and Rotations are shown in Figures 3.16A to 3.16G. In each figure, the top and bottom out-of-plane translation and the midspan deflection are shown for interior studs. Although, rotation readings were taken at the three locations described in Section 3.4.2.6, only the rotations at the location where the largest recorded rotation occurred were shown in the figures for each interior stud.

For the first five tests, as can be seen in Figure 3.16A to 3.16E, the midspan deflections of the interior studs are practically identical for each load increment plotted and are approximately linear up to load levels which caused approximately an L/180 midspan deflection. Any slight non-linearity was mostly due to the stud end translations.

In Figure 3.16A, the deflections shown for the top of the second interior stud is doubtful. Although it is included, it was probably due to a malfunction of the potentiometer at this location. The stud end deflection readings are generally linear. It was also noted that the top stud ends deflections recorded at the top nested track connections were greater than the readings recorded at the stud ends at the bottom track connection. Although the results from the steel stud to track connection tests had indicated that the deflections at the top nested track detail would be greater than at the bottom stud to track connection, the difference in deflections obtained in this phase of the test program were much greater than anticipated. Remeasurement of the spacing between the top and bottom floor beams of the test frame revealed that the beams had been spaced 4 to 5 mm further apart than had been planned. This in effect created a top movement gap of 16 to 17 mm instead of the intended 12 mm gap. This additional gap effectively reduced the top track connection stiffness and allowed more movement at this location.

The maximum stud rotations were not linear and increased rapidly as the load approached failure. The maximum stud rotation always occurred near one of the load points which were located between the midspan brace and the supports. For test 1-BW-5, the recorded stud rotation of the second interior stud shown in Figure 3.16(E), was larger than in

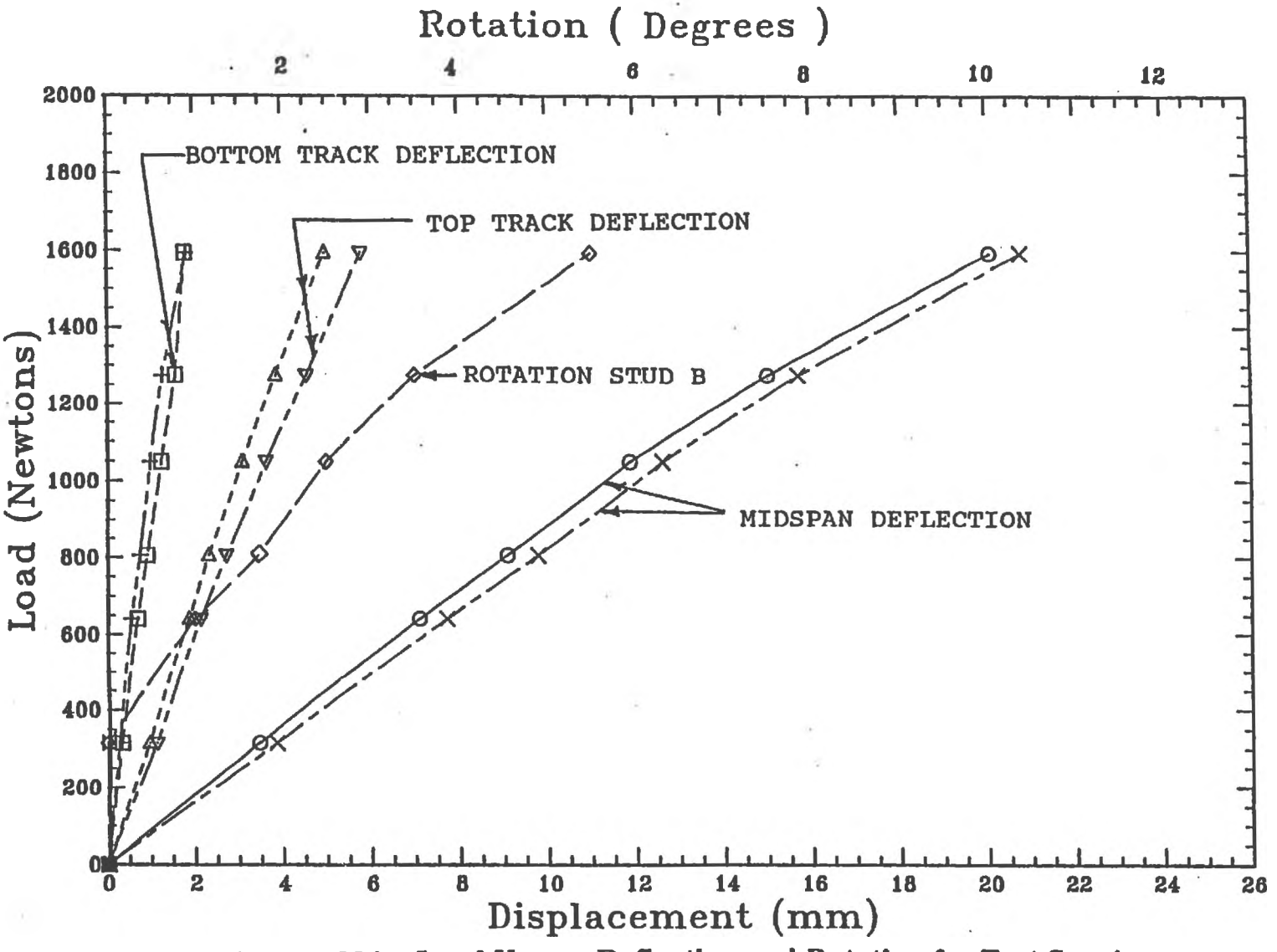

Figure 3.22A Load Versus Deflection and Rotation for Test Specimen 3-BW-1

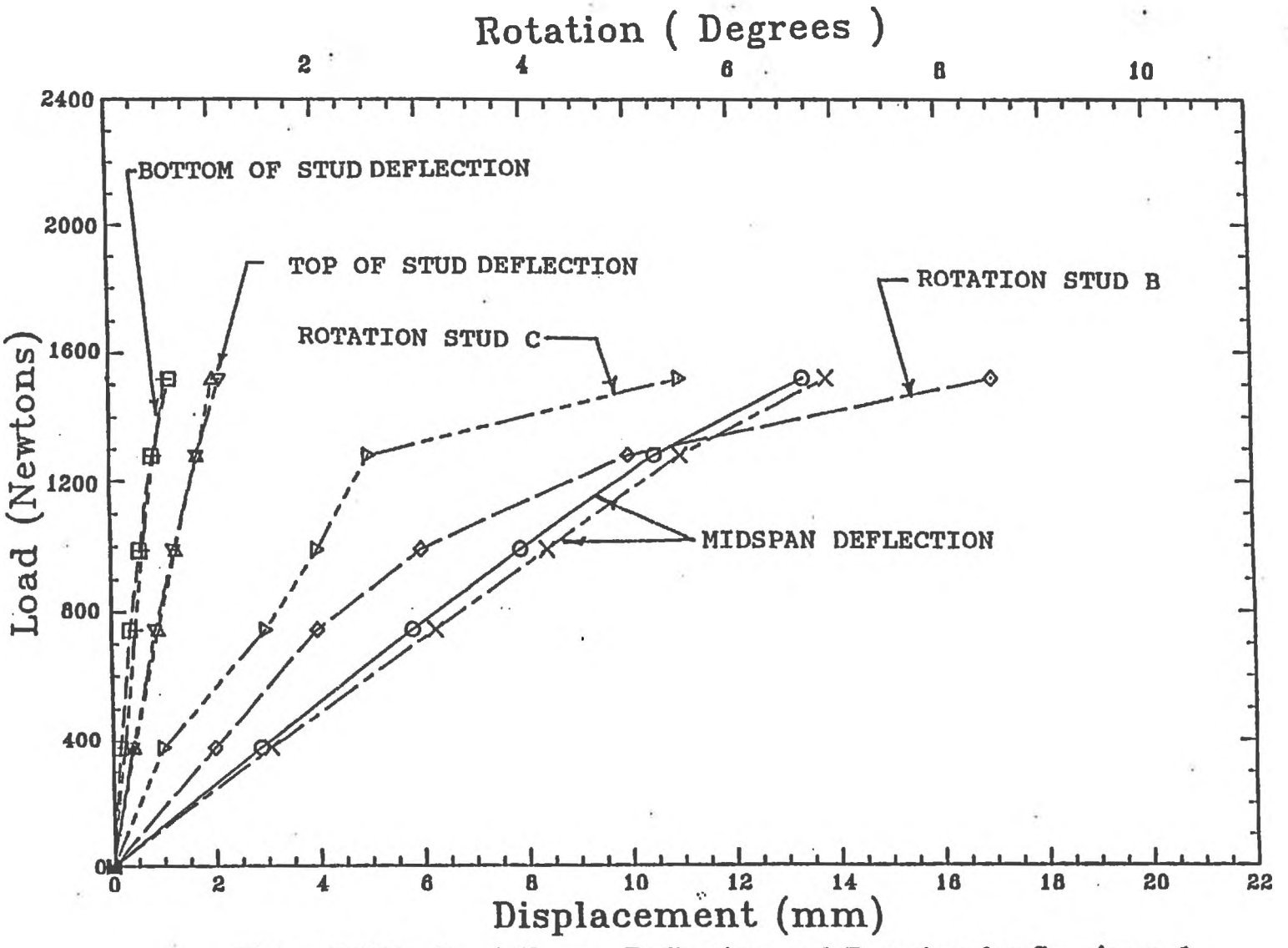

Figure 3.16B Load Versus Deflection and Rotation for Specimen 1-BW-2

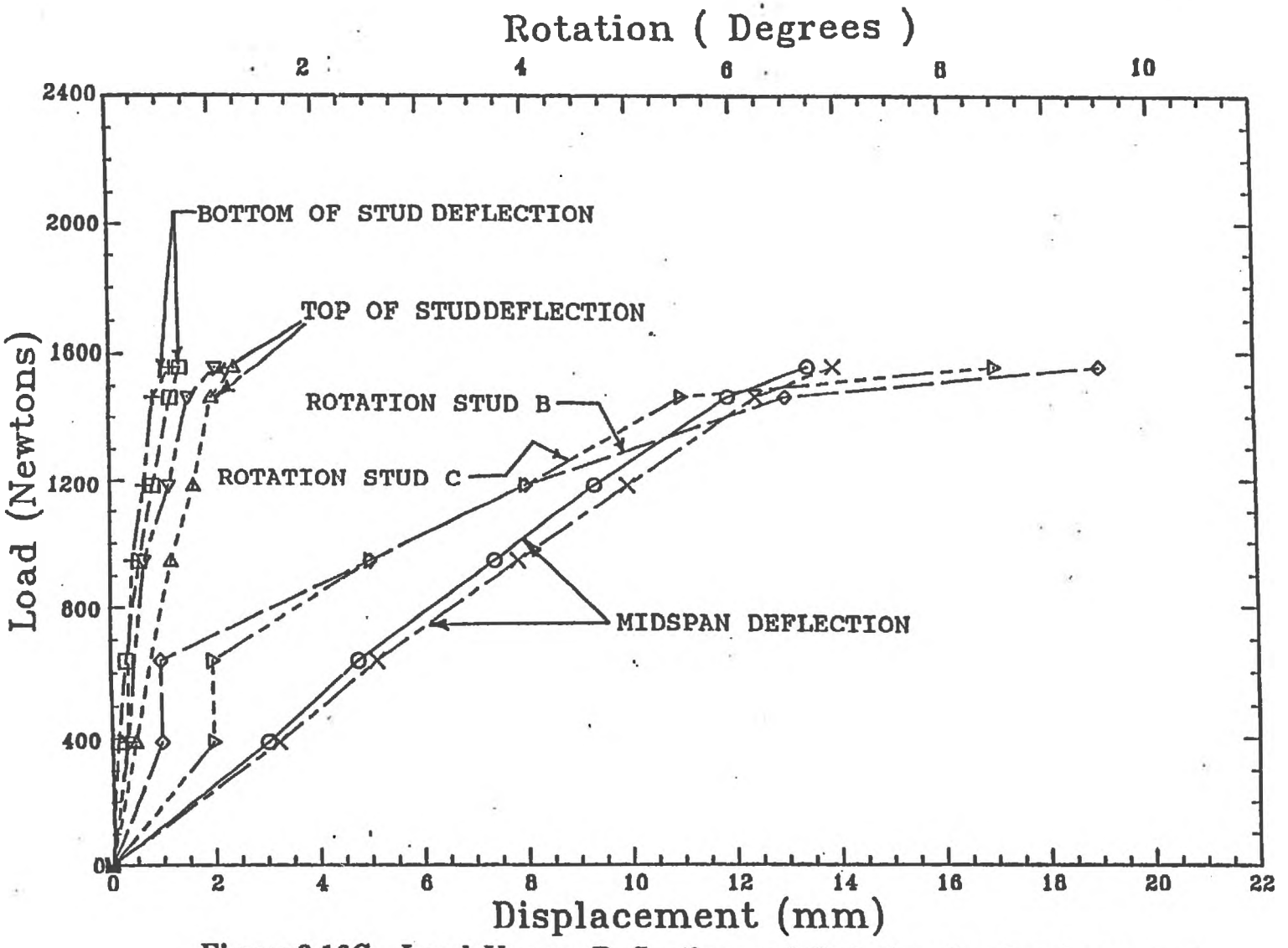

Figure 3.16C Load Versus Deflection and Rotation for Specimen 1-BW-3

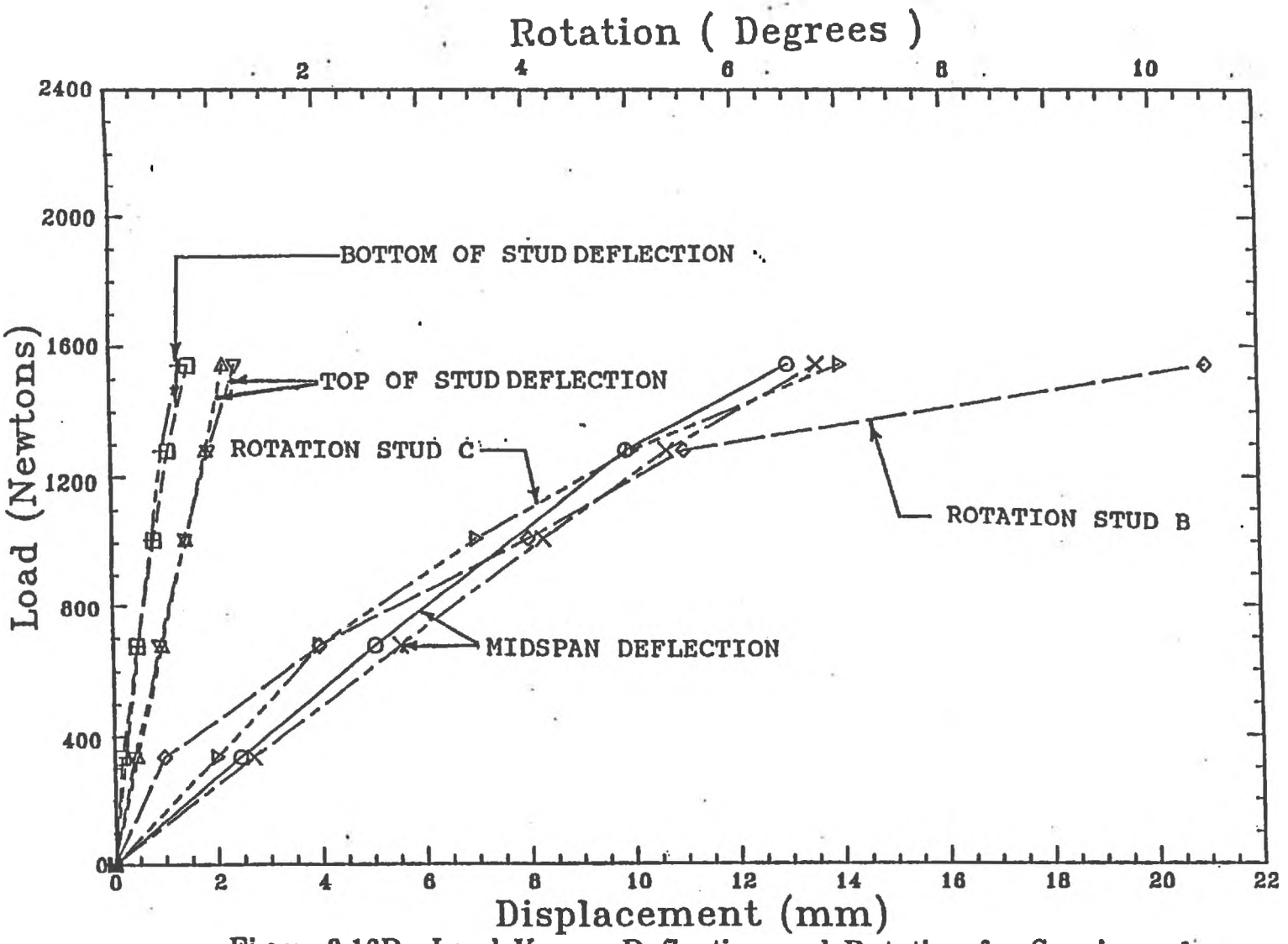

Figure 3.16D Load Versus Deflection and Rotation for Specimen 1-BW-4

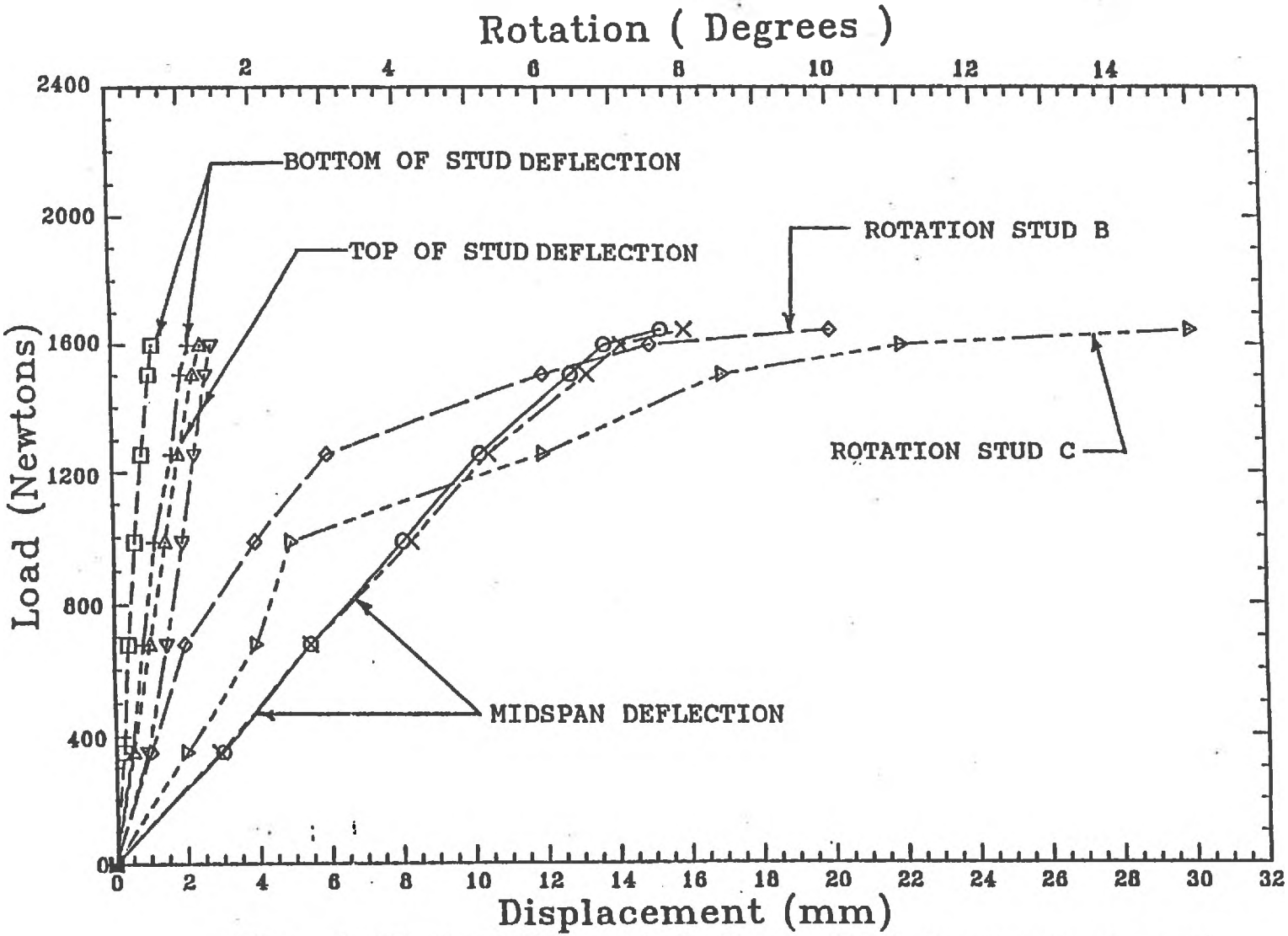

Figure 3.16E Load Versus Deflection and Rotation for Specimen 1-BW-5

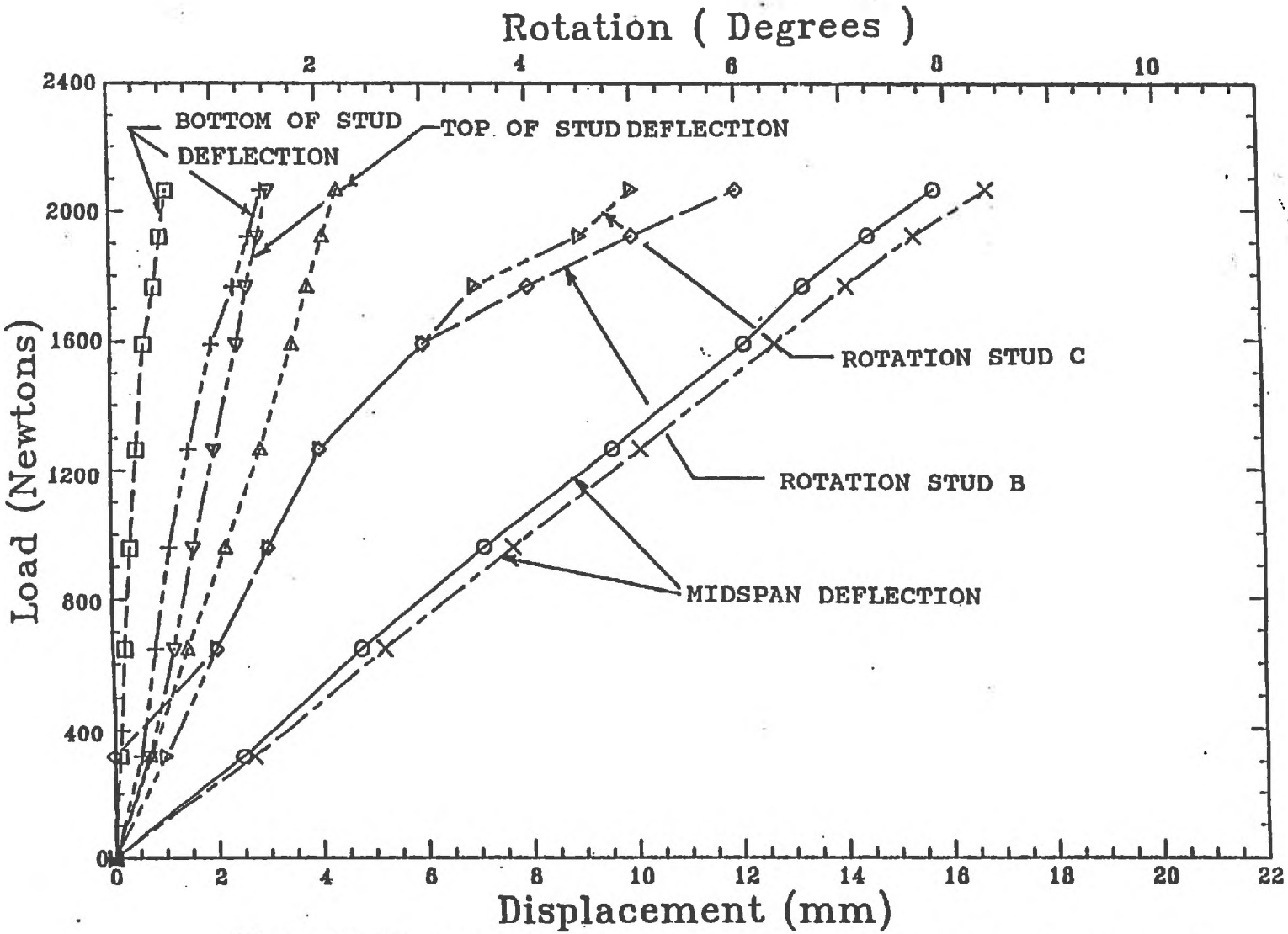

Figure 3.16F Load Versus Deflection and Rotation for Specimen 1-BW-7

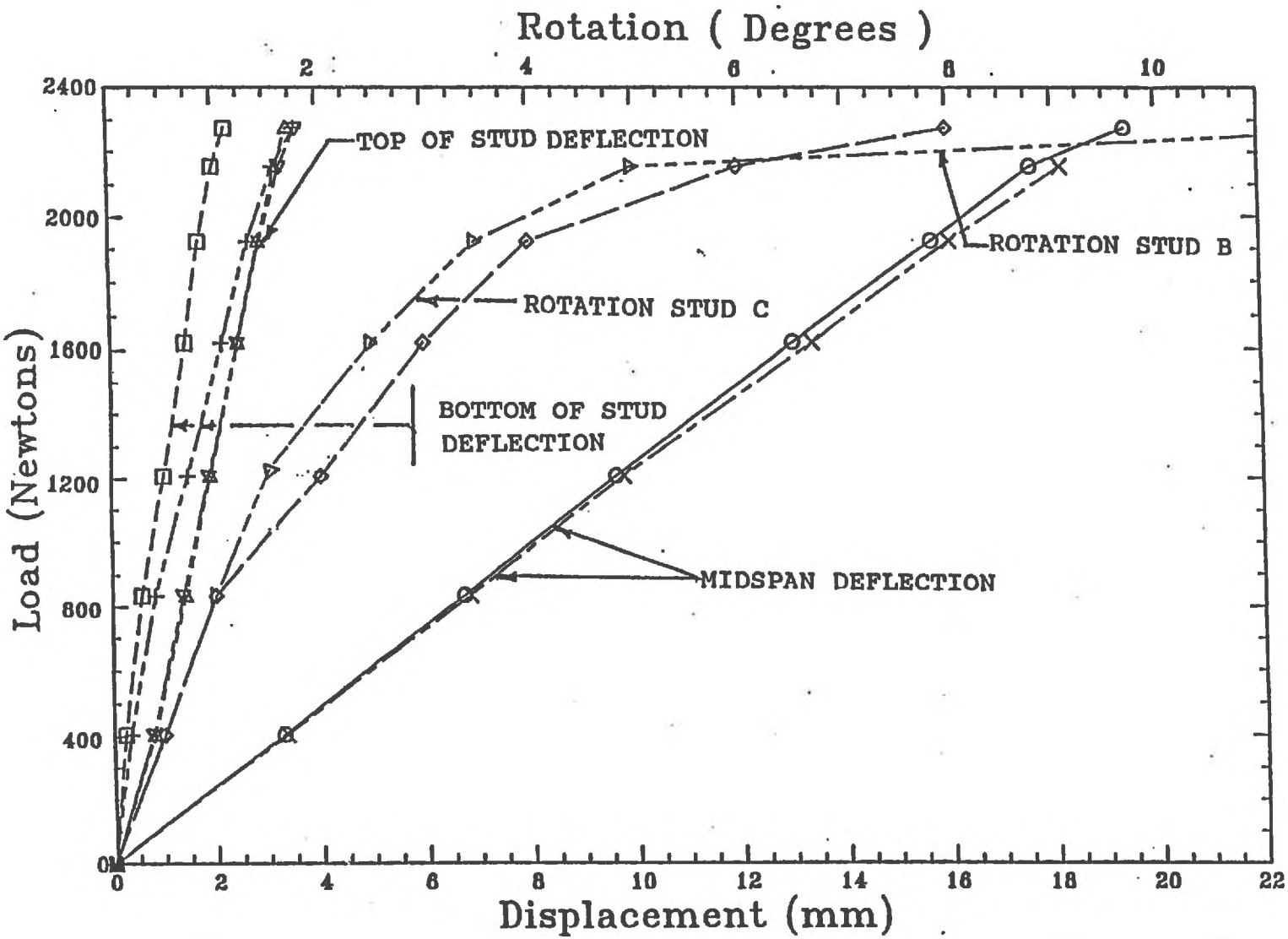

Figure 3.16G Load Versus Deflection and Rotation for Specimen 1-BW-8

the first four tests of this series. Visual examination of the panel after the test was completed, revealed that the screws which connected the stud web to the midspan steel bridging clip were loose. This was attributed to improper installation of the screw.

Although not shown, the maximum rotation obtained in test 1-BW-6 was significantly more than for the interior studs of in the previous tests. Since only two screws had been used to connect the steel stud to the bridging, instead of four used in the previous tests, it was apparent that this resulted in a more flexible connection which allowed greater rotation of the steel stud.

For tests 1-BW-7 and 1-BW-8, the midspan stud deflections shown in Figures 3.16G and 3.16H, were also approximately linear. In both these tests, some track anchorage slip occurred at the bottom track. This slippage in both tests caused the recorded stud end deflections of the second interior studs to be greater than would normally be expected. Unlike the previous tests in this series, the maximum recorded stud rotations occurred at midspan. This was due to the fact that the lines of steel bridging were located at the quarter points and not at the midspan, as in the previous tests.

For tests 1-BW-9 and 1-BW-10, equipment failure occurred and no deflection data was obtained.

3.5.2.4 Description Of Failures

Failure was initiated in the region of one or more stud web cutout holes located between the centre line of bridging and the support tracks. For panels 1-BW-1, 1-BW-2, 1-BW-4 and 1-BW-5 buckling at the cutout hole located approximately midway between the centre line of the steel bridging and bottom track for one interior stud was visible after failure. For test 1-BW-5, some local buckling was observed on the compression flange of interior stud "C1" at the steel bridging location. However, it is not known if this localized failure occurred simultaneously or shortly after the failure at the cutout hole location. A typical local buckle in

a stud is shown in Figure 3.17. This type of failure was observed to have occurred in all of the above tests.

For test 1-BW-6, two screws were used to fasten the midspan line of bridging to each stud in the panel instead of the four used in the previous tests. During the test it was observed that for a given level of applied load, both interior studs rotated significantly more than the interior studs of the first five specimens. Near the end of the test it was noted that the interior studs had rotated enough to cause the exterior lips of the top flanges to come into contact with the top flange of the interior midspan bridging. At failure, a simultaneous collapse of the interior studs in the region of the web cutout holes located midway between the top track and the line of bridging was observed. The top flange lips of the interior studs were permanently damaged at the location where each stud had made contact with the steel bridging.

For specimen 1-BW-7 failure occurred in the region of the midspan web cutout hole of both interior studs. The photograph in Figure 3.18 illustrates this failure. The picture was taken after the system of loading beams had been removed and the ends of the bridging had been unfastened from the bridging displacement control rigs. Specimen 1-BW-8 failed in a similar manner.

For test specimens 1-BW-9 and 1-BW-10, simultaneous failure of both interior studs occurred in both tests. Each stud buckled in the region of the web cutout hole located midway between the midspan line of bridging and the bottom track. It was also noted that these studs exhibited significant local top flange buckling in the region of the midspan line of steel bridging.

3.5.3 Series No. 2

3.5.3.1 Details Of Panels

Five 4 stud wide 18 gauge wall panels were fabricated in this series. Specimens 2-BW-1 to 2-BW-3 were braced at midspan with a line of exterior and interior 16 gauge face bridging. This type of bridging consisted of a 38.1mm x 19mm x 1.45mm channel, knotched 406 mm on

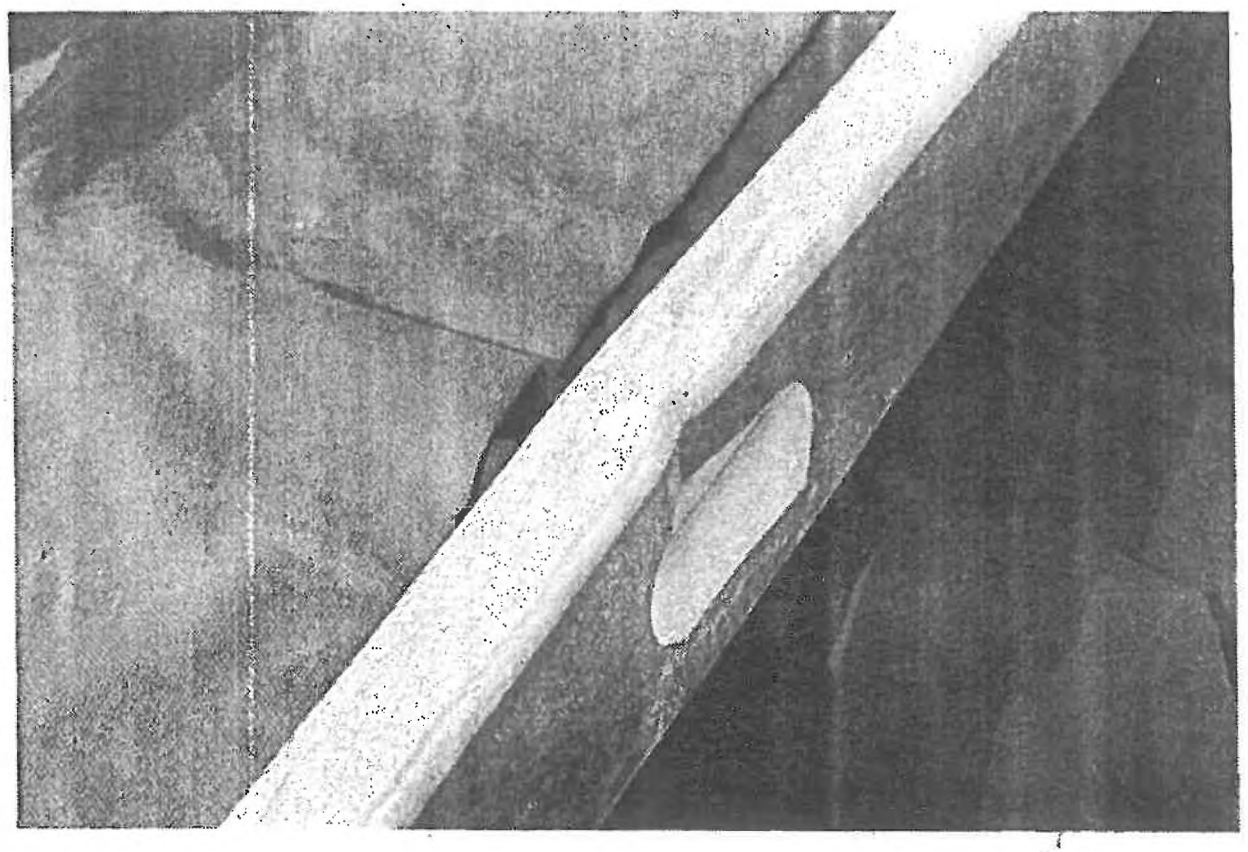

Figure 3.17 **Photograph of Typical Local Buckling Failure of Interior Steel Stud - Series 1**

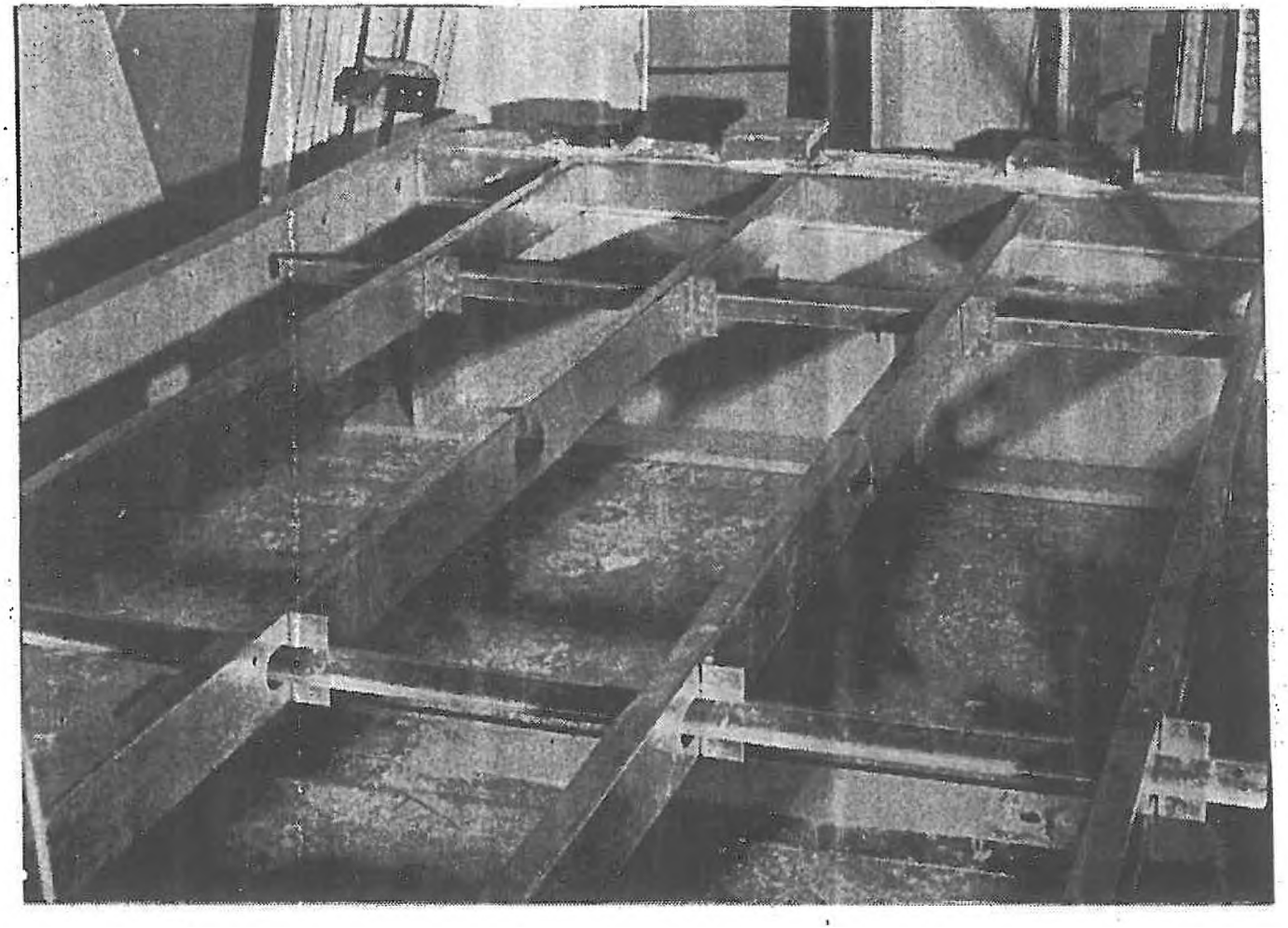

Figure 3.18 **Photograph of Local Buckling of the Two Interior Steel Studs of Specimen 1-BW-7**

centre. The bridging was fastened to the exterior and interior stud flanges with a Number 8 Tek self drilling screw. A typical panel is shown in Figure 3.19. Also shown in this Figure are the two lines of additional exterior stud bracing. The remaining two wall panels, 2-BW-4 and 2-BW-5, were braced at the quarter points with a line of face bridging attached to the exterior and interior flanges of the studs, in a manner similar to the first three specimens of this series.

3.5.3.2 Special Test Conditions

In this series the test procedure outlined in Section 3.4.3.1 was followed.

3.5.3.3 Results Of Tests

Plots of the Load versus Displacement and Rotations are shown in Figures 3.20A to 3.20E. As in Series 1, each figure shows the top and bottom displacement and midspan deflections for each interior stud. The midspan deflections were linear and roughly identical for each load increment.

The top and bottom stud end deflections were also approximately linear. In each of the first three tests the bottom track deflections shown in curves 1 and 2 in Figures 3.20A to 3.20C were practically identical. The top track deflections shown by curves and were also similar for these tests. In test 2-BW-4, the top end of each interior steel stud deflected by a different amount. This is shown in Figure 3.20D. The explanation was that the deflection gap in the nested top track connection was found to be non-uniform. In test 2-BW-5, some bottom track anchorage slip occurred which caused the deflection of the second interior stud to be greater than anticipated.

3.5.3.4 Description Of Failures

Failure of specimen 2-BW-1 was signalled by the local buckling of interior stud "B" in the region of the web cutout hole located approximately 940 mm from the top track. Similarly,

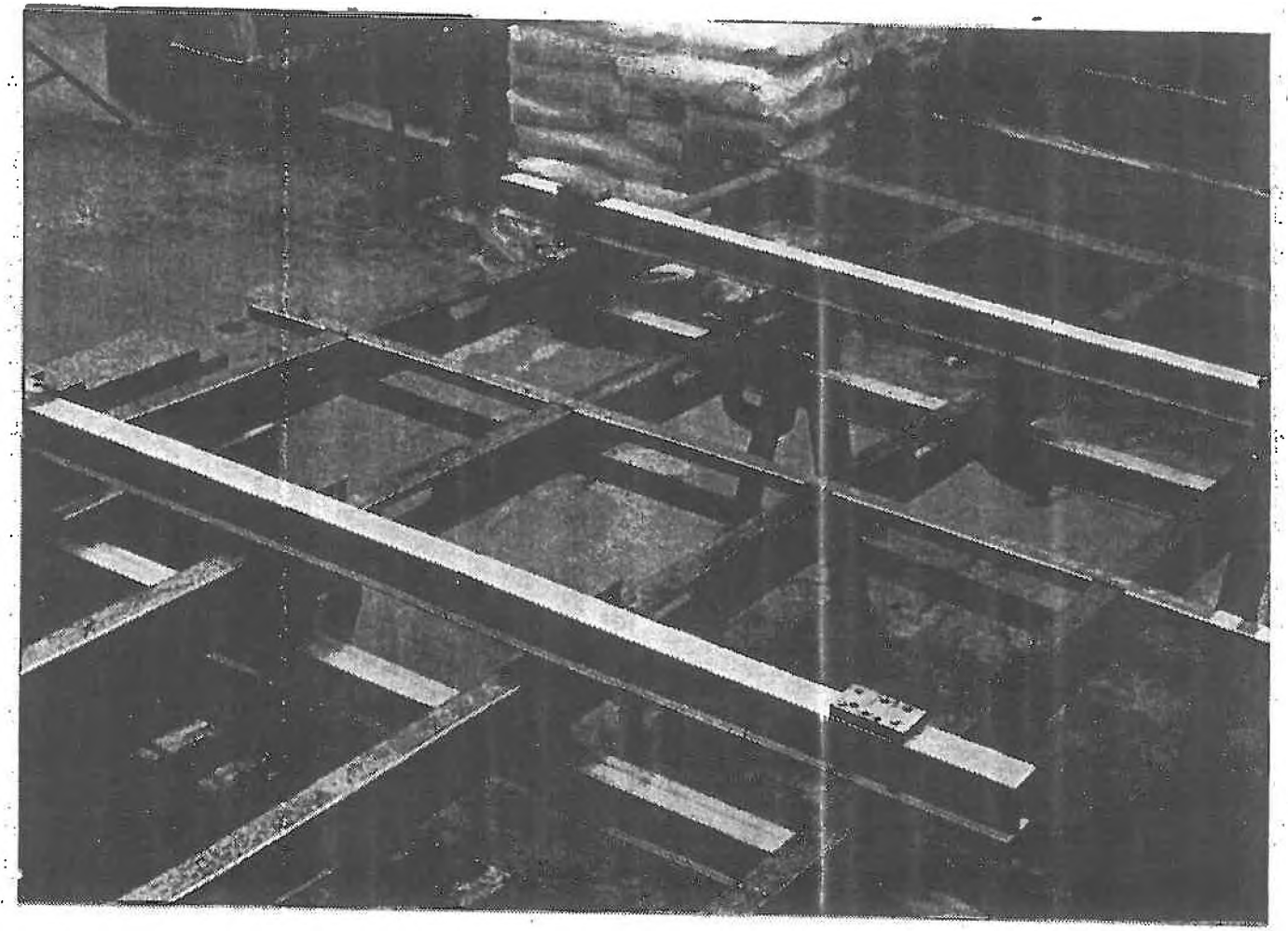

Figure 3.19 Photograph of 18 Gauge, 90 mm 4 Stud Test Specimen

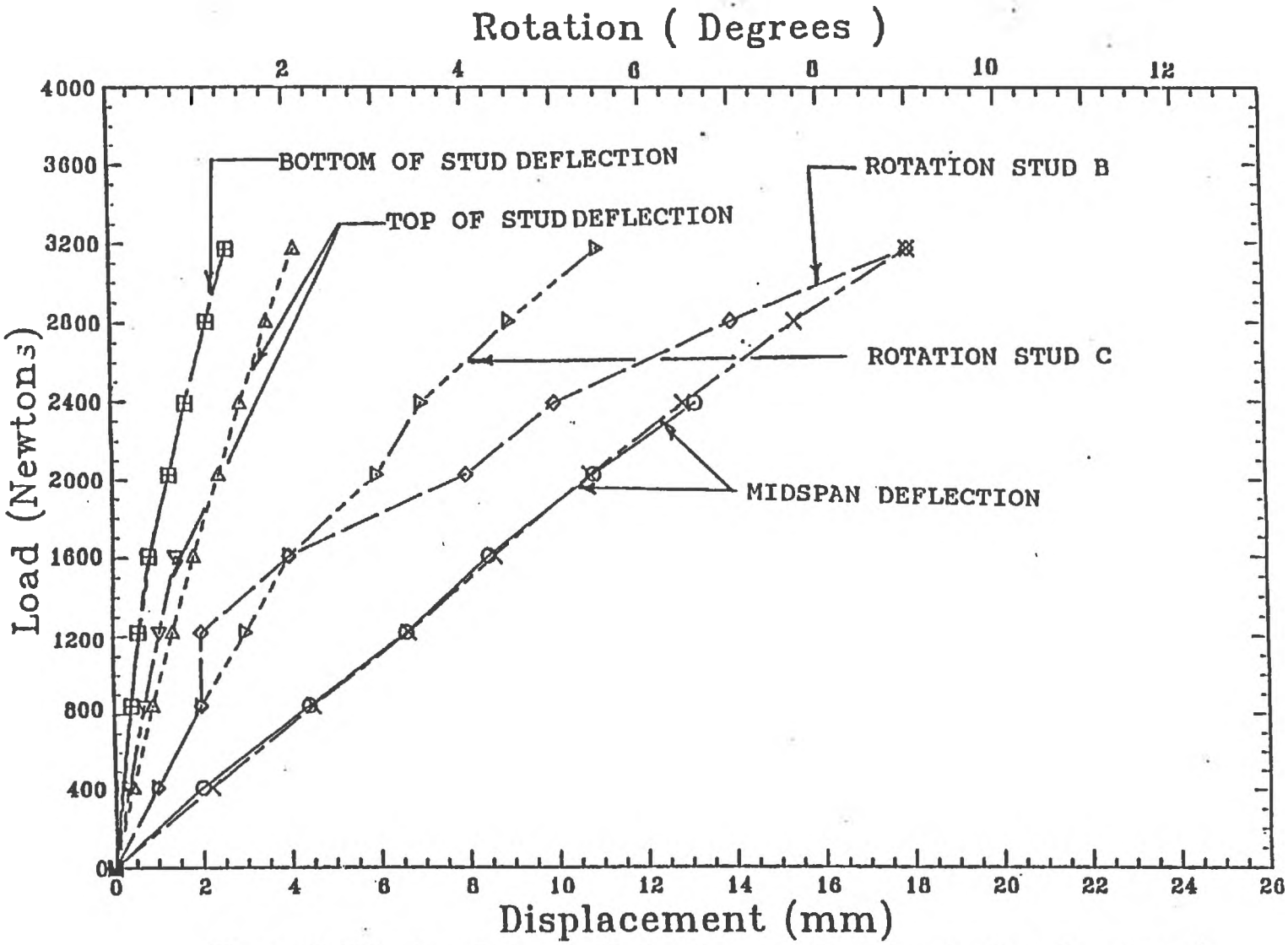

Figure 3.20A Load Versus Deflection and Rotation for Test Specimen 2-BW-1

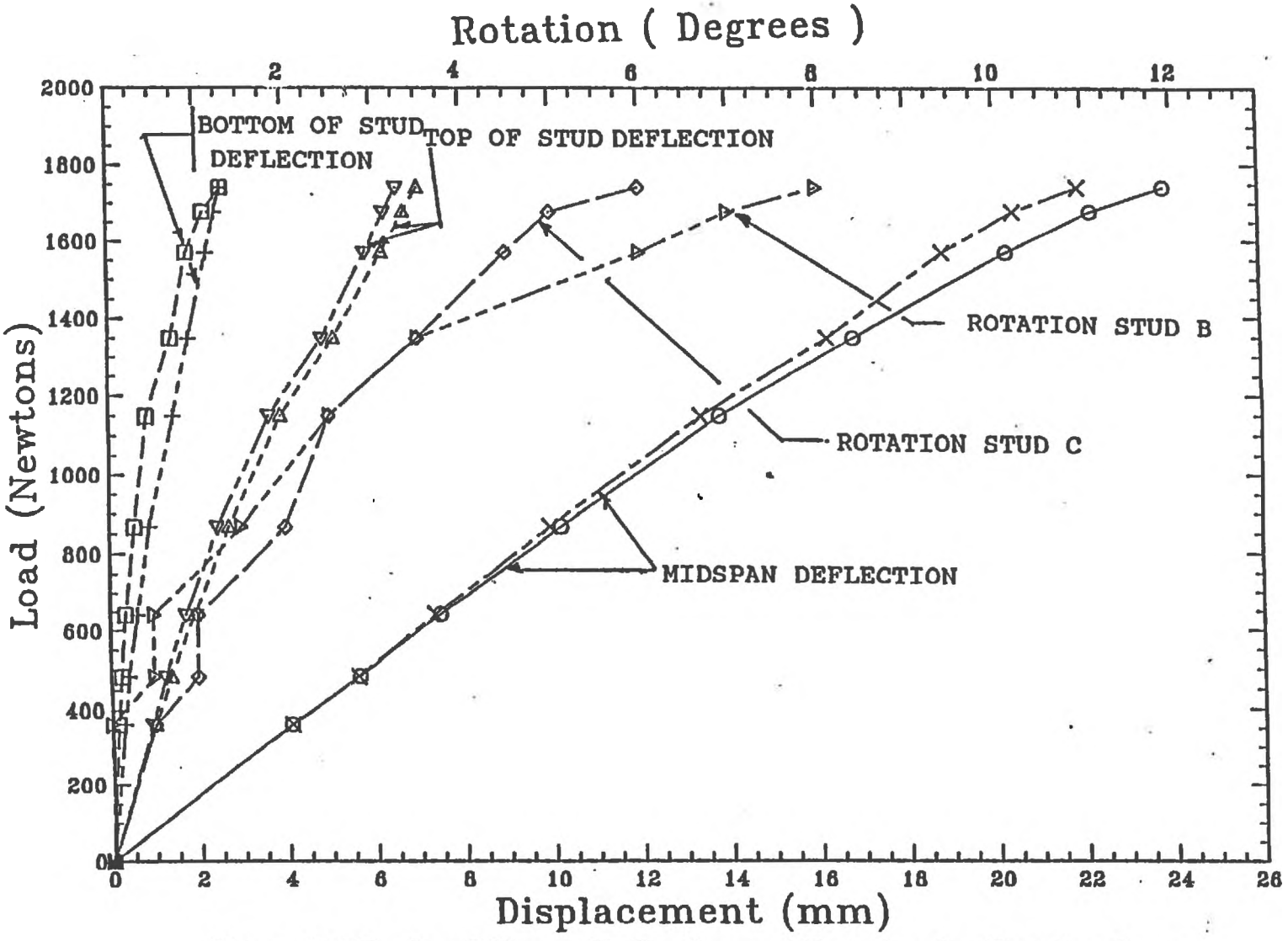

Figure 3.20B Load Versus Deflection and Rotation for Test Specimen 2-BW-2

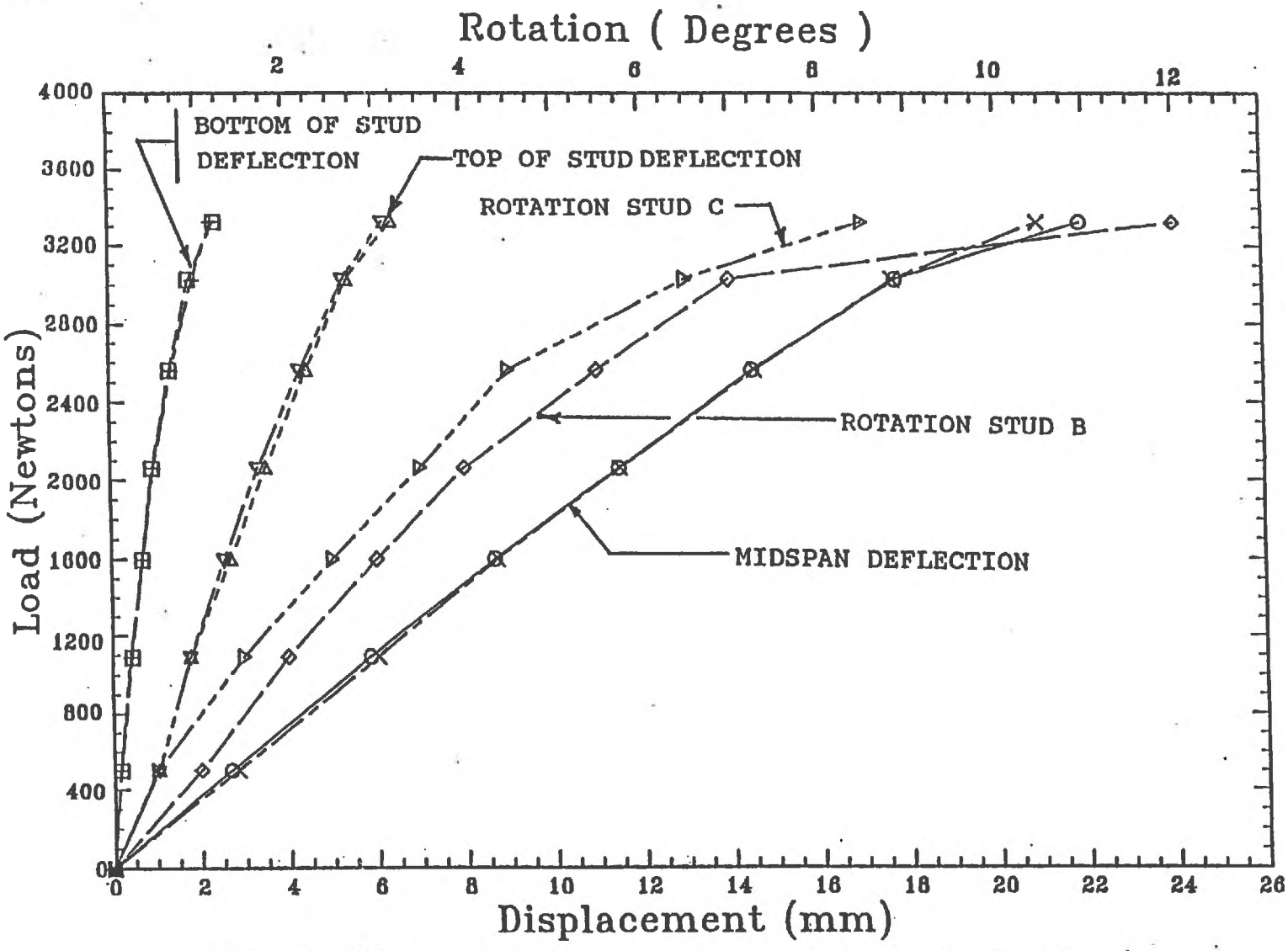

Figure 3.20C Load Versus Deflection and Rotation for Test Specimen 2-BW-3

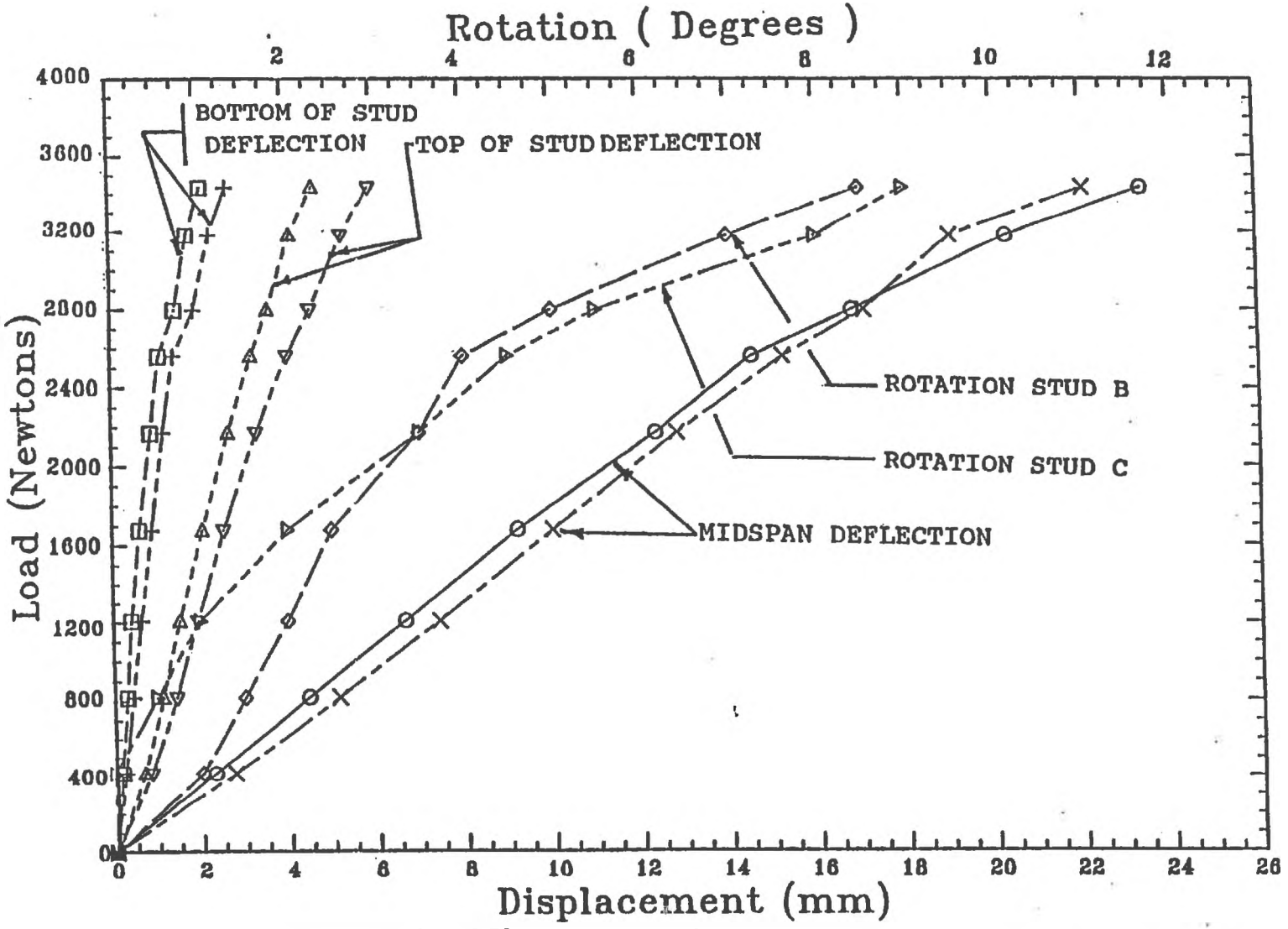

Figure 3.20D Load Versus Deflection and Rotation for Test Specimen 2-BW-4

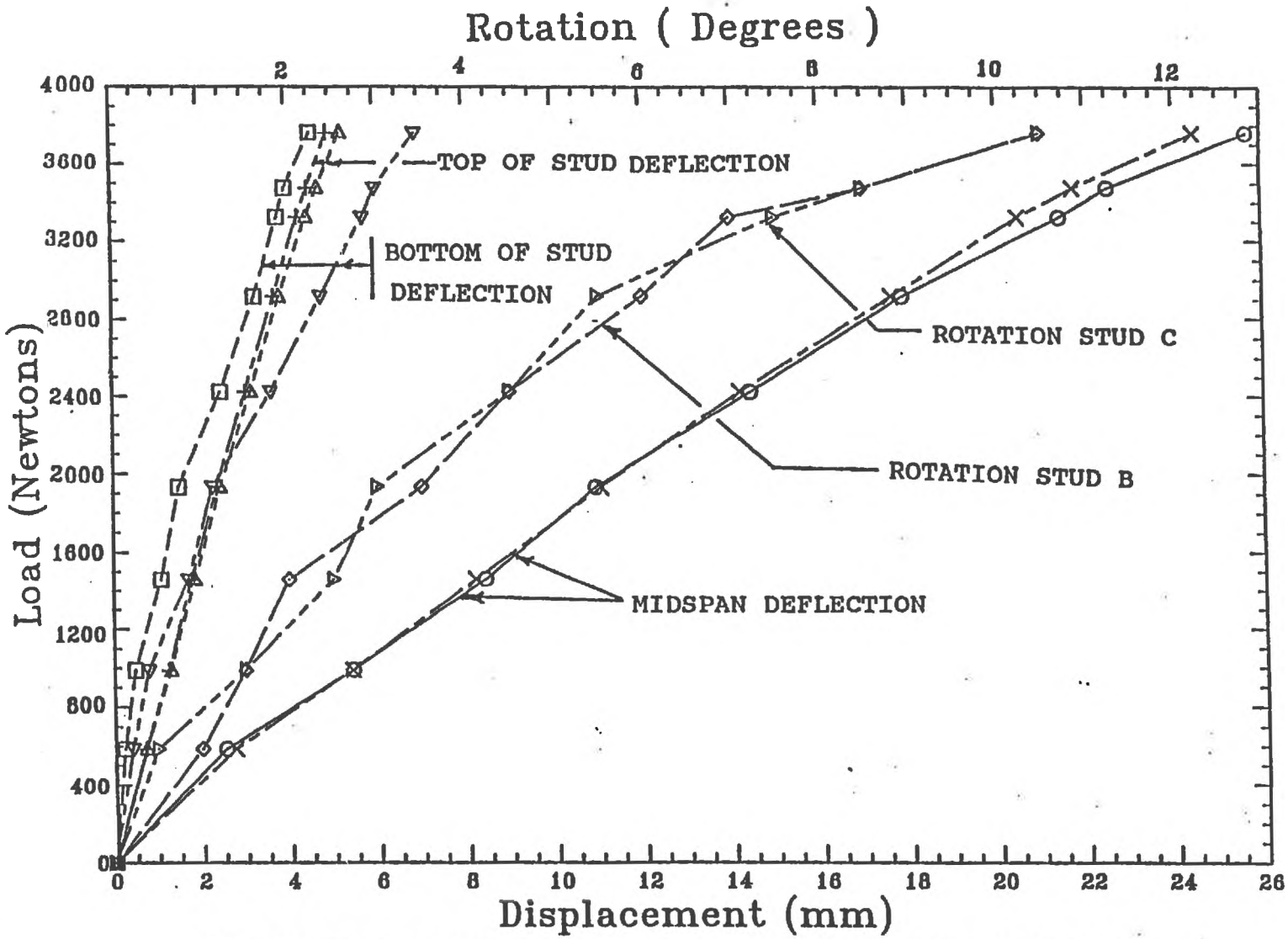

Figure 3.20E Load Versus Deflection and Rotation for Test Specimen 2-BW-5

for specimens 2-BW-2 and 2-BW-3 local failure of interior stud "B" occurred in the region of the web cutout located approximately 940 mm from the bottom track.

For specimen 2-BW-4, simultaneous local buckling of interior stud,"B", and one of the exterior studs occurred. Each stud failed locally in the region of the web cutout hole located 940 mm from the bottom track. Specimen 2-BW-5 has a similar failure pattern.

3.5.4 Series No.3

3.5.4.1 Details Of Panels

Series 3 consisted of two 4 stud wide 18 gauge wall panels braced at midspan with interior steel bridging. The bridging was attached to each stud with 16 gauge clip angles welded to each stud as shown in Figure 3.21.

The 18 gauge studs used in this series differed from the standard 18 gauge studs shown in Figure 3.3(b) since the web cutout holes were located as shown in Figure 3.3(a).

3.5.4.2 Special Test Conditions

The test procedure used in this series was identical to that outlined in Section 3.4.3.1.

3.5.4.3 Results Of Tests

The Load versus Displacement and Rotations plots for the two tests in this series are shown in Figures 3.22A and 3.22B. As in the other series the midspan deflection of each interior stud, curves 1 and 2, are nearly identical and linear for each load increment. For test 3-BW-1 only the rotations for interior stud "B" is plotted because the rotation measurement devices for interior stud "C" did not function properly. The stud rotations are shown by curves 3 and 4. For both tests, some track slippage occurred which caused the top and bottom stud end displacements to be different.

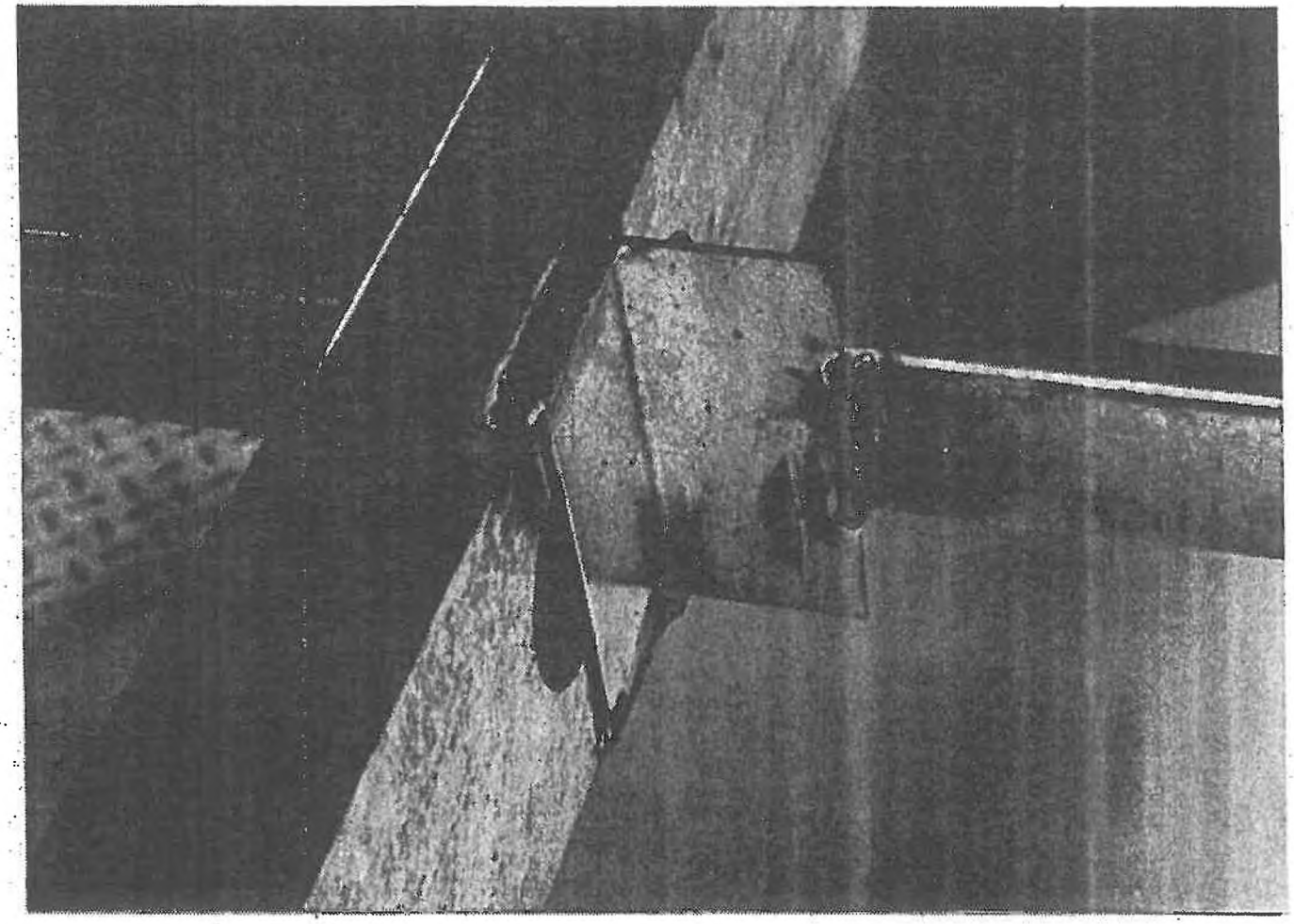

Figure 3.21 **Photograph of Welded Clip Angle Steel Bridging Connection Used in Test Program**

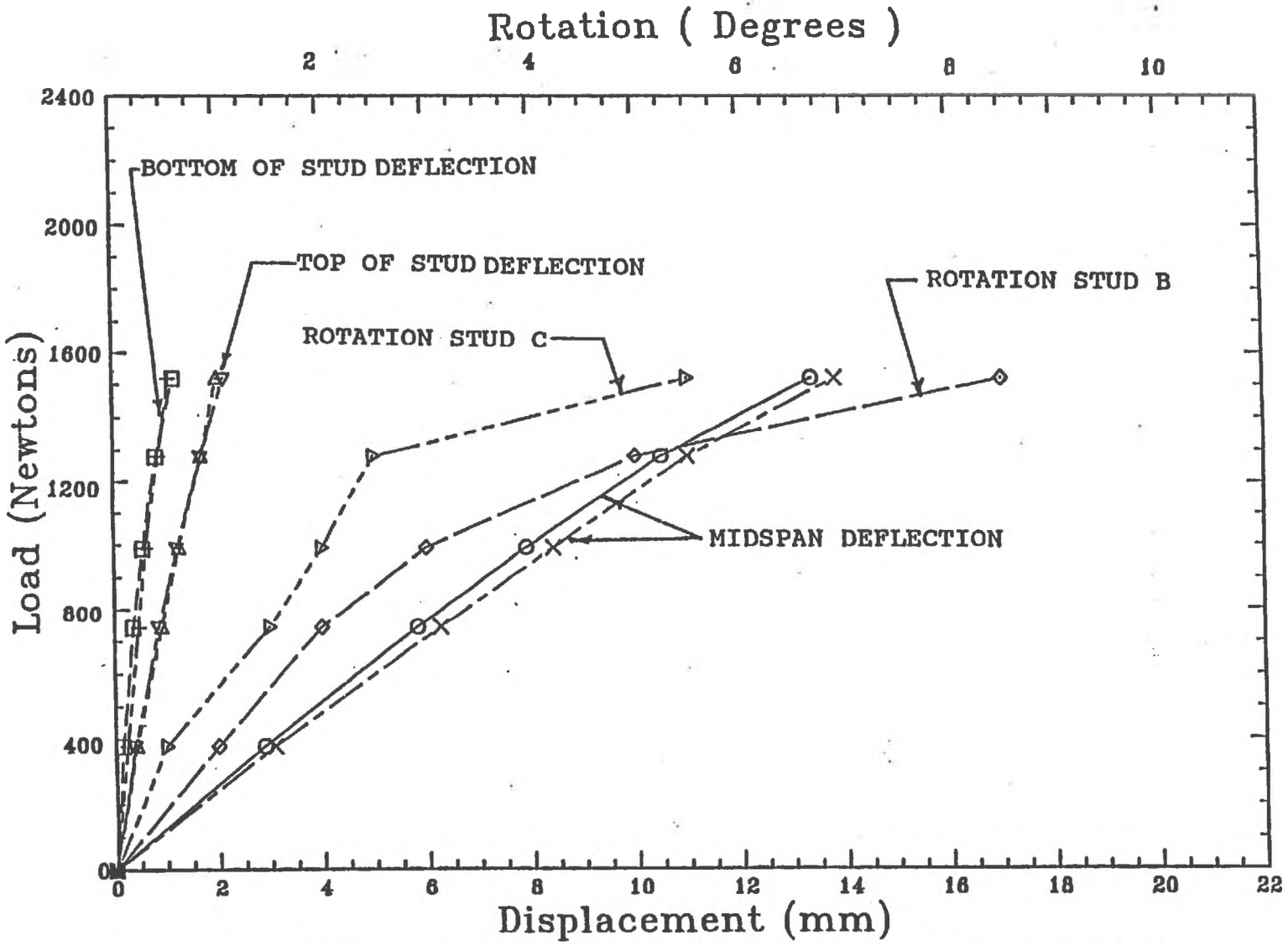

Figure 3.22A Load Versus Deflection and Rotation for Test Specimen 3-BW-1

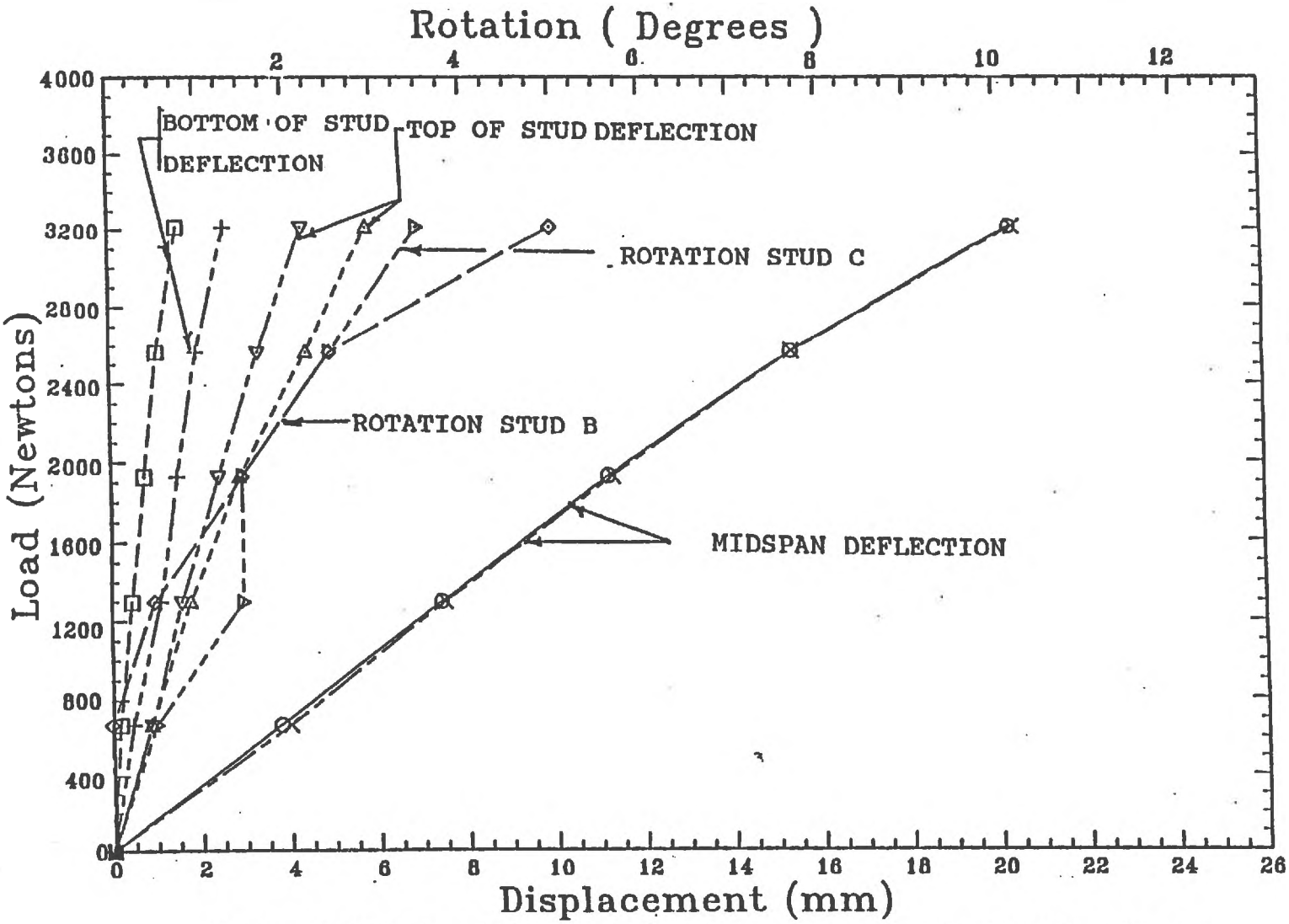

Figure 3.22B Load Versus Deflection and Rotation for Test Specimen 3-BW-2

3.5.4.3 Description Of Failures

Interior stud "B" collapsed in the region of the web cutout hole located between the centre line of bridging and the bottom track at failure of panel 3-BW-1. For 3-BW-2, buckle was in the region of the web cutout hole located between the centre line of the bridging and the top track on stud "C".

3.5.5 Series No. 4

3.5.5.1 Details of Panels

In Series 4, two 4 stud wide wall panels were fabricated. Specimen 4-BW-1 was fabricated with 20 gauge steel studs braced at midspan with steel bridging inserted through the midspan web cutout holes. In addition, the tension side of the panel was sheathed with 12 mm thick interior gypsum board fastened to the interior flanges of the studs with S-12 drywall screws, spaced 305 mm on centre. The exterior face was sheathed with 50 mm Styrofoam SM insulation. Brick veneer tie supports (B.V.T.S.), shown in Figure 3.23, were used to fasten the insulation to the compression flange of each stud. This was accomplished by pushing the legs of these 16 gauge galvanized tie support devices through the styrofoam at the locations shown in Figure 3.2 4. Two 4.5 mm diameter self tapping screws were used to fasten each B.V.T.S. device to the exterior compressive flanges of the steel studs. Specimen 4-BW-2 was fabricated with 18 gauge steel studs. A line of notched 38.1 mm by 12.7 mm by 1.2 mm face bridging was attached to the exterior flange of the studs at midspan. The interior and exterior faces of the panel were also sheathed in the same manner as test specimen 4-BW-1.

3.5.5.2 Special Test Conditions

For these tests, the bridging was not attached to the bridging displacement control rig as in test Series 1 to 3, since the interior gypsum board sheathing was expected to be sufficiently rigid to prevent in-plane translation of the panel. Since the exterior top flanges of the four studs were sheathed with 50 mm Styrofoam SM insulation, holes had to be cut into

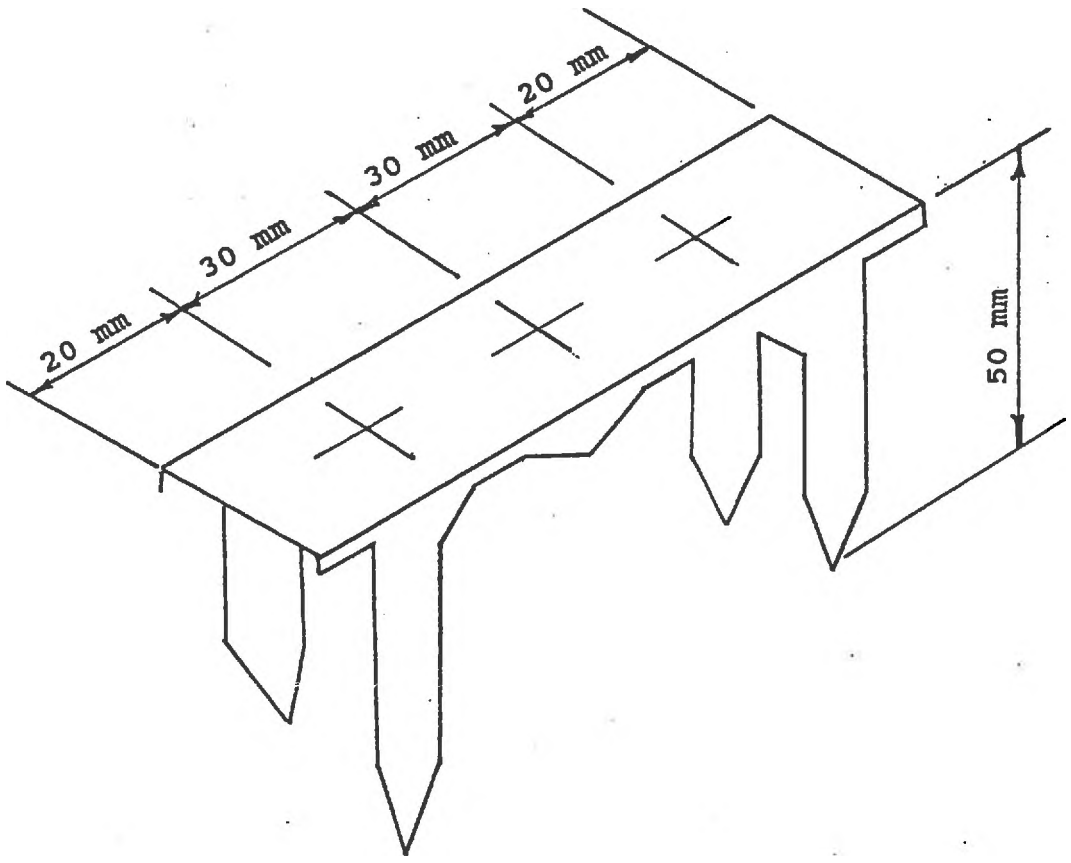

Figure 3.23 **Brick Veneer Tie Support (B.V.T.S.) Device Used in Series 4**

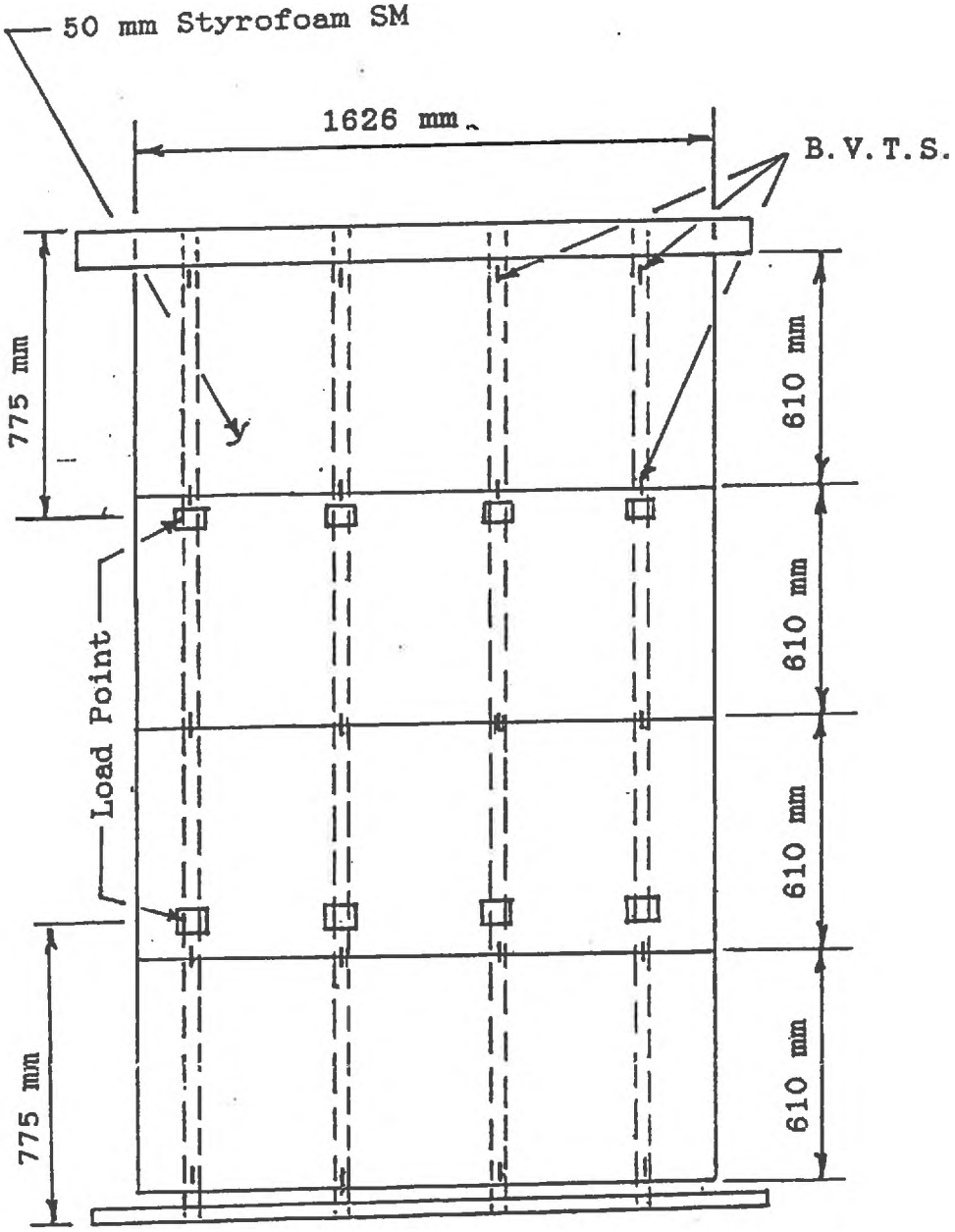

Figure 3.24 Location of the B.V.T.S. for Specimen 4-BW-1 and 4-BW-2

the SM Board during the fabrication process at the location of the points of application of the loads. This was done in order to allow the placement of loading beams A1 without any interference by the SM insulation. The holes had been cut large enough so that no additional bracing could be achieved by restricting the movement of the styrofoam in the areas surrounding the loading beams. The remaining loading beams were placed in a similar manner as in test Series 1 to 3.

Instrumentation was installed at the locations described in Section 3.4.2.2. The tests consisted of cyclic loading of each specimen. The loading was limited to 50 cycles since it had been shown previously[24], that most of the stiffness degradation takes place within the first 50 loading cycles. In each cycle, the load was increased to approximately 60 percent of the expected ultimate load. Then specimen was unloaded. At the beginning and end of every ten cycles, the deflections were recorded. On the last cycle, the load was incrementally increased until failure.

3.5.5.3 Results of Tests

For specimen 4-BW-1 the average midspan panel deflection at the two interior studs is plotted in Figure 3.25. In order to obtain the average midspan flexural deflection of the panel, the midspan flexural deflection at each stud was first determined by subtracting the average of the end deflections of the steel stud from the measured midspan deflection. Since there were two studs the average value was taken as the panel midspan flexural deflection. Also plotted in this figure is the average one cycle midspan deflection from all the 20 gauge beam tests performed in Series 6 of the test program. This value is represented by the dashed line at the top of Figure 3.25. As can be seen the panel stiffness remained practically constant over the 50 load cycles and very little composite action existed between the sheathing materials and the steel stud. Also plotted in this figure are the results for the 20 gauge tests of Series 7. These results will be discussed in Section 3.5.8.

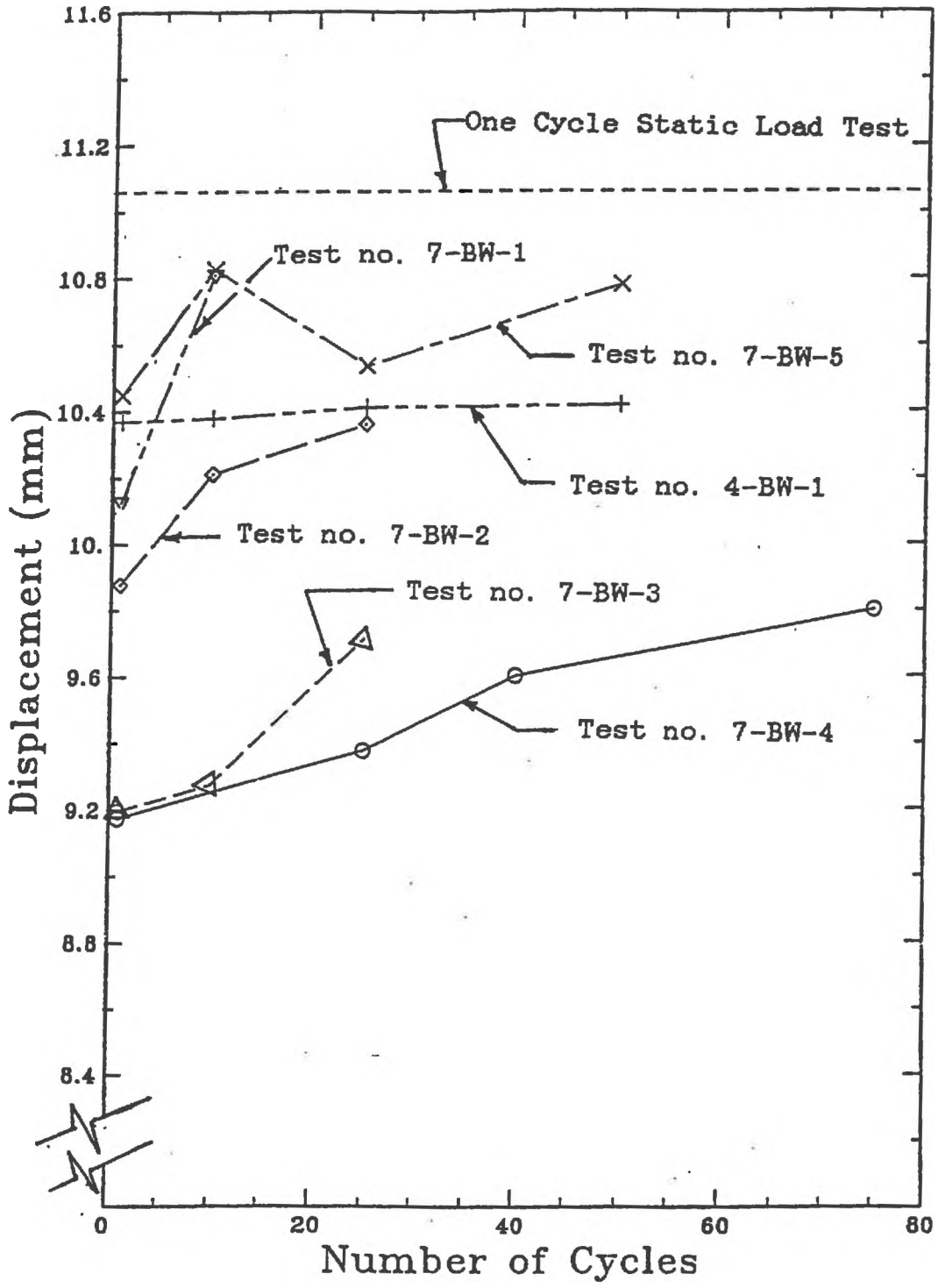

Figure 3.25 Cyclic Load Tests of 20 Gauge Steel Stud Panels

For specimen 4-BW-2, the average midspan flexural stud deflection is shown in Figure 3.26 . The average one cycle midspan deflection for the 18 gauge beam tests performed in Series 6 of the test program is also plotted for comparison purposes. As seen from this curve, the panel stiffness remained practically constant over the 50 load cycles and the overall stiffness of this specimen was slightly less than the average value obtained in the beam tests. The two other curves shown in this figure will be discussed in Section 3.5.8.

3.5.5.4 Description of Failures

The failure pattern for specimen 4-BW-1 is shown in Figure 3.27. This figure illustrates the damage sustained by the first two studs of the panel. The third stud in the panel, which is partially shown at the extreme left of the figure, also sustained damage at the same location as the first two but of lesser magnitude. This stud also had visible compression flange buckling at the intersection of the steel stud and the midspan line of steel bridging. Since the panel was sheathed with 50 mm polystyrene on the exterior face, it is not known if all three damaged studs failed simultaneously or if one stud initiated the failure of the others.

For specimen 4-BW-2, it was observed that both interior studs were severely damaged in the region of the web cutout holes located 940 mm from the bottom track. One of the interior studs also exhibited some local deformation in the region of the web cutout hole located 940 mm from the top of the panel. One of the exterior studs also sustained damage in the region of the web cutout hole located 940 mm from the top of the panel.

3.5.6 Test Series No. 5

3.5.6.1 Details Of Panels

The specimens tested in this series consisted of wall panels, two studs wide, unbraced between the top and bottom support tracks. Specimens 5-BW-1 to 5-BW-3 were fabricated with 20 guage studs and specimens 5-BW-4 to 5-BW-6 were fabricated with 18 gauge studs. Standard track was used at the top and bottom of each panel. Brick ties were fastened to the

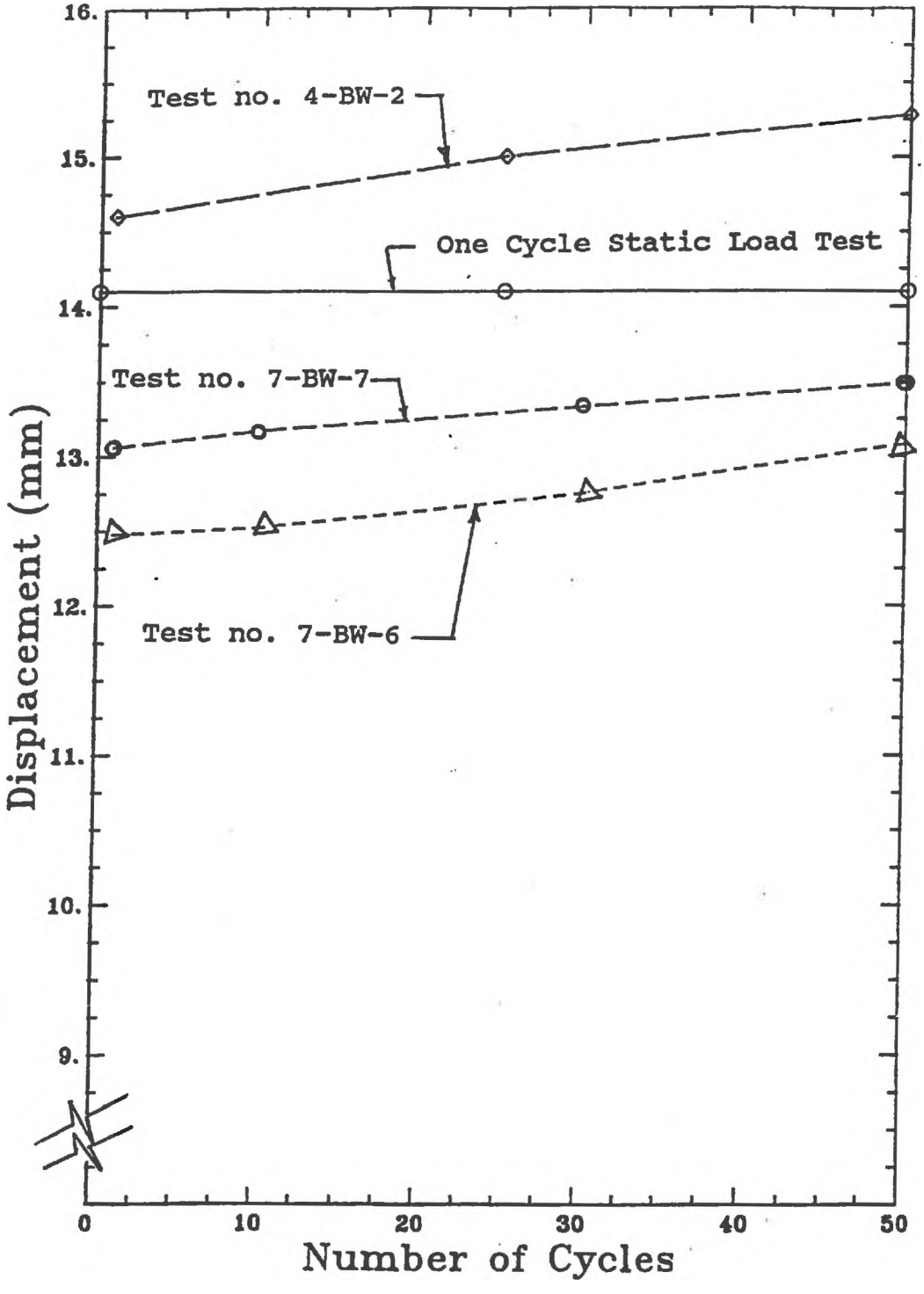

Figure 3.26 Cyclic Load Tests of 18 Gauge Steel Stud Panels

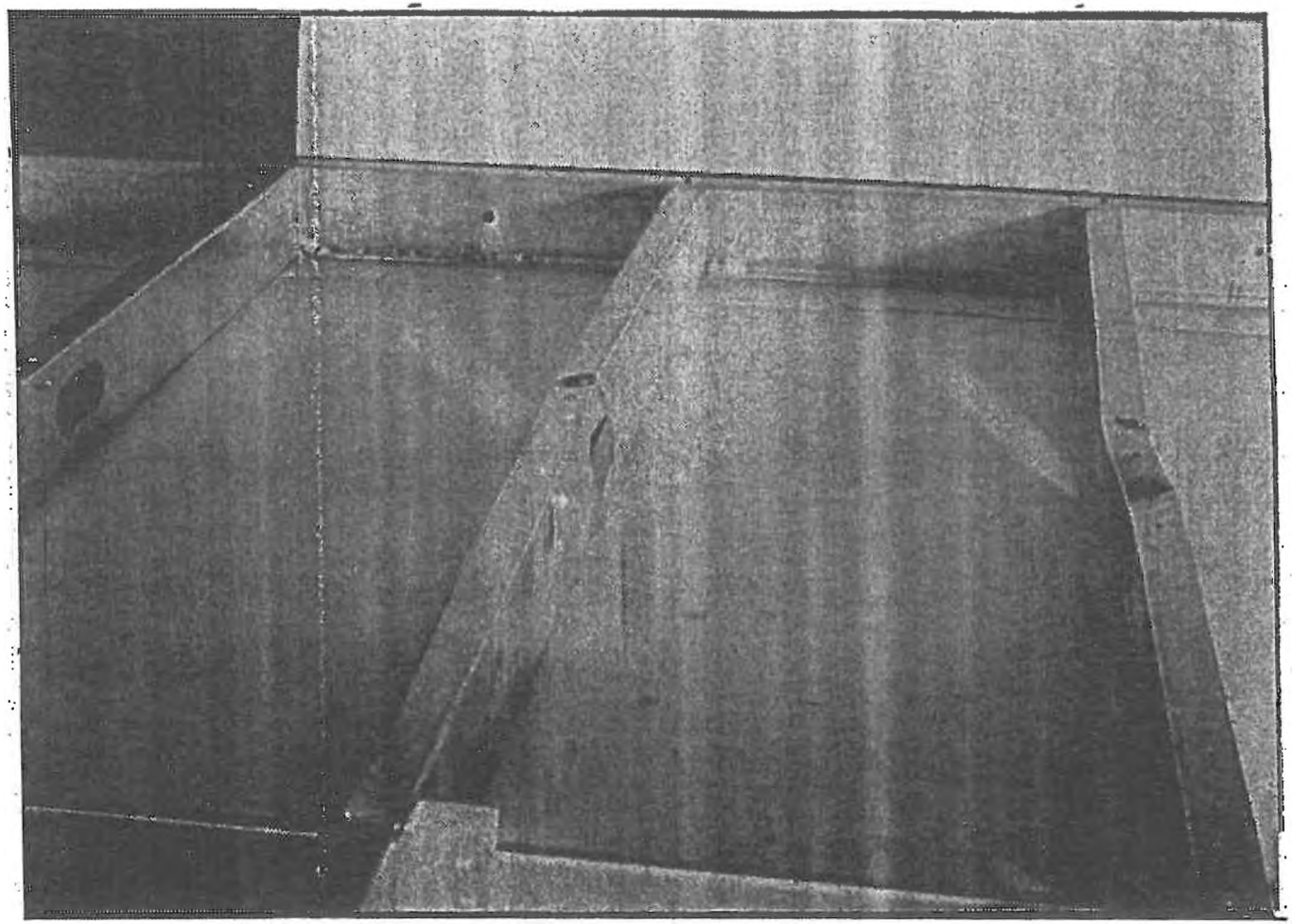

Figure 3.27 Photograph of Failure of Specimen 4-BW-1

studs at the loading points. During the fabrication process, it was observed that very little effort was required to twist the steel studs in these unbraced wall panels. Therefore it was anticipated that large rotations of the cross-sections of the studs would occur during the tests and as a result the loading beam arrangements used in the previous test series would be unstable. To load the studs, the loading arrangement shown in Figure 3.13 was used.

3.5.6.2 Special Test Conditions

The test procedure followed the outline described in Section 3.4.3.2 .

3.5.6.3 Results Of Tests

The load versus midspan rotation plots are shown in Figures 3.28A to 3.28D. As can be seen from these figures, large midspan stud rotations occurred even at very small loads. The stud rotations were also non-linear and increased rapidly with load. In Figure 3.28B, the rotation of only one stud is shown due to malfunction of the rotation measuring device for the second stud. No rotation readings were taken for the last 20 and 18 gauge specimens.

3.5.6.3 Description Of Failures

Specimens 5-BW-1 to 5-BW-3 all failed due to local buckling of the two steel studs in the region of the midspan cutout holes. For specimens 5-BW-4 to 5-BW-6, failure of each of these panels occurred when the two studs failed simultaneously in the region of of the web cutout holes located approximately 940 mm from the top track support. A typical failure of an 18 gauge specimen is shown in Figure 3.29.

3.5.7 Series No. 6

3.5.7.1 Details Of Beam Specimens

Twelve beam specimens, broken down into Series 6A and 6B, were fabricated. The first four specimens of Series 6A (6-BW-1 to 6-BW-4) were fabricated with two 20 gauge studs.

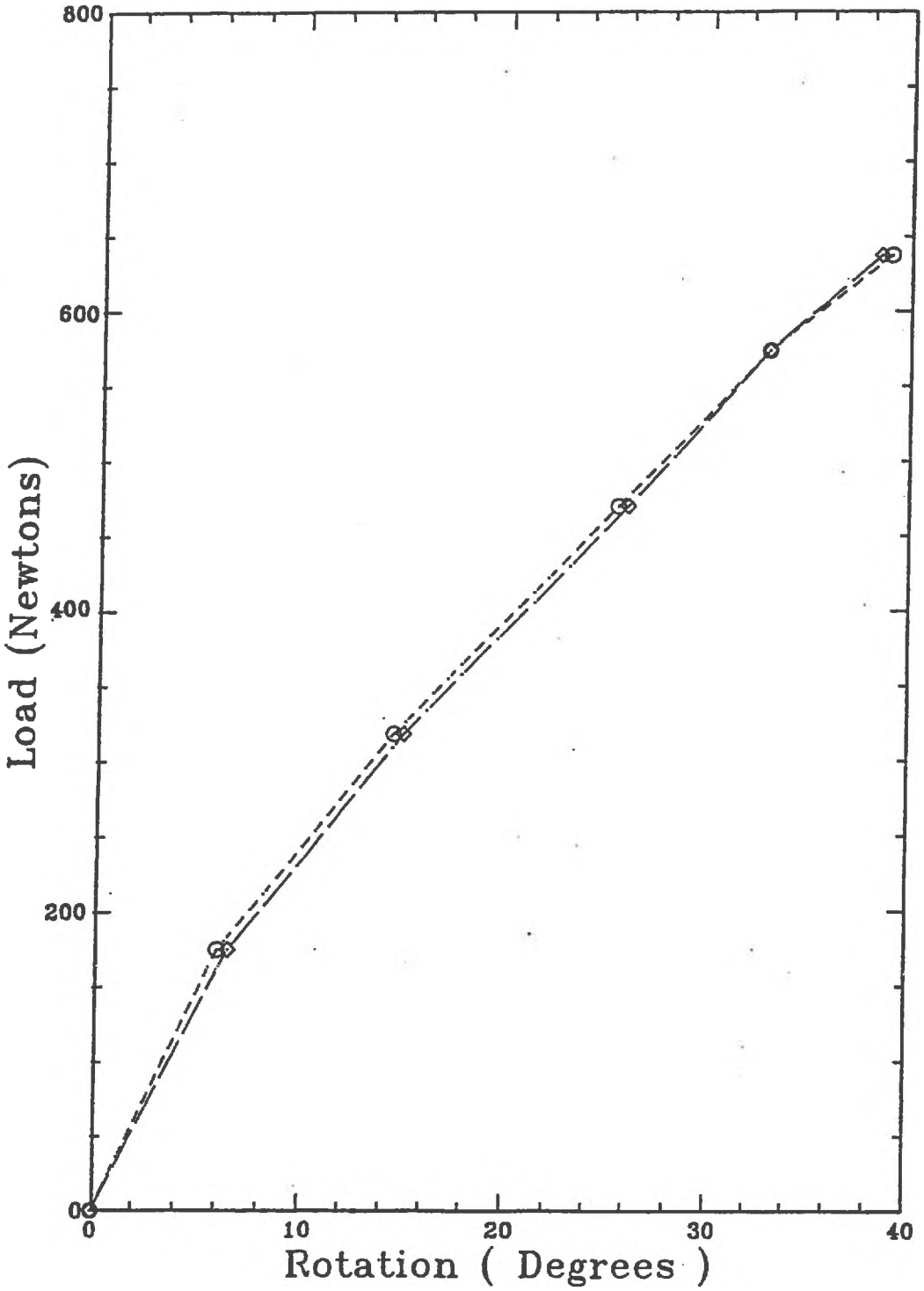

Figure 3.28A Load Versus Midspan Rotation for Specimen 5-BW-1

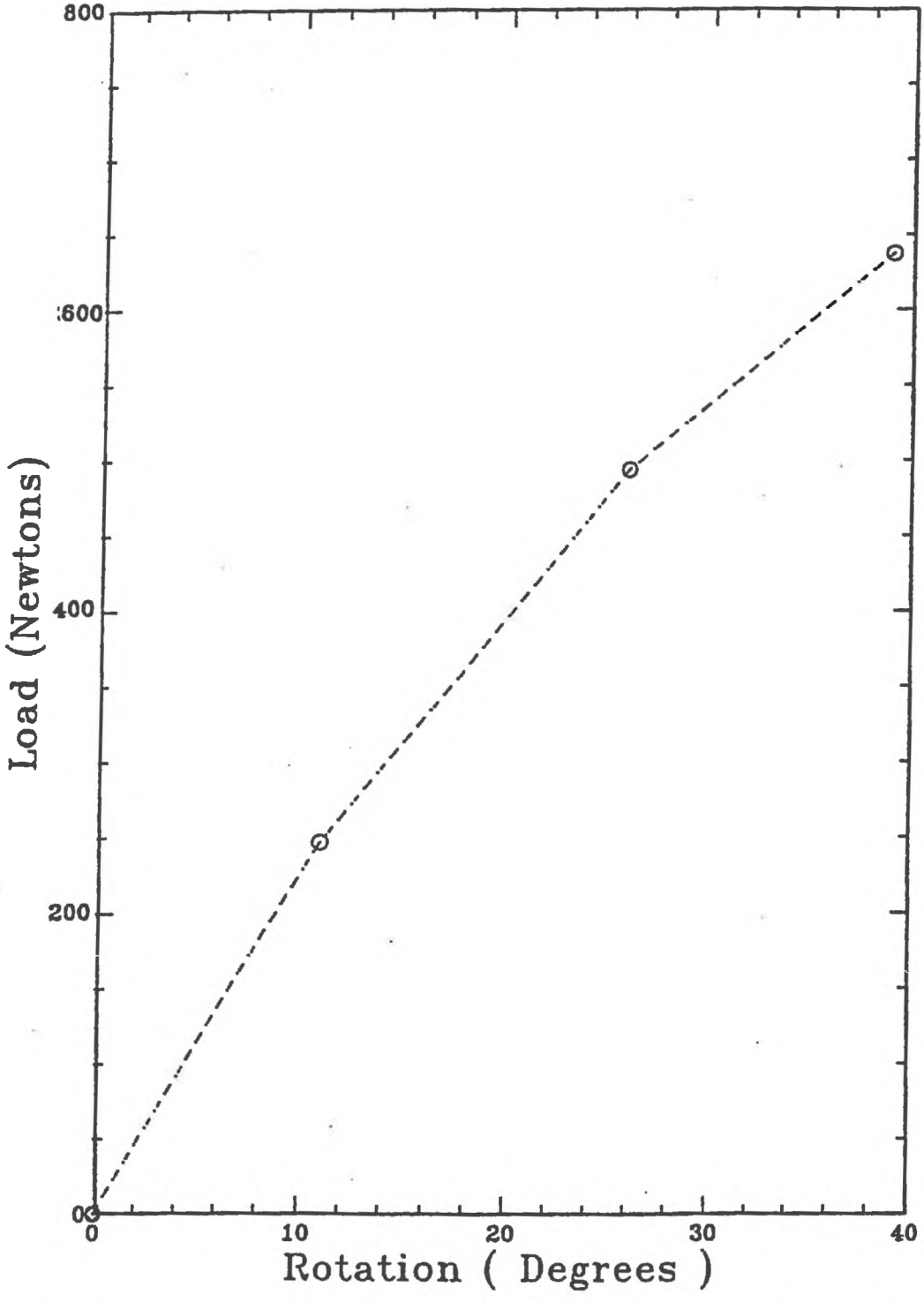

Figure 3.28B Load Versus Midspan Rotation for Specimen 5-BW-2

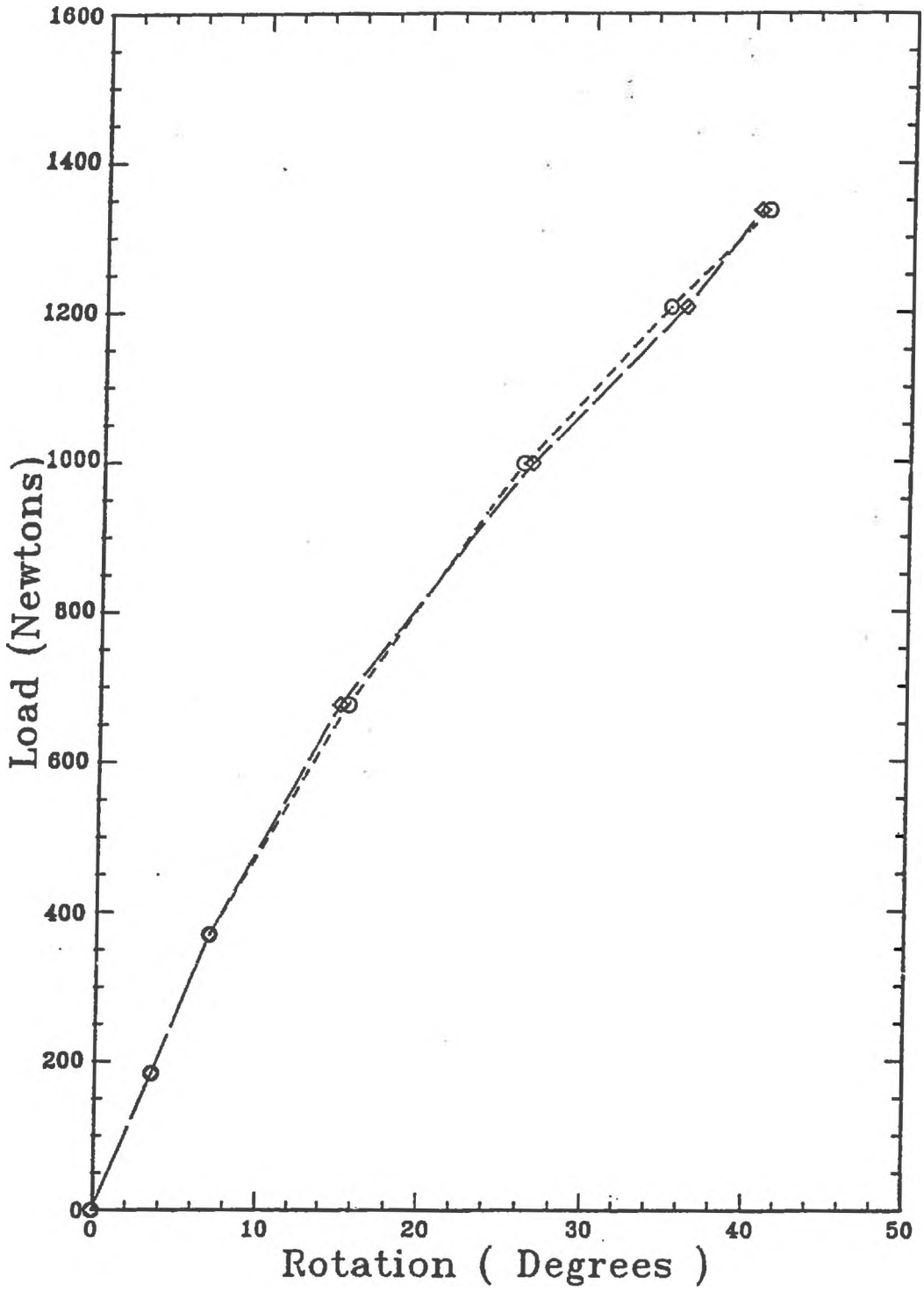

Figure 3.28C Load Versus Midspan Rotation for Specimen 5-BW-4

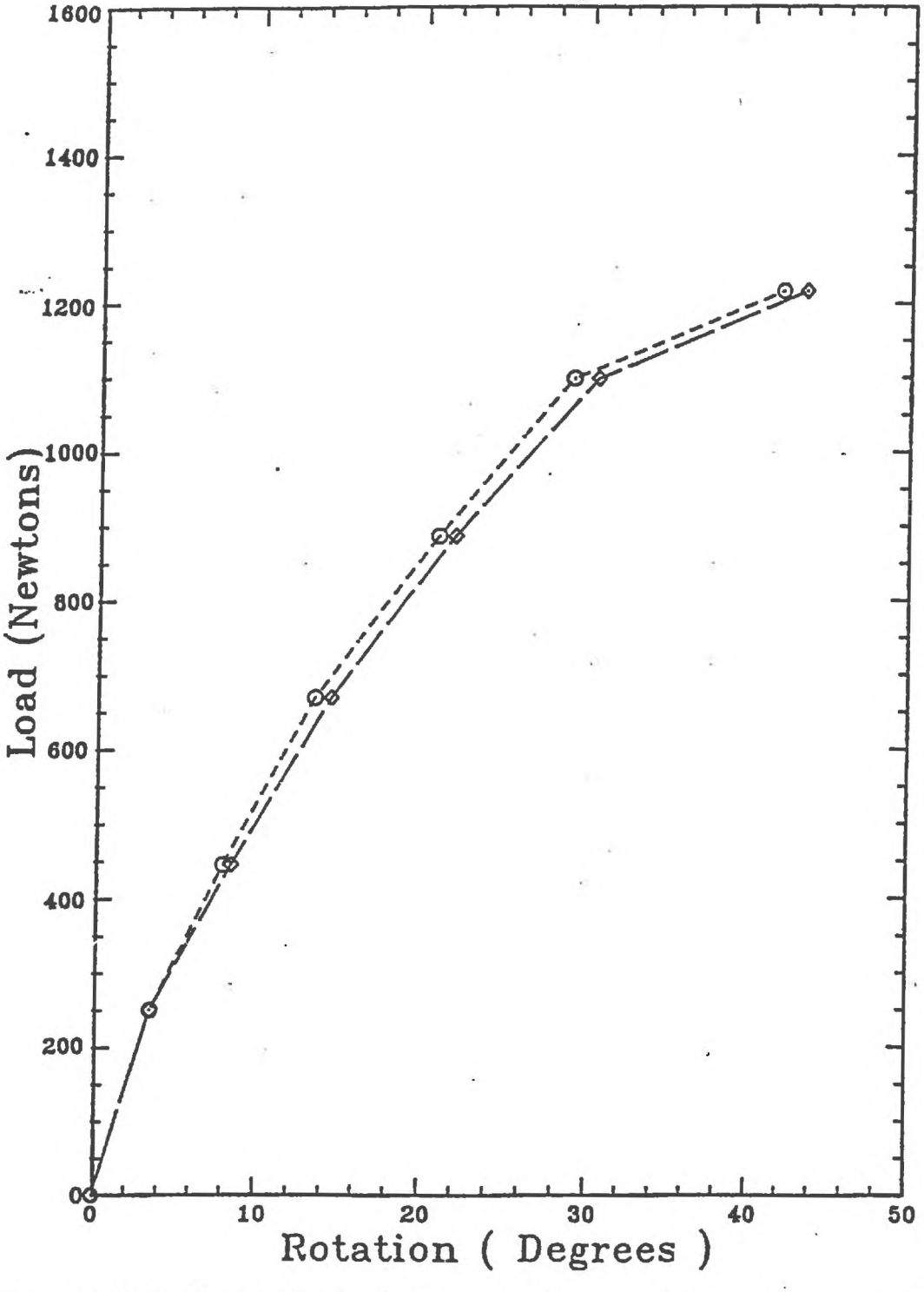

Figure 3.28D Load Versus Midspan Rotation for Specimen 5-BW-5

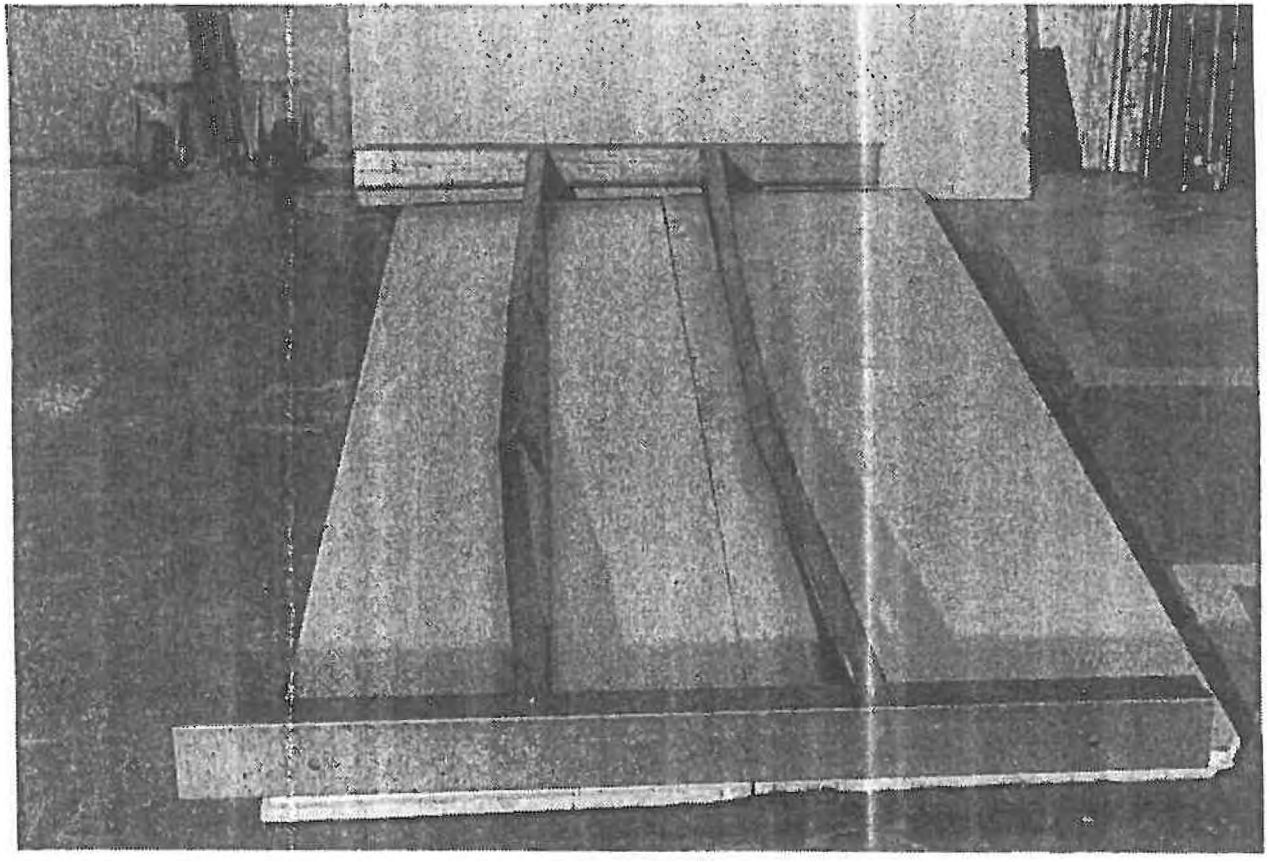

Figure 3.29 **Photograph Showing Typical Failure of an 18 Gauge Specimen - Series 5**

As shown in Figure 3.30, the studs were placed with webs back to back. The webs were separated with 25 mm thick wooden spacer blocks. To hold the studs together, 6 mm threaded rods and 6 mm plates were used at the wooden spacer locations. Specimens 6A-BW-5 and 6A-BW-6 were essentially fabricated in essentially the same manner but 18 gauge studs were used instead of the 20 gauge studs. In series 6B, specimens 6B-BW-7 to 6B-BW-9 were fabricated with two 20 gauge studs. As in Series 6A, the webs were placed back to back but instead of using wooden spacer blocks, the webs were separated by 16 gauge brick ties. The brick ties were spaced every 400 mm on centre. Two Number 6 Tek Panhead screws were used to fasten the webs to each of the brick ties. Specimens 6-BW-10 to 6-BW-12 were fabricated in a similar manner but using 18 gauge studs.

3.5.7.2 Special Test Conditions

For series 6A, each specimen was set on top of the test frame as shown in Figure 3.30. The top floor beam had been moved closer to the bottom floor beam, allowing the tests specimens to sit on the pin and roller supports. Loading plates were placed on the top flanges of the double stud specimens. Each plate was shimmed level and loading beams were set on top of the loading plates. Each specimen was loaded incrementally by the hydraulic jack until failure. For each load increment deflection readings were recorded at the midspan of each stud.

For series 6B, the specimens were placed in the Tinius Olsen test machine as shown in Figure 3.31. The loading arrangement is as shown in the figure. Otherwise the test procedure was the same as for Series 6A.

3.5.7.3 Results Of Tests

For Series 6A the load versus midspan deflection for both gauges of studs are shown in Figures 3.32A to 3.32F. The first four figures are for the 20 gauge specimens while the last two are for the 18 gauge specimens. In these tests the centreline stud deflection was found to

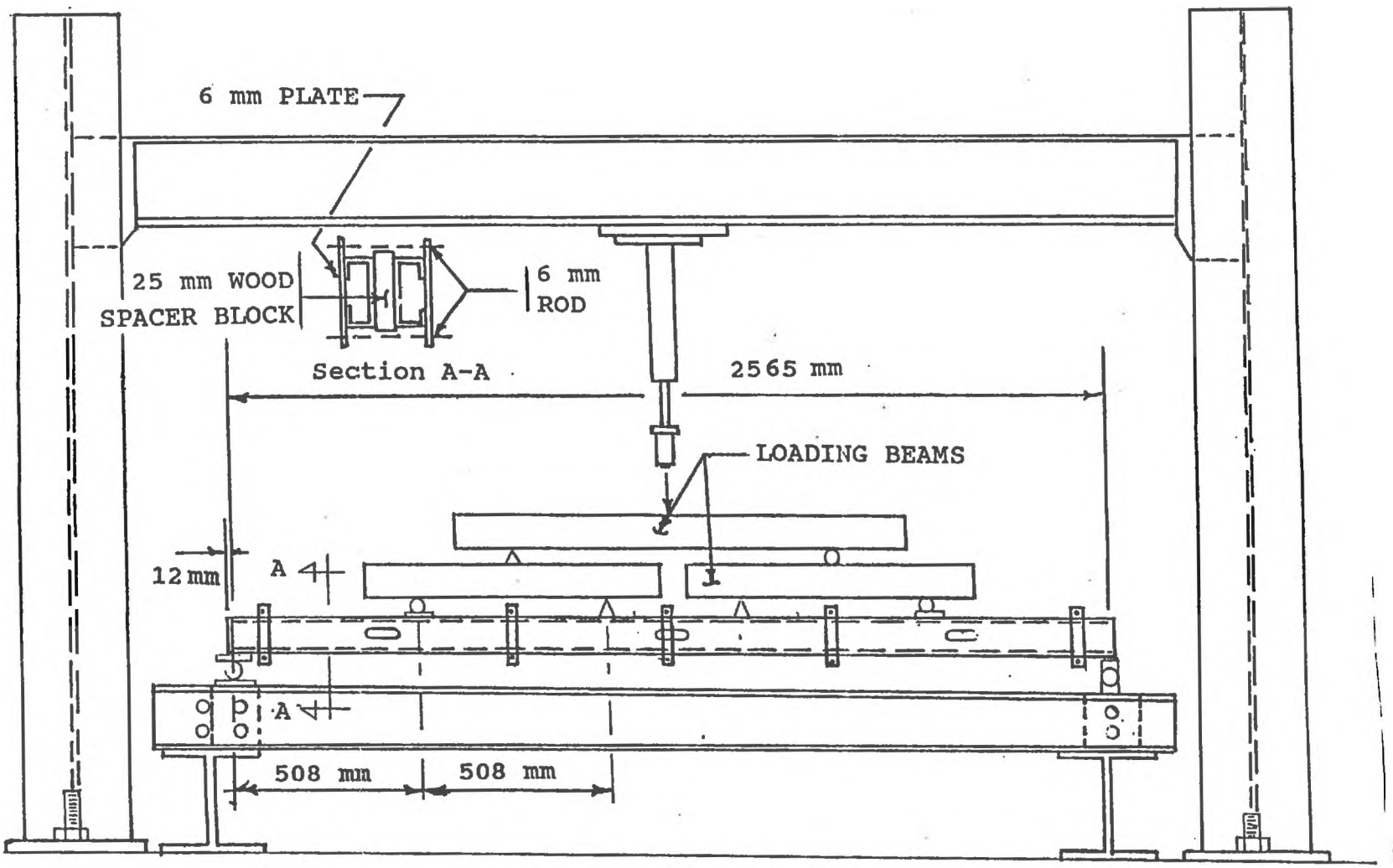

Figure 3.30 Test Setup for Beam Test Specimens - Series 6A

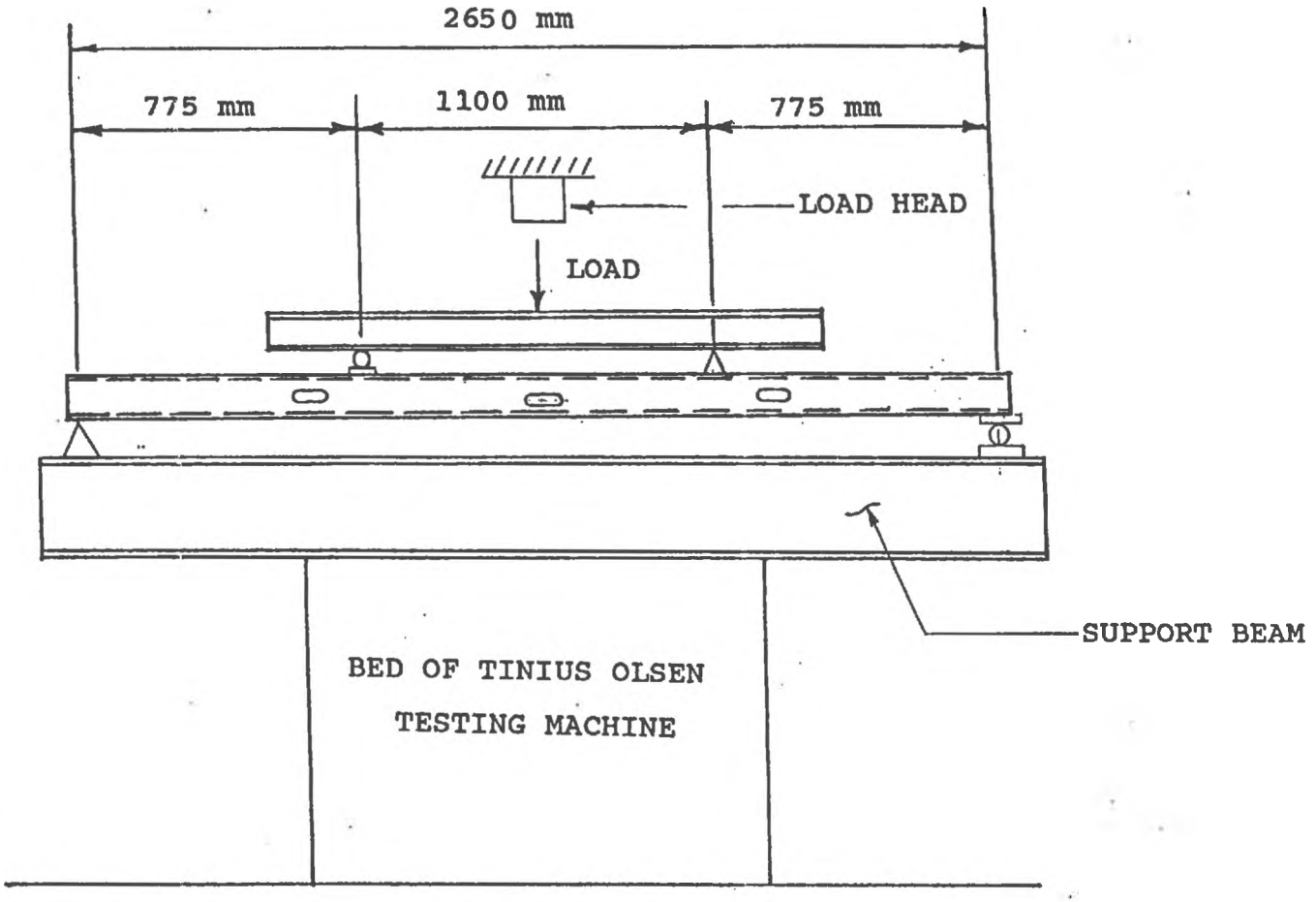

Figure 3.31 Test Setup for Beam Test Specimens - Series 6B

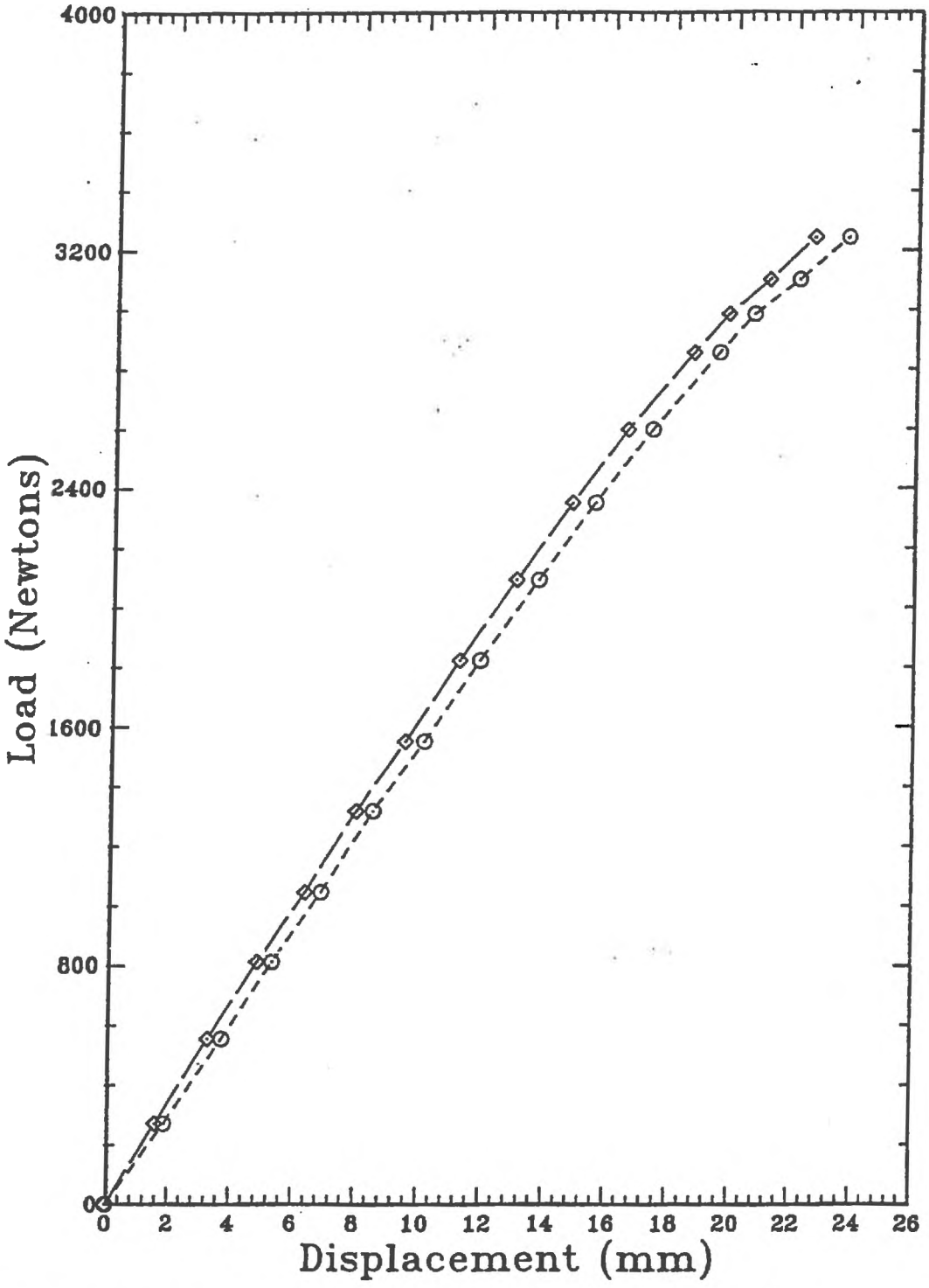

Figure 3.32A Load Versus Midspan Deflection for Specimen 6-BW-1

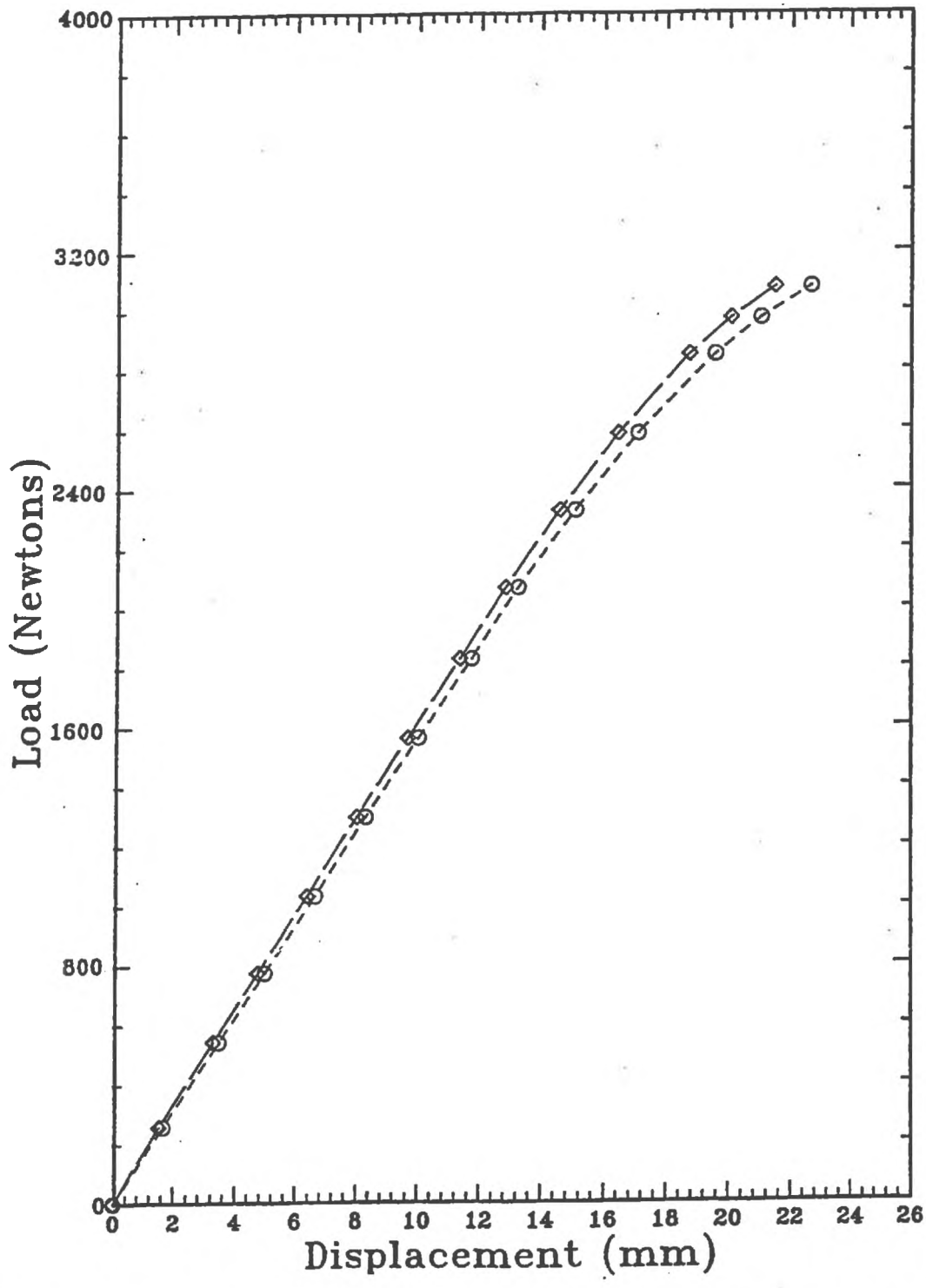

Figure 3.32B Load Versus Midspan Deflection for Specimen 6-BW-2

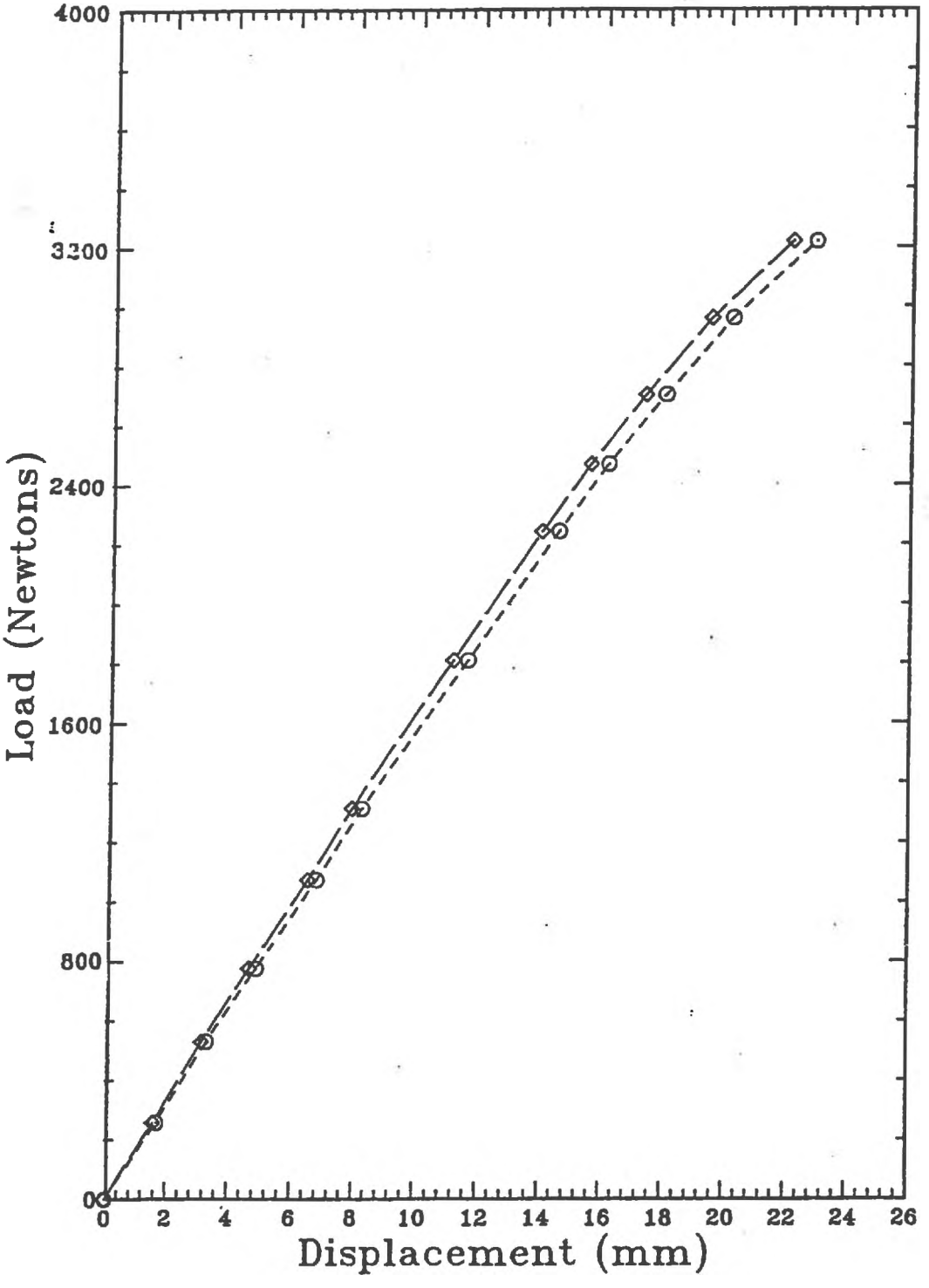

Figure 3.32C Load Versus Midspan Deflection for Specimen 6-BW-3

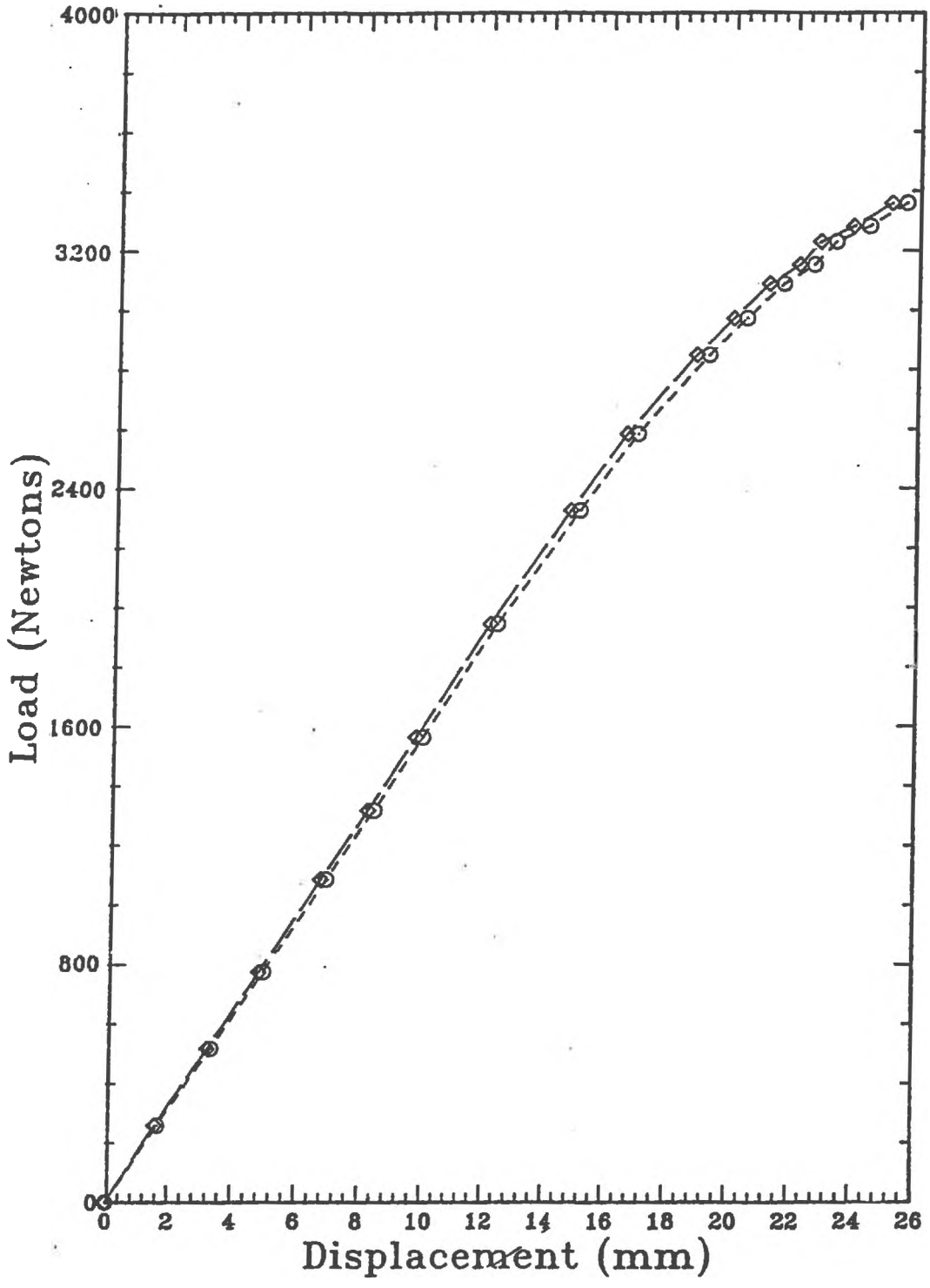

Figure 3.32D Load Versus Midspan Deflection for Specimen 6-BW-4

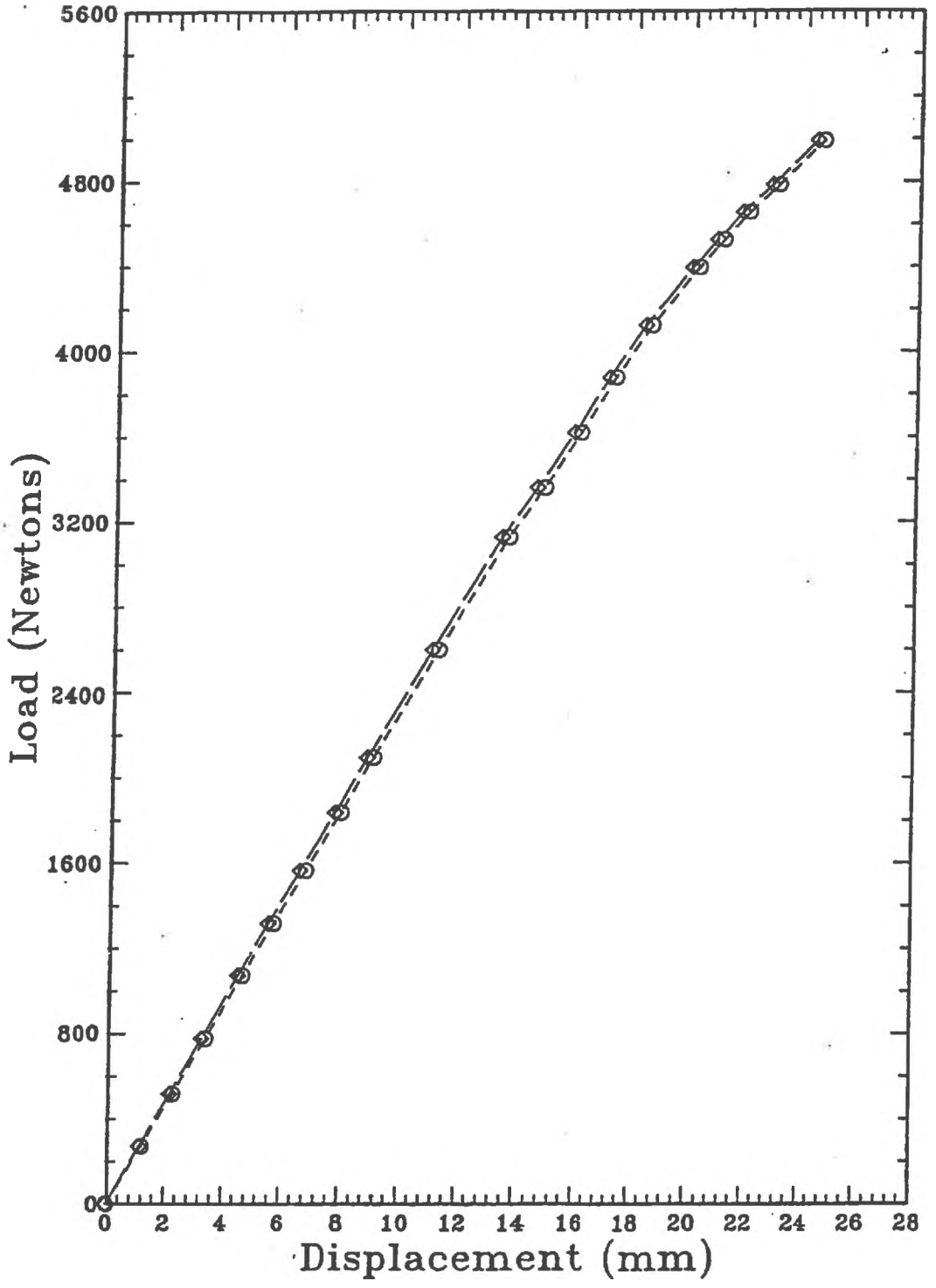

Figure 3.32E Load Versus Midspan Deflection for Specimen 6-BW-5

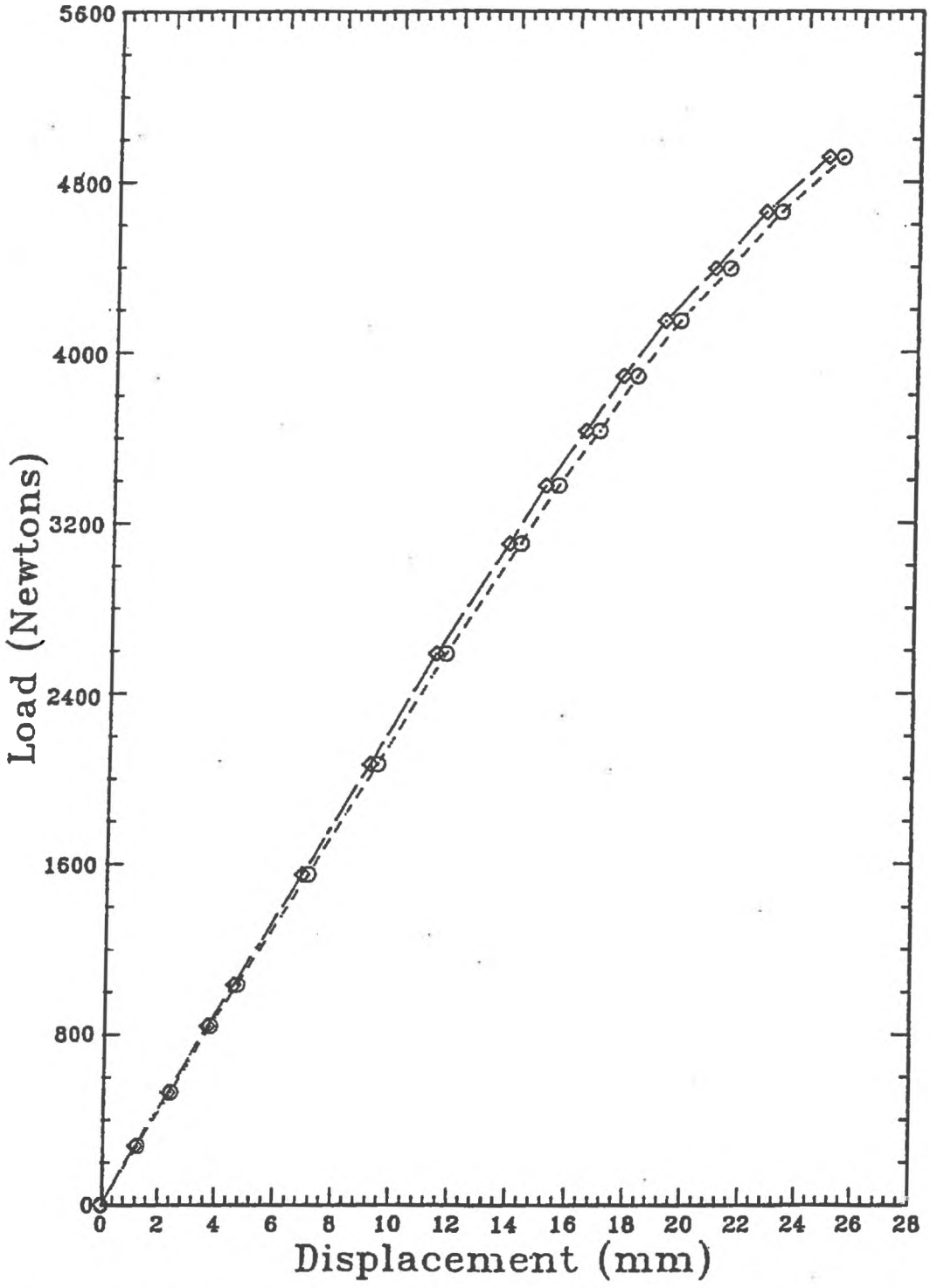

Figure 3.32F Load Versus Midspan Deflection for Specimen 6-BW-6

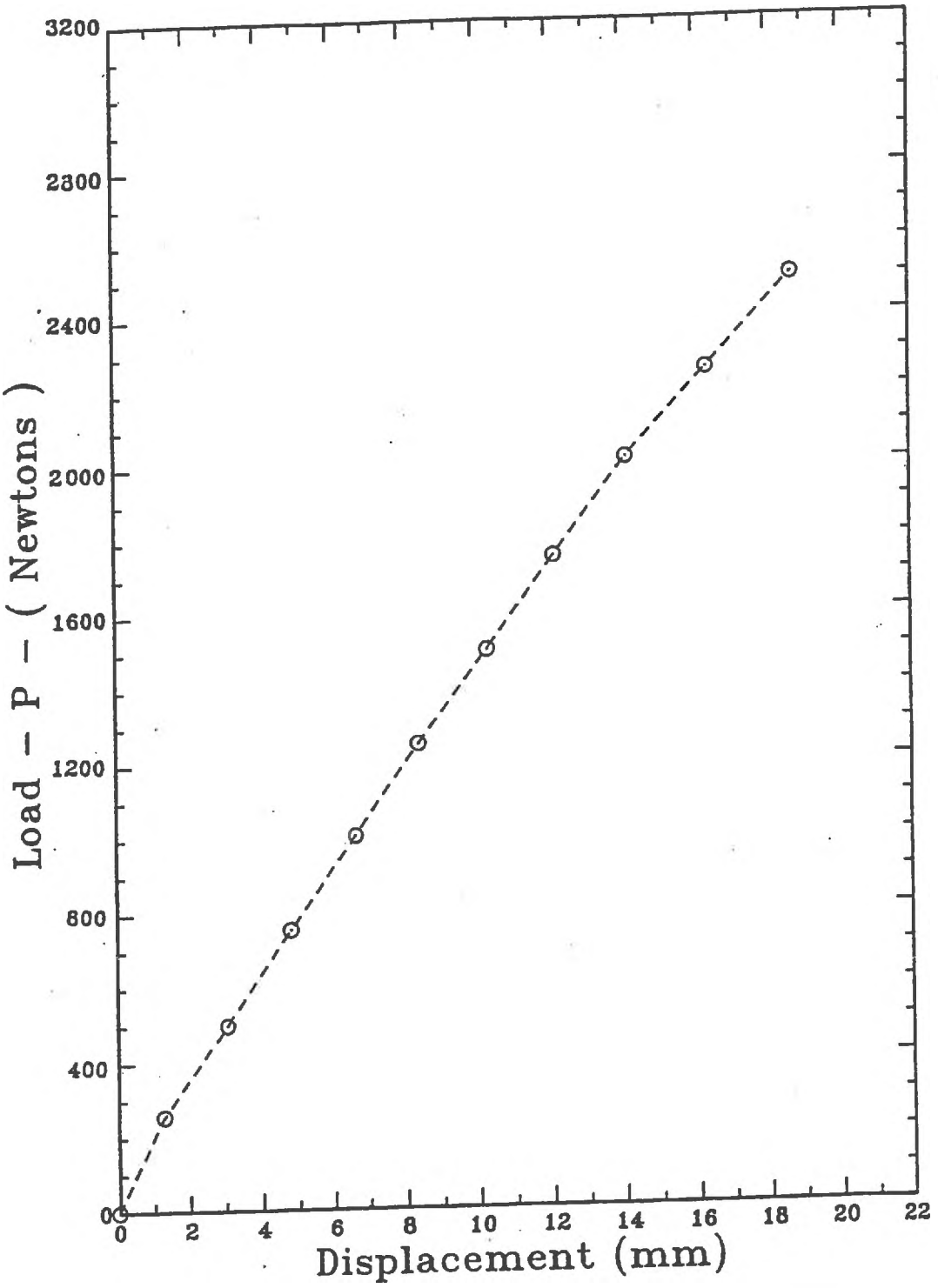

Figure 3.32G Load Versus Midspan Deflection for Specimen 6-BW-7

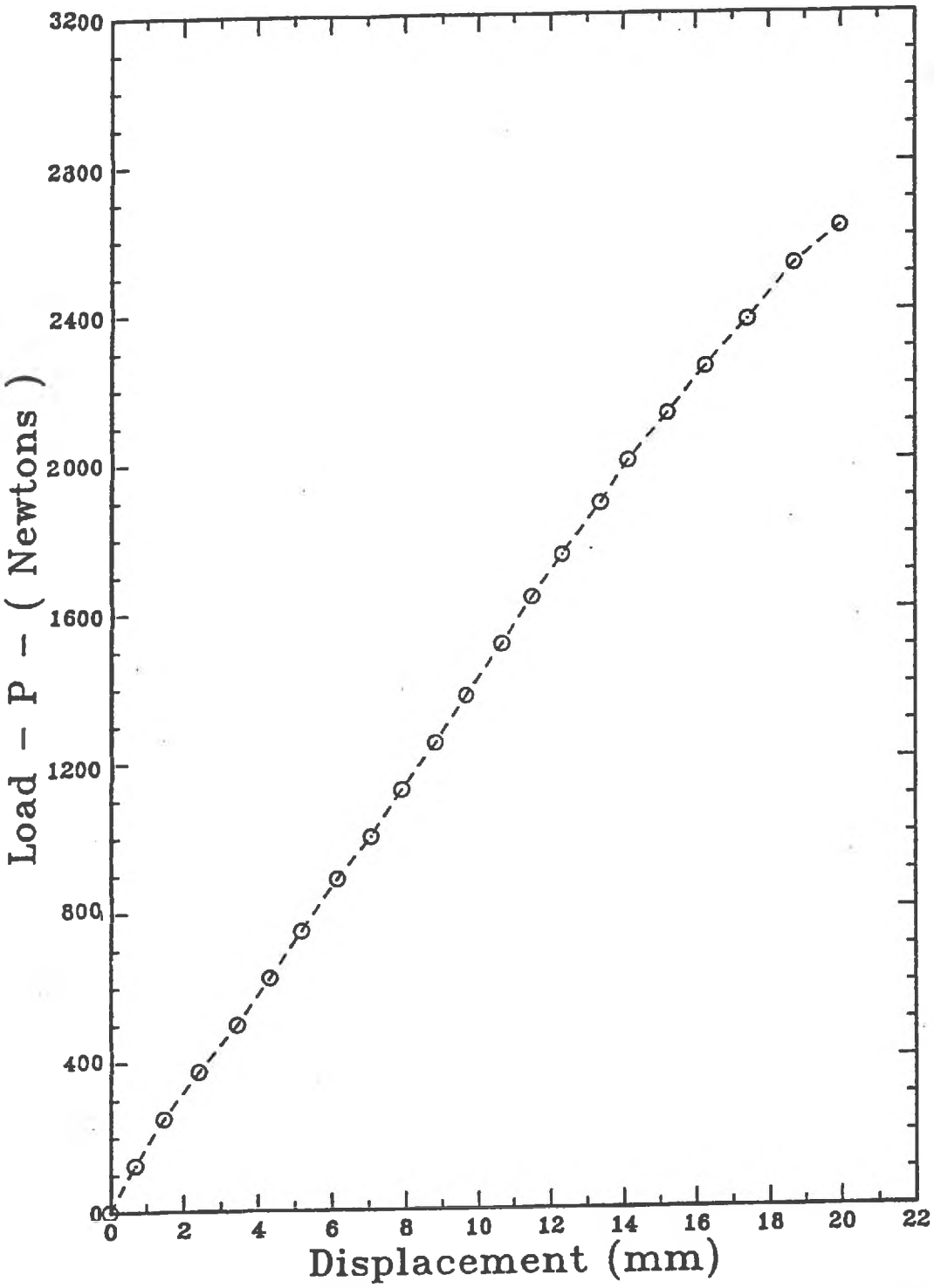

Figure 3.32H Load Versus Midspan Deflection for Specimen 6-BW-8

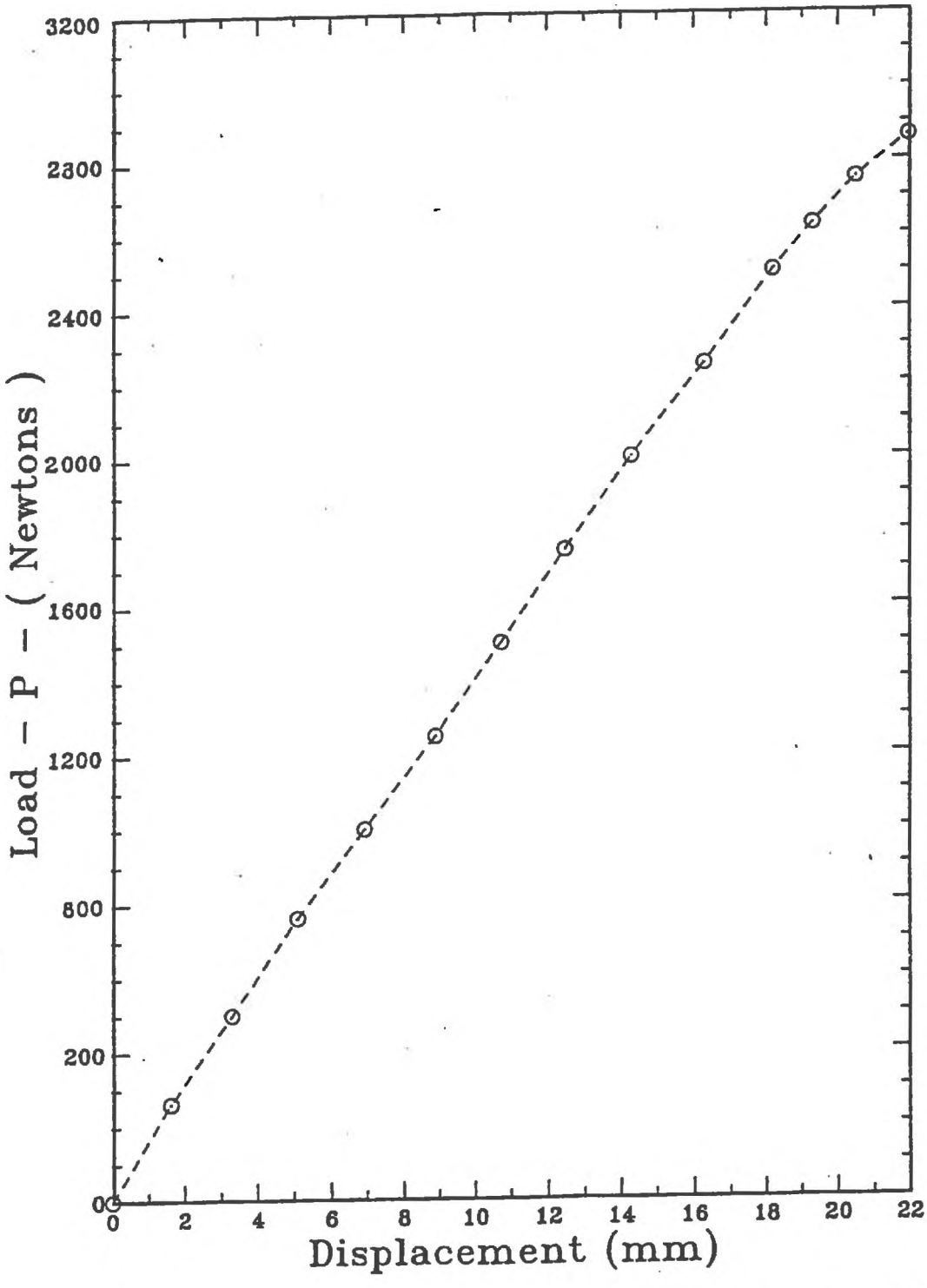

Figure 3.32I Load Versus Midspan Deflection for Specimen 6-BW-9

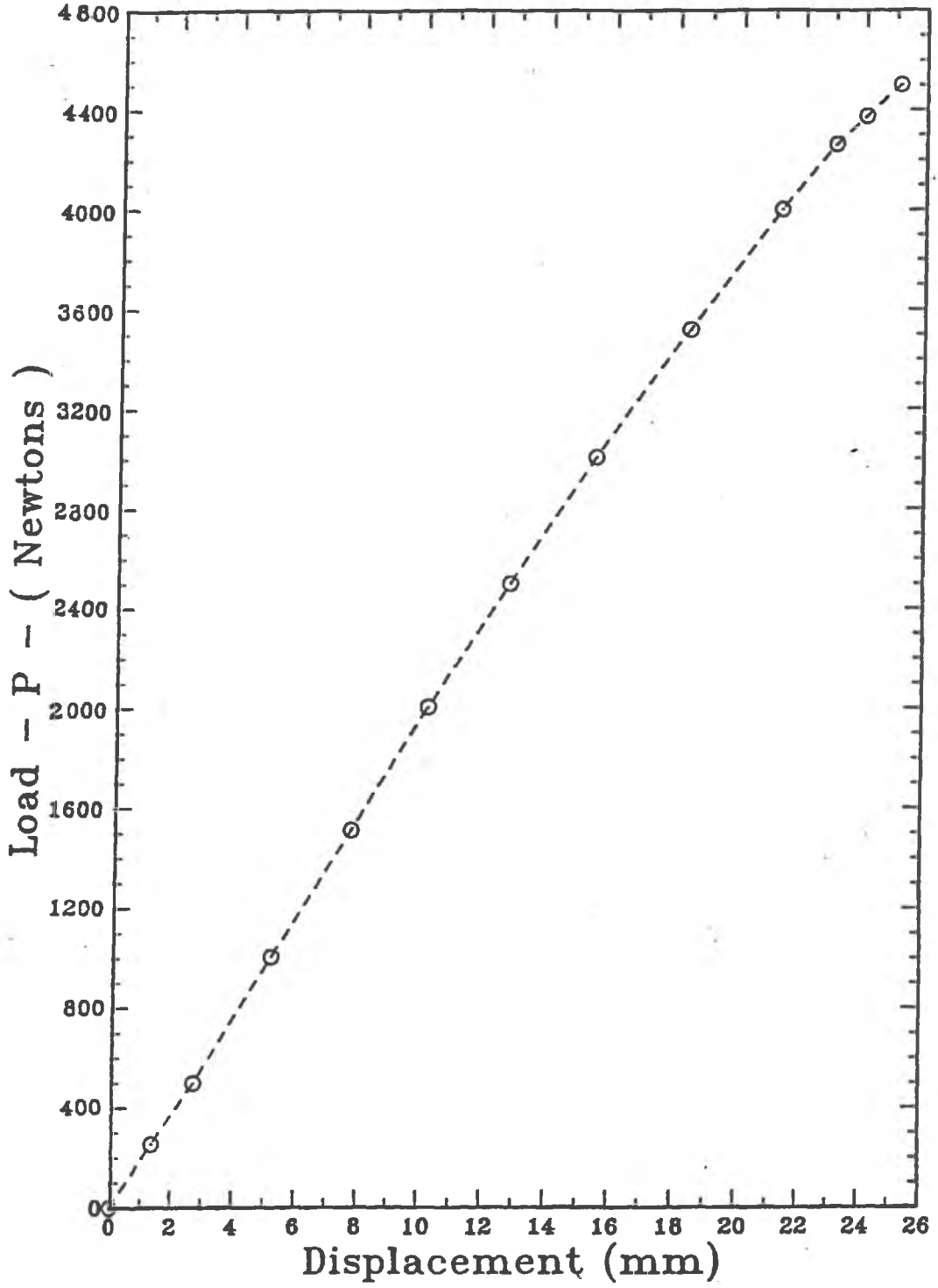

Figure 3.32J Load Versus Midspan Deflection for Specimen 6-BW-10

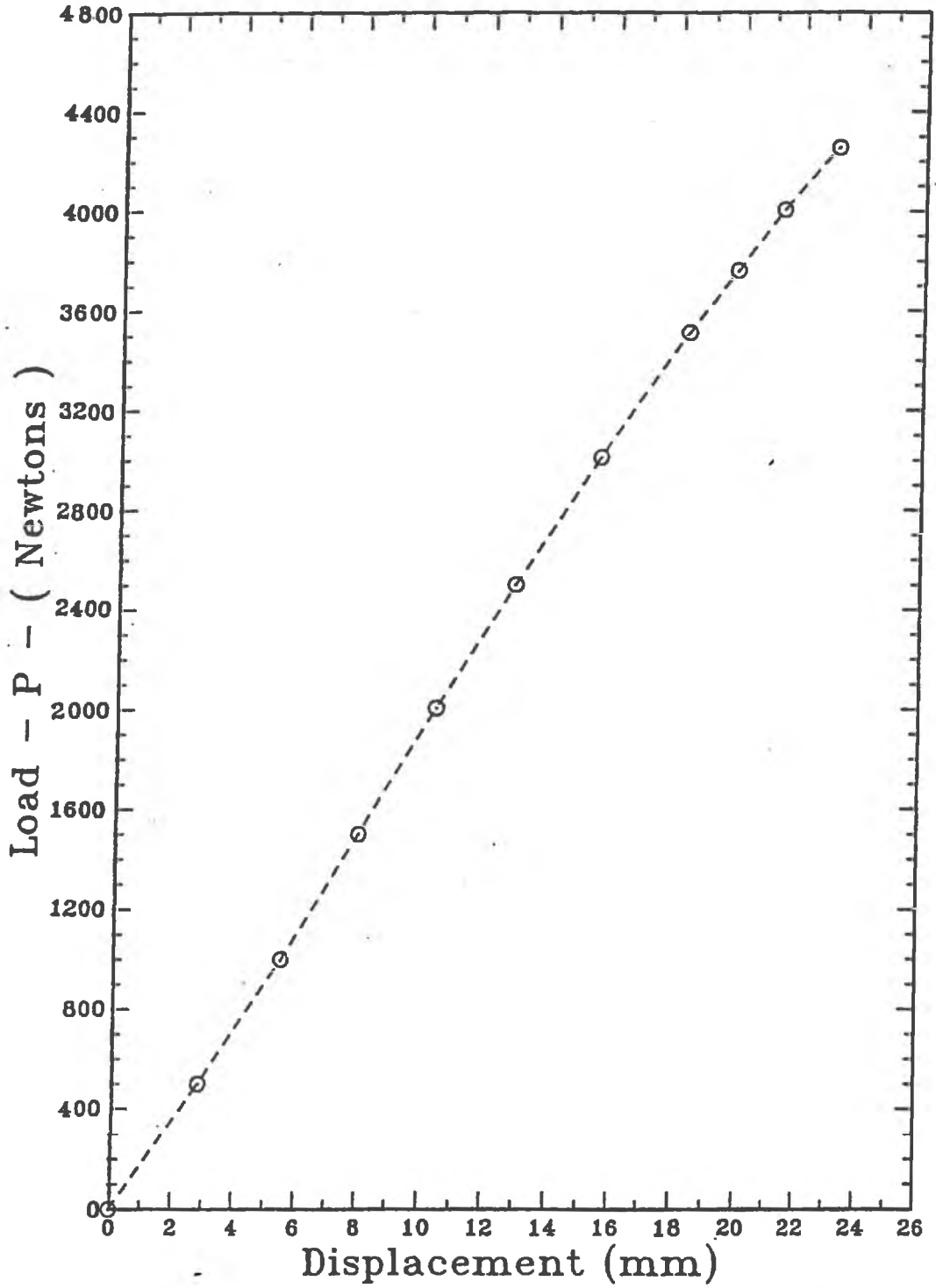

Figure 3.32K Load Versus Midspan Deflection for Specimen 6-BW-11

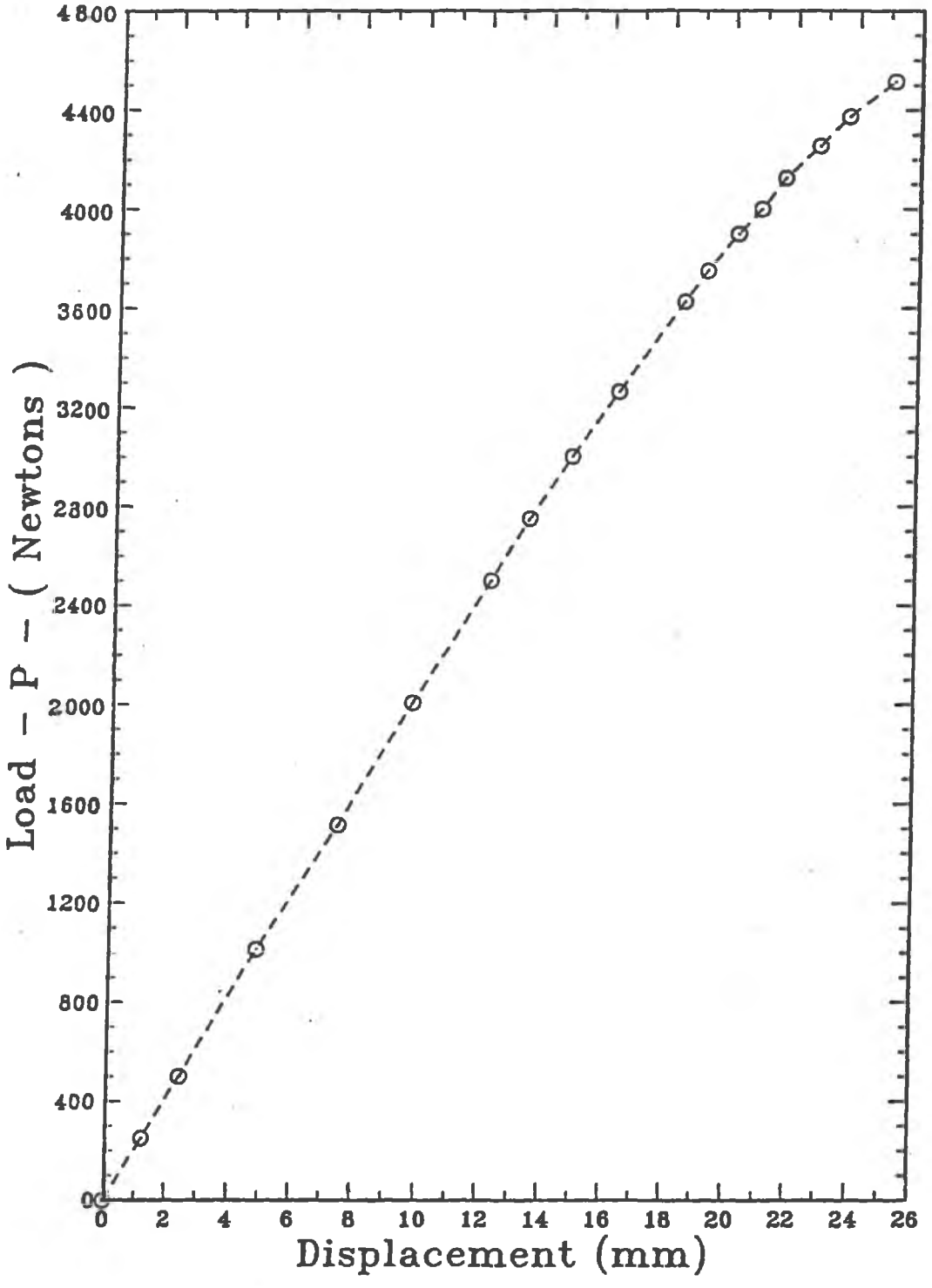

Figure 3.32L Load Versus Midspan Deflection for Specimen 6-BW-12

be linear up until the last few load increments just prior to failure. This non-linearity is not important since the design of a steel stud is usually based on a maximum allowable deflection which would be well within the linear portion of the curves.

For Series 6B the average midspan deflections of the two studs are plotted for each test as shown by Figures 3.32G to 3.32L. The first three figures are for the 20 gauge specimens while the last three are for the 18 gauge specimens. Like Series 6A, a linear relationship is evident in all of the tests until just prior to failure.

3.5.7.4 Description of Failures

Specimens 6-BW-1 to 6-BW-4 all failed when the top compression flange of one or both studs buckled in the midspan region of the two stud beam specimen. For tests 6-BW-5 and 6-BW-6, buckling of the compression flange of one or both studs occurred in the region of a web cut-out hole in the region of maximum moment. In series 6B all the specimens failed when the compression flange of one or both studs buckled at or near the midspan of the member.

3.5.8 Test Series 7

3.5.8.1 Details Of Panels

Seven, 2 stud wide steel stud panels were fabricated for this series. Specimens 7-BW-1 to 7-BW-5 were fabricated with 20 gauge steel studs. Four of the panels were braced at midspan with interior bridging fastened to each stud in a similar manner as the panels tested in Series 1. However, test specimen 7-BW-4 was not braced at midspan. These specimens were also sheathed with 12 mm thick gypsum board attached to both the interior and exterior faces of the panels.For specimens 7-BW-1 to 7-BW-3, the interior and exterior sheathing was attached to the stud flanges with S-12 drywall screws spaced at 305 mm on centre. The screw spacing was 150 mm for specimens 7-BW-4 and 7-BW-5. A typical fabricated panel is shown in Figure 3.33.

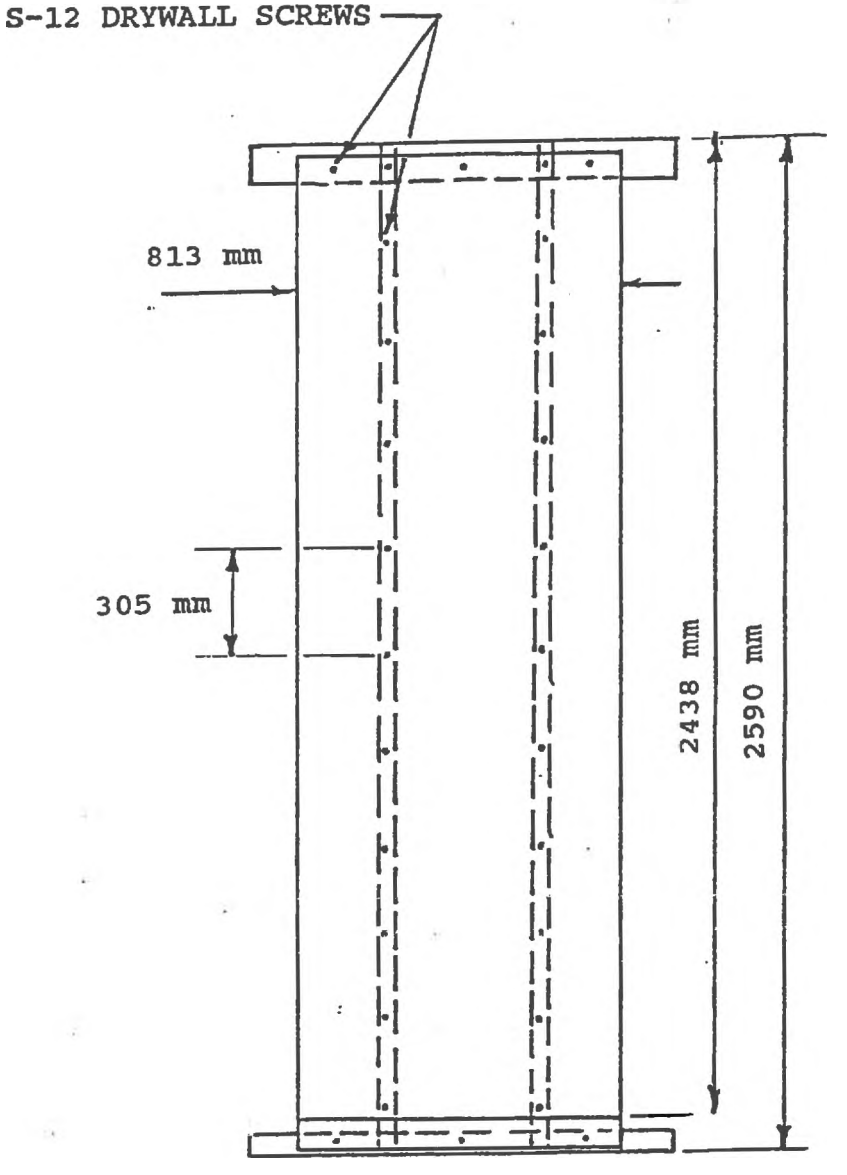

Figure 3.33 Typical Fabricated Panel Used in Series 7

Specimens 7-BW-6 and 7-BW-7 were fabricated with 18 gauge studs. Specimen 7-BW-6 was not braced at midspan with steel bridging. Specimen 7-BW-7 was braced at midspan with a line of face bridging on the compression flange. Both panels were sheathed with 12 mm gypsum board on the exterior and interior faces and fastened to the stud flanges with S-12 drywall screws spaced 305 mm on centre.

3.5.8.2 Special Test Conditions

Each fabricated specimen was attached to the test frame in a similar manner as for the test specimens in Series 5. A similar loading arrangement was also employed since it had been determined that no additional bracing occurred at the loading points using this system. Each panel was loaded in a cyclic manner using the hydraulic jack. The load was incrementally increased to approximately 60 percent of the expected panel strength. Deflection measurements were taken at the panel centreline and at the ends of the steel studs. The load was then removed and the panel was allowed to return to its unloaded state. The next load cycle was applied and the procedure was repeated. After every ten load cycles, deflection readings were also taken in order to determine if any residual panel deflection had occurred.

A special feature used in the testing of Specimen 7-BW-5 was that the exterior gypsum board sheathing was wetted prior to the test. This was accomplished by spraying a fine mist of water on the exterior facing paper of the gypsum board. The exterior sheathing was repeatedly sprayed over a period of 12 hours prior to testing in order to allow some absorbtion of the water. A small cut was made in the drywall sheathing in order to check whether the gypsum underneath the paper had aborbed any moisture. Since the gypsum felt damp to the touch, it was concluded that absorbtion had taken place. The panel was then subjected to 20 cycles of load and was allowed to dry for 24 hours after which it was subjected to another cycle of loading. This was done to determine whether any increase in panel stiffness occurred once the drywall was allowed to dry. The exterior sheathing was then wetted again and the cyclic loading of the panel was continued.

Specimens 7-BW-6 and 7-BW-7 were fabricated with 18 gauge steel studs. The loading arrangement which had been used previously for the first five tests was judged not to be strong enough to load these panels due to possible collapse of the brick ties before the tests were completed. Therefore the loading arrangement shown in Figure 3.34 was used. The test procedure followed that which was outlined for the first five panels.

3.5.8.3 Results Of Tests

For the 20 gauge steel stud wall panels, Specimens 7-BW-1 to 7-BW-5, the average midspan panel flexural deflection, Δa, is plotted against load cycle in Figure 3.25. The average midspan panel deflection was obtained in a similar manner as in Series 4. For each test, the average midspan panel deflections shown in Figure 3.25 were obtained when a total load of 1.63 KN was applied to each steel stud in the panel.

For specimens 7-BW-6 and 7-BW-7, the average midspan deflection of each panel is plotted against load cycle in Figure 3.26. Each value of Δa shown in Figure 3.26 was obtained when a total load of 2.9 KN was applied to each stud in the panel. As shown by these two curves, some loss in panel stiffness occurred as the panel were cyclically loaded. Also shown in this figure is the average midspan deflection obtained from the results for the 18 gauge specimens tested in Series 6.

An examination of Figure 3.25 showed that the 20 gauge studs sheathed with gypsum board fastened every 150 mm on centre were slightly stiffer than the wall panels that had the gypsum board attached every 300 mm on centre. This figure also showed that some loss of composite action occurred when the wall panels were subjected to a cyclic loading condition. Figure 3.25 also shows that very little composite action occurred when the gypsum board was wetted. It is interesting to note that after 20 cycles of loading the gypsum board was allowed to dry for approximately 24 hours, some minor increase in panel stiffness occurred but quickly disappeared after a few more load cycles.

In order to have a more meaningful comparison each average panel deflection, Δa, obtained for the 20 gauge panel in Series 7 was divided by the average midspan deflection of the 20 gauge steel studs, Δb, tested in Series 6. It should be noted that a direct comparison could be made since identical loading conditions existed in both series. These ratios are listed in Table 3.2 for specific load cycles. For Specimens 7-BW-1 and 7-BW-2, an initial increase in panel stiffness of approximately 8.5 to 11 percent was obtained. After only ten load cycles however, the increase in panel stiffness was found to be 2.3 to 7.7 percent. For Specimens 7-BW-3 and 7-BW-4, the number of drywall screws used to attach the sheathing was double that of the previous two tests. This caused an initial increase in panel stiffness of approximately 17 percent for these two panels. After 25 load cycles, the increase in panel stiffness had decreased to be 12.2 to 15.2 percent. For Specimen 7-BW-4, after 75 load cycles, the panel stiffness was still 11.4 percent greater than a panel with no sheathing. For Specimen 7-BW-5, which had wetted gypsum board fastened to the compression face of the studs, an initial increase in panel stiffness of 5.5 percent was obtained. After 50 load cycles, the additional increase in panel stiffness was found to be only 2.5 percent.

For test Specimens 7-BW-6 and 7-BW-7 the average midspan flexural panel deflection, Δa, of each of these 18 gauge panel was divided by the average midspan deflection of the 18 gauge steel studs tested in Series 6.

In Table 3.2 the ratio Δa/Δb for tests 7-BW-6 and 7-BW-7 indicated that an increase of panel stiffness of 7.4 to 11.7 percent occurred initially. After 50 load cycles this had decreased to 4.6 to 7.4 percent.

3.5.8.4 Description Of Failures

Failure of Specimens 7-BW-1 and 7-BW-2 occurred when the compression flange of one of the studs buckled at the midspan bridging location.

TABLE 3.2

SUMMARY OF PANEL STIFFNESS DEGRADATION

Test Number	Δa/Δb Cycle 1	Δa/Δb Cycle 10	Δa /Δb Cycle 25	Δa/Δb Cycle 30	Δa/Δb Cycle 50	Δa/Δb Cycle 75
7-BW-1	0.915	0.977				
7-BW-2	0.893	0.923	0.937			
7-BW-3	0.831	0.834	0.878			
7-BW-4	0.830		0.848			0.886
7-BW-5*	0.945	0.979	0.953		0.975	
7-BW-6**	0.883	0.889		0.902	0.926	
7-BW-7**	0.926	0.934		0.946	0.954	

* - Wetted exterior drywall

** - 18 Gauge stud panels

Failure of Specimen 7-BW-3 occurred when both studs buckled in the region of the web cut-out hole located at the quarter point near the top of the panel. Wall panel 7-BW-4 failed when one of the compression flanges of the stud buckled at the midspan bridging location.

For Specimen 7-BW-5, the exterior face of the studs were sheathed with exterior gypsum board which had been wetted. The panel had also been braced at midspan. Although the wetted gypsum board did provide some additional bracing to the top flange, it did not perform as well as in the other tests. Failure was initiated when the studs started to twist. At this point the exterior gypsum board was observed to yield around each of the drywall screws.The compression flange of both studs buckled at the midspan bridging location immediately after the studs started to twist.

For test 7-BW-6 no midspan bridging was used. Bracing was provided by the gypsum board sheathing fastened every 300 mm on centre. Failure was initiated when one of the studs twisted and pulled the screws out of the gypsum board. This immediately caused the stud to buckle in the region of one of the web cut-out holes. For Specimens 7-BW-7, which had been braced at midspan, the failure of the panel occurred when one of the studs buckled in the region of the web cut-out hole, located 940 mm from the bottom track.

3.6 Discussion of Results and Conclusions

Since a more detailed analysis of the test results will be performed in Chapter 4, only a few general conclusions will be drawn from the results presented in this chapter. Some comments will also be given based on observations made during testing of the wall panels. In general, as the number of lines of bridging increased there was a corresponding increase in the load carrying capacity of the steel studs.

In Series 5, steel bridging was not provided for the 20 and 18 gauge backup wall specimens tested. From the results shown in Table 3.1, for these tests it was found that the studs were only 26 to 33 percent efficient in carrying transverse loads and/or moment when

compared to the beam test results of Series 6B. In addition, as shown in Figures 3.28A to 3.28D, large rotations occurred at the midspan of the steel studs.

For Series 1, 2, and 3, the 20 and 18 gauge specimens tested were braced with either one or two lines of steel bridging. This effectively increased the load carrying capacity to approximately 60 and 80 percent of the full capacity for the 20 and 18 gauge steel studs respectively, with one line of bridging at midspan. With two lines of bridging, one at each quarter point, the results showed an increase in load carrying capacity to approximately 84 and 90 percent of the full capacity for the 20 and 18 gauge steel studs respectively. The steel stud rotations decreased significantly with the addition of the steel bridging.

Examination of Figures 3.14A to 3.14G showed that for a L/360 midspan deflection, the rotations which occurred were no larger than 2 to 3 degrees for the 20 gauge specimens and 1 to 2 degrees for the 18 gauge specimens. The commentary for the Canadian Code for cold formed steel structural members[7], suggests that steel bridging should be spaced at intervals no greater than that which will allow rotations in the order of 2 degrees. Rotations of magnitude greater than 2 degrees are thought to be objectionable in terms of serviceability requirements. For the backup wall panels tested with one line of bridging, the clear span between the midspan brace and either of the end supports was approximately 1280 mm. This would suggest that in order to limit rotations to a few degrees at service loads, the steel studs would have to be braced at intervals of 1280 mm or less. This will be discussed further in Chapter 4 as the spacing of braces will also depend on the strength requirements of the backup wall panels.

For the Series 7 panels sheathed with gypsum board on both faces, the capacity of the steel studs were increased to approximately the full flexural capacity. However, most of these panels were also braced at midspan with a line of bridging. In test 7-BW-5, the wetted exterior gypsum board was not as effective for bracing the steel studs as was undamaged gypsum board. The composite action provided by the gypsum board sheathing was also investigated

and it was found that under the most favourable conditions of tests 7-BW-3 and 7-BW-4, a 17 percent increase in the initial panel stiffness was obtained.

In the above two tests, the screws were spaced every 150 mm on centre. As the spacing between the fasteners increased, the initial composite action was found to decrease to approximately 10 percent or less. In all cases the initial increase in panel stiffness was found to decrease after just a few load cycles. For this test program the gypsum board had been installed in one continuous sheet, 2.44 meters long. A small end piece had been fitted to make up the remaining panel height. For most field installations the gypsum board sheathing may not be continuous. Rather, several pieces may be fastened to the steel stud along the height. Under this condition even less composite action would be anticipated. Other factors such as improper screw installation, damaged or wet gypsum board, would all tend to decrease the composite action even further.

In terms of bridging connections tested, it was found that the screwed clip angle connection shown in Figure 3.14 did increase the failure load to 60% or more of the flexural capacity of the stud if four screws were used to make the connection. It was observed that when the screws connecting the clip angle to the web of the stud were placed closer to the bend, less bending of the clip angle occurred. For these tests the 16 gauge clip angle used was found to be adequate. Preliminary tests with thinner clips showed that significant clip bending occurred. However, there is a practical limit on how close the screws can be located to the bend in the clip angle. Based on the above facts it was concluded that the clip should be made of 16 gauge material or thicker and that the screws should be placed no further than one-third the distance of the leg, away from the bend. In order to control the screw location, pre-drilled holes should be provided in the leg of the clip angle which is connected to the web of the steel stud. The holes should be as far apart as possible since this would minimize the pullout force on the screws. Also, the clip angle should be approximately the same depth as the steel stud.

The welded connection detail, shown in Figure 3.21, was found to provide the stiffest connection as it allowed little to no rotation at the bridging location. This method should be

considered for deeper and heavier steel studs since it is theoretically the strongest connection and would not be affected by improper installation or potential pullout of the screws.

The notched face bridging used in tests 2-BW-1 to 2-BW-5 was also found to increase failure load to a high percentage of the flexural capacity. However, care must be used to ensure that the ends of the lines of steel bridging are properly fastened to a building column or wall. This is necessary since it was found during a preliminary test that this type of bridging was not effective unless the ends of the bridging were adequately fastened. In general, the ends of any type of steel bridging should be adequately anchored.

The final item to be discussed deals with some visual observations made during the initial stages of the test program. When the steel studs arrived at the laboratory, it was oberved that a significant number of 20 gauge studs had sustained some visible damage. This was thought to have occurred due to the shipping and handling. An examination of the 18 gauge steel studs showed very little damage. During the fabrication process, it was also noticed that improper torquing of the sheet metal screws often led to stripped holes at the stud to track connection. This was more apparent in the 20 gauge material. Visits to some job sites in which steel studs were used inidicated that the 20 gauge steel studs sustained more damage on the site than the heavier gauges.

The above considerations as well as concern for tie connections and long term durability has contributed to the general conclusion that recommendations for good construction practice should specify 18 gauge minimum thickness.

CHAPTER 4

ANALYSIS OF STEEL STUD BACKUP WALLS

4.1 INTRODUCTION

Both the Ultimate Limit State and the Serviceability Limit States must be considered in design of BV/SS wall systems. Crack and deflection control are Serviceability Limit States and will be examined in Chapter 5. This chapter is focused on the ultimate strength of the steel stud backup walls where after cracking of the veneer, the backup wall is required to resist almost all of the lateral load. As part of the analytical study, the results of the experimental test program were evaluated. In addition, steel stud wall configurations not covered in the test program were also analyzed.

4.2 EVALUATION OF CONNECTION TEST RESULTS

4.2.1 Web Crippling Of Steel Studs Due To End Bearing

The results obtained in this part of the test program indicated that local web crippling at the end of the studs was a possible mode of failure. This is due to the fact that the steel stud must transfer the lateral wind load to the supporting top and bottom tracks. If the resulting end reactions are large enough, the local stress concentrations can cause web crippling.

Web crippling at the end of a steel stud can be thought of as the buckling of a thin, flat rectangular plate subjected to loads distributed over short segments of the plate edges. This type of problem has been extensively studied in the past by numerous investigators and the reader is referred to Reference 17 for a complete discussion and review of these analytical studies. However Yu[33] stated that the theoretical analysis of web crippling for cold rolled steel beams is further complicated by:

1. "Nonuniform stress distribution under the applied load and adjacent portions of the web.
2. Elastic and inelastic stability of the web element.

3. Local yielding in the immediate region of the load application.
4. Bending produced by eccentric load or reaction when it is applied on the bearing flange.
5. Initial out-of-plane imperfections of plate elements.
6. Various edge restraints provided by beam flanges and interaction between flange and web elements."

Because of the above mentioned factors, the present cold formed steel design provisions in CAN3-S136-M84, are based on semi-empirical equations which were essentially derived from the experimental work of Yu and Hetnakul[17], Winter and Pian[32] and Zetlin[35]. The work of Yu is the most recent and incorporated the other previously mentioned experimental studies. For end web crippling failure of a single unreinforced web, Yu derived the following equations.

1. Beams with stiffened flanges :

$$P_u = t^2(F_y/10^3)C_3\,C_4[1.0018-18.24(h/t)]\,[1+0.0102(n/t)] \qquad (4.1)$$

2. Beams with unstiffened flanges :

$$P_u = t^2(F_y/10^3)C_3\,C_4[6570-8.51(h/t)][1+0.0099(n/t)] \qquad (4.2)$$

where

$C_3 = (1.33-0.33k)$

$C_4 = (1.15-0.15R)$

$k = F_y/33$

$R = r/t$

n = bearing length (in)

t = thickness of web (in)

F_y = tensile yield strength (ksi)

r = inside bend radius at web to flange stud junction (in)

h = clear distance between the flats of the flanges measured in the plane of the web (in)

The parameters used in the above equations are limited to the following conditions:

1. $h/t < 200$

2. $n/t < 60$

3. F_y ranging from 33 to 54 k.s.i.

4. Corner radii $< 4t$

5. $n/h < 1$

For steel stud wall applications however, the sizes and thickness usually fall well within the limitations listed above.

The above equations form the basis for the current Canadian code equations[6] which are written as :

For stiffened flange :

$$Pr = \phi_s\, 10\, t^2\, F_y(1.33\text{-}0.33k)(1.15\text{-}0.15R)(1+0.01n/t)(1\text{-}0.0018H) \qquad (4.3)$$

For unstiffened flange :

$$Pr = \phi_s\, 6.6\, t^2\, F_y(1.33\text{-}0.33k)(1.15\text{-}0.15R)(1+0.01n/t)(1\text{-}0.0013H) \qquad (4.4)$$

where,

ϕ_s = Resistence factor for web crippling in beams with a single unreinforced web and is equal to 0.80.

$H = h/t$

n = bearing length (mm)

F_y = tensile yield strength (MPa)

$k = F_y/230$

r = inside bend radius (mm)

n = bearing length (mm)

The other constants are the same as defined previously.

Equations 4.3 and 4.4 are essentially the S136[6] of Equations 4.1 and 4.2 multiplied by a resistence factor of 0.8.

4.2.2 Comparison of Experimental and Predicted Web Crippling Loads

The experimental and predicted ultimate loads for web crippling at the stud end were compared for all the specimens in this phase of the test program. The results are shown in Table 4.1. For each test specimen the predicted failure load, P_u, was calculated using a resistance factor of 1.0 in Equation 4.3. The physical parameters used in this equation are listed in Table 4.2 for each of the test specimens. In some of the tests, web crippling did not occur at the track to stud junction. Instead, failure of the stud under the top flange loading plate or by other means described earlier in Section 2.3.4 caused unloading of the specimen. For each of these tests, the experimental result is marked by an asterisk in Tables 4.1 and represents the maximum load attained at the stud to track connection before the specimen failed.

Equations 4.3 and 4.4 were derived for the case where the minimum clear distance between the edge of the bearing plates, for the top flange concentrated load and the edge of the end reaction was not less than 1.5 times the clear distance, h, between flanges. For some tests, the clear distance was slightly less than 1.5h but Equation 4.3 was found to give adequate results even for this condition. The actual clear distance between the interior top plate and the edge of the track are listed in Column 6 of Table 4.2.

The last column in Table 4.1 is the ratio of the experimental failure load, P_{test} to the ultimate predicted load, P_u. For all tests specimens, this ratio was greater than one. The mean value of P_{test}/P_u was found to be 1.335 with a standard deviation of 0.162. (Note: $\phi = 1$ for P_u calculation.) As stated in Reference 17, the accuracy of prediction using Equations 4.1 and 4.2 were expected to be within ± 20 percent. Based on this degree of accuracy, use of Equation 4.1 or 4.3 with a resistence factor of 1.0 was found to provide a reasonable estimate of the experimental web crippling strengths. An examination of Tables 4.1 also showed that on average the web crippling strength of the steel stud specimens fastened to the supporting steel track with two screws was greater than when one screw was used. For Series D7 and D8, no

TABLE 4.1

COMPARISON OF EXPERIMENTAL AND PREDICTED FAILURE LOADS FOR STUD TO TRACK CONNECTIONS

Specimen no.	P_{test} (KN)	P_u (KN)	$\frac{P_{test}}{P_u}$
20A-D1-1	2.997	2.325	1.29
20A-D1-2	2.680	2.325	1.15
20A-D1-3	3.010	2.325	1.29
20A-D1-4	2.661	2.325	1.14
20A-D1-5	3.044	2.325	1.31
20A-D1-6	2.889	2.325	1.24
20A-D1-7	2.600	2.325	1.12
20A-D1-8	2.550	2.325	1.10
20A-D1-9	2.986	2.325	1.28
18A-D1-1	4.971	4.289	1.16
18A-D1-2	4.767	4.289	1.11
18A-D1-3	4.951	4.289	1.15
18A-D1-4	4.473	4.289	1.04
18A-D1-5	4.554	4.289	1.06
20B-D1-1	2.480	2.001	1.24
20B-D1-2	2.630	2.001	1.31
20B-D1-3	2.840	2.001	1.41
20B-D1-4	2.470	2.001	1.23
20B-D1-5	2.800	2.001	1.40
20B-D1-6	2.674	2.001	1.34
18B-D1-1	4.300	3.864	1.11
18B-D1-2	4.740	3.864	1.23
18B-D1-3	4.545	3.864	1.18
18B-D1-4	4.292	3.864	1.11
18B-D1-5	4.624	3.864	1.20
18B-D1-6	4.082	3.864	1.06
20A-D2-1	2.588	2.103	1.23
20A-D2-2	2.900	2.103	1.38
20A-D2-3	2.770	2.103	1.32
20A-D2-4	2.976	2.103	1.42
20B-D2-1	2.410	1.811	1.33
20B-D2-2	2.650	1.811	1.46
20B-D2-3	2.411	1.811	1.33
20B-D2-4	2.520	1.811	1.39

TABLE 4.2

PARAMETERS FOR STUD TO TRACK TEST SPECIMENS

Specimen No.	n[1] (mm)	h[1] (mm)	t (mm)	r[1] (mm)	a (mm)	F_y[2] (MPa)
20A-D1-1	30.81	90.18	0.95	1.90	1.50h	287.9
20A-D1-2	30.81	90.18	0.95	1.90	1.50h	287.9
20A-D1-3	30.81	90.18	0.95	1.90	1.50h	287.9
20A-D1-4	30.81	90.18	0.95	1.90	1.50h	287.9
20A-D1-5	30.81	90.18	0.95	1.90	1.50h	287.9
20A-D1-6	30.81	90.18	0.95	1.90	1.50h	287.9
20A-D1-7	30.81	90.18	0.95	1.90	1.50h	287.9
20A-D1-8	30.81	90.18	0.95	1.90	1.50h	287.9
20A-D1-9	30.81	90.18	0.95	1.90	1.50h	287.9
18A-D1-1	30.50	89.55	1.27	2.53	1.50h	287.9
18A-D1-2	30.50	89.55	1.27	2.53	1.50h	287.9
18A-D1-3	30.50	89.55	1.27	2.53	1.50h	287.9
18A-D1-4	30.50	89.55	1.27	2.53	1.50h	287.9
18A-D1-5	30.50	89.55	1.27	2.53	1.50h	287.9
20B-D1-1	30.81	151.00	0.95	1.90	1.27h	287.9
20B-D1-2	30.81	151.00	0.95	1.90	1.27h	287.9
20B-D1-3	30.81	151.00	0.95	1.90	1.27h	287.9
20B-D1-4	30.81	151.00	0.95	1.90	1.27h	287.9
20B-D1-5	30.81	151.00	0.95	1.90	1.27h	287.9
20B-D1-6	30.81	151.00	0.95	1.90	1.27h	287.9
18B-D1-1	30.50	150.38	1.27	2.53	1.25h	306.9
18B-D1-2	30.50	150.38	1.27	2.53	1.25h	306.9
18B-D1-3	30.50	150.38	1.27	2.53	1.25h	306.9
18B-D1-4	30.50	150.38	1.27	2.53	1.50h	306.9
18B-D1-5	30.50	150.38	1.27	2.53	1.25h	306.9
18B-D1-6	30.50	150.38	1.27	2.53	1.25h	306.9
20A-D2-1	18.81	90.18	0.95	1.90	1.50h	287.9
20A-D2-2	18.81	90.18	0.95	1.90	1.50h	287.9
20A-D2-3	18.81	90.18	0.95	1.90	1.50h	287.9
20A-D2-4	18.81	90.18	0.95	1.90	1.50h	287.9
20B-D2-1	18.81	151.00	0.95	1.90	1.25h	287.9
20B-D2-2	18.81	151.00	0.95	1.90	1.25h	287.9
20B-D2-3	18.81	151.00	0.95	1.90	1.25h	287.9
20B-D2-4	18.81	151.00	0.95	1.90	1.25h	287.9

TABLE 4.1 (continued)

Specimen no.	P_{test} (KN)	P_u (KN)	$\frac{P_{test}}{P_u}$
18A-D7-1	4.329	4.289	1.01
18A-D7-2	4.815	4.289	1.12
18A-D7-3	UNR.	4.289	
18A-D8-1	5.176	3.962	1.31
18A-D8-2	4.444	3.962	1.12
18A-D8-3	4.844	3.962	1.22
18A-D9-1	4.378	4.289	1.02
18A-D9-2	4.148	4.289	0.97
18A-D9-3	UNR.	4.289	
20A-D10-1	3.132	2.307	1.36
20A-D10-2	3.059	2.307	1.33
20A-D10-3	3.022	2.307	1.31
20B-D11-1	3.090	1.997	1.55
20B-D11-2	3.056	1.997	1.53
20B-D11-3	3.359	1.997	1.68
20A-D12-1	2.903	2.882	1.01
20A-D12-2	2.825	2.882	0.98
20A-D12-3	3.058	2.882	1.06
20B-D12-1	2.359	2.522	0.94
20B-D12-2	2.694	2.522	1.07
20B-D12-3	2.449	2.522	0.97
18B-D13-1	4.575	3.864	1.18
18B-D13-2	5.022	3.864	1.30
18B-D13-3	5.790	3.864	1.50
18A-D13-1*	5.700	4.289	1.33
18A-D13-2*	4.937	4.289	1.15
18A-D13-3*	4.823	4.289	1.12
18A-D13-4*	4.791	4.289	1.12
18A-D13-5*	4.776	4.289	1.11
18A-D13-6*	4.849	4.289	1.13

TABLE 4.1 (continued)

Specimen no.	P_{test} (KN)	P_u (KN)	$\frac{P_{test}}{P_u}$
18A-D2-1	4.817	3.962	1.21
18A-D2-2	4.760	3.962	1.20
18A-D2-3	4.565	3.962	1.15
18A-D2-4	4.461	3.962	1.13
18B-D2-1	4.269	3.569	1.20
18B-D2-2	4.102	3.569	1.15
18B-D2-3	3.901	3.569	1.09
20A-D3-1	2.422	2.325	1.04
20A-D3-2	2.837	2.325	1.22
20A-D3-3	2.615	2.325	1.12
20A-D3-4	2.429	2.325	1.04
18A-D3-1	4.385	4.289	1.02
18A-D3-2	4.415	4.289	1.03
18A-D3-3	4.540	4.289	1.06
18A-D3-4	4.110	4.289	0.96
20B-D3-1	2.344	2.001	1.17
20B-D3-2	2.271	2.001	1.13
20B-D3-3	2.280	2.001	1.14
18B-D3-1	4.155	3.864	1.08
18B-D3-2	3.734	3.864	0.97
18B-D3-3	3.969	3.864	1.03
18A-D4-1	3.811	4.289	0.89
18A-D4-2	4.600	4.289	1.07
18A-D4-3	4.478	4.289	1.04
18A-D4-4	4.644	4.289	1.08
20A-D5-1	2.284	2.103	0.09
20A-D5-2	2.050	2.103	0.97
20A-D5-3	2.560	2.103	1.21
20A-D5-4	2.522	2.103	1.20
20B-D6-1	2.218	2.001	1.11
20B-D6-2	2.555	2.001	1.28

TABLE 4.2 (continued)

Specimen No.	n[1] (mm)	h[1] (mm)	t (mm)	r[1] (mm)	a (mm)	F_y[2] (MPa)
18A-D2-1	18.50	89.55	1.27	2.53	1.50h	306.9
18A-D2-2	18.50	89.55	1.27	2.53	1.50h	306.9
18A-D2-3	18.50	89.55	1.27	2.53	1.50h	306.9
18A-D2-4	18.50	89.55	1.27	2.53	1.50h	306.9
18B-D2-1	18.50	150.38	1.27	2.53	1.25h	306.9
18B-D2-2	18.50	150.38	1.27	2.53	1.43h	306.9
18B-D2-3	18.50	150.38	1.27	2.53	1.25h	306.9
20A-D3-1	30.81	90.18	0.95	1.90	1.50h	287.9
20A-D3-2	30.81	90.18	0.95	1.90	1.50h	287.9
20A-D3-3	30.81	90.18	0.95	1.90	1.50h	287.9
20A-D3-4	30.81	90.18	0.95	1.90	1.50h	287.9
18A-D3-1	30.50	89.55	1.27	2.53	1.50h	306.9
18A-D3-2	30.50	89.55	1.27	2.53	1.50h	306.9
18A-D3-3	30.50	89.55	1.27	2.53	1.50h	306.9
18A-D3-4	30.50	89.55	1.27	2.53	1.50h	306.9
20B-D3-1	30.81	151.00	0.95	1.90	1.50h	287.9
20B-D3-2	30.81	151.00	0.95	1.90	1.43h	287.9
20B-D3-3	30.81	151.00	0.95	1.90	1.43h	287.9
18B-D3-1	30.50	150.38	1.27	2.53	1.50h	306.9
18B-D3-2	30.50	150.38	1.27	2.53	1.25h	306.9
18B-D3-3	30.50	150.38	1.27	2.53	1.43h	306.9
18A-D4-1	30.50	89.55	1.27	2.53	1.50h	306.9
18A-D4-2	30.50	89.55	1.27	2.53	1.50h	306.9
18A-D4-3	30.50	89.55	1.27	2.53	1.50h	306.9
18A-D4-4	30.50	89.55	1.27	2.53	1.50h	306.9
20A-D5-1	18.81	90.18	0.95	1.90	1.50h	287.9
20A-D5-2	18.81	90.18	0.95	1.90	1.50h	287.9
20A-D5-3	18.81	90.18	0.95	1.90	1.50h	287.9
20A-D5-4	18.81	90.18	0.95	1.90	1.50h	287.9
20B-D6-1	30.81	151.00	0.95	1.90	1.25h	287.9
20B-D6-2	30.81	151.00	0.95	1.90	1.25h	287.9

TABLE 4.2 (continued)

Specimen No.	n[1] (mm)	h[1] (mm)	t (mm)	r[1] (mm)	a (mm)	F_y[2] (MPa)
18A-D7-1	30.50	89.55	1.27	2.53	1.50h	306.9
18A-D7-2	30.50	89.55	1.27	2.53	1.50h	306.9
18A-D7-3	30.50	89.55	1.27	2.53	1.50h	306.9
18A-D8-1	18.50	89.55	1.27	2.53	1.50h	306.9
18A-D8-2	18.50	89.55	1.27	2.53	1.50h	306.9
18A-D8-3	18.50	89.55	1.27	2.53	1.50h	306.9
18A-D9-1	30.50	89.55	1.27	2.53	1.50h	306.9
18A-D9-2	30.50	89.55	1.27	2.53	1.50h	306.9
18A-D9-3	30.50	89.55	1.27	2.53	1.50h	306.9
20A-D10-1	29.86	90.18	0.95	1.90	1.50h	287.9
20A-D10-2	29.86	90.18	0.95	1.90	1.50h	287.9
20A-D10-3	29.86	90.18	0.95	1.90	1.50h	287.9
20B-D11-1	30.50	151.00	0.95	1.90	1.43h	287.9
20B-D11-2	30.50	151.00	0.95	1.90	1.43h	287.9
20B-D11-3	30.50	151.00	0.95	1.90	1.50h	287.9
20A-D12-1	60.77	90.18	0.95	1.90	1.50h	287.9
20A-D12-2	60.97	90.18	0.95	1.90	1.50h	287.9
20A-D12-3	60.97	90.18	0.95	1.90	1.50h	287.9
20B-D12-1	60.97	151.00	0.95	1.90	1.50h	287.9
20B-D12-2	60.97	151.00	0.95	1.90	1.50h	287.9
20B-D12-3	60.97	151.00	0.95	1.90	1.50h	287.9
18B-D13-1	30.50	150.38	1.27	2.53	1.50h	306.7
18B-D13-2	30.50	150.38	1.27	2.53	1.50h	306.7
18B-D13-3	30.50	150.38	1.27	2.53	1.50h	306.7
18A-D13-1	30.50	89.55	1.27	2.53	1.50h	306.7
18A-D13-2	30.50	89.55	1.27	2.53	1.50h	306.7
18A-D13-3	30.50	89.55	1.27	2.53	1.50h	306.7
18A-D13-4	30.50	89.55	1.27	2.53	1.50h	306.7
18A-D13-5	30.50	89.55	1.27	2.53	1.50h	306.7
18A-D13-6	30.50	89.55	1.27	2.53	1.50h	306.7

1. Catalogue values, not measured.
2. F_y = average value obtained from tensile tests on coupons cut from webs of studs. (specified yield strength = 228 MPa[6])

bearing failure was found to occur at the stud to track connection. This was due to fact that the end reaction was not transferred from the end of the stud to the track by direct bearing of the stud end on the track flange. For the tests of welded stud to track connections, Series D12, web crippling did occur in some of these tests and Equation 4.1 was shown to give a conservative estimate of the web crippling strength of these specimens.

Since web crippling was shown to be a possible mode of failure, this should be considered when designing the steel stud backup wall. Equations 4.3 and 4.4 with an appropriate resistance factor should be used.

4.3 EVALUATION OF STEEL STUD BACKUP WALL TESTS RESULTS

4.3.1 Moment Resisting Capacity Of Steel Stud

In Series 6, beam tests were performed to evaluate the moment capacity of cold rolled steel studs. Since each of the beams tested in this series consisted of two steel studs, the total applied load was divided by two to obtain the load applied to each steel stud. The series was divided into two parts. In Series 6A, each steel stud of a typical beam specimen was symmetrically loaded by four equal transverse loads. The total failure per steel stud was listed in Table 3.1 for each test. Since each steel stud was simply supported, the maximum applied bending moment, M_a, was easily calculated from statics.

For Series 6B, each steel stud of a typical beam specimen was symmetrically loaded by two equal transverse loads. For each of these tests the total failure load per steel stud was also listed in Table 3.1. The applied bending moment, M_a, for the simply supported steel stud was determined from statics.

The resulting applied bending moments for Series 6A and 6B are listed in column 3 of Table 4.3. As a benchmark for comparison, the resisting moment at yield stress, M_r,was calculated for each type of steel stud tested using elastic plane section bending theory:

$$M_r = S_{xx} F_y \tag{4.5}$$

where the section modulus, S_{xx}, was taken at the perforated section since it was observed during the tests that the steel studs normally failed at a web cut-out hole located in the zone of maximum applied bending moment. The values of S_{xx} are listed in Table 4.4. The yield point, F_y, of the virgin steel used in the fabrication of the steel stud specimens was established by standard tensile tests conforming to A.S.T.M. Standard A370. Two tests were performed for each of the 18 and 20 gauge steel materials. Both values of yield stress are listed in Table 4.4 and for each gauge of steel stud specimens, the two corresponding values of M_r were obtained and are listed in Table 4.3. This resulted in the range of ratios of M_a/M_r given in column 5 of Table 4.3.

As described in Section 3.5.7.1, each specimen tested in Series 6 consisted of two steel studs placed back to back. Therefore it was expected that the full yield moment of each steel stud would be obtained since torsional loads had been minimized in this test setup. An inspection of column 5 in Table 4.3 showed that the full yield moment was obtained in Series 6A and that, in Series 6B, the full yield moment was obtained for some tests and nearly attained for others. A likely reason that the full moment capacity was not obtained in some tests of Series 6B may be associated with some observed slight twisting between the two load points. This could have been caused by accidental load eccentricity which would weaken the steel studs slightly. In Series 6A, the studs were braced at the four load point locations and any small load eccentricity which may have occurred would not have had as detrimental an effect on the moment capacity of the steel stud. The closer spacing of the braces would significantly reduce any tendency of the steel stud to twist.

Not withstanding the above, it was concluded that,for all practical purposes the full moment capacity of the steel studs were attained in these tests.

TABLE 4.4

SECTION AND MATERIAL PROPERTIES OF STEEL STUDS

Section Properties†

Stud Type	a (mm)	b (mm)	c (mm)	d (mm)	t (mm)
20 gauge	92.08	34.93	9.53	38.1	0.95
18 gauge	92.08	41.28	12.70	38.1	1.26

Unperforated Properties*

	Cross-Sectional Area	I_{xx} (mm^4)	I_{yy} (mm^4)	J (mm^4)	Cw ($mm^6 \times 10^6$)
20 gauge	164.4	214734.0	26639.0	49.5	45.3
18 gauge	240.0	322163.1	57440.0	131.9	103.9

	Wn_1++ (mm^2)	Wn_2++ (mm^2)	Wn_3++ (mm^2)
20 gauge	1264.5	813.0	735.5
18 gauge	1613.0	884.0	935.5

Perforated Properties*

	Cross-Sectional Area (mm^2)	I_{xx} (mm^4)	I_{yy} (mm^4)	S_{xx} (mm^3)
20 gauge	128.2	210197.0	22019.0	4565.5
18 gauge	191.8	316539.0	47502.0	6875.3

Material Properties**

	Yield Stress (MPa)	E*** (MPa)	G*** (MPa)
20 gauge	287.9	203,000	78,000
18 gauge	306.9	203,000	78,000

* Catalogue properties modified for actual mean black metal thickness, t.

** Coupons from webs of studs tested in accordance with A.S.T.M.-A370.

*** Assumed material properties.

† See Figure 2.3 for description of dimensions.

++ torsional warping constants.

d = depth of perforation in web of stud.

4.3.2 Bending Capacity of Steel Stud Walls Tested with Sheathing Attached

4.3.2.1 Steel Stud Panels with Sheathing on Both Sides

The moment capacity of steel studs braced with sheathing material is evaluated in this section. In Series 7, each panel was sheathed on both sides with 12 mm thick gypsum board. Some of these panels were additionally braced at midspan with a line of steel bridging. Each simply supported steel stud in the panels was loaded under equal two-point load as described in Section 3.5.8.2. For each test the maximum bending moment per steel stud at ultimate load was calculated using simple beam theory. The values obtained are listed in column 4 of Table 4.5. The previously calculated theoretical yield moment capacities, M_r, are listed again in column 5 of Table 4.5. Column 6 is the ratio of maximum applied bending moment, M_a, to the theoretical moment capacity, M_r. From the resulting ratios it was observed that the experimental moment capacities were equal to or greater than M_r under the following conditions:

1. For 20 gauge studs with both sides sheathed with 12 mm thick gypsum board fastened every 150 mm on centre, (Specimen7-BW-4), no additional bridging was necessary.
2. For 20 gauge studs with both sides sheathed with 12 mm thick gypsum board fastened every 305 mm on centre (Specimens 7-BW-1and 7-BW-2),an additional line of bridging was necessary.
3. For 18 gauge studs with both sides of the stud sheathed with 12 mm thick gypsum board attached to both flanges every 305 mm on centre, (Specimen 7-BW-7),an additional line of bridging was included.

Although no test was performed on a 20 gauge steel stud backup wall panel braced with gypsum board, attached every 305 mm on centre with no additional line of bridging, it was expected that the full moment capacity would be attained. This is based on test 7-BW-6,where an 18 gauge steel stud backup wall panel,braced on both sides with 12 mm thick gypsum board attached every 305 mm on centre with no additional line of bridging, attained approximately 90 percent of the full moment capacity.

TABLE 4.5

COMPARISON OF EXPERIMENTAL MOMENT CAPACITY TO THEORETICAL YIELD CAPACITY FOR BACKUP WALL PANELS SHEATHED ON BOTH SIDES

Specimen Number	Stud Type	Fastener Spacing (mm)	M_a* (N mm) *10^6	M_r (N mm) *10^6	$\frac{M_a}{M_r}$
7-BW-1	20 ga.	305	1.25	1.32	0.95
7-BW-2	20 ga.	305	1.19	1.32	0.90
7-BW-3	20 ga.	150	1.36	1.32	1.03
7-BW-4	20 ga.	150	1.29	1.32	0.98
7-BW-5	20 ga.	305	0.94	1.32	0.71
7-BW-6	18 ga.	305	1.64	2.11	0.78
7-BW-7	18 ga.	305	1.92	2.11	0.91
4-BW-1 **	20 ga.		1.07	2.11	0.81
4-BW-2 **	18 ga.		1.42	2.11	0.67

* includes self-weight of drywall

** 50 mm Styrofoam SM on compression face

Note: M_r is based on F_y from tests of coupons from webs of steel studs (specified yield strength = 228 MPa[6])

In test 7-BW-5, the gypsum board sheathing attached to the compression face was wetted as described earlier in Section 3.8.2.1. The results of M_a/M_r indicated that a reduction of approximately 20 percent in the moment capacity of the stud occurred under this condition. However, the steel studs in this panel were also braced at midspan with a line of bridging. Without the additional line of bridging, it was anticipated that the value of M_a/M_r would have been reduced even further.

In Series 4 the compression face of the two backup wall panels tested were sheathed with 50 mm styrofoam SM™ boards. The other side of each wall panel was sheathed with interior grade 12 mm thick gypsum board sheathing fastened to the studs at 305 mm on centre. In addition each panel was braced at midspan with a line of bridging. For each of these tests, the maximum bending moment attained per stud is listed in column 4 of Table 4.5. The M_a/M_r ratios listed in column 6 of Table 4.5 indicate the full moment capacity of the 20 gauge and 18 gauge studs tested was not attained. Therefore it can be concluded that that undamaged gypsum board sheathing is a more effective bracing material than 50 mm thick styrofoam sheathing.

4.3.2.2 Bending Capacity of Steel Stud Walls Tested with Sheathing Attached to One Side

For specimens 1-BW-9 and 1-BW-10, the steel stud backup wall panels were sheathed with 12 mm thick interior gypsum board, fastened to the tension face of the steel studs every 305 mm on centre. In addition, one line of steel bridging was provided at the midspan of the panels. The applied bending moment, M_a, calculated for these two tests are listed in column 4 of Table 4.6. The theoretical yield moment capacity, M_r, calculated earlier is again listed in column 5 of this table. The ratios of M_a/M_r in column 6 indicate that the steel studs were not sufficiently braced even though a line of steel bridging was provided at midspan.

TABLE 4.6

COMPARISON OF EXPERIMENTAL MOMENT TO THEORETICAL YIELD MOMENT CAPACITY FOR BACKUP WALL PANELS SHEATHED ON THE TENSION SIDE

Specimen No.	M_a 10^6	M_r* 10^6	$\frac{M_a}{M_r}$
1-BW-9	0.794	1.315	0.60
1-BW-10	0.744	1.315	0.57

* M_r is based on F_y = 287.9 Mpa
(Specified Yield Strength = 228 MPa[6])

The gypsum board sheathing on the tension face did provide some bracing since an increase of 6 to 10 percent in moment was achieved. This conclusion was based on comparison of the results of these two tests with those obtained for specimens 1-BW-1 to 1-BW-5, which were identical to specimens 1-BW-9 and 1-BW-10 except that they were not sheathed on the tension side.

4.3.3 Analysis of Discretely Braced Steel Stud Backup Wall Tests Results

4.3.3.1 General

In all of the tests performed, the steel studs were loaded by transverse loads which did not pass through the shear centre of the cross-section. As a result, these studs were subjected to a combination of plane bending and torsional moments. In Series 1, 2 and 3, the steel stud backup wall specimens were braced at discrete locations with steel bridging. The moment capacities of these panels were considerably lower than similar sheathed panels. A simplified analysis of these test results is provided in this section. Influences of residual stresses, plate buckling and effects of cold working were not considered. Before proceeding a synopsis of the theory of combined torsion and bending is presented. A more complete treatment of this topic is available elsewhere.[13,14,29,33]

4.3.3.2 Classical Theory Of Bending And Torsion

If a steel stud is sufficiently braced so that the expected deformations are small, then the linear theory of thin walled open sections may be used. The relevant differential equations, obtained from Reference 3 are :

$$E * I_x * \frac{d^4 v}{dz^4} = q_y \qquad (4.6)$$

$$E * I_y * \frac{d^4 u}{dz^4} = q_x \qquad (4.7)$$

$$E * C_w * \frac{d^4\phi}{dz^4} - \frac{GJd^4\phi}{dz^2} = mt \qquad (4.8)$$

where,

E = Modulus of Elasticity

G = Shear Modulus of Elasticity

x,y,z = Coordinate axes

u,v = Horizontal and Vertical Displacements

ϕ = Angle of Twist

I_x, I_y = Principal Moments of Inertia

q_x, q_y = Uniformly distributed load in x and y direction

J = St. Venant torsional constant

C_w = Warping constant

m_t = Distributed torque along z-axis

The assumptions used in the derivation of the above equations are given in References 13 and 29. Equations 4.6 and 4.7 are the well known equations of bending. Equation 4.8 is the torsion equation derived by considering the equilibrium of moments on an element of length dz, loaded along its length with a uniformly distributed twisting moment, m_t.

In the case of the steel studs tested, the transverse loads were applied parallel to the plane of the web. As suggested by Lansing[19], if the rotations are held to no more than a few degrees, the influence of minor axis bending can be ignored. As a consequence the equations of equilibrium were approximated as follows :

$$E * I_x * \frac{d^2v}{dz^2} = M_x \qquad (4.9)$$

$$E * I_y * \frac{d^2u}{dz^2} = 0 \qquad (4.10)$$

$$E * C_w * \frac{d^4\phi}{dz^4} - \frac{GJd^2\phi}{dz^2} = m_t \qquad (4.11)$$

Equation 4.9 represents Equation 4.6 rewritten in the more familiar form in terms of the bending moment, Mx. The longitudinal bending and shear stresses associated with this equation are easily evaluated using the simple theory of bending found in elementary textbooks on strength of materials. The stresses due to torsion were calculated as follows :

1. Warping Longitudinal Stress

$$\sigma w = -E * C_w * \frac{d^2\phi}{dz^2} \qquad (4.12)$$

2. Warping Shear Stress

$$\lambda_w = E * \frac{S_w}{t} * \frac{d^3\phi}{dz^{42}} \qquad (4.12)$$

3. St. Venant Shear Stress

$$\lambda_w = G * t * \frac{d\phi}{dz} \qquad (4.14)$$

where,

$C_{w_A} = \int w^2 \, dA$

$S_{w_A} = \int w \, dA$

t = thickness

S_w, C_w and w are called sectorial properties of the section and the reader is referred to the literature for a more detailed explanation of the terms. Using the principle of superposition, the stresses due to bending and torsion are added vectorially.

4.3.3.3 Finite Element Torsion Analysis Of Discretely Braced Steel Stud Backup Wall Tests

Since the steel studs tested in Series 1, 2 and 3 were subjected to a simple loading condition, the longitudinal stresses due to bending were easily evaluated using simple beam theory. In order that the longitudinal stresses due to torsion be determined at any point in the cross-section of a stud, a solution of the fourth order equation, Equation 4.8, was required. To

solve this equation in an efficient manner, a one-dimensional finite element torsion analysis program was developed. It must be emphasized that the intent of this study was not to develop a sophisticated finite element model. The simple model developed was intended to be used to study the general distribution of torsional stresses in the steel studs. The theory used in the development of the program is given in Appendix A. A general description of the modeling employed in this program will be given and then the results of the analysis will be presented.

A steel stud was modeled as a number of one-dimensional line elements. However the model could not properly take into account the effects of the web cut-out holes. As a result, the torsional stresses obtained at these locations are nominal. However for studs without web cut-out holes, the model will be able to give an accurate solution, for small stud rotations. The steel stud was divided into six, three noded elements with two degrees of freedom at each node, namely, the twist, ϕ, and the rate of change of twist, ϕ'. In the analysis, the ends of the stud were considered to be restrained from twisting and free to warp. The kinematic boundary conditions at these locations were simply :

$$\phi = 0.0$$

At the locations of the steel bridging, the kinematic boundary condition was taken as :

$$\phi = \phi_i$$

Where ϕ_i is equal to the experimentally measured rotation at the brace. Since there were two equal applied transverse loads, each applied torsional moment was assumed equal to the total applied load on the stud divided by two and multiplied by the the distance from the shear centre to the point of application on the top flange of the steel stud.

In order to evaluate the test results of Series 1, 2, and 3, the analyses on five different cases were carried out. For Case 1, the results for the 20 gauge steel stud backup wall panels braced at midspan, (Specimens 1-BW-1to 1-BW-5), were evaluated. In this analysis,the interior steel stud which failed in the panel was modeled as shown in Figure 4.1. The applied transverse loads on this stud were taken as the average of the applied stud transverse loads obtained from the results of tests 1-BW-1 to 1-BW-5. The specified rotation of the midspan

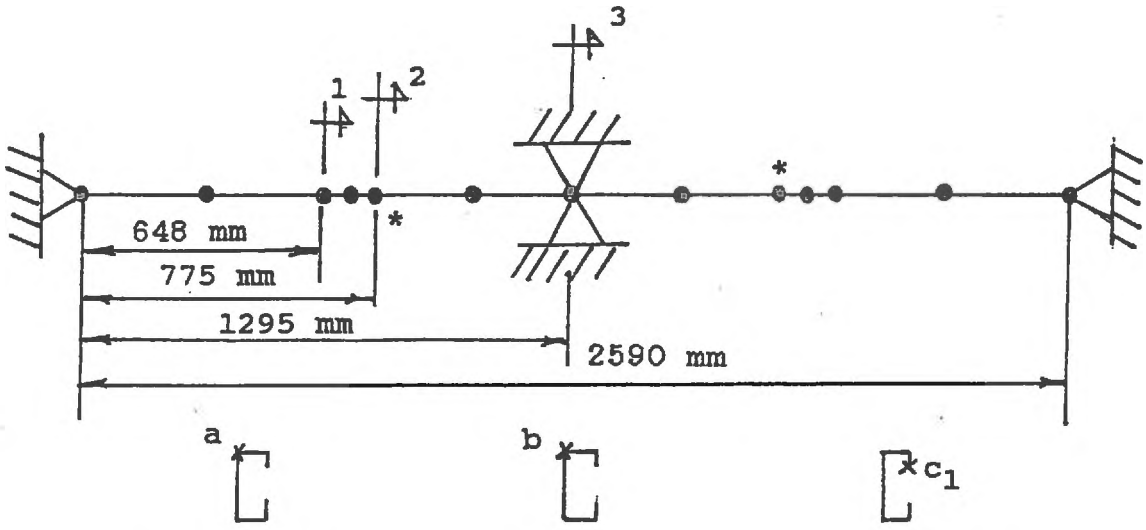

Section 1-1 Section 2-2 Section 3-3

* = Location of Applied Load

= Support or Steel Bridging Location

Figure 4.1 Torsional Model Case 1

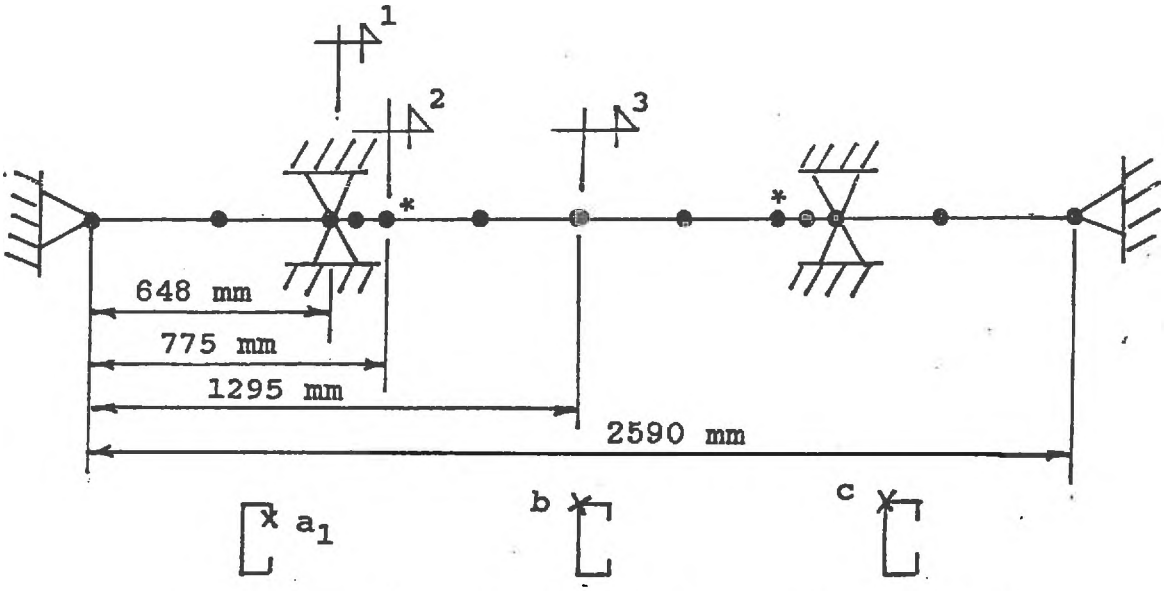

Section 1-1 Section 2-2 Section 3-3

Figure 4.2 Torsional Model Case 2

brace was taken as 2 degrees since it was found that rotations of this magnitude occurred at this location as the load approached its ultimate value. The rotation at the brace was included in order to obtain a more accurate comparison with the test results. The effects of assuming no rotation at this location will be commented on later. The applied torques used for this case are listed in Table 4.7.

In Case 2, the results for the 20 gauge steel stud backup wall panels braced at the quarter points,(Specimens 1-BW-7 and 1-BW-8), were evaluated. In this analysis the interior steel stud which failed in the panel was modeled as shown in Figure 4.2. The applied transverse loads were taken as the average of the applied stud transverse loads obtained in tests 1-BW-7 and 1-BW-8. In these tests the measured rotations at the two lines of bridging were again found to be approximately 2 degrees. This was accounted for by specifying a rotation of 2 degrees at each brace location. The applied torques used are given in Table 4.7.

For Case 3, the results for the 18 gauge steel studs panels braced at midspan with a line of face bridging,(Specimens 2-BW-1 to 2-BW-3), were evaluated. For this analysis the interior steel stud in the panel was modeled as shown in Figure 4.3. The applied transverse loads were taken as the average of the maximum transverse loads obtained in tests 2-BW-1 to 2-BW-3. The specified rotation at the midspan brace was taken as 5 degrees, as measured at this location in these tests. The applied torques are listed in Table 4.7.

For Case 4, the torsional behavior for the 18 gauge steel stud panels braced at the quarter points with a line of face bridging at each location,(Specimens 2-BW-4 and 2-BW-5), was evaluated. For this analysis the interior steel stud which failed was modeled as shown in Figure 4.4. The transverse loads were taken as the average of the maximum loads obtained in tests 2-BW-4 and 2-BW-5. The specified rotation at each brace location was taken as the measured 5 degrees. The applied torque used is listed in Table 4.7.

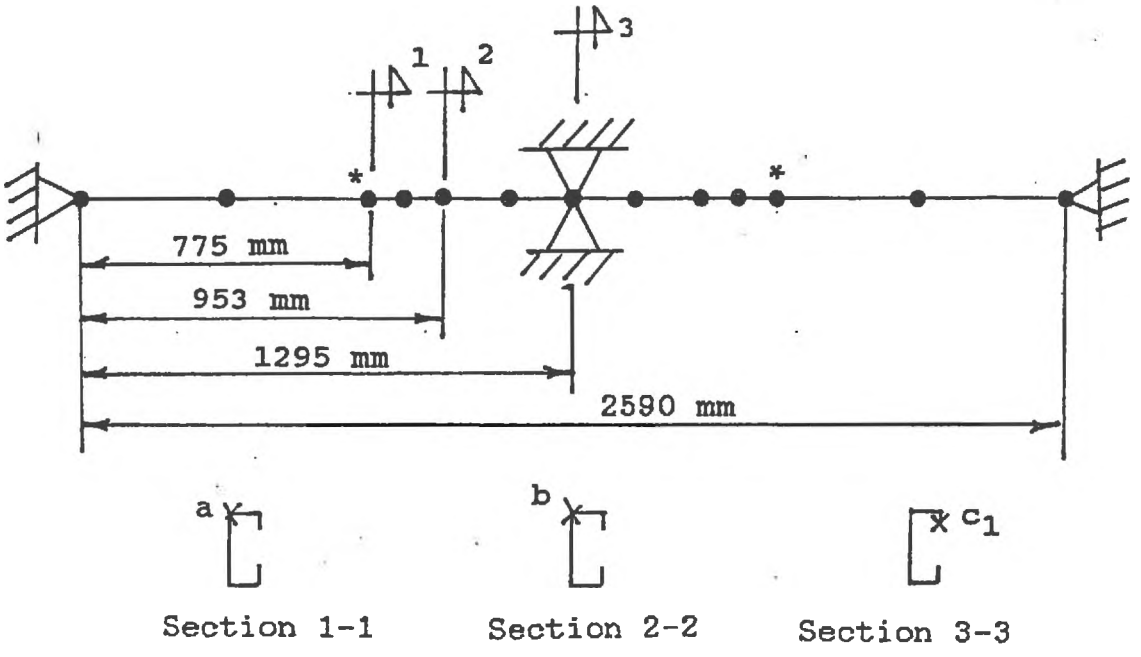

Figure 4.3 Torsional Model Case 3

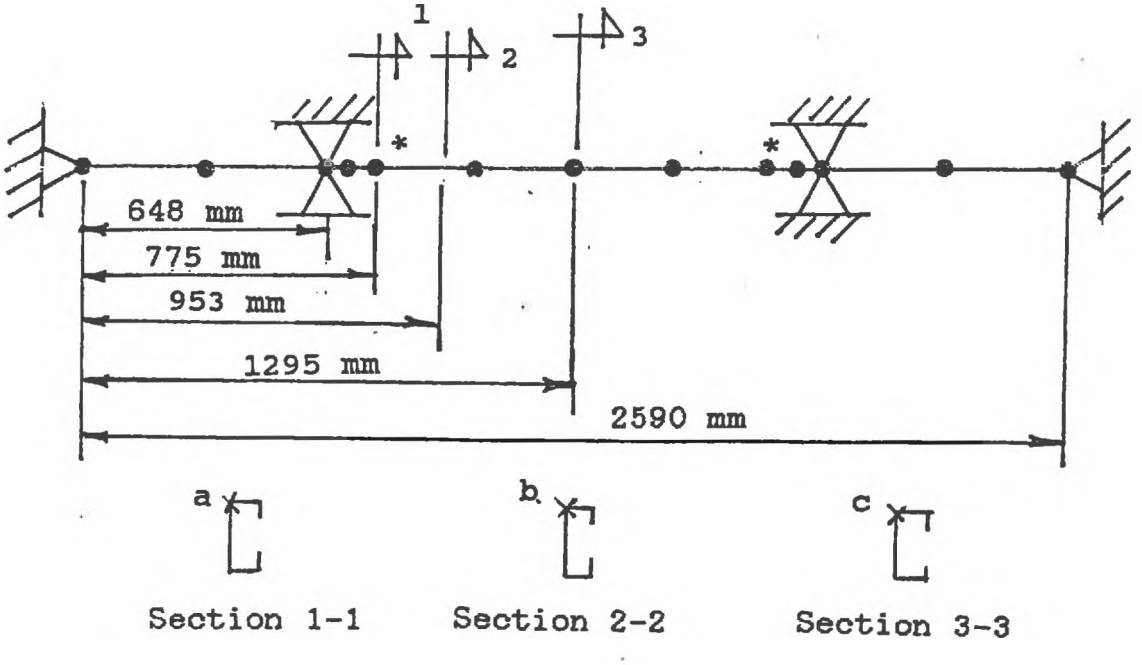

Figure 4.4 Torsional Model Case 4

TABLE 4.7

ANALYSIS OF TORSIONAL AND FLEXURAL STRESSES AT ULTIMATE LOADS FROM BENDING TESTS OF STUD PANELS

Loading Information				Results of Analysis					
Case No.	Ultimate Load ($N * 10^3$)	Measured Eccentricity e (mm)	Applied Torque ($N.mm * 10^3$)	Location* (Mpa)	σb (Mpa)	σw (Mpa)	σt (Mpa)	Computed Ultimate Load ($N * 10^3$)	% Difference (Computed - Experimental)
1	0.87	30.0	26.16	a	-121.00	-59.00	-180.00	0.91	+4.5
				b	-144.00	-71.60	-216.40		
				c1	-114.80	-161.50	-276.30		
2	1.19	30.0	35.64	a1	-143.80	-66.40	-210.20	1.48	+24.2
				b	-197.40	-34.40	-231.80		
				c	-197.40	32.13	-229.50		
3	1.86	34.0	63.92	a	-208.20	-111.30	-319.50	1.73	-8.0
				b	-208.20	-32.80	-241.00		
				c	-150.80	183.40	-334.20		
4	1.96	34.0	66.50	a	-216.60	-61.70	-278.30	2.16	+10.2
				b	-216.60	-58.90	-275.50		
				c	-216.60	-58.00	274.60		
5	1.81	34.0	61.37	a	-167.10	-71.70	-238.80	1.50	-17.1
				b	-199.80	-87.00	-286.80		
				c	-144.70	-224.40	-369.10		

* For location where stresses calculated, see Figures 4.1 to 4.3.

For Case 5 panels with the 18 gauge steel studs braced at midspan with a line of interior steel bridging welded to the steel stud (Specimens 3-BW-1 and 3-BW-2), were studied. In this analysis the interior steel stud which failed in the panel was modeled as shown in Figure 4.5. The applied transverse loads were taken as the average of the maximum transverse loads obtained from tests 3-BW-1 and 3-BW-2. In these tests, the rotations at the midspan brace were found be to much less than in the previous tests. In the analysis, a specified rotation of 0.5 degrees was used. The applied torques used are listed in Table 4.7.

The results of the analyses are given in Table 4.7. For each case analyzed, the longitudinal stresses were checked at three critical locations on the steel stud. For each case the locations checked are shown in Figures 4.1 to 4.5. This was done since it is normally not possible to know at what location the combined bending and torsional longitudinal stresses will be critical. The bending stress, σ_b, was obtained at each location for each case using simple bending theory and the values obtained are listed in column 6 of Table 4.7. The steel stud section properties used in the analyses are listed in Table 4.4 The warping longitudinal stresses, σw, due to the torsional loads are given in column 7 of Table 4.7. These values were calculated at each location with the use of Equation 4.12 and the torsional section properties listed in Table 4.4. The combined stresses, σ_t, are listed in column 8 of Table 4.7. The combined stress values marked with an asterisk in column 8, show the location of observed failures for the steel stud specimens tested in Series 1 to 3.

In all the tests, the observed failure location on the stud was found to have occurred at a cross-section with a hole. The results of the analyses at these locations show that the total longitudinal compressive stresses were lower than the yield stress, F_y. However, the stresses calculated at these locations were based on a solid cross-section. Also, the measured rotations at these locations in some cases approached 10 degrees and the minor axis stresses, which were not considered in the analysis would have increased the stresses at these locations. Also some distortion of the cross section did occur during the tests. This was more evident near ultimate load. This effect would also change the distribution of stresses. Stress concentrations

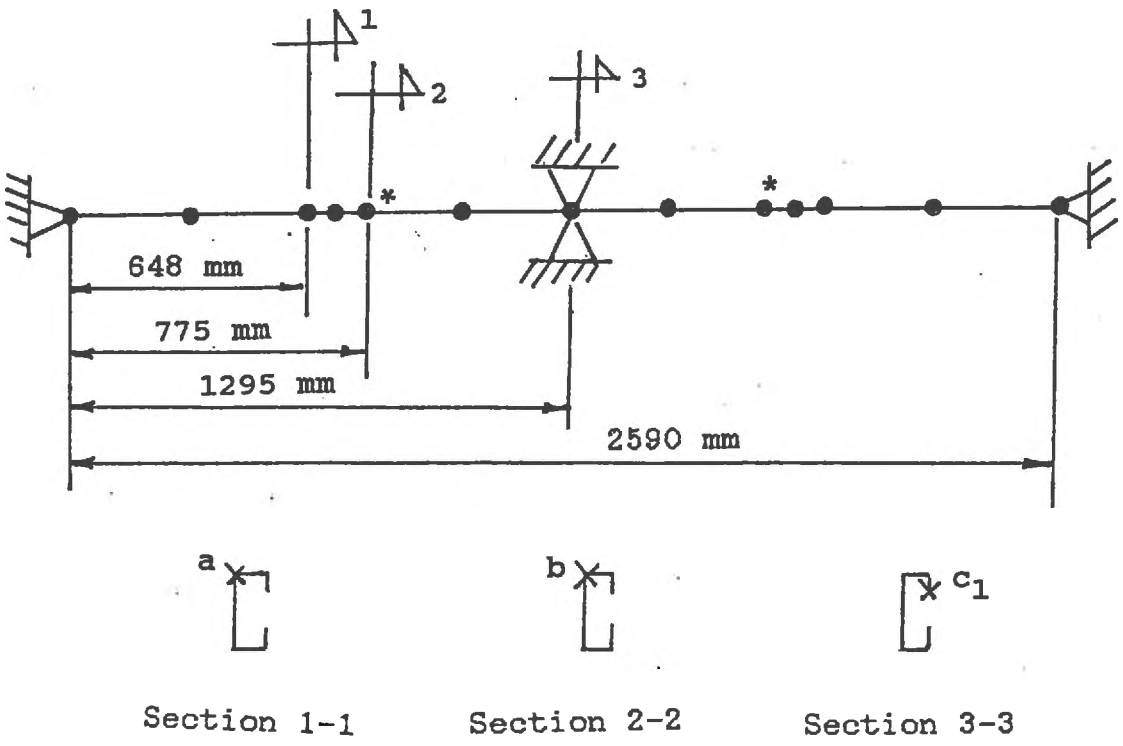

Figure 4.5 Torsional Model Case 5

in the region around the hole would also increase the stresses. While the torsion model used was not able to predict the distribution of stresses at these locations, the results of the test program indicated that any hole located in a region of high bending and torsional stress between the brace point locations may cause premature failure at this location.

Premature failure at a web cut-out can be prevented by not allowing additional web cut-out holes in regions of high combined stresses other than at the brace point locations on the steel stud. This will be commented on again later. For Cases 1, 3 and 5, the calculated magnitudes of the total compressive stress at location C1 was found to be greater than F_y. This can be explained partially by the fact that the rotations which did occur were greater than the rotations measured at the last load increment just prior to failure. This effect would have reduced the stresses at this location.

In each analysis the measured rotation at the midspan brace location was used. If no rotation at the braces had been assumed, then the analysis would have shown an increase in the torsional stresses at the brace locations and a reduction of the torsional stresses at locations between braces. In order to examine how this would affect the analysis, Case 3 was analyzed again assuming the rotation at the midspan brace to be zero. The results showed an increase in torsional stresses of approximately 28 percent at the brace location and a reduction of approximately 18 percent at location a. For Case 3, the tests were on 18 gauge steel stud backup wall panels braced with notched surface bridging fastened to both faces of the steel studs at midspan. The rotation of approximately 5 degrees which occurred at midspan was due to the inability of the bridging displacement control rig to fully restrain this type of bridging from displacing in the plane of the backup wall. Rotations of this magnitude are undesirable and proper anchoring of the ends of the line of steel bridging is required in order that the steel stud rotations at the bridging location be limited to approximately 1 degree. In the other tests, the rotations at the lines of steel bridging were much smaller and the difference resulting from assuming no rotation at the brace locations would be in the range of 5 to 10 percent.

If no holes are allowed between brace points and the rotations are kept within linear theory, then the torsion model will satisfactorily predict the torsional stress distribution along the member length. Assuming that failure is considered to occur when the total compressive stress reaches F_y at any location the computed ultimate loads for each case considered are listed in column 9 of Table 4.7.

4.4 ANALYSIS OF OTHER STEEL STUD BACKUP WALL CONFIGURATIONS

4.4.1 General

The primary structural function of the steel stud backup wall is to resist some or all of the applied wind load. The wind load is usually transferred to the steel stud by means of brick ties, point loads and/or by uniform loading on the exterior wall sheathing. Since these transverse loads do not pass through the shear centre of the cross-section, the steel studs will be subjected to a combined flexural and torsional loading condition.

In the current Canadian cold formed steel design code, CAN3-S136-M84[6], Clauses 6.8 and 6.8.1, state that wall studs which are sheathed on one or both sides may be designed using the assumption that the sheathing material furnishes adequate lateral and rotational support to the studs in the plane of the wall. The studs, sheathing material and attachments must comply with the restrictions imposed in Clause 6.8.1. It is then left up to the designer to decide whether or not additional steel bracing is required.

Some steel stud manufacturers recommend a minimum number of braces so that adequate structural integrity can be maintained during construction and in the completed structure. However it is also stated[25,30] that this minimum recommended bracing requirement may not be adequate for all possible conditions. A qualified engineer or architect must decide on the suitability of the manufacturers' recommendations. Conditions such as improper installation of sheathing material, effects of water damage and accidental damage of gypsum board must all be considered. The designer may decide to provide a sufficient number of steel braces so that the sheathing material is not required to provide any additional bracing.

The use of exterior sheathing materials such as polystyrene,which may not be rigid enough to prevent stud twisting, may necessitate the use of steel bracing in order to prevent premature failure of the steel stud.

The current Canadian code[6] provides guidance on the requirements for discrete bracing. For a channel section, Clause 8.3.2.1 states that,

> "Braces shall be connected so as to effectively restrain both flanges of the section at the ends and at intervals not greater than one-quarter of the span length in such a manner as to prevent tipping at the ends and lateral deflection of either flange in either direction at intermediate braces "

In addition, a brace must be located at or near a concentrated load which is greater than one third of the total load on the beam. This clause is intended to ensure that the torsional stresses will be small enough so that the load carrying capacity of the member will not be adversely affected. This clause is also limited to the case where the transverse loads are applied in the plane of the web of the channel. These provisions where derived from the experimental and theoretical work of Winter et al[31]. which contains a more complete discussion. Clause 8.3.2.1 also allows the use of fewer braces if this can be shown to be acceptable by load tests or by rational analysis. These load tests must be in accordance with Clause 9 of the code. No specific guidance is provided for members with holes.

For a BV/SS wall system, the design of the steel stud may be controlled by deflection limits. Therefore in many cases, the full moment resisting capacity of the steel stud may not be required. An attempt was made in the following section to determine the minimum bracing requirements for steel stud backup walls. In order to accomplish this, two BV/SS wall systems were analyzed.

4.4.2 Computer Analysis

Two BV/SS wall systems were analyzed to provide information on critical stress conditions in steel stud backup walls. Model 1 shown in Figure 4.6 is typical of wall systems

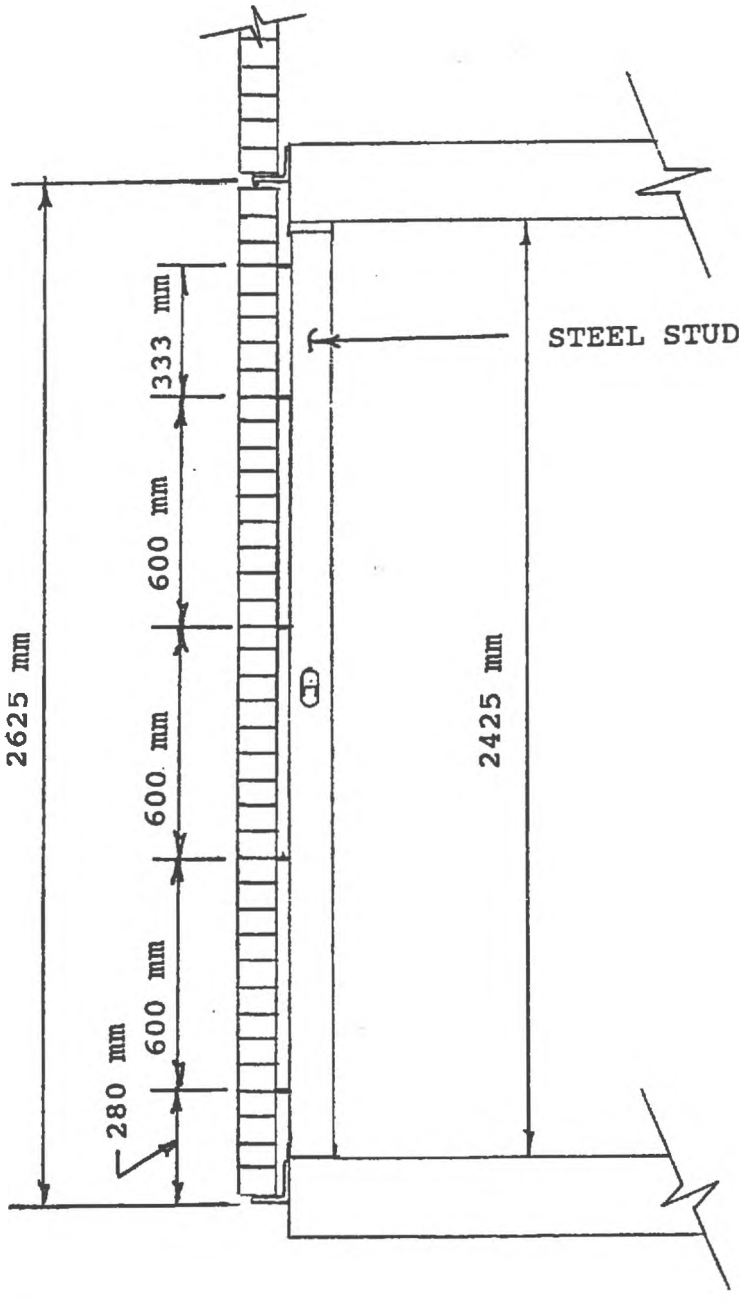

Figure 4.6 2.6 Meter High.BV/SS Wall 1

used in residential construction of low to medium rise buildings. Model 2 shown in Figure 4.7 represents a BV/SS wall system such as might be typically used to clad the exteriors of shopping malls or warehouses. Figures 4.8 and 4.9 are sketches which illustrates the mathematical models used to analyze the two wall systems. In these analytical models the two wythes were modeled as beam elements and the brick ties and the stud end supports were modeled as axial springs. These numerical values will be discussed in greater detail in Chapter 5.

In the analyses, the brick veneer wythe were assumed to be cracked. This was done since preliminary analysis had shown that the steel stud backup wall was more critically loaded under this condition. An explanation is that after cracking, the brick veneer is a less stiff element and the steel stud backup wall shares a greater portion of the wind load. Although the formation of a crack in the brick veneer would be expected to occur at the location of maximum flexural tensile stress, normal to the bed joints, the analysis was carried out assuming the crack could occur anywhere in the brick veneer. This was done since a crack can form in the brick veneer wherever a weak joint may exist. The crack was modeled as a hinge which was introduced in the models at the assumed crack location. Table 4.8 and 4.9 list the location of the crack for each computer analysis. The wind load was assumed to act on the exterior face of the brick veneer. For Wall Model 1, a 20 gauge 90 mm deep stud was used since this would be the smallest size stud used for this wall configuration. For Wall Model 2, the steel stud was specified to be 18 gauge and 150 mm deep. The spacing of the studs was set at 400 mm on centre. The brick veneer tributary width was taken to be the same as the steel stud spacing. Computer analyses were carried out for the cases listed in Tables 4.8 and 4.9 to obtain the bending stress distribution in the steel stud. These were subsequently combined with the torsional stresses obtained in the second analysis.

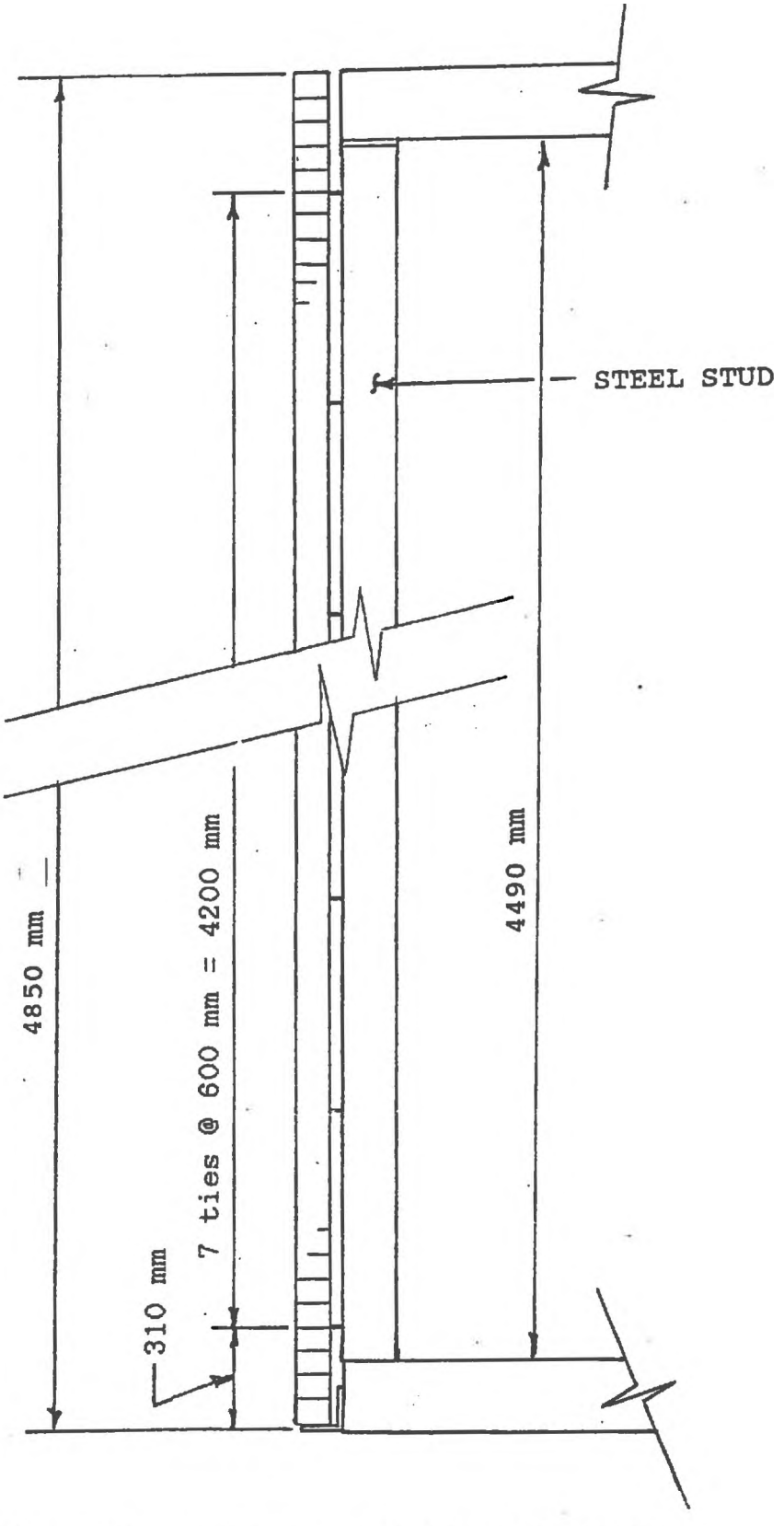

Figure 4.7 4.85 Metre High B.V.S.S. Wall 2

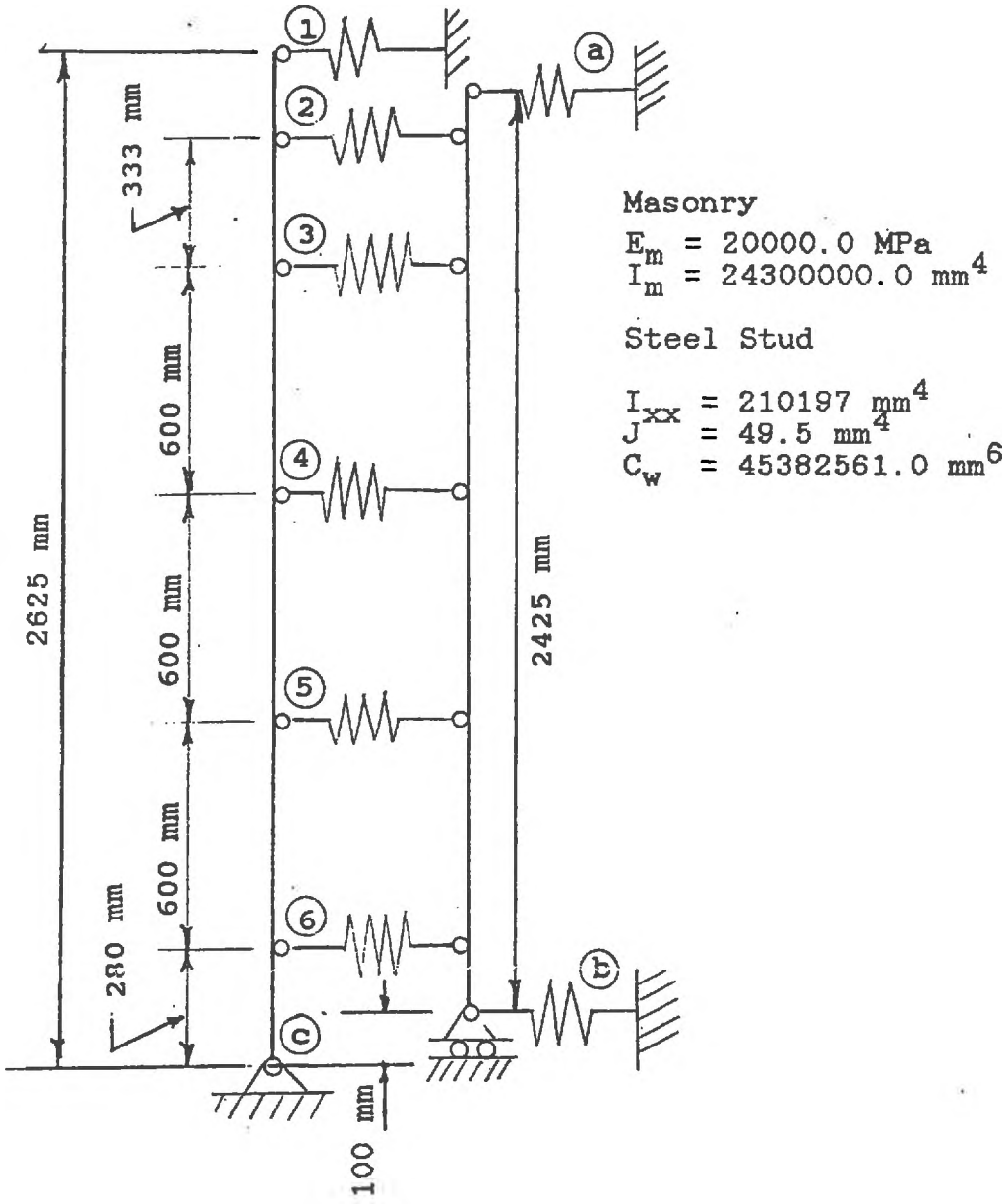

Figure 4.8 Mathematical Model Wall 1

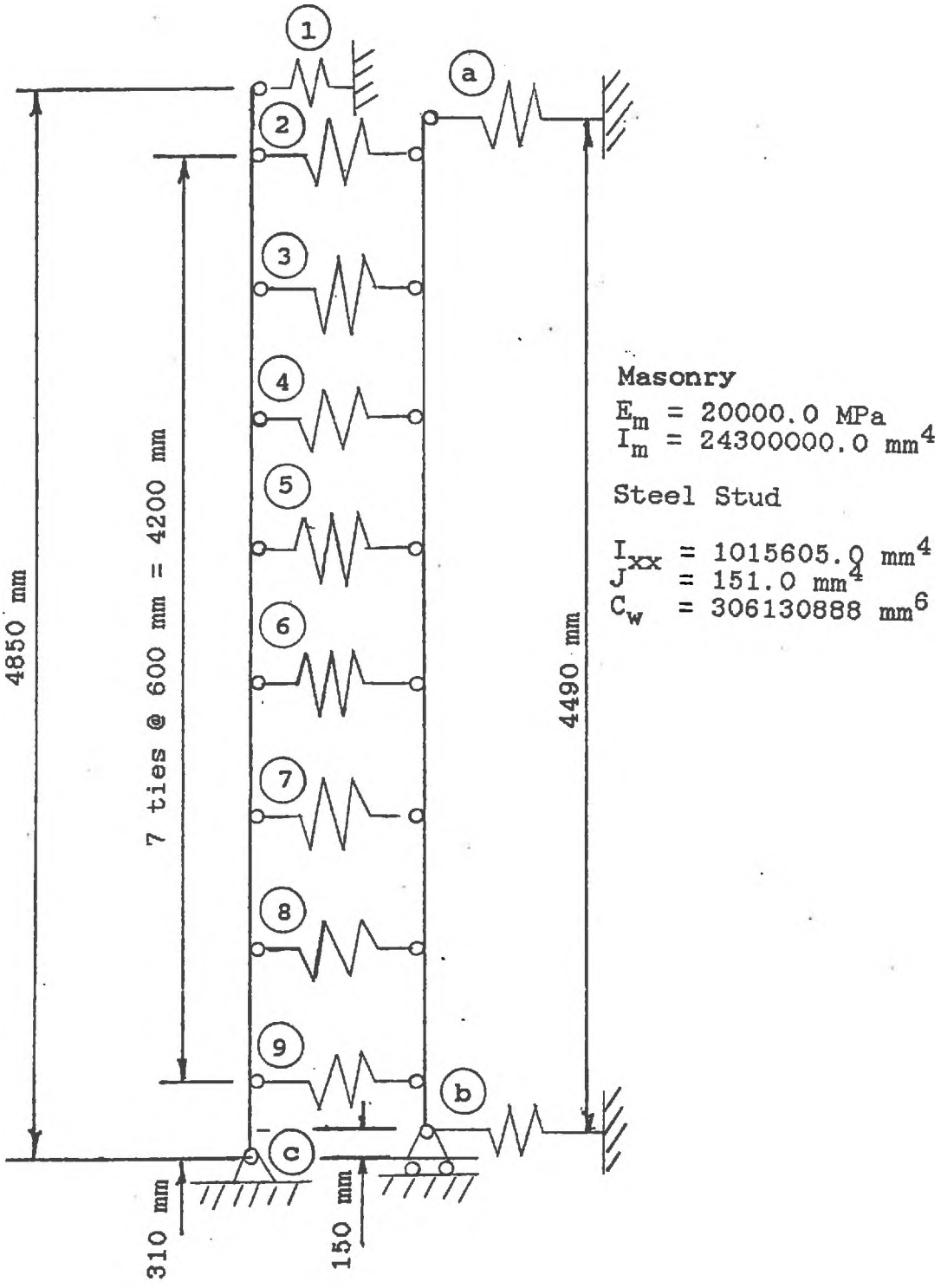

Figure 4.9 Mathematical Model Wall 2

TABLE 4.8

PREDICTED WIND LOADS REQUIRED TO CAUSE STEEL STUD FAILURE IN WALL MODEL 1

Case No.	Crack Location (αL)	**Predicted Failure Load ÷ 1.5 (KN/m²)		
		a*	b*	c*
1	0.335	1.98	1.53	1.31
2	0.335	1.70	1.39	1.18
3	0.411	1.85	1.57	1.34
4	0.488	1.81	1.47	1.23
5	0.488	1.82	1.49	1.26
6	0.564	2.25	1.88	1.62
7	0.716	1.97	1.49	1.38
8	0.716	2.05	1.60	1.33

* Location of Tie loads from web of stud

a = in the plane of the web.

b = 1/3 flange width from web

c = 2/3 flange width from web

** = Based on specified yield strength of 228 MPa.

TABLE 4.9

PREDICTED WIND LOADS REQUIRED TO CAUSE STEEL STUD FAILURE IN WALL MODEL 2

Case No.	Crack Location (αL)	**Predicted Failure Load ÷ 1.5 (KN/m^2)		
		a*	b*	c*
1	0.311	2.15	2.02	1.90
2	0.373	1.91	1.81	1.71
3	0.435	1.78	1.65	1.53
4	0.435	1.75	1.60	1.46
5	0.497	1.87	1.82	1.75
6	0.559	1.82	1.72	1.59
7	0.559	1.76	1.60	1.47
8	0.620	1.89	1.77	1.66

* Location of Tie loads from web of stud

a = in the plane of the web.

b = 1/3 flange width from web

c = 2/3 flange width from web

** = Based on specified yield strength of 228 MPa.

The steel studs were re-analyzed using the finite element torsion program described earlier to determine the distribution of torsional stresses in each steel stud.

The two finite element torsion models used for Wall Models 1 and 2, are shown in Figures 4.10 (a) and 4.10 (b). The location of braces are shown in these figures. The brace point locations were modeled as torsionally simply supported which is the case most likely to occur in practice. The braces were spaced approximately 1.2 meters apart because tests indicated that recommended maximum spacing of 1.5 meter might not be adequate. The tie loads obtained in the previous analyses were multiplied by a specified load eccentricity to obtain the torsional loads .Three cases of load eccentricity were considered in the analysis for each of the two torsion models. In Case A the tie loads were assumed to act in the plane of the web. In Case B the tie loads were assumed to act on the top flange of the stud, at a distance of one-third the width of the flange from the outside face of the web. In Case C the tie loads were assumed to act on the top flange of the stud at a distance of two-thirds the width of the flange from the outside face of the web.

For each assumed crack location, the longitudinal stresses due to torsion and bending were combined vectorially. The wind load required to raise the combined torsional and bending stresses to a level equal to the yield stress, F_y, at the critically stressed location in the steel stud, was subsequently determined. This value was then divided by a load factor of 1.5 to obtain the specified wind load. The calculated wind loads for each case of load eccentricity considered are listed in Tables 4.8 and 4.9. It should be pointed out that plate buckling, lateral instability, the interaction of lateral instability and torsion and effects of cold working were not included.

As shown from the results in Tables 4.8 and 4.9, the unfactored wind loads corresponding to stud failure are generally in excess of the expected design wind loads for most locations in Canada. [Note: These values should also be multiplied by a resistance factor of 0.9.] The results also indicate that the tie eccentricity can significantly affect the steel stud capacity. It is not always possible to control the exact location where the ties will be fastened

on the flange of the steel stud. This is due to fact that the exterior wall sheathing obstructs the view of the steel studs. Therefore surface mounted ties will be located in an approximate manner on the flange. If the locations of attachment of the brick tie on the flange of the steel stud cannot be guaranteed, the variability of the tie eccentricity should be considered.

The results of the analyses were for a steel bridging spacing of approximately 1.2 metres on centre. For the minimum eccentricity of Case A, the results in column 3 of Table 4.8 seem to indicate that a more liberal spacing of steel bridging would be justifiable. However, the results of the flexural analysis showed that once the brick veneer was cracked, the ties located in the midheight region of the wall became heavily loaded. If too liberal a spacing of steel bracing is adopted, a large concentrated tie load could cause twisting of the stud which may not be acceptable. The results of the experimental program indicated that a spacing of braces of approximately 1.22 meters on center limited the stud rotation to no more than a few degrees under working load. Based on the results of the analyses and of the experimental work, a spacing of 1.22 meters for the steel bracing would seem to be reasonable for the design of steel stud backup walls. For commonly occurring BV/SS walls the maximum spacing of steel bridging of 1.22 meters would result in the following bridging schedule.

Backup Wall Height (meters)	Number of Braces Required	Location
0 - 2.44	1	midspan
2.44 - 3.66	2	1/3 points
3.66 - 4.88	3	1/4 points

In the above analysis bracing due to the sheathing was not considered.

4.5 SUMMARY AND CONCLUSIONS

4.5.1 Summary

In this chapter the results of the test program were evaluated in terms of strength requirements.

As was shown by the results, steel studs braced with gypsum board sheathing plus a minimum amount of steel bridging were capable of developing the full moment capacity. However, if the gypsum board was wetted, the bracing capacity was reduced and the full flexural capacity of the steel stud was not achieved. This would also be anticipated to occur if the gypsum board was damaged or if fasteners were spaced too far apart, or if the screw fasteners were not properly installed. It is hard to predict with any degree of accuracy how much reduction in flexural capacity would occur under these conditions. However, unless the integrity of the sheathing can be guaranteed over the life of the structure, some other form of bracing must be provided. This is usually accomplished by bracing the steel studs with steel bridging.

If steel bridging is to be used to brace the steel studs, a maximum spacing between braces must be established in order to control the amount of stud twisting and to prevent premature failure. The current Canadian code[6] bracing specification for spacing not to exceed one-quarter of the span length is quite conservative for short steel stud walls which are commonly used in residential construction. The spacing of steel braces should be such that the steel stud performs in an adequate manner structurally and that no unacceptable twisting occurs between braces. In Series 1, 2 and 3, the steel bridging provided in these tests was spaced at approximately 1.23 metres on centre. For this spacing it was found that acceptable rotations of 1 to 2 degrees occurred under service loads.

The structural analysis performed in order to evaluate the tests results obtained in Series 1, 2 and 3, was not able to predict accurately the stresses in the region of the holes where failure was observed to occur. However the analysis showed that for most of these tests the maximum expected combined stresses occurred at the midspan brace location and if the total combined stress was limited to F_y at this location, the computed failure loads were generally conservative. Assuming no holes existed in areas of high combined stress,analyses of two BV/SS walls indicated that a spacing of approximately 1.2 metres on centre would be structurally adequate.

4.5.2 Conclusions

Based on the results presented in this chapter some important conclusions are drawn.

1. Web crippling at the end of the steel stud is a possible mode of failure. The current Canadian code for cold formed steel members can be used to provide reasonable predictions of the web crippling strength at these locations.
2. The full moment resisting capacities of the types of studs tested in the experimental program were developed only when the studs were fully braced.
3. Gypsum board sheathing attached to both flanges of the steel stud satisfied the full bracing requirement only under the conditions described in Section 4.3.
4. Gypsum board sheathing attached to the tension side only did not significantly improve the capacity of the steel stud.
5. The bracing capacity of the gypsum board was significantly reduced when it was wet.
6. 50 mm styrofoam SM was able to provide some bracing for the steel stud. However the full moment resisting capacity was not achieved under this condition.
7. Holes located in regions of high stress weaken the steel stud.
8. Location of tie loads on the flange of the steel stud significantly affected the capacity of the steel stud.
9. Steel bridging provided at 1220 mm on centre or less will provide sufficient bracing for the steel stud.
10. If additional web cut-out holes are required for services at locations other than at the bracing points it is suggested that they be located 300 to 400 mm from either end of the steel stud. In addition no brick ties which induce web crippling should be located directly over these holes.

CHAPTER 5

ANALYSIS OF BRICK VENEER STEEL STUD WALL SYSTEMS

5.1 INTRODUCTION

The influences of various features of steel stud backup walls on the overall behaviour of BV/SS wall systems were examined analytically in this chapter. The two analytical wall models introduced in Chapter 4 (Figures 4.6 and 4.7) were again used. For this study, findings of the experimental work were incorporated into the analytical models as input for some structural properties. The influence of the following variables were examined:

1. Stud stiffness
2. Top track stiffness
3. Bottom track stiffness
4. Brick veneer stiffness
5. Tie stiffness
6. Top of brick restraint
7. Wind loading condition

5.2 BRICK VENEER MASONRY PROPERTIES

5.2.1 Elastic Material Properties

Since brick masonry is composed of both brick and mortar, the elastic properties are dependent on the material properties of both components. Empirical relationships have been developed to predict the elastic modulus of brick masonry. The Canadian masonry code[22] specifies:

$$E_m = 1000\, f'_m \quad \text{(MPa)}$$

$$\text{but} \; < 20{,}000 \text{ MPa}$$

where f'_m is the ultimate compressive strength of masonry

However for brick masonry, Drysdale[11] suggested that a more realistic value be given by :

$$E_m = 700 f'_m \quad (MPa)$$

Also, an expression given by Grim [15] for this quantity is :

$$E_m = 7957 (\ln(f'_m) - 1.12)$$

This expression also gives values of E_m which are lower than the values predicted by the masonry code.

5.2.2 Flexural Bond Strength Of Brick Masonry Veneer

Since a BV/SS wall system resists primarily out-of-plane forces such as wind and earthquake, the response is mostly flexural in nature. When a brittle material such as brick masonry is subjected to flexural forces, cracking of the wall can occur. The bond strength of masonry governs its flexural strength. A brick veneer wall subjected to out-of-plane forces develops flexural tensile stresses normal to the bed joints. These joints are essentially planes of weakness in the brick veneer. Once the tensile stresses have exceeded the bond strength between the unit and the mortar, cracking occurs. Most research into the bond strength of brick masonry has been focused on testing of small stack bonded prisms. Some researchers[2,20] have attempted to relate bond strength to overall flexural strength of brick masonry walls. However, there are other factors such as poor workmanship and effects of temperature which also contribute to overall wall strength. Therefore, it is difficult to accurately predict the ultimate flexural capacity of a brick wall. Testing of a large number of stacked bonded prisms can provide a lower bound on the ultimate flexural capacity as well as indicate the range of strengths that are possible for a brick veneer wall. Typical ultimate flexural bond strength values obtained from the work of Gazzola and Drysdale[10] for clay brick masonry are as follows:

1. Clay brick with type S mortar 0.4 – 0.9 MPa
2. Clay brick with type S mortar with masonry cement 0.2 – 0.4 MPa

In this study an ultimate flexural bond strength of 0.6 MPa was chosen as the representative flexural capacity of the brick veneer. However in some cases this value could be optimistic in view of the typical values listed above.

5.3 ANALYTIC MODEL

5.3.1 General

A more comprehensive description and discussion of the analytical wall models introduced in Chapter 4 is included in this section. Since the models incorporated some of the results obtained in the experimental work, a brief discussion on the experimental parameters will be presented before proceeding with the above.

5.3.2 Top And Bottom Track Stiffness

Based on the the experimental results presented in Chapter 2, the top and bottom stud to track connections were modelled as linear elastic springs which allowed out-of-plane displacements to occur. The axial stiffness of each of these springs was determined by the following relationship :

$$K_s = \frac{A_e E_s}{L} \tag{5.1}$$

where

E_s = Elastic modulus of elasticity of steel and is assumed as 203,000 MPa.

L = Length of spring assumed (mm)

K_s = Slope of line taken from Figures 2.13 to 2.16 for a particular type of connection.

A_e = Equivalent cross-sectional area required to satisfy Equation 5.1

Based on the above, an equivalent axial force type member was provided at the ends of the steel stud.

5.3.3 Tie Stiffness

Although no experimental investigation of the various types of ties was performed by the author, an experimental tie testing program[12] was undertaken at McMaster University as

part of the C.H.M.C. program. Results of twelve types of ties were obtained and based on this information, the following representative range of tie stiffness was used :

$$K_t = 500 \text{ to } 1000 \text{ (N/mm)}$$

where

K_t = Tie stiffness considering all local stud flange and tie deformation.

Based on the above stiffness values, the wall ties were modelled as equivalent axial load members with an equivalent axial stiffness.

5.3.4 Stud and Sheathing Interaction

Based on the results of the experimental work presented in Chapter 3, it was shown that the initial composite action between the gypsum board sheathing and the steel stud increased the backup wall stiffness by a small percentage. Under cyclic loading most of this small increase in stiffness diminished until the interaction between the two was insignificant. If the sheathing is not continuous, as is often the case, it is expected that there would be even less composite action. Therefore it can be assumed that no composite action takes place. In the case of Styrofoam SM board, the results of the experimental work showed that little to no composite action existed. Therefore the backup walls were modelled using only the stiffness of the steel studs.

5.3.5 Analytical Investigation

The two BV/SS walls shown in Figures 4.6 and 4.7 were considered in the analysis. These wall configurations were chosen since they represented the range of the wall heights which are normally found in practice. As discussed earlier these walls were modelled as shown in Figures 4.8 and 4.9. The top and bottom tracks were modelled as linear springs with stiffness K_t and K_b respectively. The wall ties were also modelled as springs with a stiffness K_{ts}. The spacing of the steel studs and the effective tributary brick width were both taken as 400 mm.

Computer analyses of the models described above were performed for the walls prior to cracking of the brick veneer and after the formation of a crack. The crack was modelled as a hinge. The location of the hinge was determined by the location of the maximum brick veneer stress from the uncracked wall analysis. The hinge was then introduced into the wall at a node in the region of maximum stress and the computer analysis was repeated. In order to determine the degree to which various factors influenced the deflection and strength of the wall system, the cases listed in Tables 5.1 and 5.2 were analysed.

For the short wall, Model 1, Cases 1 to 4 modelled the wind load acting on the exterior face of the brick veneer. This type of wind action usually occurs when a strong gust of wind rapidly loads the wall in such a manner that cavity equalization does not have a chance to develop. For Cases 5 to 8 the wind load acted fully on the backup wall. This type of wind loading will only happen in an adequately vented cavity in which the wind load has a chance to pressure equalize the cavity. In reality, the actual wind load will act partly on the brick veneer face and partly on the backup wall. Case 9 is identical to Case 1 except that the stiffness of the backup wall was increased by approximately 50 percent. Cases 10 to 15 were also identical to Case 1, except for the changes noted in Table 5.1.

For Model 2, Cases 16 to 19 pertained to wind load acting on the exterior face of the brick veneer, while Cases 20 to 23 were for the wind load acting on the exterior face of the backup wall. Cases 24 and 25 were identical to Case 16 except for the noted changes shown in Table 5.2.

TABLE 5.1

DESCRIPTION OF PARAMETERS USED FOR WALL MODEL 1

Case No.	Modulus of Elasticity of Brick Masonry (MPa)	Steel Stud Ixx (mm^4)	Top Track Stiff. K_t (N/mm)	Bottom Track Stiff. K_b (N/mm)	Tie Stiff. K_{ts} (N/mm)
1	20000.0	a	517	554	500
2	10000.0	a	517	554	1000
3	20000.0	a	517	554	500
4	10000.0	a	517	554	1000
5	20000.0	a	517	554	500
6	10000.0	a	517	554	1000
7	20000.0	a	517	554	500
8	10000.0	a	517	554	1000
9	20000.0	b	517	1012	500
10	20000.0	a	517	247	500
11	Same as Case 1 except top of brick restrained.				
12	Same as Case 1 except top of brick supported by spring with stiffness of 500 N/mm.				
13	Same as Case 1 except top track spring constant reduced to 243 N/mm.				
14	Same as Case 1 except bottom stud spring axial stiffness increased to K_b = 10,000 N/mm.				
15	Top of steel stud spring stiffness increased to K_t = 10,000 N/mm.				

a - I_{xx} = 214730 mm^4

b - I_{xx} = 322160 mm^4

TABLE 5.2

DESCRIPTION OF PARAMETERS USED FOR WALL MODEL 2

Case No.	Modulus of Elasticity (MPa)	Steel Stud Ixx (mm^4)	Top Track Spring Stiff. K_t (N/mm)	Bottom Track Spring Stiff. K_b (N/mm)	Tie Stiff. K_{ts} (N/mm)
16	20000.0	a	650	1014	500
17	10000.0	a	650	1014	1000
18	20000.0	a	650	1014	500
19	10000.0	a	650	1014	1000
20	20000.0	a	650	1014	500
21	10000.0	a	650	1014	1000
22	20000.0	a	650	1014	500
23	10000.0	a	650	1014	1000
24	20000.0	b	650	1014	500
25	20000.0	a	650	10000.0	500

a - $I_{xx} = 1015605\ mm^4$

b - $I_{xx} = 1.5 * a\ mm^4$

5.4 RESULTS OF COMPUTER ANALYSIS

5.4.1 Wall Model 1

For Cases 1 to 9, the deflection responses for a 1 KN/m^2 wind load are plotted in Figures 5.1 to 5.9. Both the displacement of the brick veneer and backup wall are shown in the pre and post cracked stages. The wind pressures required to cause cracking of the brick veneer are listed in Table 5.3. In addition to the above cases, additional computer analyses were performed in order to further investigate the influence of the other parameters listed in Table 5.1 for Cases 11 to 15. Only the uncracked condition was considered for these cases. The wind pressure required to cause cracking of the brick veneer are also listed in Table 5.3 for each of these cases. In all the cases considered, the wind pressures listed in Table 5.3 were based on a flexural tensile strength, normal to the bed joints of brick veneer, of 0.6 MPa. The influence of the brick self weight was also included.

Table 5.4 contains a summary of the tie loads obtained from the analysis of Cases 1 to 16. For Cases 1 to 9, there are two values given. The first is the maximum load each tie will sustain prior to brick cracking and the second value is the tie load after the wall has cracked. For the other computer runs, only the tie loads prior to flexural cracking of the brick veneer are given.

5.4.2 Wall Model 2

For Cases 16 to 23, the displacement responses for a 0.9 KN/m^2 wind load are plotted in Figures 5.15 to 5.22. The displacement of the brick veneer and backup wall are plotted for both the pre and post cracking conditions. The wind pressures required to cause brick veneer cracking are also listed in Table 5.3. For Cases 24 and 25, only the uncracked analysis was performed. The wind pressures required to cause flexural cracking in the brick veneer for each of these additional cases were also listed in Table 5.3. Table 5.4 contains a summary of the tie loads obtained from the analyses.

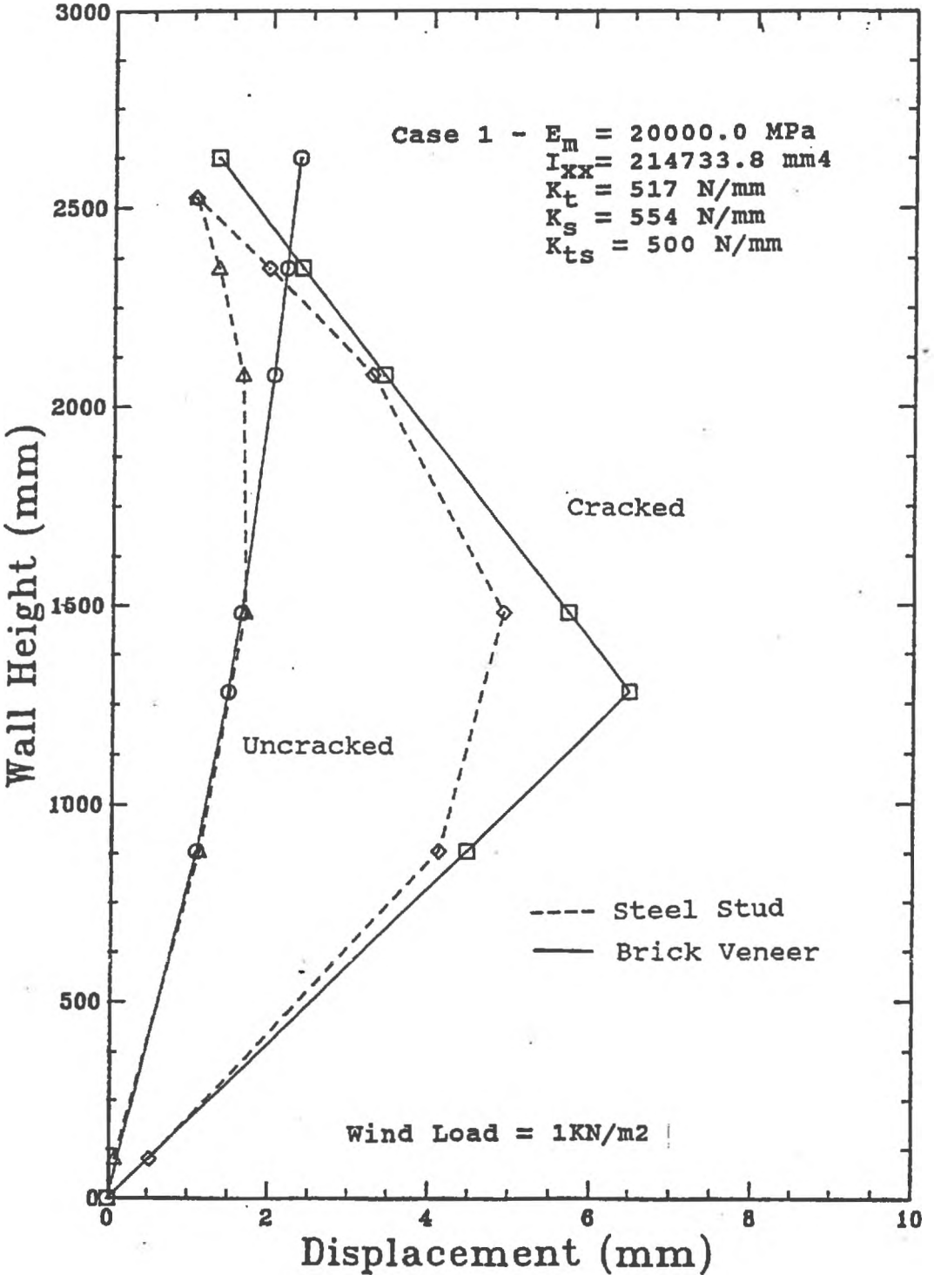

Figure 5.1 Deflection Profile for 2.63 Meter High BV/SS Wall - Case 1

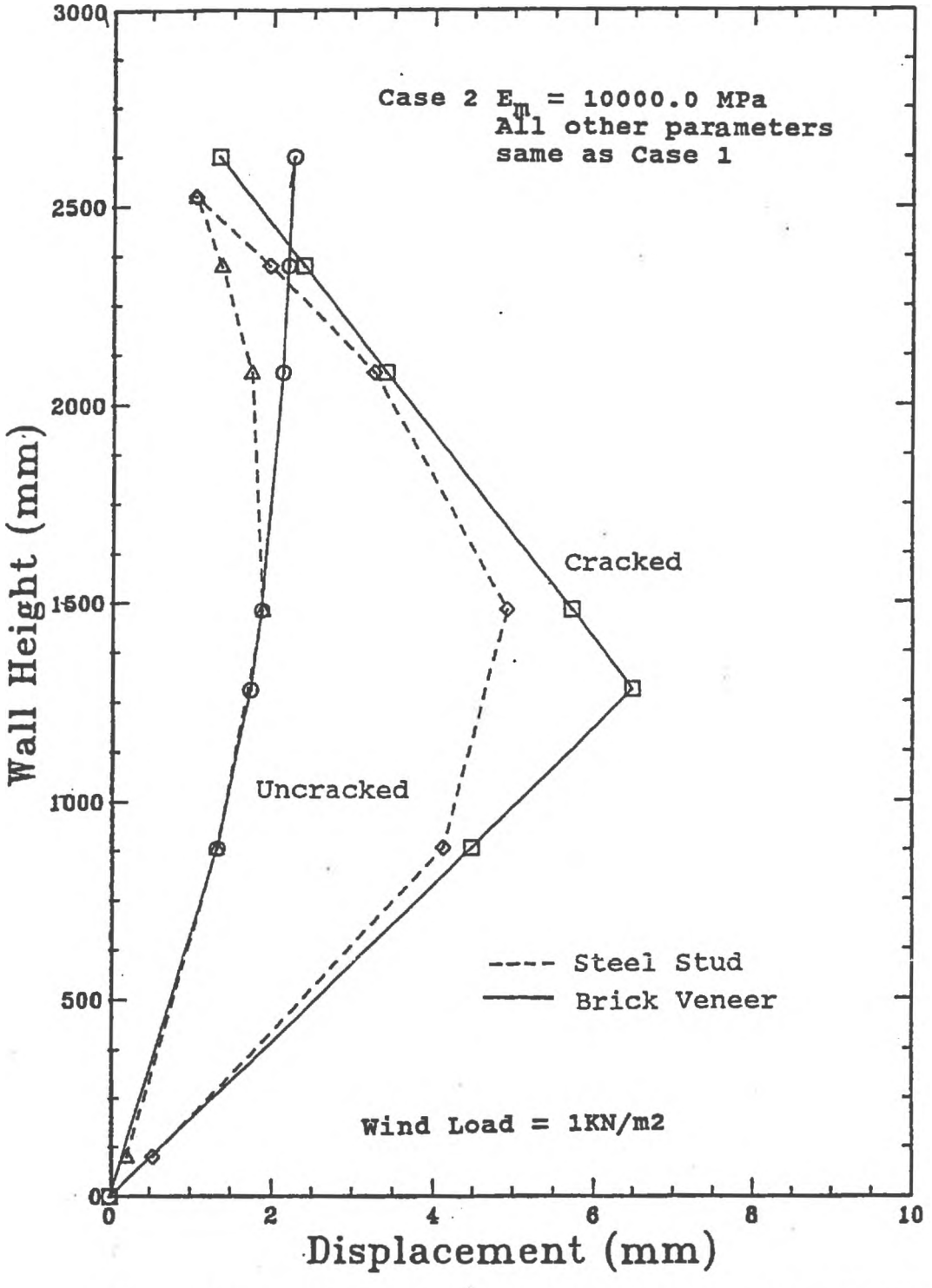

Figure 5.2 **Deflection Profile for 2.63 Meer High BV/SS Wall - Case 2**

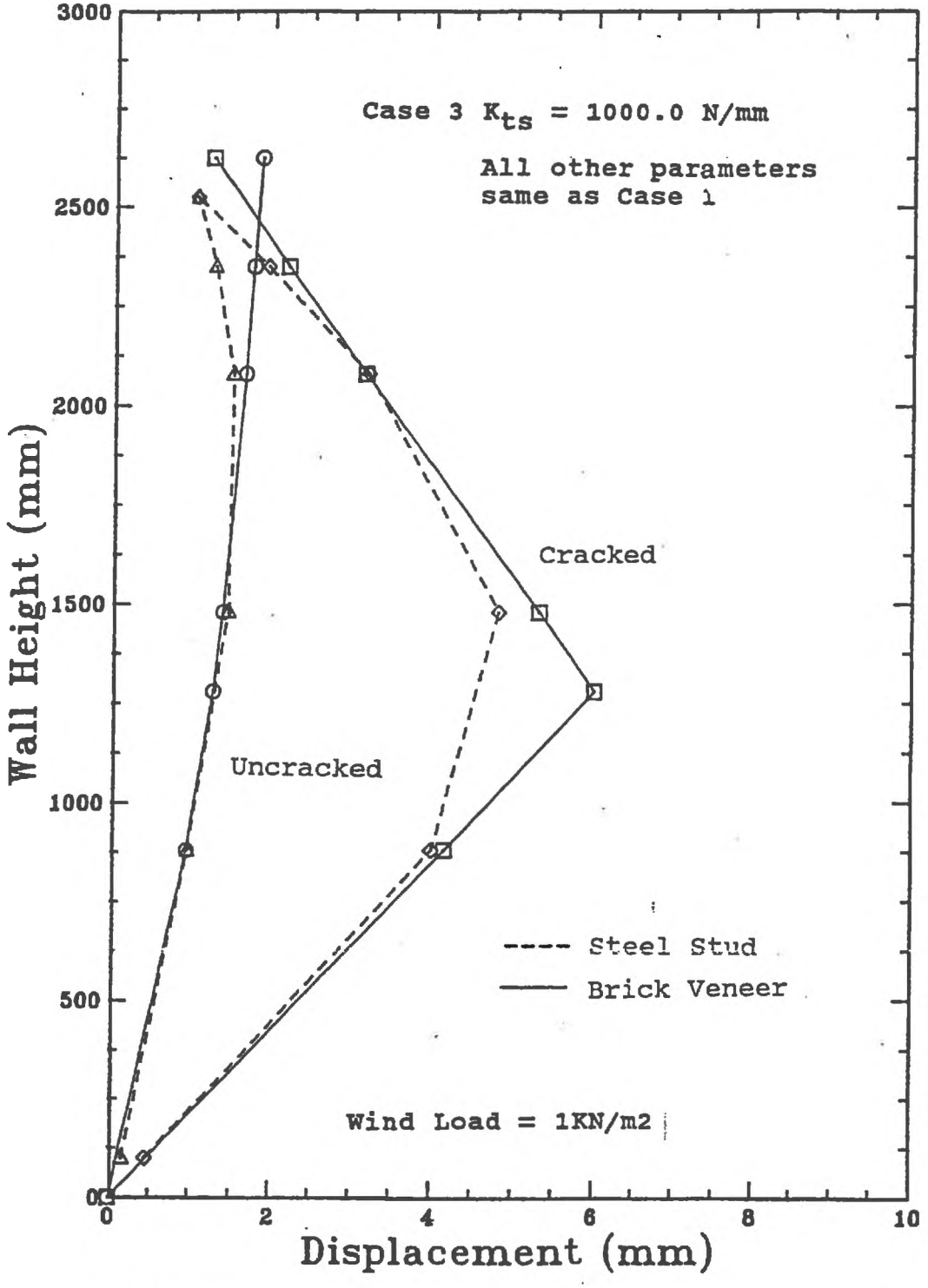

Figure 5.3 Deflection Profile for 2.63 Meter High BV/SS Wall - Case 3

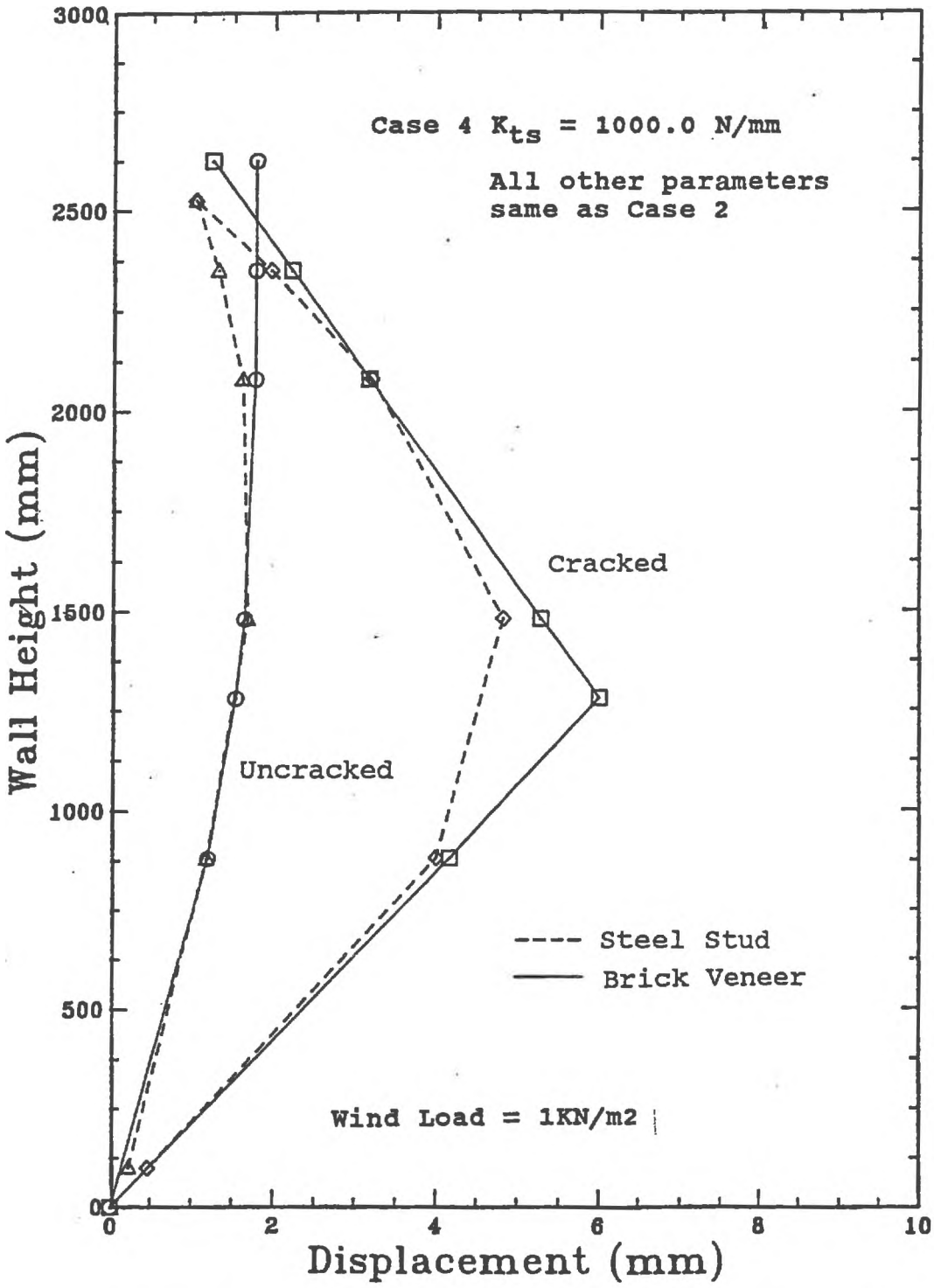

Figure 5.4 Deflection Profile for 2.63 Meter High BV/SS Wall - Case 4

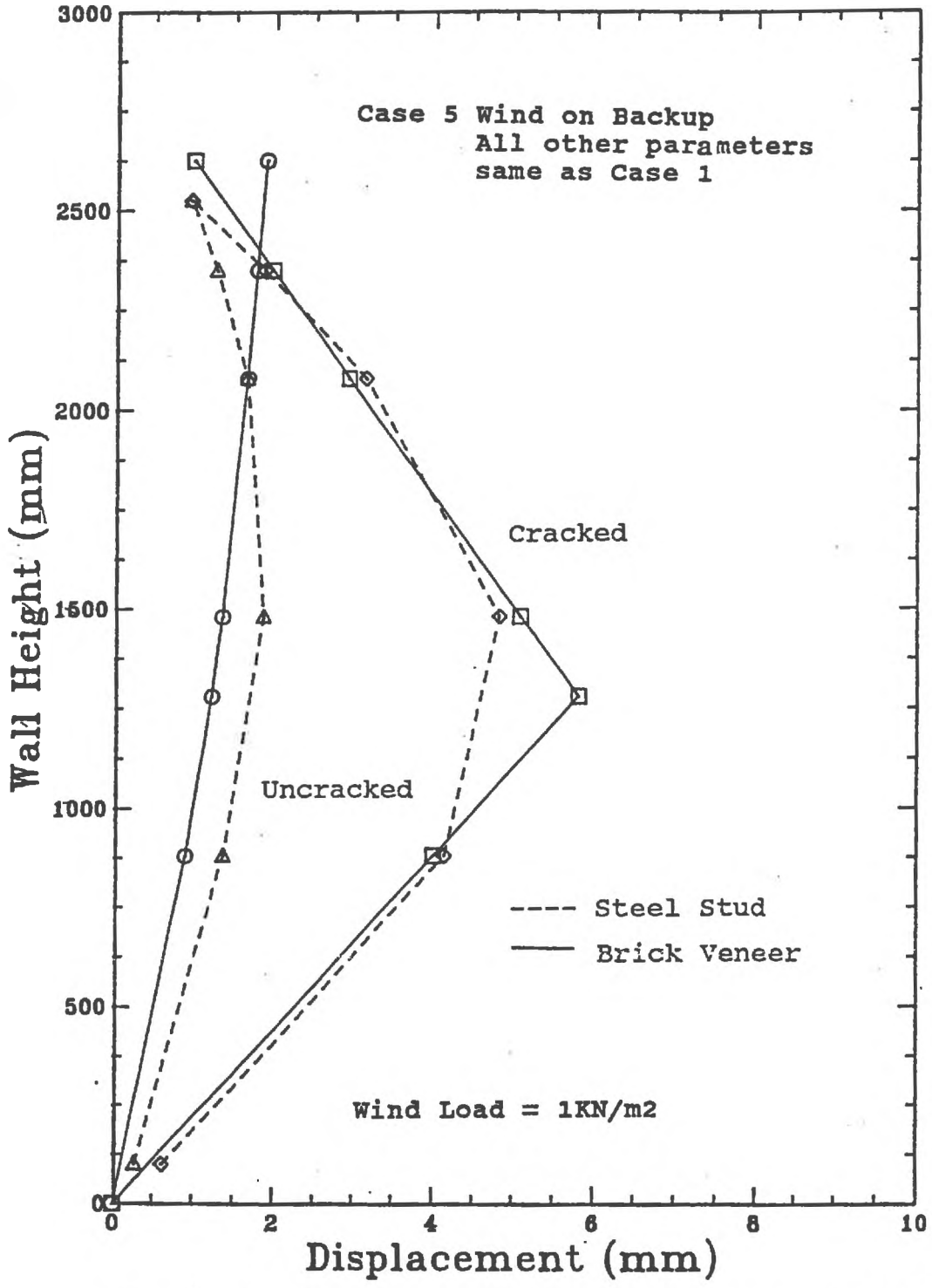

Figure 5.5 Deflection Profile for 2.63 Meter High BV/SS Wall - Case 5

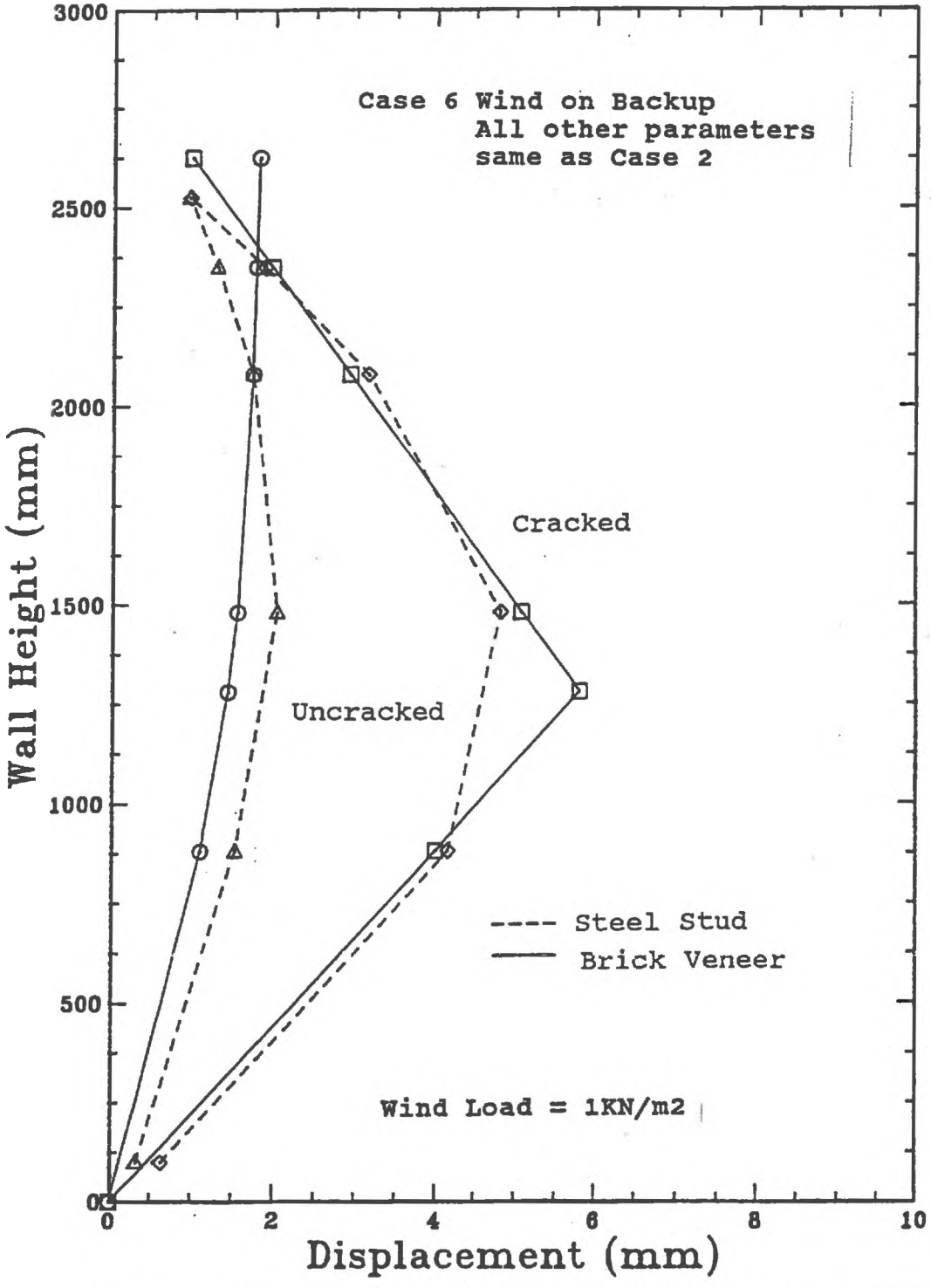

Figure 5.6 Deflection Profile for 2.63 Meter High BV/SS Wall - Case 6

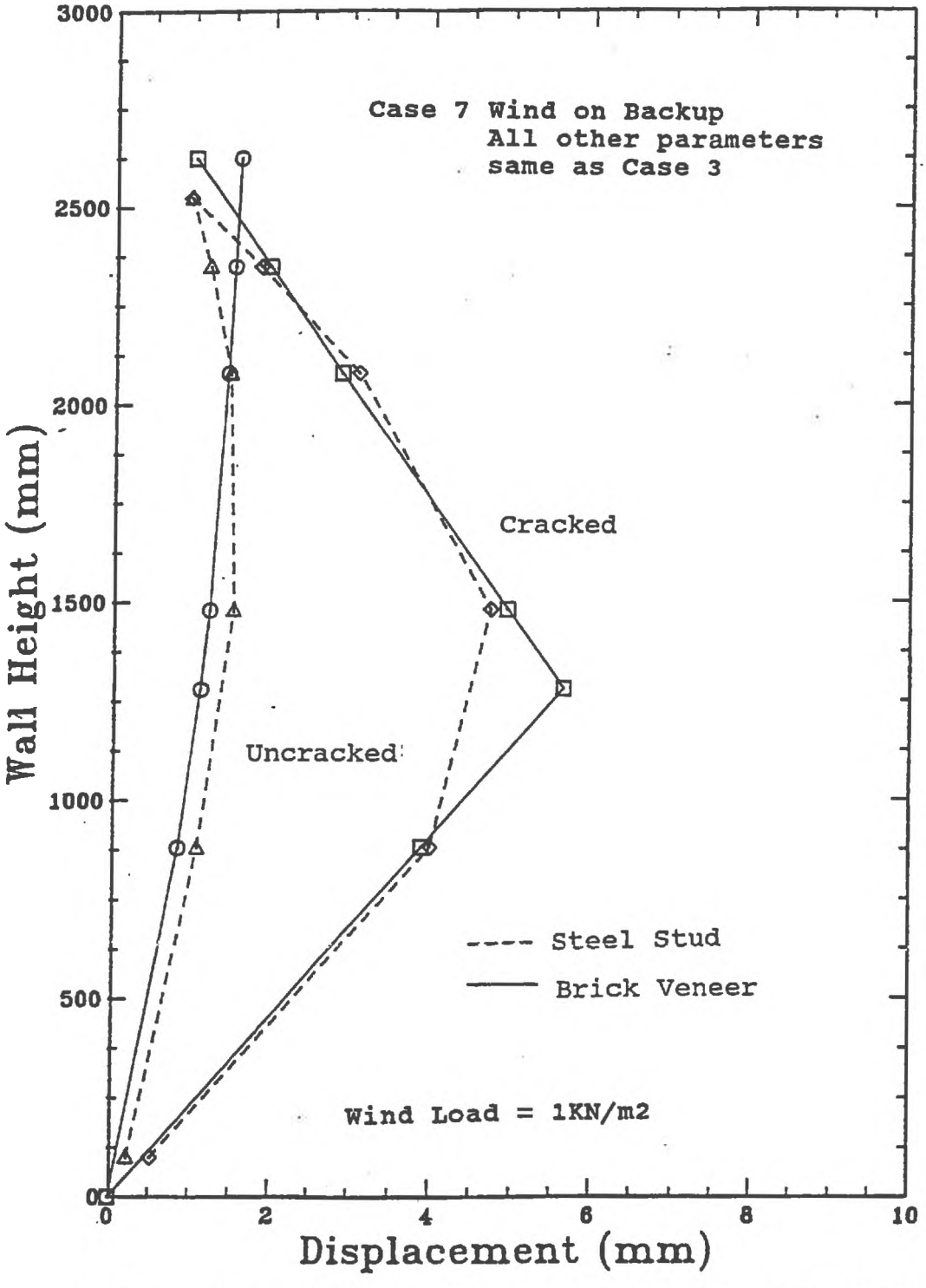

Figure 5.7 **Deflection Profile for 2.63 Meter High BV/SS Wall - Case 7**

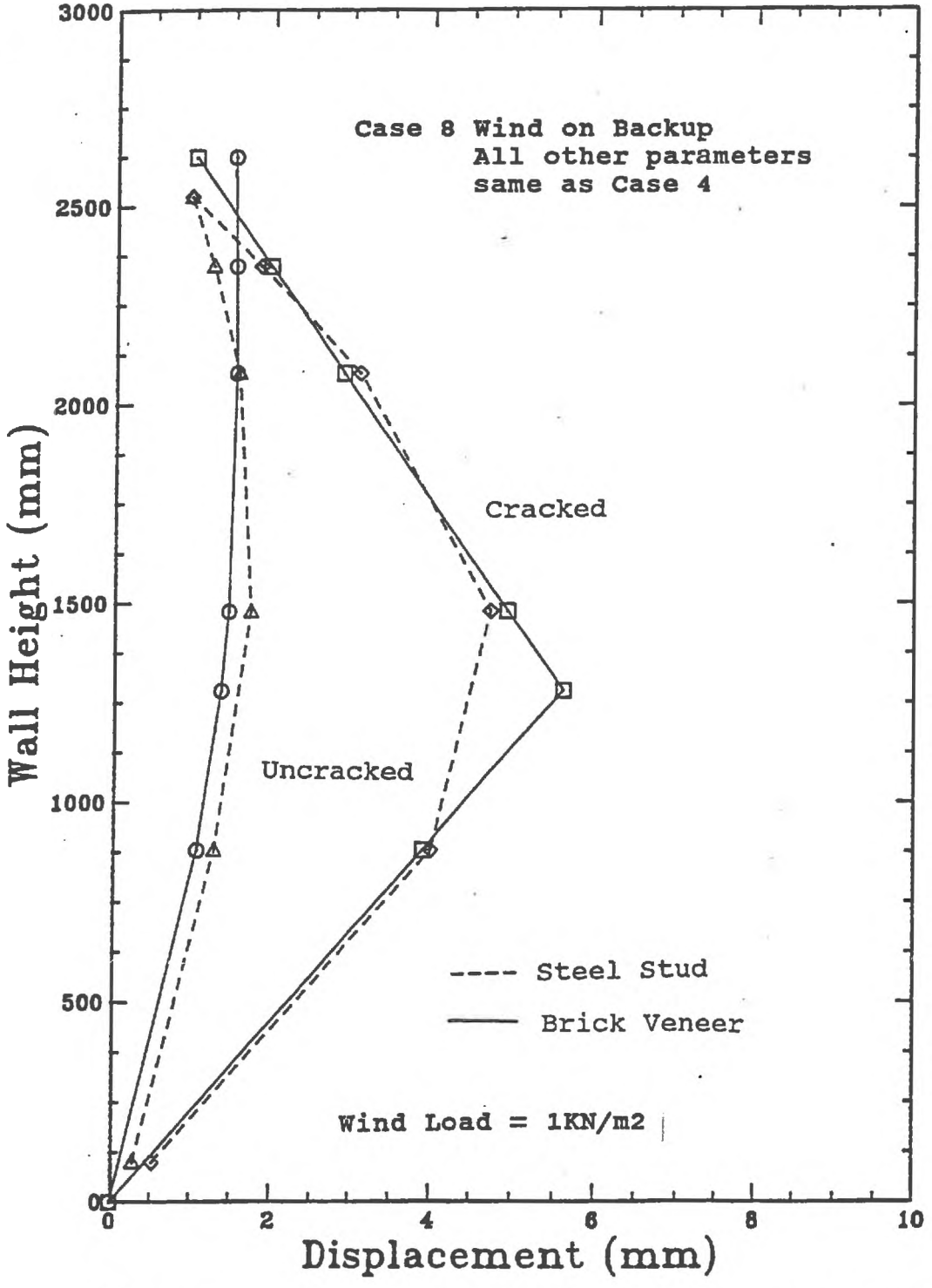

Figure 5.8 **Deflection Profile for 2.63 Meter High BV/SS Wall - Case 8**

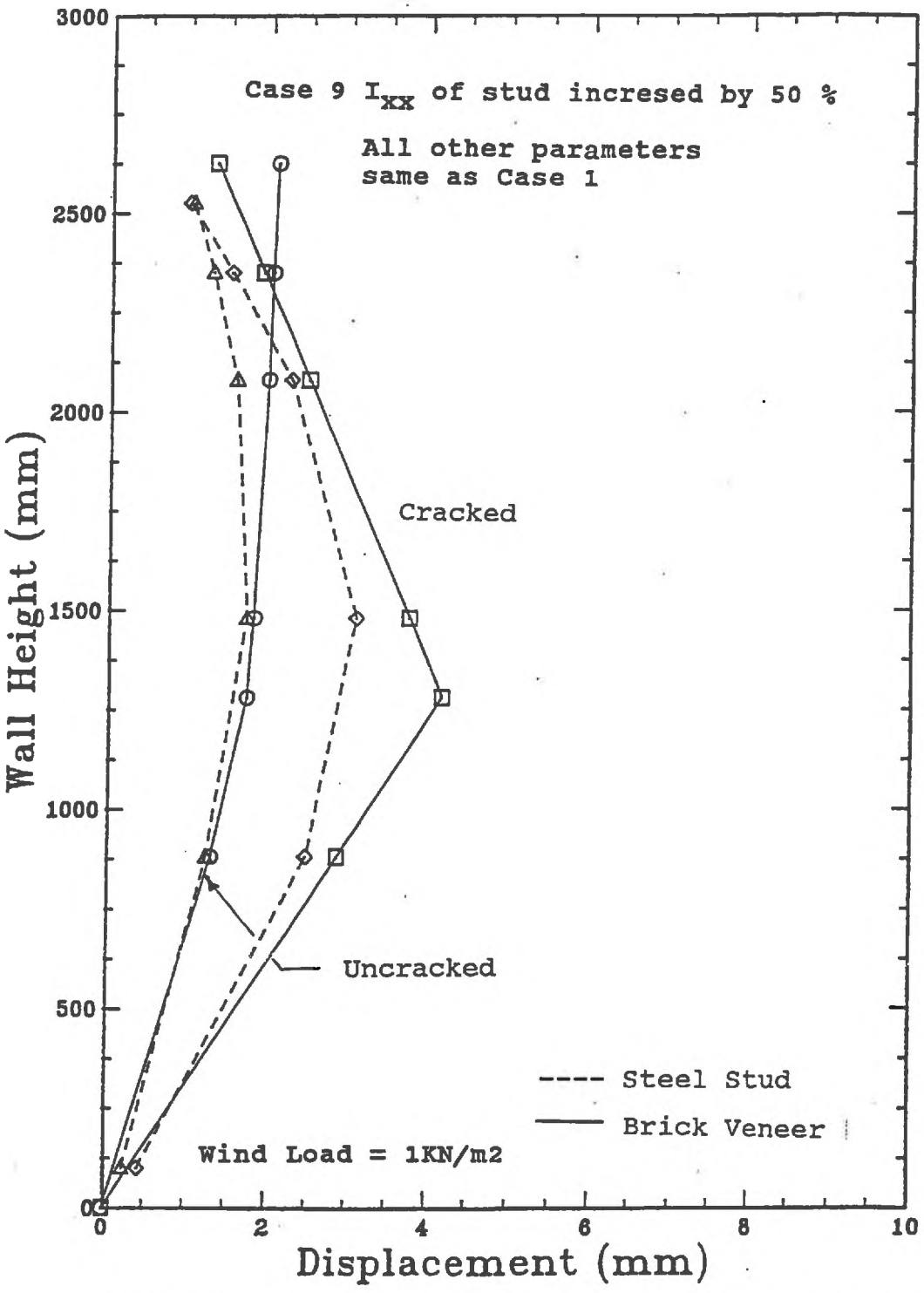

Figure 5.9 Deflection Profile for 2.63 Meter High BV/SS Wall - Case 9

TABLE 5.3

RESULTS OF COMPUTER ANALYSIS

Case No.	Predicted Wall 1 Cracking Load (KN/m^2)	Max. Stud Stress Prior to First Crack (MPa)	Max. Stud * Stress After First Crack (MPa)
1	1.273	34.00	90.90
2	1.361	37.46	96.96
3	1.210	28.65	88.46
4	1.304	32.18	94.94
5	1.400	33.59	93.10
6	1.499	38.93	99.57
7	1.280	26.63	87.96
8	1.377	30.52	94.34
9	1.577	31.43	67.56
10	1.260	34.02	
11	1.069	6.02	
12	1.129	11.38	
13	1.275	34.06	
14	1.298	34.64	
15	1.270		

Case No.	Predicted Wall 2 Cracking Load (KN/m^2)	Max. Stud Stress Prior to First Crack (MPa)	Max. Stud * Stress After First Crack (MPa)
16	0.483	13.50	37.02
17	0.630	23.50	48.86
18	0.476	16.99	36.70
19	0.618	15.09	48.10
20	0.486	12.95	36.96
21	0.630	22.83	47.66
22	0.473	11.03	36.02
23	0.618	21.47	46.77
24	0.561	18.76	
25	0.494	13.69	

* - Maximum flexural Stress only

TABLE 5.4

SUMMARY OF TIE LOADS

Tie * No.	Case 1 Uncracked	Case 1 Cracked	Case 2 Uncracked	Case 2 Cracked
1	0.0w	0.0w	0.0w	0.0w
2	−0.414w	−0.198w	−0.400w	−0.198w
3	−0.190w	−0.071w	−0.187w	−0.071w
4	0.231w	−0.381w	0.007w	−0.378w
5	0.029w	−0.162w	−0.009w	−0.165w
6	−0.011w	0.024w	0.016w	0.022w
a	−0.514w	−0.509w	−0.517w	−0.509w
b	−0.046w	−0.279w	−0.070w	−0.282w
c	−0.437w	−0.212w	−0.414w	−0.209w

Tie * No.	Case 3 Uncracked	Case 3 Cracked	Case 4 Uncracked	Case 4 Cracked
1	0.0w	0.0w	0.0w	0.0w
2	−0.464w	−0.260w	−0.446w	−0.260w
3	−0.154w	0.030w	−0.150w	0.029w
4	0.059w	−0.450w	0.039w	−0.443w
5	0.021w	−0.129w	−0.002w	0.054w
6	−0.024w	0.057w	−0.028w	−0.137w
a	−0.518w	−0.510w	−0.517w	−0.510w
b	−0.044w	−0.241w	−0.070w	−0.246w
c	−0.437w	−0.248w	−0.413w	−0.244w

Tie * No.	Case 5 Uncracked	Case 5 Cracked	Case 6 Uncracked	Case 6 Cracked
1	0.0w	0.0w	0.0w	0.0w
2	−0.270w	−0.060w	−0.255w	−0.056w
3	−0.009w	0.109w	−0.006w	0.108w
4	0.265w	−0.135w	0.249w	−0.133w
5	0.260w	0.073w	0.240w	0.071w
6	0.113w	0.149w	0.109w	0.147w
a	−0.510w	−0.501w	−0.514w	−0.506w
b	−0.125w	−0.353w	−0.148w	−0.358w
c	−0.357w	−0.138w	−0.338w	−0.137w

TABLE 5.4 (continued)

Tie * No.	Tie Loads Case No. 7		Tie Loads Case No. 8	
1	0.0w	0.0w	0.0w	0.0w
2	−0.329w	−0.118w	−0.332w	−0.118w
3	0.024w	0.213w	0.027w	0.211w
4	0.307w	−0.218w	0.286w	−0.213w
5	0.267w	0.115w	0.244w	0.110w
6	0.120w	0.204w	0.117w	0.200w
7	−0.516w	−0.508w	−0.515w	−0.508w
8	−0.095w	−0.297w	−0.121w	−0.301w
a	−0.389w	−0.195w	−0.364w	−0.191w

Tie * No.	Tie Loads Case No. 9		Tie Loads Case No. 10	Case No. 11
1	0.0w	0.0w	0.0w	−0.466w
2	−0.358w	−0.183w	−0.415w	−0.003w
3	−0.188w	−0.108w	−0.191w	−0.013w
4	−0.039w	−0.311w	0.022w	−0.023w
5	−0.020w	−0.193w	0.031w	−0.022w
6	−0.016w	−0.100w	0.004w	−0.006w
7	−0.515w	−0.488w	−0.519w	−0.034w
8	−0.105w	−0.406w	−0.031w	−0.032w
a	−0.379w	−0.106w	−0.450w	−0.467w

Tie * No.	Tie Loads Case No. 12	Case No. 13	Tie Loads Case No. 14	Case No. 15
1	−0.330w	0.0w	0.0w	0.0w
2	−0.123w	−0.414w	−0.413w	−0.415w
3	−0.065w	−0.189w	−0.188w	−0.190w
4	−0.010w	0.024w	0.026w	0.022w
5	−0.015w	0.027w	0.025w	0.030w
6	−0.008w	−0.022w	−0.040w	−0.003w
7	−0.176w	−0.518w	−0.517w	−0.518w
8	−0.037w	−0.056w	−0.074w	−0.037w
a	−0.458w	−0.426w	−0.409w	−0.444w

TABLE 5.4 (continued)

Tie * No.	Tie Loads Case No. 16		Tie Loads Case No. 17	
1	0.0w	0.0w	0.0w	0.0w
2	−0.340w	−0.239w	−0.301w	−0.234w
3	−0.146w	−0.024w	−0.135w	−0.032w
4	−0.045w	0.008w	−0.056w	0.003w
5	−0.015w	−0.275w	−0.038w	−0.253w
6	−0.018w	−0.277w	−0.045w	−0.265w
7	−0.030w	0.019w	−0.056w	0.004w
8	−0.039w	0.044w	−0.060w	0.002w
9	−0.039w	−0.049w	−0.051w	−0.056w
10	−0.518w	−0.514w	−0.515w	−0.513w
11	−0.153w	−0.281w	−0.227w	−0.305w
a	−0.326w	−0.205w	−0.257w	−0.182w

Tie * No.	Tie Loads Case No. 18		Tie Loads Case No. 19	
1	0.0w	0.0w	0.0w	0.0w
2	−0.371w	−0.311w	−0.325w	−0.293w
3	−0.124w	0.032w	−0.116w	0.014w
4	−0.023w	0.105w	−0.040w	0.087w
5	−0.009w	−0.348w	−0.036w	−0.321w
6	−0.023w	−0.357w	−0.049w	−0.330w
7	−0.037w	0.097w	−0.060w	0.072w
8	−0.047w	0.087w	−0.070w	0.050w
9	−0.050w	−0.090w	−0.066w	−0.096w
10	−0.517w	−0.514w	−0.515w	−0.513w
11	−0.168w	−0.270w	−0.246w	−0.305w
a	−0.314w	−0.216w	−0.239w	−0.182w

Tie * No.	Tie Loads Case No. 20		Tie Loads Case No. 21	
1	0.0w	0.0w	0.0w	0.0w
2	−0.225w	−0.117w	−0.181w	−0.110w
3	−0.020w	0.108w	−0.009w	0.100w
4	0.088w	0.144w	0.074w	0.137w
5	0.122w	−0.154w	0.096w	−0.140w
6	0.120w	−0.154w	0.091w	−0.142w
7	0.100w	0.152w	0.075w	0.138w
8	0.066w	0.154w	0.046w	0.134w
9	0.015w	0.004w	0.003w	−0.002w
10	−0.509w	−0.504w	−0.506w	−0.504w
11	−0.224w	−0.359w	−0.298w	−0.380w
a	−0.267w	−0.136w	−0.196w	−0.116w

TABLE 5.4 (continued)

Tie * No.	Tie Loads Case No. 22		Tie Loads Case No. 23	
1	0.0w	0.0w	0.0w	0.0w
2	−0.257w	−0.192w	−0.205w	−0.172w
3	0.001w	0.169w	0.009w	0.148w
4	0.108w	0.245w	0.090w	0.224w
5	0.125w	−0.236w	0.096w	−0.208w
6	0.114w	−0.242w	0.086w	−0.215w
7	0.097w	0.240w	0.074w	0.215w
8	0.067w	0.210w	0.047w	0.164w
9	0.014w	−0.029w	−0.002w	−0.034w
10	−0.509w	−0.506w	−0.506w	−0.504w
11	−0.220w	−0.329w	−0.299w	−0.363w
a	−0.271w	−0.166w	−0.194w	−0.133w

Tie * No.	Tie Loads Case No. 24
1	0.0w
2	−0.303w
3	−0.149w
4	−0.064w
5	−0.034w
6	−0.033w
7	−0.040w
8	−0.039w
9	−0.024w
10	−0.517w
11	−0.168w
a	−0.315w

* See Figures 4 8 and 4.9.

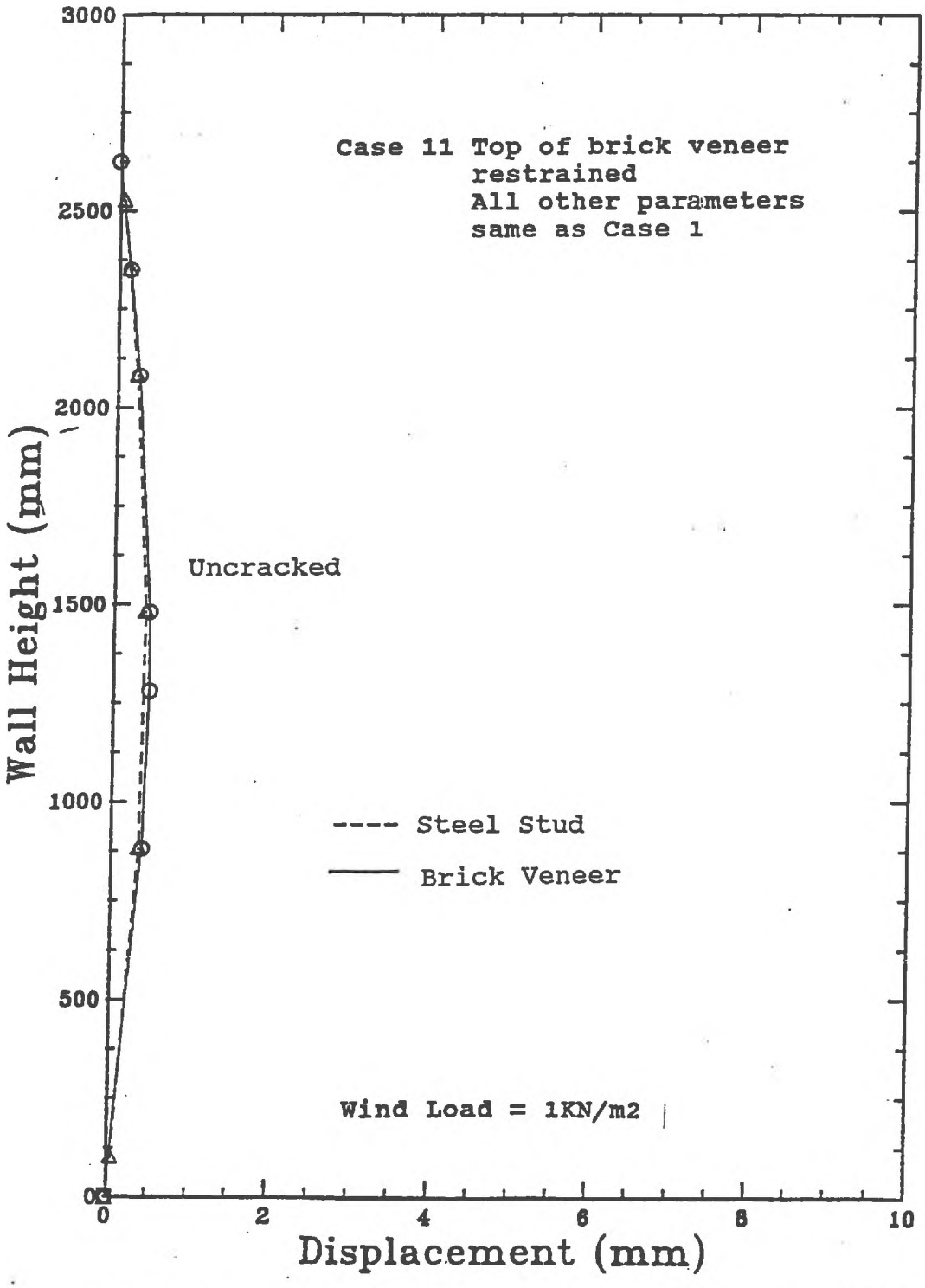

Figure 5.10 Deflection Profile for 2.63 Meter High BV/SS Wall - Case 11

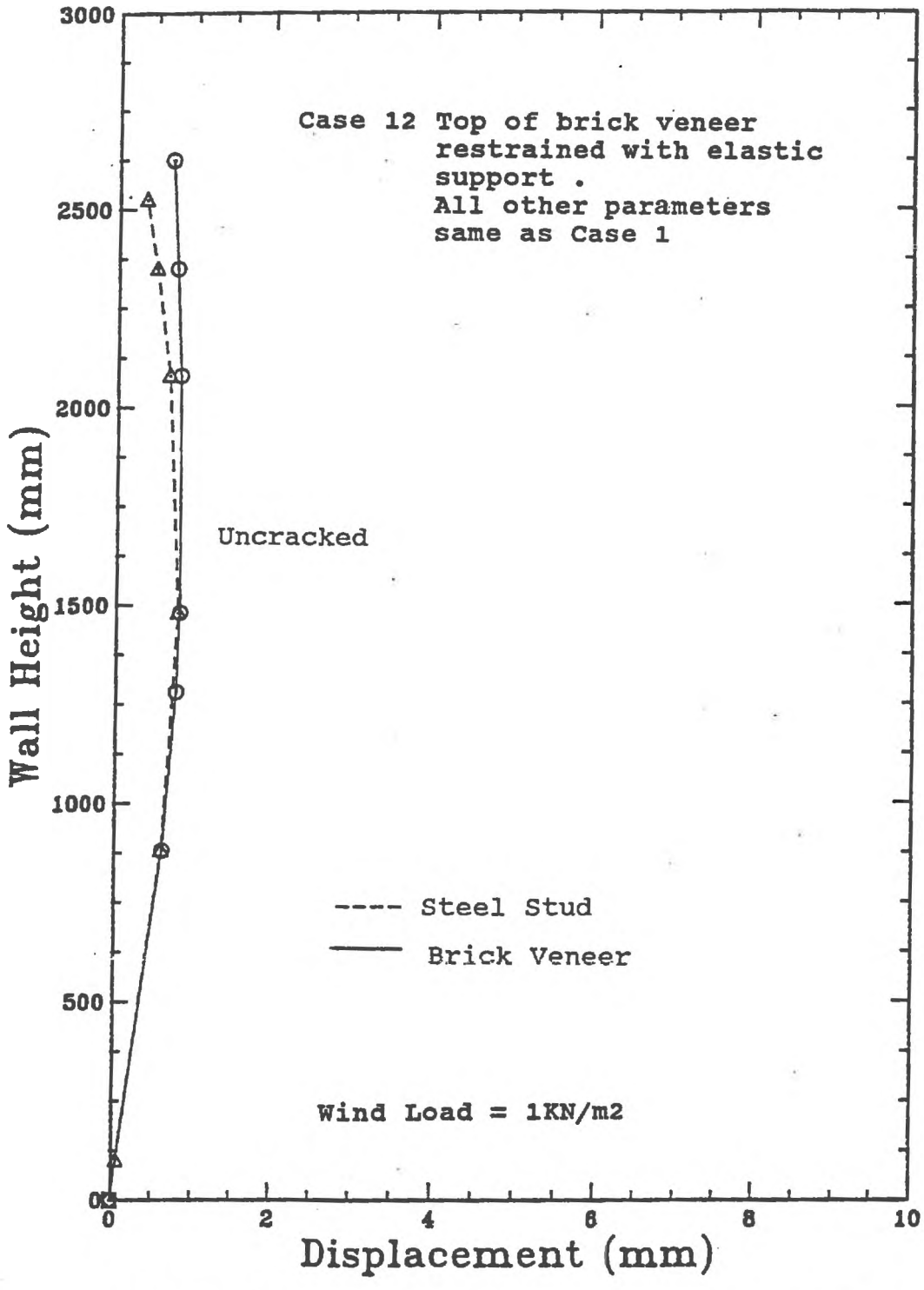

Figure 5.11 Deflection Profile for 2.63 Meter High BV/SS Wall - Case 12

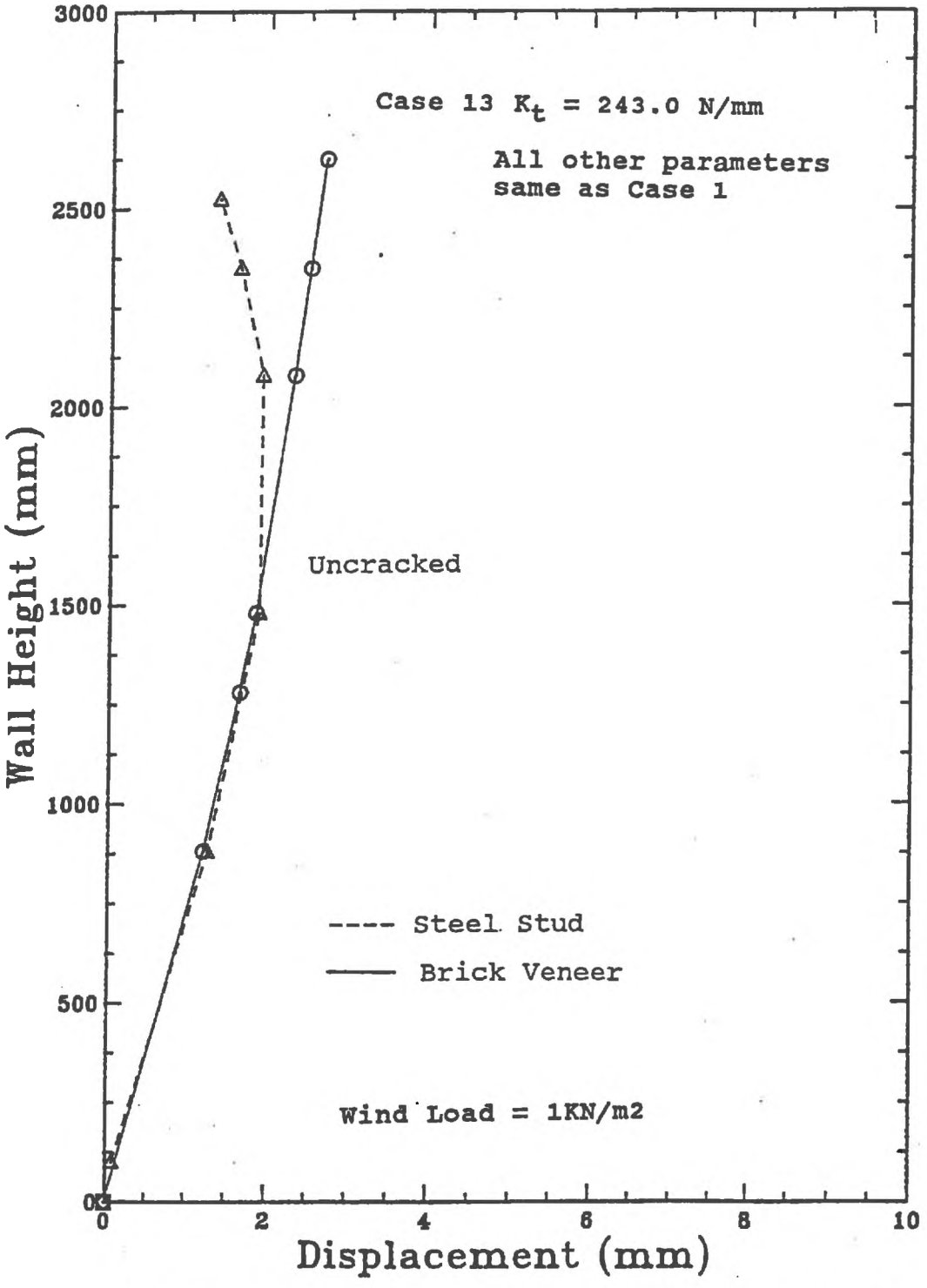

Figure 5.12 Deflection Profile for 2.63 Meter High BV/SS Wall - Case 13

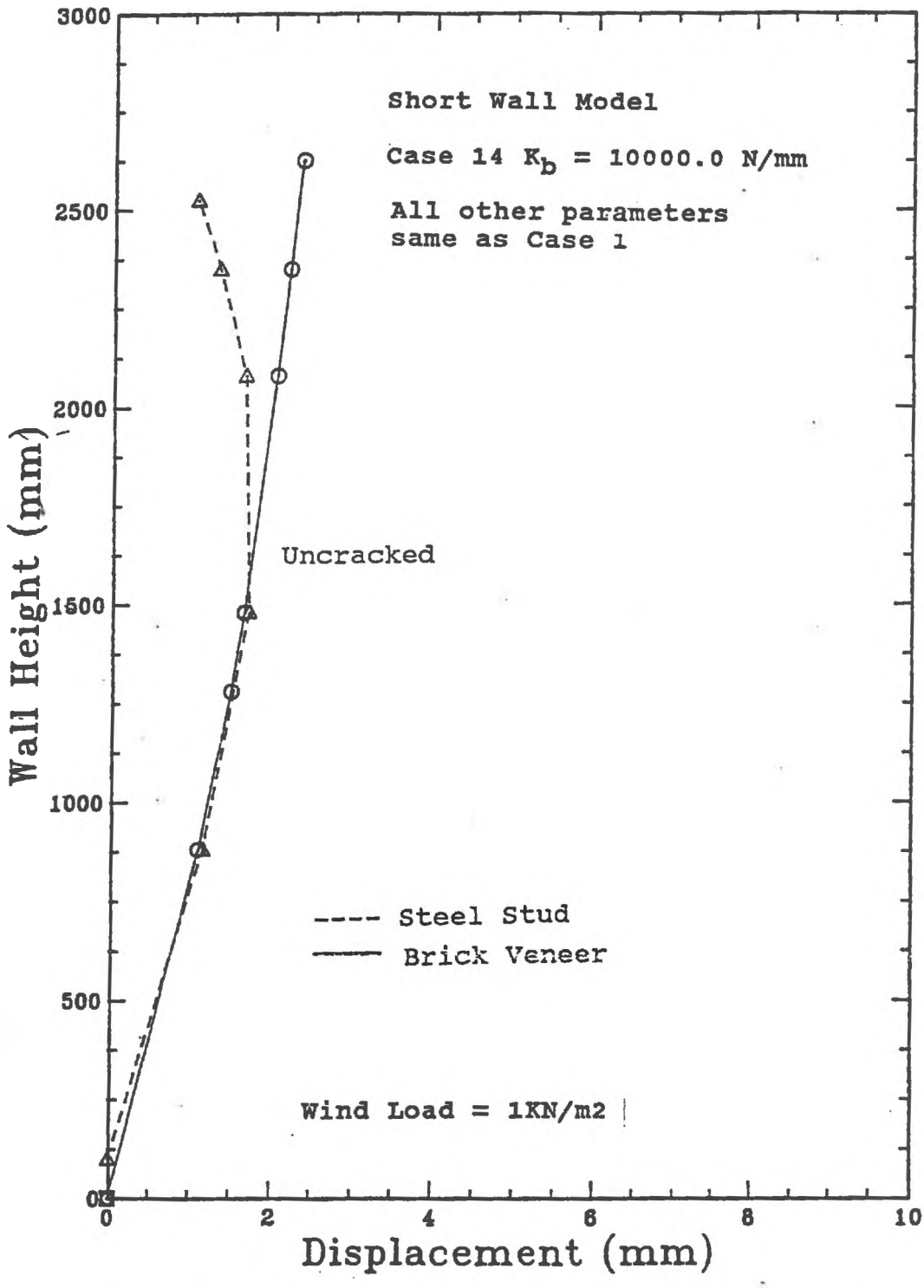

Figure 5.13 Deflection Profile for 2.63 Meter High BV/SS Wall - Case 14

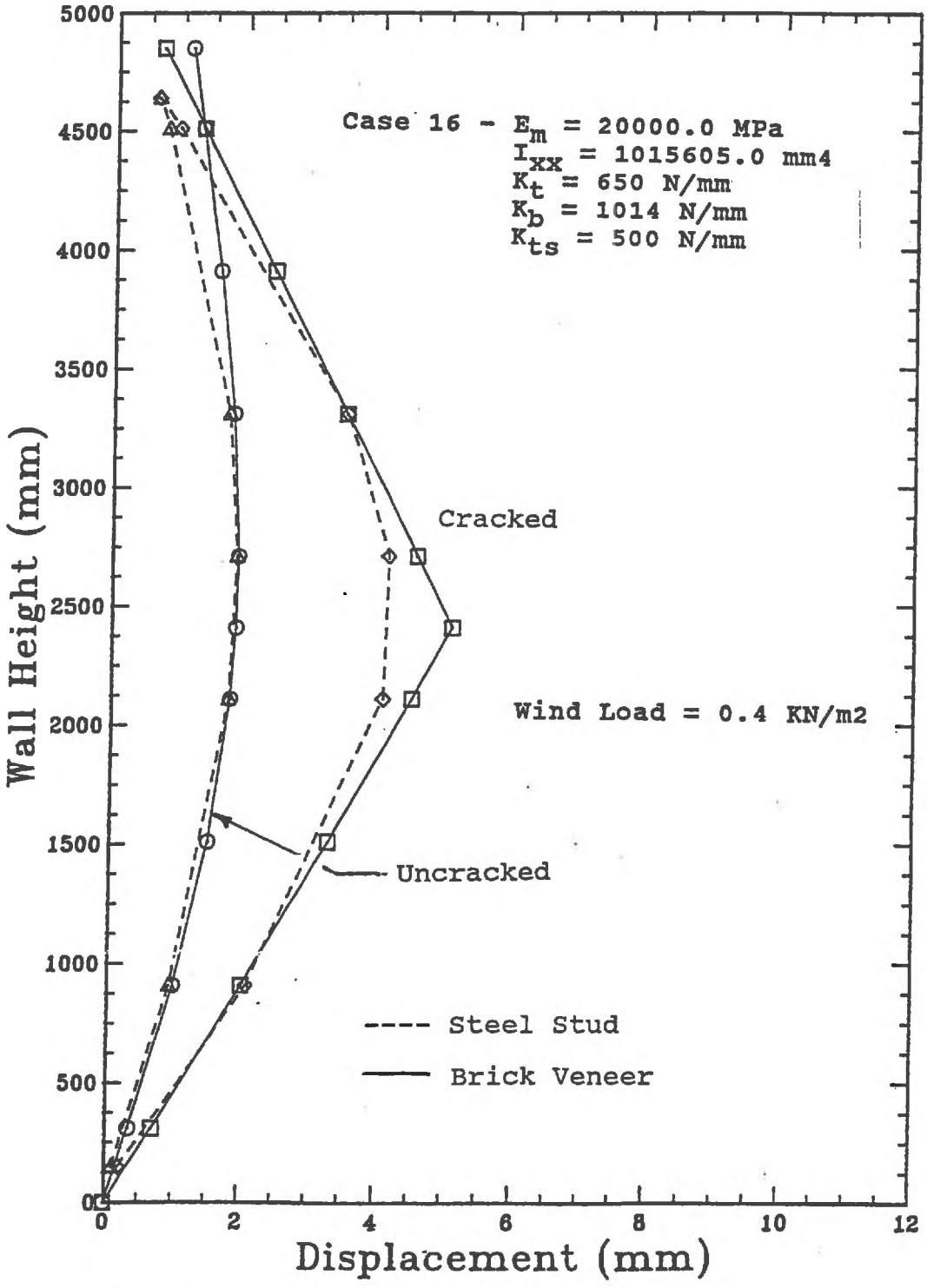

Figure 5.15 Deflection Profile for 4.85 Meter High BV/SS Wall - Case 16

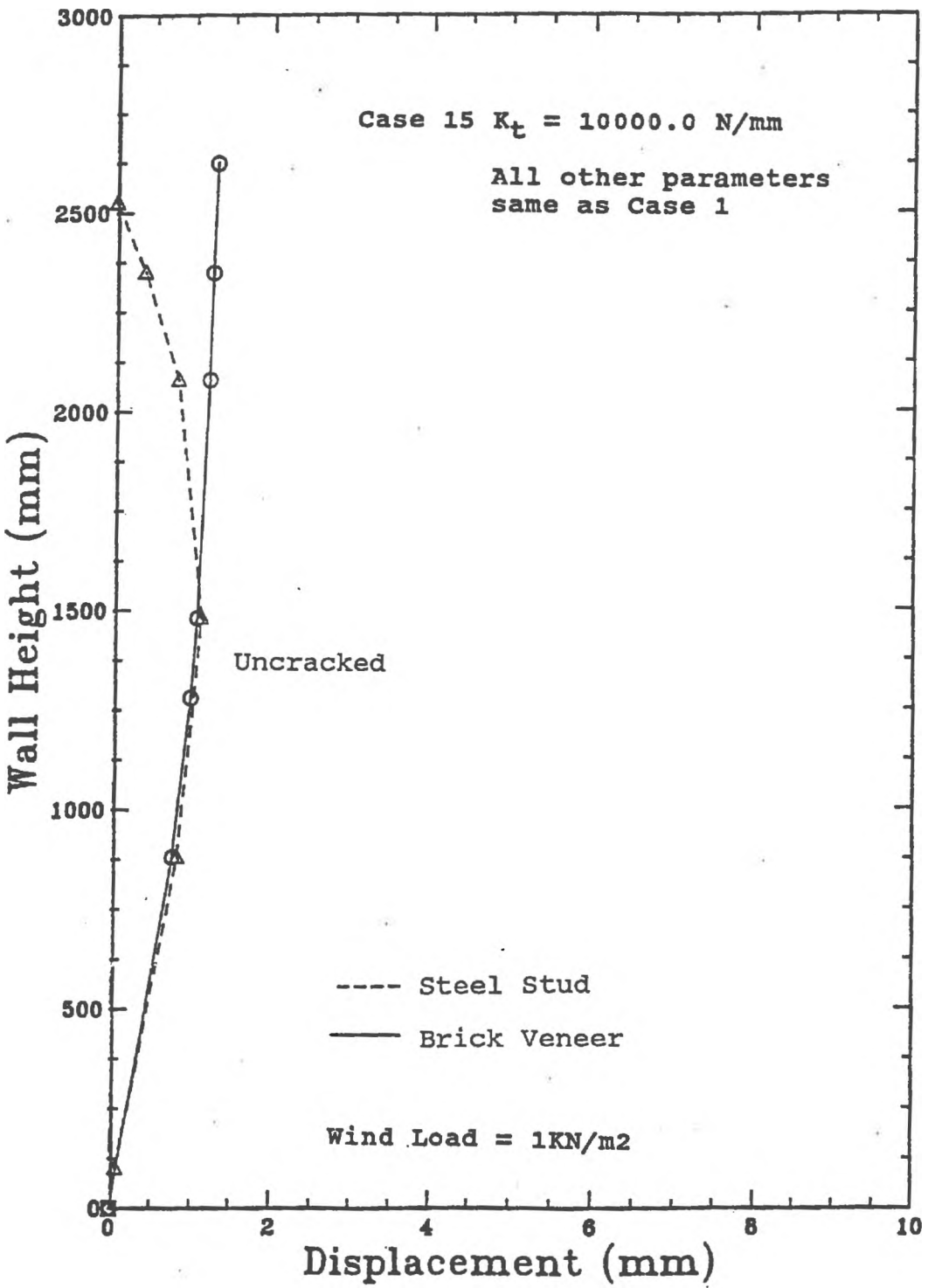

Figure 5.14 Deflection Profile for 2.63 Meter High BV/SS Wall - Case 15

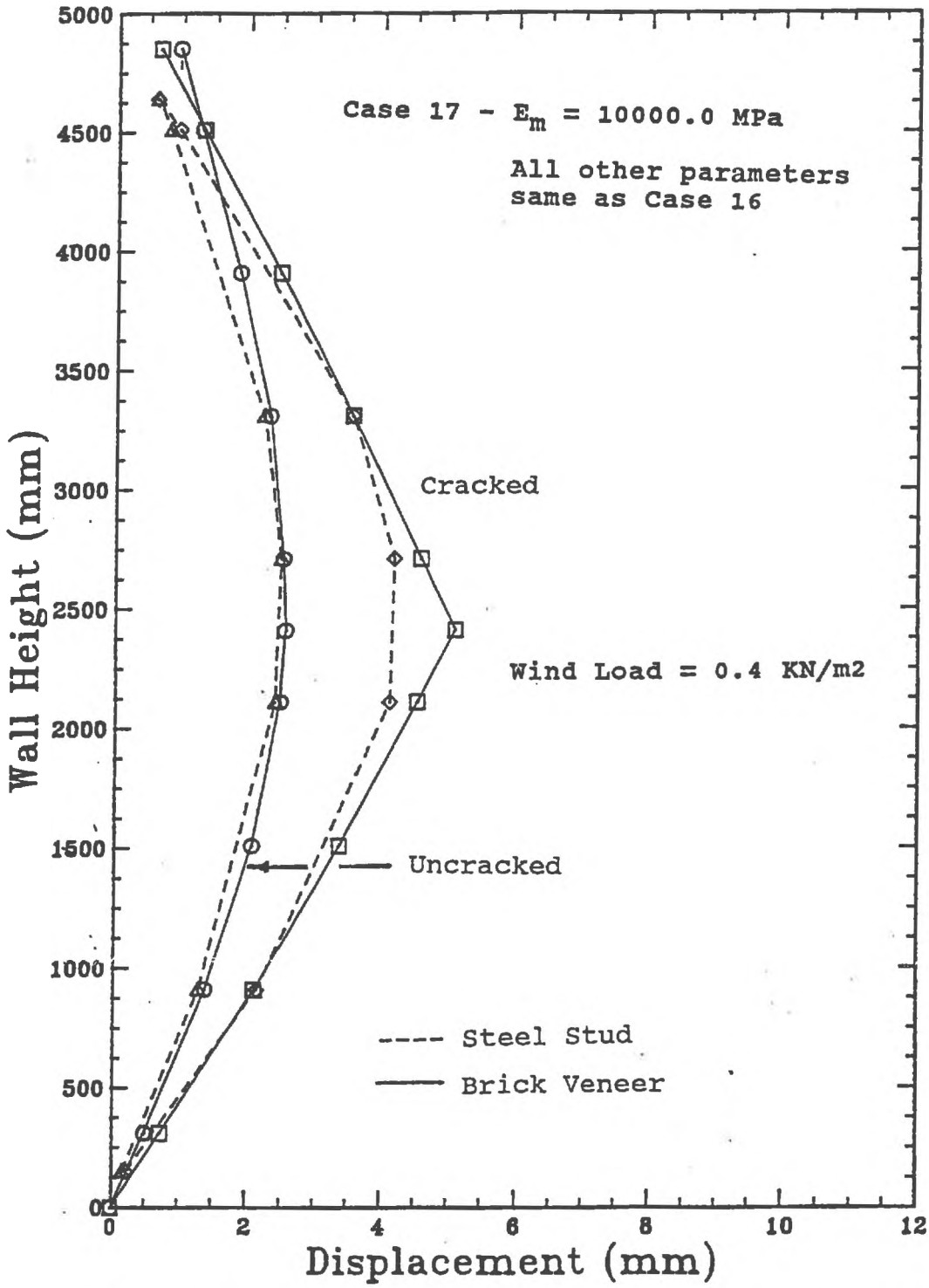

Figure 5.16 Deflection Profile for 4.85 Meter High BV/SS Wall - Case 17

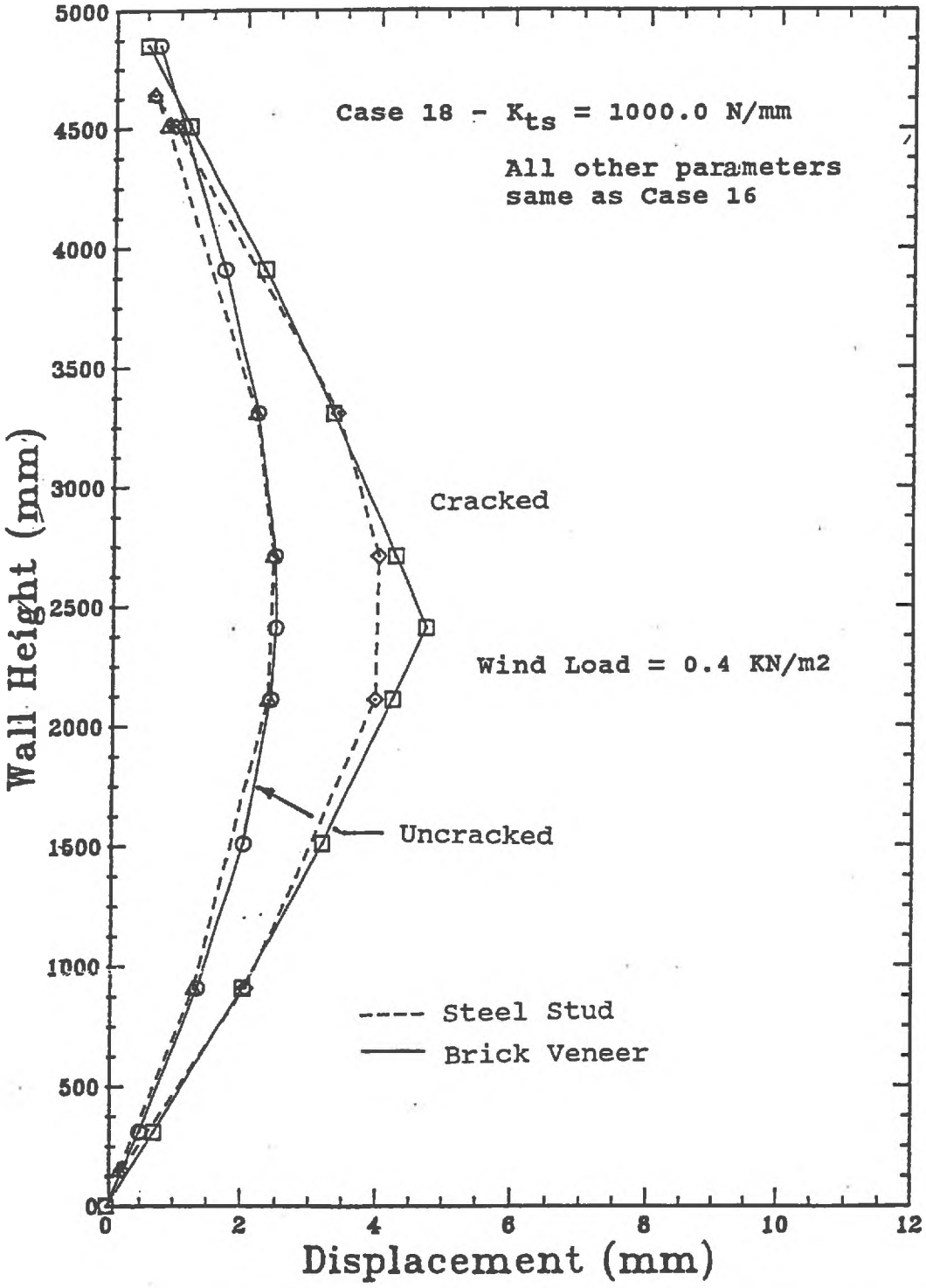

Figure 5.17 Deflection Profile for 4.65 Meter High BV/SS Wall - Case 18

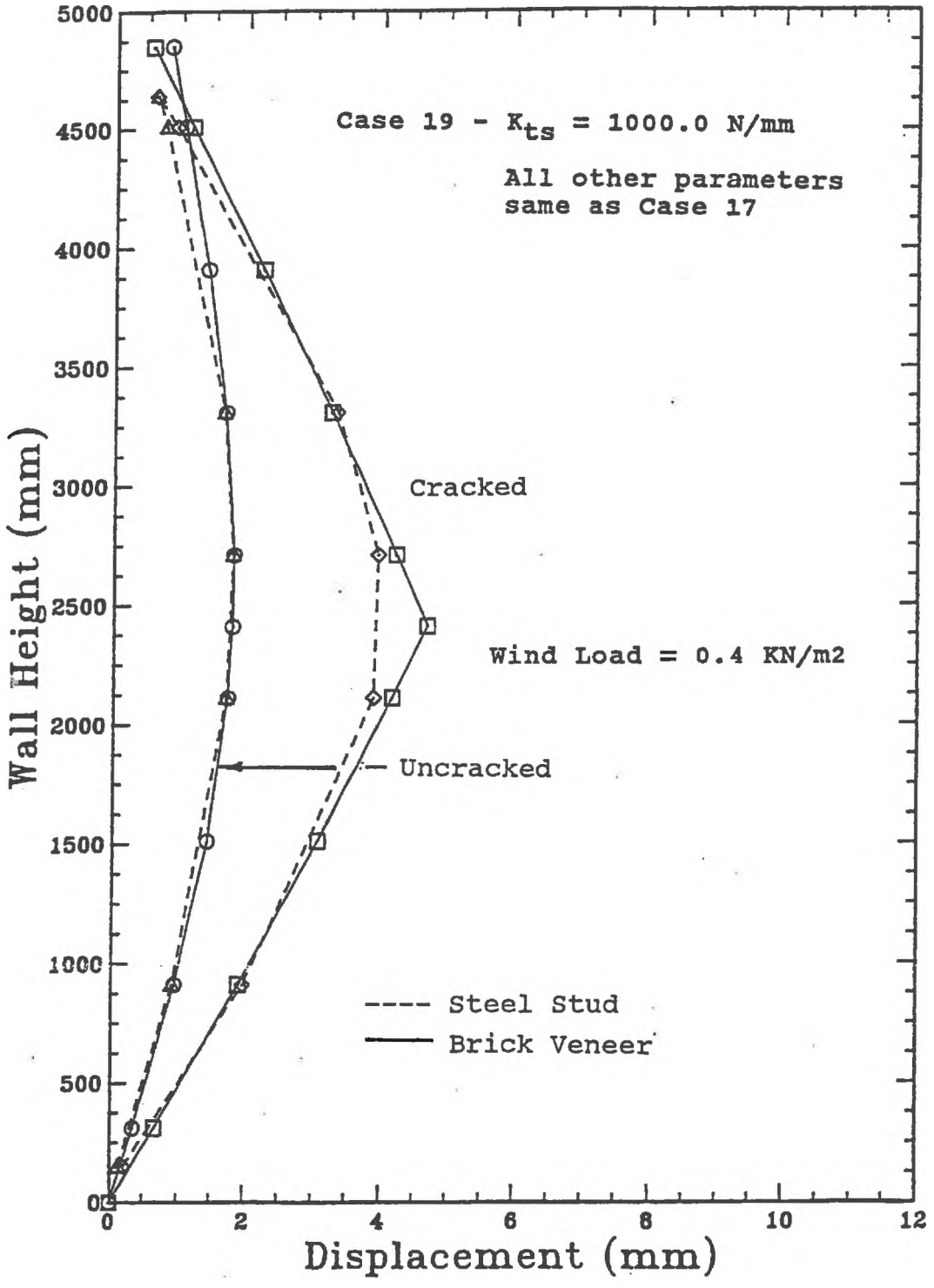

Figure 5.18 Deflection Profile for 4.85 Meter High BV/SS Wall - Case 19

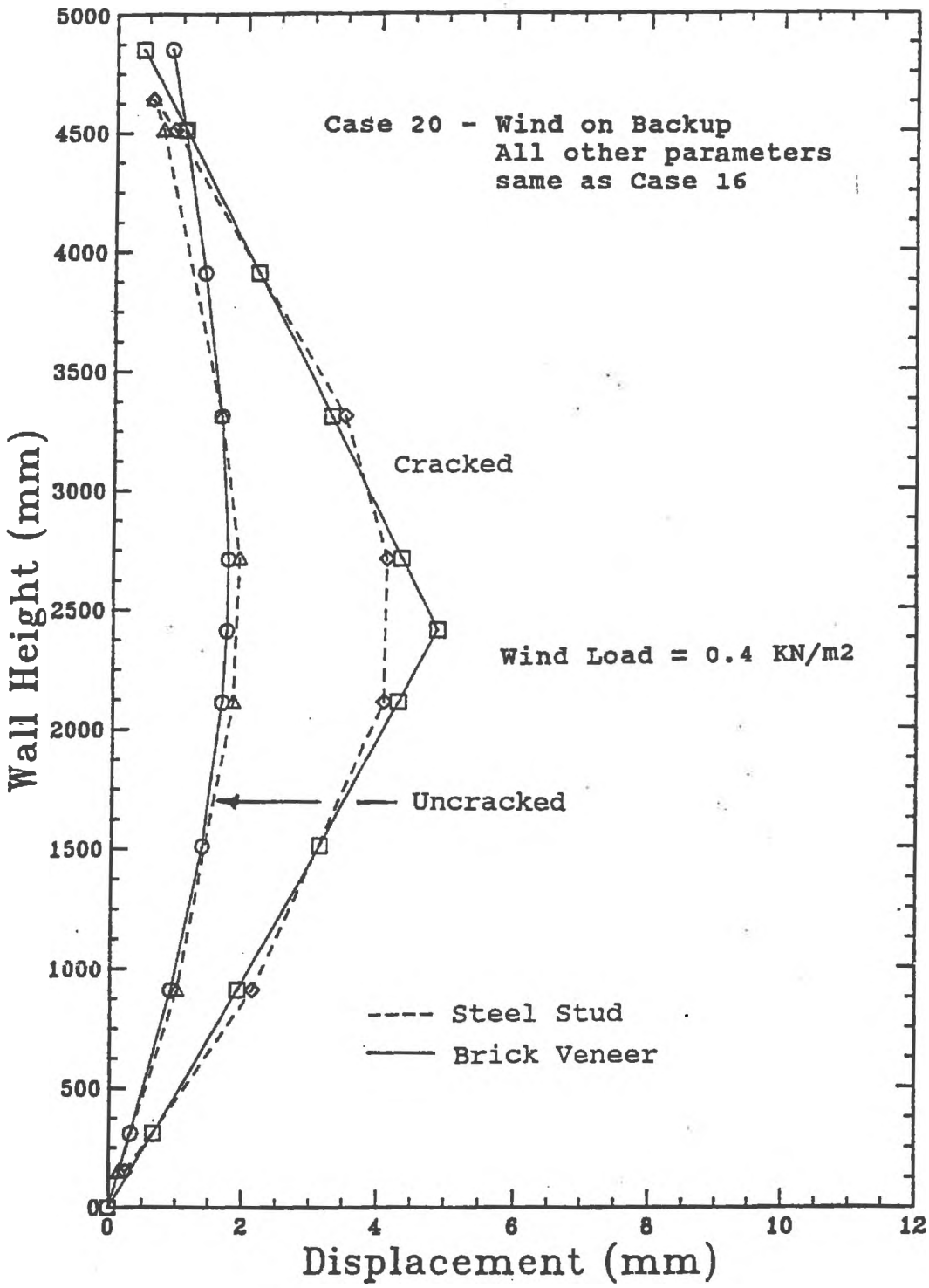

Figure 5.19 Deflection Profile for 4.85 Meter High BV/SS Wall - Case 20

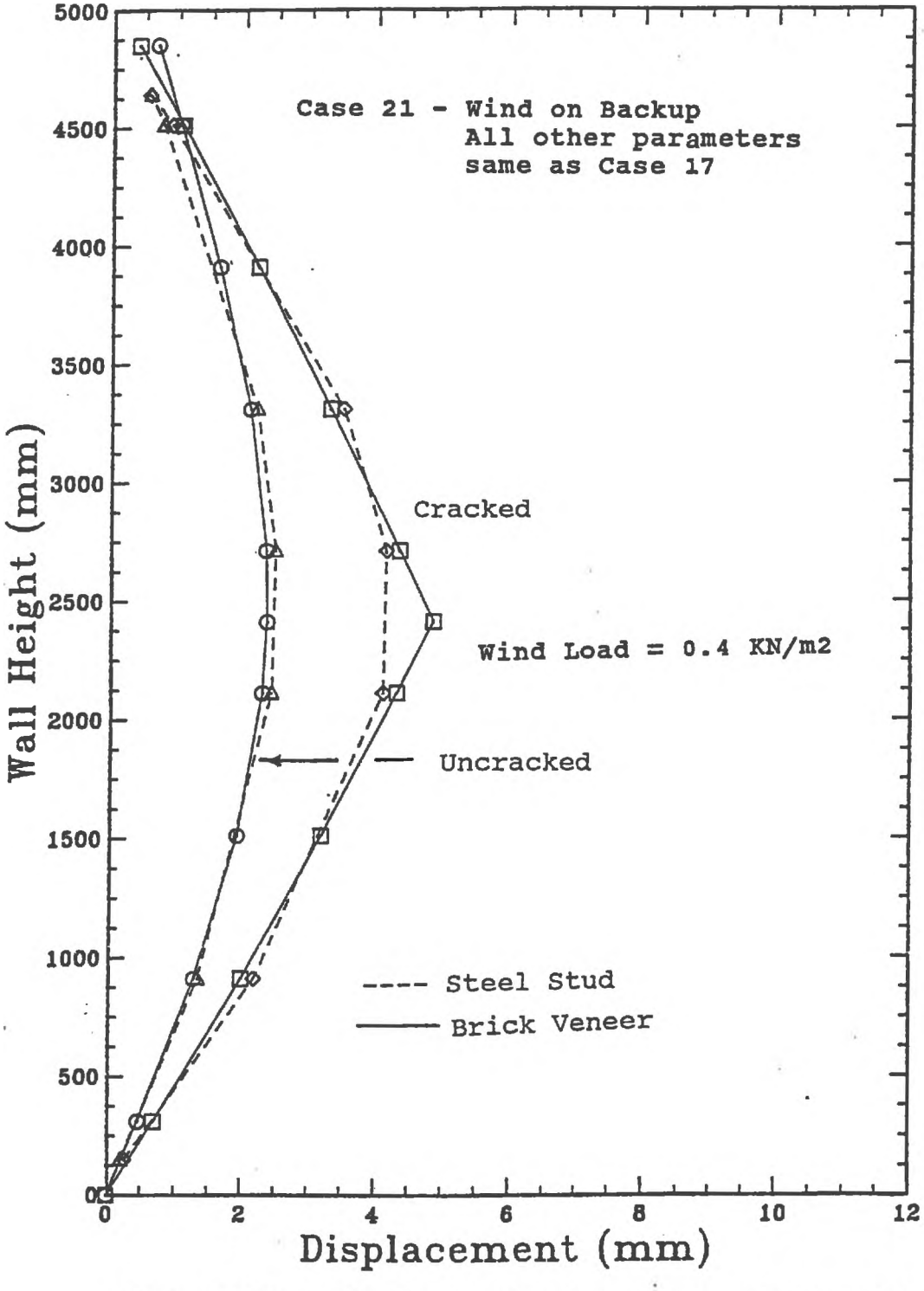

Figure 5.20 Deflection Profile for 4.85 Meter High BV/SS Wall - Case 21

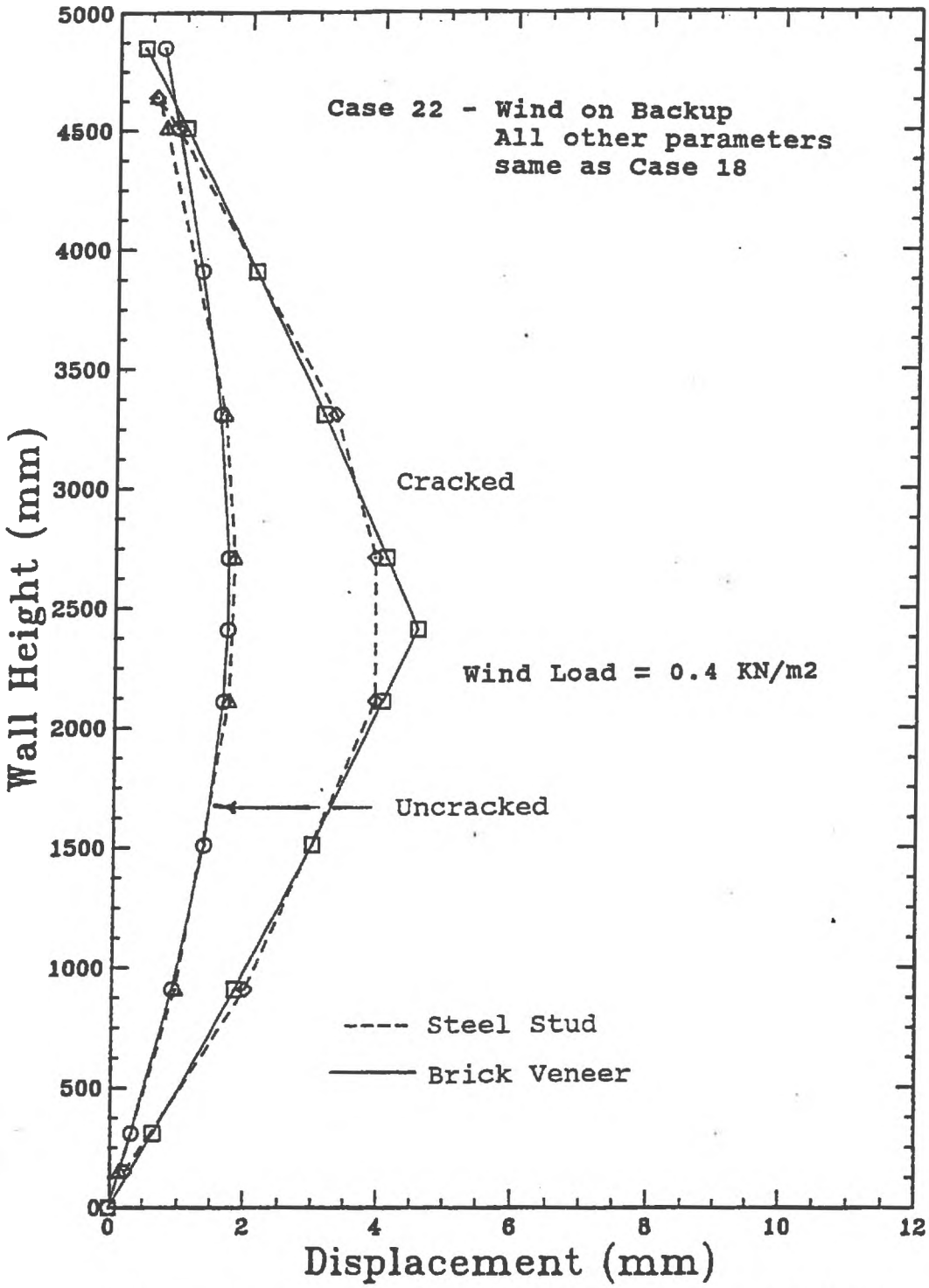

Figure 5.21 Deflection Profile for 4.85 Meter High BV/SS Wall - Case 22

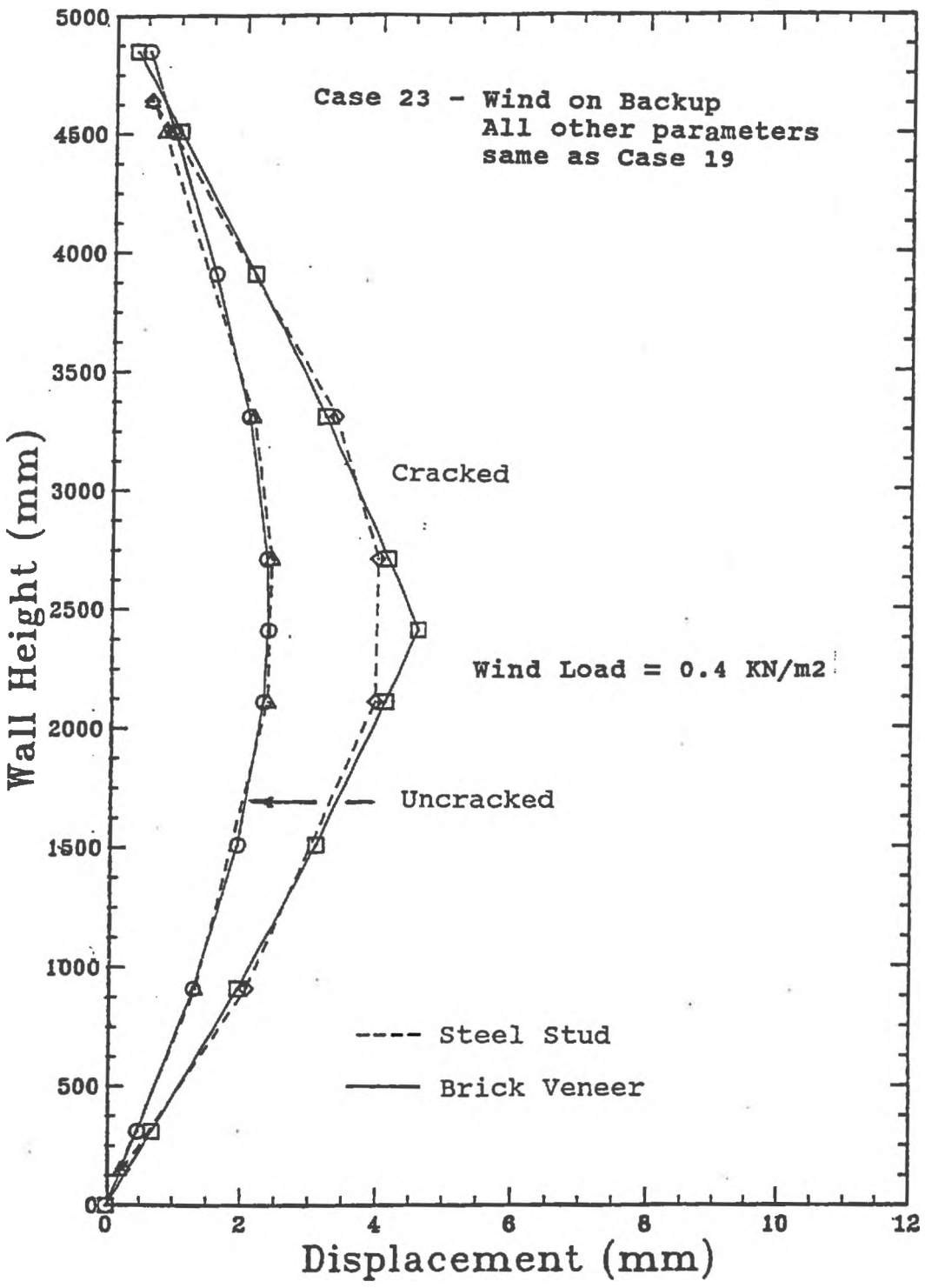

Figure 5.22 **Deflection Profile for 4.85 Meter High BV/SS Wall - Case 23**

5.4.3 Steel Stud Flexural Stresses

For both models, the maximum flexural stress in the steel stud prior to the formation of the first brick veneer crack is listed in Column 3 of Table 5.3. The maximum flexural stud stress for the cases which included post cracking behaviour are given in Column 4 of Table 5.3. It should be noted that the location of the maximum flexural stress in the steel stud before and after brick veneer cracking was not the same.

5.5 DISCUSSION OF RESULTS

5.5.1 General

In the following sections the influence of the various parameters investigated using the computer analysis will be discussed. However, before proceeding with the above, some general observations obtained from the results of the analyses concerning the general behaviour of the BV/SS wall system will be given. Firstly it was noted from the analysis that a large component of the out-of-plane displacements in the uncracked wall resulted from translation of the top track. This was due to the fact that the top of the brick veneer was assumed to be unrestrained and this effectively made the top stud to track connection the only lateral support at the top of the wall. Once the wall was cracked, the deflection at midspan was found to increase significantly. This was anticipated since the cracked brick veneer is a much less stiff element and the steel stud backup wall would resist a greater portion of the lateral wind load. In doing so, it would deflect to a much greater extent.

The results of the analysis also showed that before the brick veneer cracked, the top tie was heavily loaded. Once the brick veneer cracked, a redistribution of tie loads occurred and it was found that the ties near the midspan of the wall became more heavily loaded. More will be said about these results in the following sections.

5.5.1.1 Effect of Bottom Track Stiffness

In the case of Wall Model 1, the influence of bottom track stiffness on the predicted cracking load of the brick veneer can be seen by comparing the predicted failure load of Case 1 to those obtained for Cases 10 and 14. A summary of the failure loads is listed in Table 5.3. As the bottom track restraint to out-of-plane translation was increased from a stiffness of K_b = 554 N/mm for Case 1, to K_b = 10,000 N/mm for Case 14, the wind load required to cause brick veneer cracking increased by only 2 percent. The stiffness value used for Case 1 modelled the 2 screw minimum gap connection detail from Series 20A-D1 (Section 2.3.6). Increasing the bottom track translational stiffness by increasing the support track gauge, for example, will not significantly decrease the proportion of load carried by the brick veneer prior to cracking. When the bottom track stiffness was decreased for Case 10, only a minor decrease in the predicted ultimate cracking load was obtained. The bottom stud to track connection for this case was modelled as a linear spring with a stiffness equivalent to the slope of the load displacement curve for the 2 screw, 12 mm gap connection detail of Series 20B-D2.

The results of the analysis showed that for Wall Model 2, the influence of this variable was approximately similar to that of Model 1. Only a 2 percent decrease in the brick veneer stress resulted when the axial stiffness of the bottom of the stud spring support was increased from K_b = 1014 N/mm for Case 16, to 10,000 N/mm for Case 25.

5.5.1.2 Influence Of The Top Track Stiffness

For Wall Model 1, the results of the analysis indicated that the flexibility of the top steel stud to track connection greatly influenced the overall out-of-plane deflections of the BV/SS wall system. A significant portion of the out-of-plane movement of the wall was a direct result of the out-of-plane translation at the top of the steel stud.

For the cases represented in Figures 5.5 to 5.12, the top of the steel stud was assumed to be supported by a linear elastic spring with an axial stiffness of K_t = 517 N/mm. This stiffness was made for the nested top track connection detail of Series 20A-D12. As can be seen

from these figures, a significant portion of the out-of-plane deflections of the BV/SS wall system is due to the top translation of the steel stud.

For Case 15, the axial stiffness of the top of the steel stud spring was increased to K_t = 10,000 N/mm. Only the uncracked analysis was performed and the results are plotted in Figure 5.18. When this figure was compared to Figure 5.1 for Case 1, it was evident that the out-of-plane deflections were reduced for this condition. For both these cases the assumed wind load was taken as 1 KN/m^2. Increasing the top track stiffness to K_t = 10,000 N/mm did not greatly affect the predicted cracking load.

For Wall Model 2, no computer runs were made to specifically check the influence of the top track stiffness since the results obtained for Wall Model 1 clearly indicated that very little influence on the reduction in brick veneer stress was obtained. However, as indicated in Section 5.5.1.2, the flexibility of the top steel stud to track connection greatly influenced the total out-of-plane deflections of the BV/SS wall system.

5.5.1.3 Influence of Steel Stud Stiffness

In order to determine the influence of this variable on Wall Model 1, the out-of-plane flexural stiffness of the steel stud was increased by 50 percent in Case 9. The results of the analysis showed that this effectively reduced the stress in the brick veneer by 23 percent when compared to Case 1. This was due to the fact that the stiffer stud used in Case 9 shared a greater portion of the total lateral wind load. When Case 9 was compared to the case of the wind load acting on the backup wall, Case 5, the reduction in brick veneer stress was found to be only approximately 12 percent.

Increasing the stiffness of the steel stud also influenced the out-of-plane deflections. When the deflection profile of Case 1 shown in Figure 5.1 was compared to Figure 5.9 for Case 9, the BV/SS wall with the stiffer backup wall, shown in the second figure, deflected significantly less after the brick veneer was cracked.

For Wall Model 2, the flexural stiffness of the steel stud was increased by 50 percent in Case 24. The results of the analysis showed a 16 and 15 percent decrease in brick veneer stress when compared to Cases 16 and 20, respectively.

5.5.1.4 Effect Of Brick Veneer Stiffness

For Cases 2, 4, 6 and 8, related to Wall Model 1, the brick veneer stiffness was reduced to 10,000 MPa from the 20,000 MPa value used for Cases 1, 3, 5 and 7. For the reduced brick veneer stiffness, the steel stud backup wall was found to share a greater portion of the total lateral wind load. This effectively reduced the brick veneer stress by 7 to 8 percent.

The brick veneer stiffness for Wall Model 2 was reduced from 20,000 MPa to 10,000 MPa in Cases 17, 19, 21 and 23. This resulted in a decrease of approximately 30 percent in brick veneer stress when these cases were compared to Cases 16, 18, 20 and 22 respectively.

5.5.1.5 Influence of Brick Tie Stiffness

For the analysis of the short wall (Wall Model 1), the axial stiffness of the brick tie was increased to K_{ts} = 1000 N/mm for cases 3, 4, 7 and 8 from K_{ts} = 500 N/mm used in Cases 1, 2, 5 and 6. The results of the analysis indicated that this caused an increase of 4 to 9 percent in the brick veneer stress for the stiffer tie condition. In all cases considered, the tie loads were found to be non-uniform. This aspect will be discussed further in Section 5.5.3.

In the case of Wall Model 2, increasing the axial stiffness of the wall ties from K_{ts} = 500 N/mm to K_{ts} = 1000 N/mm for the cases listed in Table 5.1, resulted in an increase of 1 to 3 percent in the brick veneer stress.

5.5.1.6 Effect Of Top Of Brick Restraint

To determine the influence of restraint at the top of the veneer on Wall Model 1, three cases were compared. In Case 1 (Figure 5.1), the top of the brick veneer was assumed unrestrained. In Case 12 (Figure 5.11), the top of the brick veneer was assumed to be

supported by a linear spring with a stiffness of K_{bt} = 500 N/mm. In Case 11 (Figure 5.10), the axial stiffness of the spring was increased to 10,000 N/mm.

As the stiffness of the restraint at the top of the veneer increased, the brick veneer stress increased and the the out-of-plane deflections decreased significantly.

5.5.1.7 Influence Of Wind Load Location

Generally the results of the analysis for Wall Model 1 showed that the location of wind load on the BV/SS wall system had some influence on the amount of load shared by the brick veneer and the steel stud backup wall. In all the cases which considered the wind load to act on the face of the steel stud backup wall, the brick veneer stresses were reduced 5 to 10 percent lower than for similar cases with the wind load acting on the exterior face of the brick veneer.

For Wall Model 2,the location of the wind load did not have as significant an effect on the brick veneer stresses as was the case for Wall Model 1.

5.5.1.8 Influence of Cracked Brick Veneer

For Wall Model 1, cracking of the brick veneer occurred at approximately mid-height. Figures 5.1 to 5.9 are plots of the deflected profile of the BV/SS wall system before and after brick veneer cracking occurred for Cases 1 to 9. From these deflections, it is obvious that the out-of-plane deflections at midspan of the veneer increased significantly due to the loss of stiffness in the cracked brick veneer.

For Wall Model 2, cracking of the brick veneer also occurred near mid-height. The increased midspan deflection of the BV/SS wall system for Cases 16 to 23 are shown in Figures 5.15 to 5.20.

The formation of a crack in the brick veneer does not necessarily signify inadequate structural performance. However the crack width must be controlled since water penetration or leakage is more likely to occur through a cracked mortar joint. This topic is covered in more detail in other parts of the McMaster BV/SS research program. However, at a conceptual level,

if an average crack width of 0.1 to 0.2 mm was assumed, at the centre of the brick veneer, as the maximum allowable crack width as suggested by Drysdale[9], then an estimate of the allowable steel stud deflection which would result in a crack width of of this magnitude can be made. Based on this criteria, the results for Case 2 were used to calculate the allowable steel stud deflection for a maximum allowable crack width of 0.1 to 0.2 mm. This was accomplished by using the rotation data obtained at the joints of the cracked brick veneer. By using geometry, the width of the crack was determined. By setting the crack width successively at a value of 0.1 and 0.2 mm, the corresponding stud deflection was determined to be approximately L/1800 and L/900 respectively where cracking was assumed to occur at mid-height. Further research is needed to compare this information with leakage rates through brick veneer. However, based on the calculated stud deflections obtained in this study, it was concluded that an L/360 deflection criteria will lead to the formation of visible cracks of 1 mm in width or greater. The B.I.A.[4] recommendation of L/600 to L/720 should be considered an absolute maximum allowable steel stud deflection under full design wind load. It should also be noted that this deflection limitation is based on the flexural component of steel stud displacement and does not include the displacement of the stud due to end translations.

5.5.2 Steel Stud Stresses

The analysis of Wall Model 1 after cracking showed an increase in the maximum steel stud flexural stresses of more than 2.5 times that for the uncracked wall from Cases 1 to 8. The increase in steel stud stress indicated that the brick veneer no longer carried the greater portion of the wind load. As noted earlier, the location of maximum flexural steel stud stress varied. In the uncracked wall analysis, the cross-section under maximum stress was located near tie 3. In the cracked analysis the cross-section under maximum flexural stress was located at tie 4, which was very near to the mid-height of the steel stud. Stresses due to torsional loads were not considered in this analysis but a more detailed discussion on this aspect was covered in Chapter 4.

For Wall Model 2, the maximum flexural stresses were located between Tie 5 and Tie 6. For the cracked wall analysis, the cross-section under maximum flexural stress was located at Tie 6.

5.5.3 Distribution of Brick Tie Loads

For all the cases considered, the tie load distributions shown in Table 5.4 were found to be non-uniform. For the cases in which the top of the brick veneer was not restrained and the wind load was applied to act on the exterior face of the brick veneer, the top brick tie acted as the primary support point for the brick veneer. As a result, the top tie was heavily loaded. For these cases, the introduction of a crack in the brick veneer resulted in a significant decrease in load for the top tie. In addition to reducing the top tie load, the cracking resulted in a complete re-distribution of loads to the other ties. For Wall Model 1, Tie 4, which was located near midspan, carried approximately 40 percent of the total lateral wind load. For Wall Model 2, Ties 6 and 7 were both heavily loaded and each carried approximately 28 to 33 percent of the total lateral wind load. The higher tie loads occurred when the brick tie stiffness was increased from K_{ts} = 500 N/mm to K_{ts} = 1000.0 N/mm.

For Cases 5 to 8 and 20 to 23, the wind load was assumed to act on the exterior face of the steel stud and the top of brick veneer was assumed to be unrestrained. Again, the top tie was also found to be heavily loaded prior to veneer cracking. The redistribution of the tie loads after cracking resulted in a significantly reduced load in the top brick tie. For Wall Model 1, Tie 4 which was in tension prior to brick veneer cracking, was found to be not as heavily loaded in compression when compared to a similar case in which the wind load was acting on the exterior face of the brick veneer. For Wall Model 2, after cracking of the veneer, the portion of load taken by Ties 6 and 7 was less than for similar cases in which the wind load acted on the exterior face of the brick veneer.

For the cases in which the top of the brick veneer was restrained (Cases 11 and 12 for Wall Model 1), the top tie assumed more load as the top restraint decreased. This is consistent with the condition of no restraint in which case the top tie assumed the role of primary support for the top of the brick veneer wall.

5.6 DISCUSSIONS AND CONCLUSIONS

The results of the computer analyses clearly showed that the parameters which were investigated in this chapter all had some influence on the predicted cracking load of the brick veneer, on the distribution of tie loads and on the deflections of the BV/SS wall system.

For Wall Model 1, the wind pressure required to cause brick veneer cracking, was found to range from 1.2 to 1.58 KN/m2 for Cases 1 to 9. These values were obtained by limiting the flexural tensile stress in the brick to 0.6 MPa. Under more moderate wind load, this wall would not be expected to crack. However the flexural bond strength of brick masonry is highly variable and in some cases where flexural bond is poor or where other stresses exist, the veneer may crack.

For Wall Model 2, the design wind pressures required to crack the veneer was found to range from 0.47 KN/m^2 to 0.63 KN/m^2 The maximum flexural tensile stress was again limited to 0.6 MPa. Any combination of wind pressures greater than about 0.6 KN/m^2 would likely crack this brick veneer.

Based on the results presented in this chapter, it was concluded that any design criteria based solely on a limiting maximum deflection of the steel stud is not satisfactory because of significant influences of the deformations and displacements of the ends of the steel studs in the track. Unless arbitrary values are provided, determination of the appropriate design loads for this system requires a more extensive analysis. The design of the BV/SS wall system using either a rigiorous structural analysis or approximate criteria based on the rigorous analysis should consider the following:

1. Brick veneer and backup wall interaction

2. Stiffness of the top and bottom track connection detail
3. Steel stud stiffness
4. Tie stiffness
5. Brick veneer stiffness
6. Flexural bond strength

The designer must also consider the possibility of brick veneer cracking. For high walls this cracking is highly probable and in order to control water penetration through the veneer and into the cavity, the width of the crack should be controlled. This was shown to be possible by controlling the brick veneer deflections after the wall cracked. Control of deflections was shown to be possible by considering the stiffness of the backup wall. For the time being, a limitation on the maximum allowable veneer deflection to L/720 is recommended.

The design of the backup wall system must also satisfy the ultimate strength requirements for the backup wall. This aspect was discussed in Chapter 4.

CHAPTER 6
SUMMARY AND RECOMMENDATIONS

6.1 GENERAL OVERVIEW

The primary purpose of this study was to investigate and document the structural behaviour of the steel stud backup wall construction in the context of how it influences the overall behaviour of the BV/SS wall system. Experimental research to obtain this information was necessary because no previous comprehensive investigation had been undertaken. In addition to the direct benefit of providing useful data, these results have been put into forms suitable for use by others. Also, interpretation and use of this information in various analyses has permitted incorporation of illustrations of the impact of changing characteristics of the steel stud backup form of construction. Some recommendations have been provided.

6.2 SUMMARY

Discussion of the various findings of this research program were included in the body of this report. A brief summary of the main points is provided below.

6.2.1 Steel Stud to Track Connection Tests

A simple experiment was designed to isolate the behaviour of various steel stud to track connection details. The 109 connections tested included variation of parameters such as the size and thickness of the steel stud and track, number of screws used to make the connection, and amount of gap left between the end of the steel stud and the inside face of the track. In addition, welded connections and a variety of movement connections were tested. In the majority of tests, web crippling was the observed mode of failure. The specimens that used some type of clip angle to connect the web of the stud to the track did not fail in this manner. Also, it was found that some of the welded connections did not fail by web crippling at the stud to track connection.

Load-deflection curves obtained from these tests showed that the lateral displacement of the stud at the track was greatly influenced by the type of connection used to fasten the stud to the track. Since the load-displacement relationships were found to be reasonably linear to load levels well above expected service loads, linear best fit curves for each test series were presented to represent their out-of-plane stiffnesses.

In order to evaluate the web crippling strength of the steel studs at the stud to track connection, the experimental failure loads were compared with theoretically ultimate loads predicted using code equations. The experimental values were greater than the predicted values for all cases.

6.2.2 Steel Stud Backup Wall Tests

The strength and deformation characteristics of full size steel stud backup wall assemblies were evaluated using bending tests. The backup wall panels were fabricated with either two or four steel studs. The four-stud panels were used to investigate the strength and deformation characteristics of steel studs braced at discrete locations with steel bridging or with studs braced with a combination of sheathing and discrete bracing. The parameters varied included the thickness of stud, number of rows of bridging and type of bridging connection details. For these tests, the observed mode of failure was local buckling in the region of the web cutout holes located between the steel bridging and the supports. This type of failure always occurred after significant stud twisting was observed in the region of the web cutout hole. The rotation measurements showed that for L/360 panel deflections, the maximum stud rotations were not greater than a few degrees.

In all of the above tests, the maximum unbraced span length was approximately 1280 mm. Different types of steel bridging were used and various commonly used methods of attaching the bridging to the steel studs were also investigated. The results showed that all types of bridging tested improved the bending capacity of the panels. However, it was concluded that special consideration was required to ensure that each type of bridging would

function properly. Chapter 4 contains a more detailed description and summary of this particular aspect of the research.

Two 4 stud wall panels sheathed with 50 mm of Styrofoam S.M. insulation on the compression face were also tested. The results showed that the polystyrene did provide some bracing for the stud but that it was not sufficient to develop the full expected moment capacity of the steel studs.

6.2.3 Two-Stud Backup Wall Panels

Panels constructed with two studs were used primarily to test steel studs with drywall sheathing on both faces of the panels. Tests on unbraced two-stud backup wall panels were also performed in order to investigate the strength and deformation characteristics of panels under this condition.

The beam test specimens were fabricated with two studs placed symmetrically to minimize torsional loads and allow the studs to brace each other. Under this condition the full moment capacity of the steel stud was expected to be achieved. When compared to the theoretical yielded moment, it was concluded that the full moment capacity was obtained for the beam test specimens.

Tests showed that the studs in unbraced panels underwent longer rotations even at low load levels and that the panels developed only 26 to 33 percent of the capacity from the braced beam tests. Hence, it was concluded tht unbraced steel stud panels are structurally inefficient and basically undesirable.

For stud panels sheathed with gypsum board on both faces, some composite action was shown to exist initially and it was found to be a function of the spacing of the drywall screws. For a screw spacing of 150 mm on centre, a 17 percent increase in initial panel stiffness was observed. For panels with sheathing attached every 300 mm on centre, the initial increase in panel stiffness was found to be 10 percent or less. In all cases, the amount of composite action was found to decrease rapidly under cyclic loading. The effect of dampening the gypsum board

was also investigated and it was shown that under this condition, very little initial composite action existed. In these tests, the gypsum board sheathing was fastened in a continuous manner to the steel studs. The research by Murden[24] showed that gypsum board attached in pieces rather than in continuous sheaths provided even less composite action. It was concluded that the composite action between the steel stud and the gypsum board is very small under ideal laboratory conditions and is anticipated to be even less under field conditions.

Gypsum board sheathing was found to provide sufficient bracing to allow the full moment capacity of the steel stud to be developed. For dampened conditions, the much weaker gypsum board was unable to provide much bracing capability.

6.2.4 Backup Wall Panels Braced With Discrete Bracing

Since the results of the test program indicated that the torsion loads significantly reduced the moment capacity of the steel studs, a simple finite element torsion program was developed to evaluate the effects of discrete bracing. The results of the simplified analysis showed that the maximum combined flexural and torsional stresses occurred at the lip of the cross-section at the midspan brace. As noted earlier, at failure buckling was often found to have occurred in the region of the web cut-out hole located between the midspan bridging and the support. The results of the analysis showed that the stresses in an unperforated section at this location would not be expected to cause failure. However, for the reasons stated in Chapter 4, the stresses at this web cut-out were greater than that shown by the analysis since the torsion program was unable to properly model the stud at the cross-sections with holes.

In some of the tests, it was also observed that some local buckling of the compression flange occurred at the midspan brace location almost simultaneously with the local buckling in the region of the web cut-out hole. This observation lends support to the suggestion that failure at the centre was imminent or had started to occur. Release of torsional restraint would significantly increase torsional stresses near the load points. The predicted failure loads were calculated and compared to the experimental failure loads. In all but one case, it

was found that by limiting the combined bending and torsional longitudinal stresses at any location in the steel stud to the yield strength F_y, the predicted failure loads were conservative. Logically, it is rational to conclude that a steel stud with web perforation holes may be weakened if these holes are located in zones of high stress. Therefore, care should be taken to locate these cut-outs only near the bottom of the stud.

6.2.5 Theoretical Analysis

The analyses carried out on two BV/SS wall systems were done to determine the bracing requirements of steel studs in the backup wall. In this analysis, it was assumed that, over the long term, the sheathing could not be relied upon to offer additional bracing for the steel stud. Both these results and the results of the test program, which had shown that a brace spacing of 1280 mm was reasonably effective for control of stud twisting, led to the conclusion that steel bridging should be spaced at no more than 1200 mm on centre.

In terms of serviceability requirements, the two BV/SS wall models were again used to examine the influence of various structural and loading parameters on the overall behaviour of the BV/SS wall system. The results showed that all these parameters affected the behaviour of the BV/SS wall system to some degree. Since in some cases it was concluded that cracking of the brick veneer was inevitable, an attempt was made to determine what allowable steel stud deflection would lead to the formation of cracks in the mortar joints which would be no larger, on average, than 0.2 mm. Based on this criteria, an allowable stud deflection of L/900 under full design wind load was obtained. Therefore, the currently often used value of L/720 is thought to represent a maximum limit for deflection.

6.3 RECOMMENDATIONS

Based on the results and conclusions presented in this study, the following recommendations are proposed:

1. The maximum spacing of track anchors should be 900 mm on centre.

2. For screwed stud to track connnections, the ends of the steel should be fastened to the support tracks with one self-drilling sheet metal screw in each flange.
3. Web crippling at the stud to track connection should be checked using the relevant Canadian design code provisions[6].
4. The track thickness should not be less than the thickness of steel stud.
5. While a minimum allowable thickness of steel stud and track of 0.91 mm (20 gauge) can be used, consideration of handling, storage and erection, and long term durability leads to the recommendation thay the minimum thickness be 1.22 mm (18 gauge).
6. The maximum spacing of steel brdiging should be 1220 mm.
7. Generally, web cut-out holes should not be provided at locations other than where a line of steel bridging is to be provided. In particular, under no condition should there be a hole at the midspan of the steel stud unless a line of bridging is provided at this location with connection detailing that will reinforce the hole. This recommendation applies only to lipped channel steel studs with web cutout holes similar to that used in the test program. For other types of steel studs such as studs with regular openings in the web, it is recommended that load tests be performed under bending and torsional loading condition in order to establish the capacity of these types of studs. [Clause 9 of the code[6] should be consulted.] Where web cut-outs are required for services, they should be kept near the bottom of the wall where lower concentrated loads exist. As a rough empirical guide, these cut-outs should not be located in regions where the combined effects of bending and torsion under factored and load exceeds 60 percent of F_y.
8. Ties that induce web crippling should not be located directly over web cut-out holes.
9. Clip angles used in steel bridging connections should be 16 gauge or thicker.
10. Screwed bridging to stud connections should be made with a minimum of four screws. The clip angle should be predrilled at the screw locations. The holes in the leg of the clip angle which is to be fastened to the web of the stud should be located no further

than one-third the distance of the width of the clip angle away from the bend. These holes should be as far apart as possible since this will minimize the pullout force on the screws.

11. For heavier and deeper studs, a welded clip angle connection is suggested.

12. In terms of serviceability requirements, the maximum stud deflection should not be greater than L/720 under full design wind load. Other experimental research is ongoing to evaluate leakage rates through cracked brick veneer.

6.4 CLOSING REMARKS

The results, conclusions and recommendations resulting from this research will serve as background for the development of guides for the structural design and the fabrication of steel stud backup wall assemblies. From an overall perspective, however, the design of a BV/SS wall system must also address other issues such as moisture problems which can also play an important role in the performance of this wall system.

REFERENCES

1. Arumala, J.O., Brown, R.H., "Performance Evaluation of Brick Veneer and Steel Stud Backup", Department of Civil Engineering, Clemson University, Clemson, North Carolina, 1982.
2. Baker, L.R., "The Flexural Action of Masonry Structures Under Lateral Load", Ph.D. Thesis, Deakin University, 1981.
3. Black, M.M., "Thin Walled Steel Structures", Gordon and Breach, Science Publishers Inc., New York, 1969, pp. 173-196.
4. Brick Institute of America, "Technical Notes on Brick Construction", No. 28B, Revision II, 1987.
5. Brook, M.S., "Masonry Veneer with Steel Stud Backup Wall", M. Eng. Project Report, McMaster University, April 1985.
6. "Cold Formed Steel Structural Members", CSA Standard CAN3-S136-M84, 1984.
7. "Commentary on CSA Standard CAN3-S136-M84", CSA Special Publication S136. 1-M86, 1986.
8. Dawe, D.J., "Matrix and Finite Element Displacement Analysis of Structures", Clarendon Press, Oxford, 1984.
9. Drysdale, R.G., "Seminar on BV/SS Research", McMaster University, November 9, 1988.
10. Drysdale, R.G., Gazzola, E., "Influence of Mortar Properties on the Tensile Bond Strength of Brick Masonry", Proceedings of the 7th Australian Conference, 1985.
11. Drysdale, R.G., Suter, G.T., "Modern Engineering Masonry".
12. Drysdale, R.G., Wilson, M.J., "A Report on the Behaviour of Masonry Veneer/Steel Stud Tie Systems", C.M.H.C. Report (in Press) 1989.
13. Galambos, T.V., "Structural Members and Frames", Prentice-Hall Inc., Englewood Cliffs, New Jersey, 1968.
14. Gjelsuik, A., "The Theory of Thin Walled Bars", John Wiley and Sons Inc., New York, 1981.
15. Grim, C.T., "Dimensional Stability of Clay Masonry", Internal Report, University of Texas, Austin, 1981.
16. Hatzinikolas, M., Lee, R., Longworth J., and Warwaruk, J., "The Behaviour of Styrofoam SM Insulation as Exterior Sheating in Brick Veneer and Metal Stud Wall Systems", Dept. of Civil Engineering, University of Civil Engineering,University of Alberta, 1986.
17. Hetnakul, N., Yu, W.W., "Webs for Cold-Formed Steel Flexural Members and Structural Behaviour of Beam Webs Subjected to Web Crippling and Combination of Web Crippling and Bending", University of Missouri-Rolla, June 1978.
18. Hill, H.N., "Lateral Buckling of Channels and Z Beams", ASCE Transactions Paper No. 2700, 1954, pp. 826-841.
19. Lansing, W., "Stresses in Thin Walled Open Section Beams Due to Combined Torsion and Flexure", Ph.D. Thesis, Cornell University, June 1949.
20. Lawrence, S.J., "Behaviour of Brick Masonry Panels Under Lateral Loading", Ph.D. Thesis, University of New South Wales, November 1983.

21. "Lightweight Steel Framing Manual", Canadian Sheet Steel Building Institute Publication, Willowdale, Ontario, August 1987.

22. "Masonry Design for Buildings", CSA Standard CAN3-S304-M-84.

23. Metal Lath/Steel Framing Association, "Here are the Facts", Publication, Chicago, Illinois.

24. Murden, J.A., "Evaluation of Lateral Stiffness for Gypsum-Faced Steel Stud Backup Panels", Master of Science Thesis, Department of Civil Engineering, Clemson University, Clemson, North Carolina, August, 1984.

25. "Steel Framing Systems", Baily Metal Products Ltd., Publication, Toronto Ontario.

26. Tong, P., Rossetos, J.N., "Finite Element Method", MIT Press, Cambridge, Massachusetts, 1977.

27. "Torsional Analysis of Steel Members", American Institute of Steel Construction, Chicago, Ill., 1983.

28. "USG Steel Framing Systems", United States Gypsum Company Publication, 1986.

29. Vlasov, U.A., "Thin Walled Elastic Beams", Israel Program for Scientific Translations, Jerusalem, 1961.

30. "Wheeling Steel Framing", Wheeling Corrugating Company, Wheeling, West Virginia, Catalogue 1981 Edition.

31. Winter, G., Lansing W., and McCalley, R.B., "Performance of Laterally Loaded Channel Beams", Symposium on Engineering Structures (Colston Papers, Vol. 2) Butterworths Scientific Publications, London, 1949.

32. Winter, G., Pian, R.H., "Crushing Strength of Thin Steel Webs", Engineering Experiment Station Bulletin No. 35, Part 1, Cornell University, Ithaca, New York, April 1946.

33. Yu, W.W., "Cold Formed Steel Design", John Wiley and Sons Inc., New York, 1985.

34. Zbirohowjki, K., "Thin Walled Beams", Crosby Lockwood and Son Ltd., London, 1967.

35. Zetlin, L., "Elastic Instability of Flat Plates Subjected to Partial Edge Loads", Journal of the Structural Division, ASCE Proceedings, Vol. 81, September 1955.

APPENDIX A

FINITE ELEMENT FORMULATION OF TORSION PROBLEM

To detemine the torsional stresses in a steel stud subjected to torsional loads, the governing differential equation, Eq. 4.11, with its associated boundary conditions, must be solved. Closed formed solutions for relatively simple loading and boundary conditions are available[27,33]. However, for more complicated loading and boundary conditions, a closed form solution is not practical and is often impossible to obtain. In order to efficiently solve the differential equatoin of torsion, it is necessary to use a numerical method. The Finite Element Method is a popular numerical method and was used to obtain a numerical solution to the mixed torsion problem under general loading and boundary conditions.

The total potential energy in a thin wall beam subjected to load is given by:

$$\pi(\phi) = \frac{EC_W}{2}\int_0^L \left(\frac{d^2\phi}{dz}\right)^2 dz + \frac{GJ}{2}\int_0^L \left(\frac{d\phi}{dz}\right)^2 dz - Ti\cdot\phi i - \int_0^L mt\cdot\phi\cdot dz$$

The first two integrals represent the strain energy in the beam while the last two terms represent the loss or gain in potential energy due to the applied concentrated torques and uniformly distributed torques, respectively. To obtain a finite element solution, the beam was first divided into a number of a number elements. A typical element is shown in Figure A.1. For this study, a three node element with two degrees of freedom, ϕ and ϕ', was chosen. Since there are six degrees of freedom in each element, a fifth order polynomial was required to approximate the rotation, ϕ, inside each element domain. In the finite element formulation, the rotation ϕ is given by the following[26]:

$$\phi^e = N_1\phi_1 + N_2\phi_1' + N_3\phi_2 + N_4\phi_2' + N_5\phi_3 + N_6\phi_3'$$

where

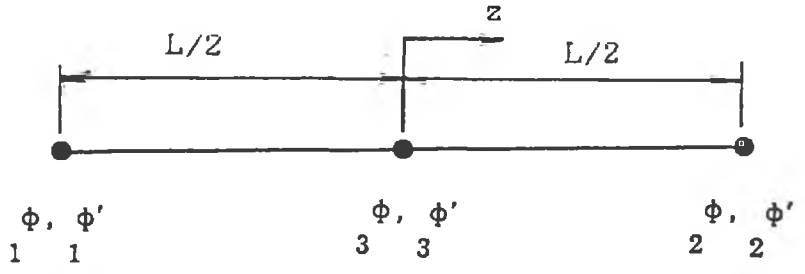

Figure A1 - Typical Torsion Element

$$\bar{x} = z/L$$

$$N_1 = 4\bar{x}^{-2} - 10\bar{x}^{-3} - 8\bar{x}^{-4} + 24\bar{x}^{-5}$$

$$N_2 = \ell * (0.5\bar{x}^{-2} - \bar{x}^{-3} - 2\bar{x}^{-4} + 4\bar{x}^{-5})$$

$$N_3 = 4\bar{x}^{-2} + 10\bar{x}^{-3} - 8\bar{x}^{-4} - 24\bar{x}^{-5}$$

$$N_4 = \ell * (-0.5\bar{x}^{-2} - \bar{x}^{-3} + 2\bar{x}^{-4} + 4\bar{x}^{-5})$$

$$N_5 = 1 - 8\bar{x}^{-2} + 16\bar{x}^{-4}$$

$$N_6 = \ell(\bar{x} - 8\bar{x}^{-3} + 16\bar{x}^{-5})$$

$$\{\phi^e\} = <\phi_1, \phi_1', \phi_3, \phi_3', \phi_2, \phi_2'>$$

The total potential energy of the beam can now be considered as the sum of the energies of each element[26]. Substitution of ϕ^e into the total potential energy expression for each individual element, ϕ^e, and minimizing the potential energy of the element with respect to each degree of freedom yields the following element stiffness matrix and load vector:

$$[K_V] = G \cdot J \begin{bmatrix} \frac{278}{105\,\ell} & \frac{13}{210} & \frac{-22}{105\,\ell} & \frac{-1}{70} & \frac{-256}{105\,\ell} & \frac{8}{21} \\ \frac{13}{210} & \frac{2\,\ell}{45} & \frac{1}{70} & \frac{-1}{126} & \frac{-8}{105} & \frac{-4\,\ell}{315} \\ \frac{-22}{105\,\ell} & \frac{1}{70} & \frac{278}{105\,\ell} & \frac{-13}{210} & \frac{-256}{105\,\ell} & \frac{-8}{21} \\ \frac{-1}{70} & \frac{-1}{126} & \frac{-13}{210} & \frac{2\,\ell}{45} & \frac{8}{105} & \frac{-4\,\ell}{315} \\ \frac{-256}{105\,\ell} & \frac{-8}{105} & \frac{-256}{105\,\ell} & \frac{8}{105} & \frac{512}{105\,\ell} & 0 \\ \frac{8}{21} & \frac{-4\,\ell}{315} & \frac{-8}{21} & \frac{-4\,\ell}{315} & 0 & \frac{128\,\ell}{315} \end{bmatrix}$$

$$[K_W] = \frac{EC_W}{35\ell^3}\begin{bmatrix} 5092 & 1138\,\ell & -1508 & 242\,\ell & -3584 & 1920\,\ell \\ 1138\,\ell & 332\,\ell^2 & -242\,\ell & 38\,\ell^2 & -896\,\ell & 320\,\ell^2 \\ -1508 & -242\,\ell & 5092 & -138\,\ell & -3584 & -1920\,\ell \\ 242\,\ell & 38\,\ell^2 & -138\,\ell & 332\,\ell^2 & 896\,\ell & 320\,\ell^2 \\ -3584 & -898\,\ell & -3584 & 896\,\ell & 7168 & 0 \\ 1920\,\ell & 320\,\ell^2 & -1920\,\ell & 320\,\ell^2 & 0 & 1280\,\ell^2 \end{bmatrix}$$

The potential energy of the beam can now be considered as the sum of the energies of each element. Substitution of ϕ^e into the total potential energy expression for each individual element, and minimizing the potential energy of the element with respect to each degree of freedom yields the following element stiffness matrix and load vector:

$$[K_T] = [K_V] + [K_W]$$

For each element, the potential energy is given by:

$$\pi(\phi)^e = \frac{EC_W}{2}\int_0^L \left(\frac{d^2\phi}{dz}\right)^2 dz + \frac{GJ}{2}\int_0^L \left(\frac{d\phi}{dz}\right)^2 dz - \int_0^L mt \cdot \phi \cdot dz$$

Element marix $[K_W]$ was adapted from Reference [8]. For element matrix $[K_V]$, the author performed the intergration using the following:

$$Kij = GJ\int_{-1/2}^{1/2} Ni' \cdot Nj'\, d\bar{x}$$

For a constant distributed torque, the load ector is given as:

$$\{M\} = \frac{m_t \cdot \ell}{60}\begin{bmatrix} 14 \\ 14 \\ 32 \\ \ell \\ 0 \\ -\ell \end{bmatrix}$$

where m_t is the uniiformly distributed torque.

Assembly of the individual elements to obrain the global stiffness and load matrices is done in the usual manner, by enforcing nodal compatibility and equilibrium. The applied concentrated nodal torques are thus incorporated into the global load vector. Finally, the rigid or

kinematic boundary conditions are applied. This procedure yields a set of simultaneous equations from which a solution for the unknown nodal degrees of freedom is obtained.

In the finite element formulation, only the kinematic boundary conditions need to be enforced. For the torsion problem, the kinematic boundary conditions are as follows:

$$\phi = 0.0 \qquad z = 0, L$$

$$\phi' = 0.0 \qquad z = 0, L$$

The secondary quantities which needed to be evaluated at each node are the warping normal stresses.

These quantities are determined using Equations 4.15. Upon examination of these equations, it is noted that evaluation of the second derivatives of the twist, ϕ, was required at the nodes.

The second derivative is evaluated at each node of each element using the second following equation:

$$\phi''_{ki} = \sum_{j=1}^{6} N''_j + S_i * U_{kj}, \qquad i = 1,2,3,\ldots,()$$

$$k = 1 \text{ to number of elements}$$

where

N''_j = Second derivative of shape function j

U_{kj} = Nodal degree of freedom j in elements k

$S_1 = -1/2, \quad S_2 = +1/2, \quad S_3 = 0.0$

APPENDIX B

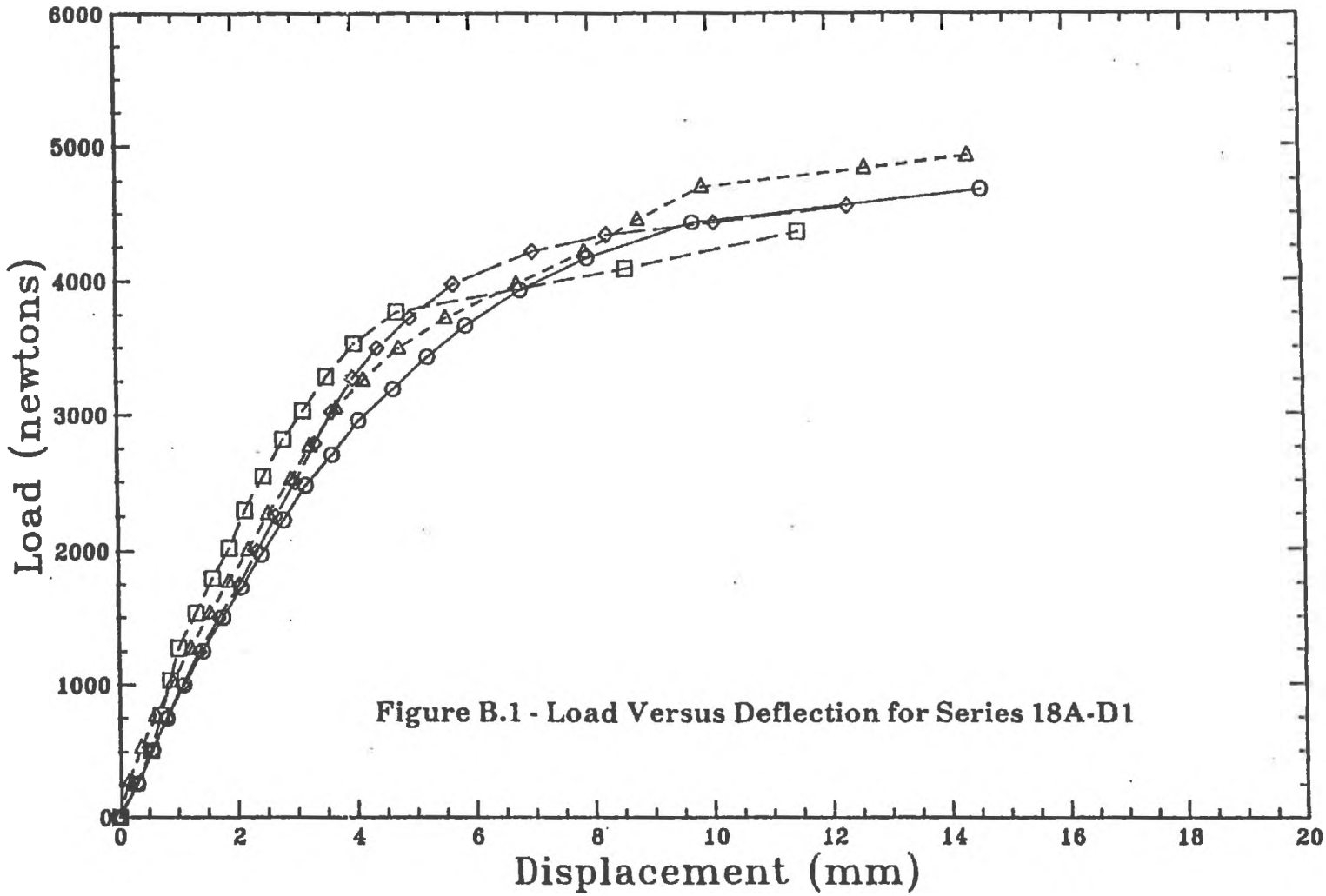

Figure B.1 - Load Versus Deflection for Series 18A-D1

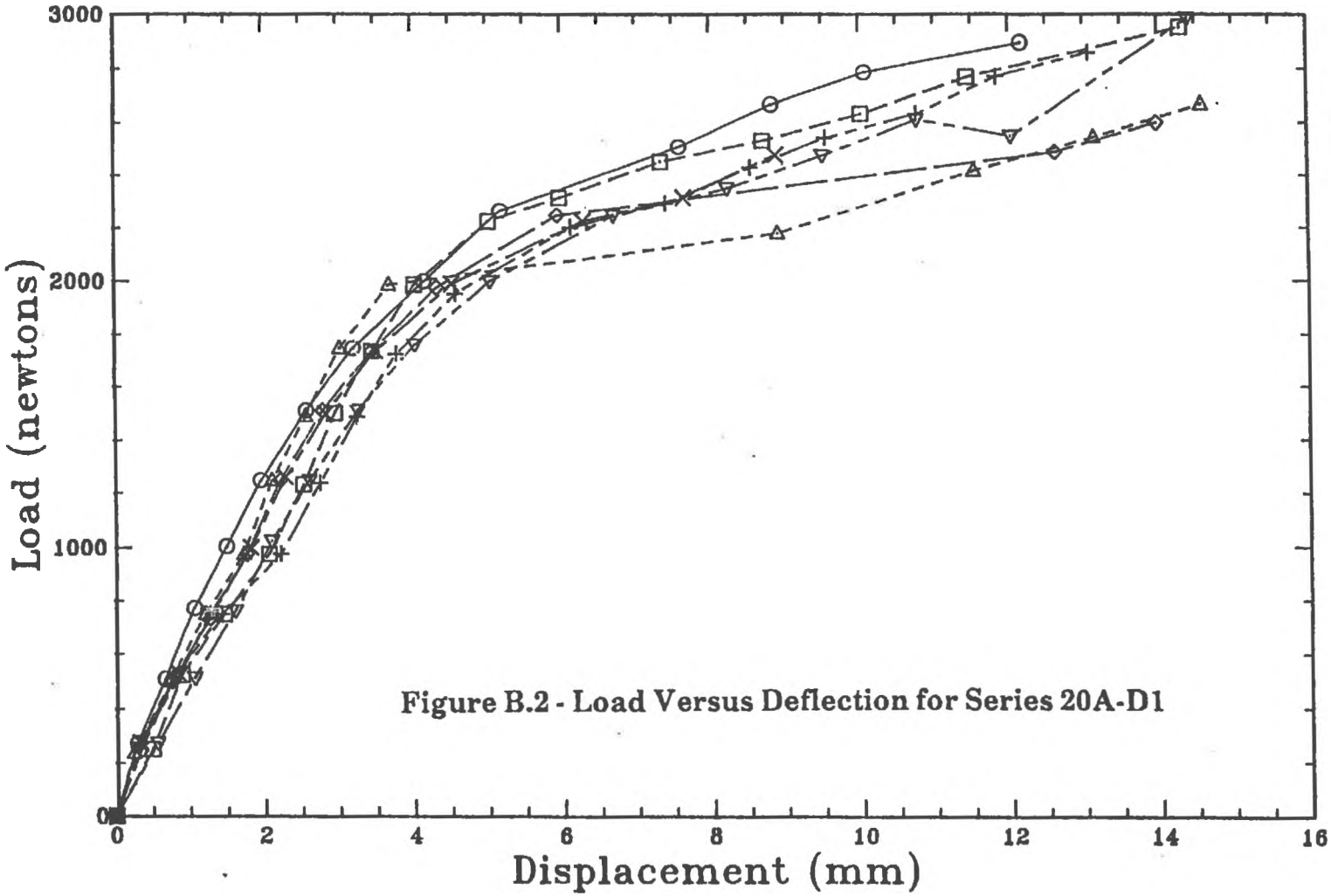

Figure B.2 - Load Versus Deflection for Series 20A-D1

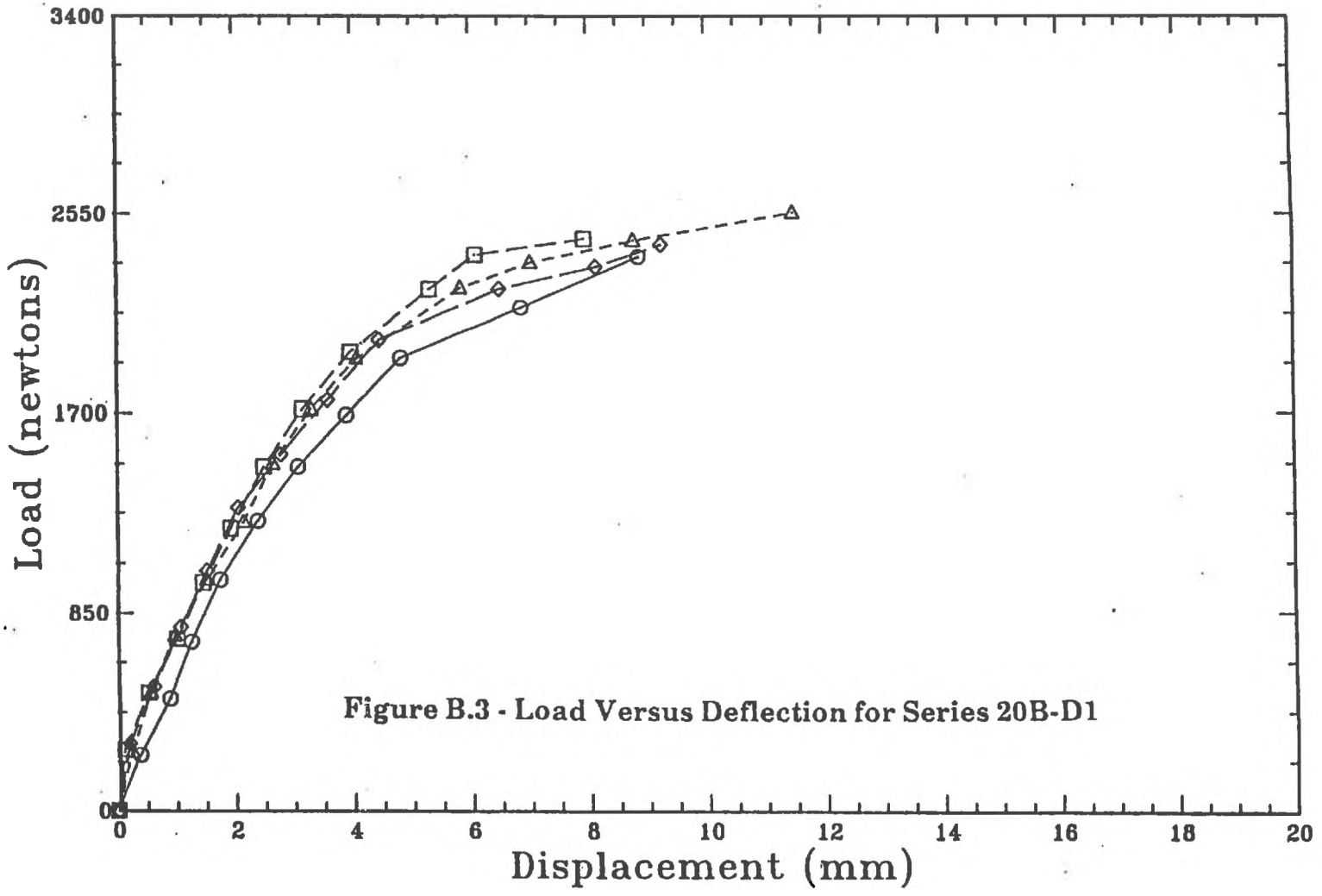

Figure B.3 - Load Versus Deflection for Series 20B-D1

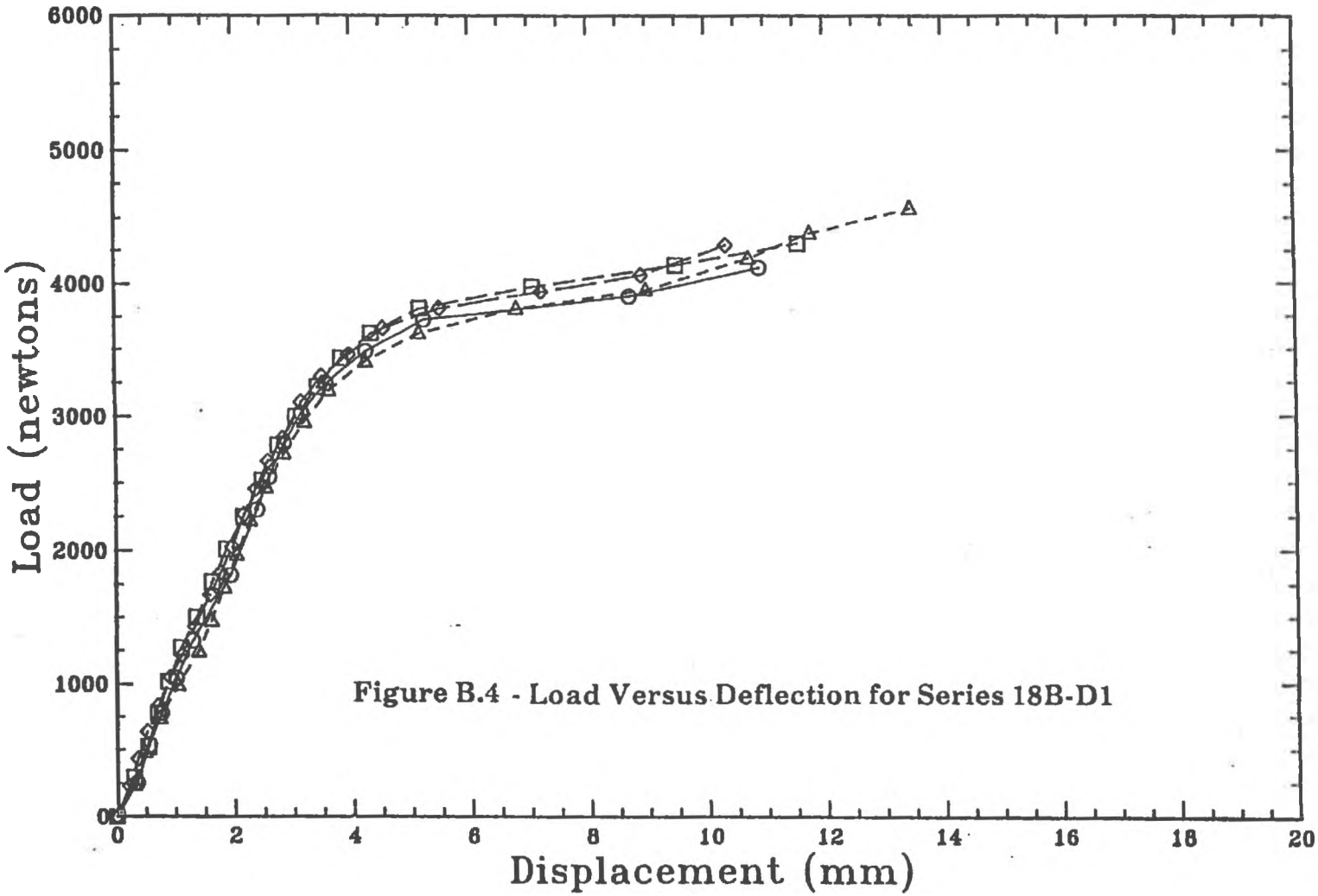

Figure B.4 - Load Versus Deflection for Series 18B-D1

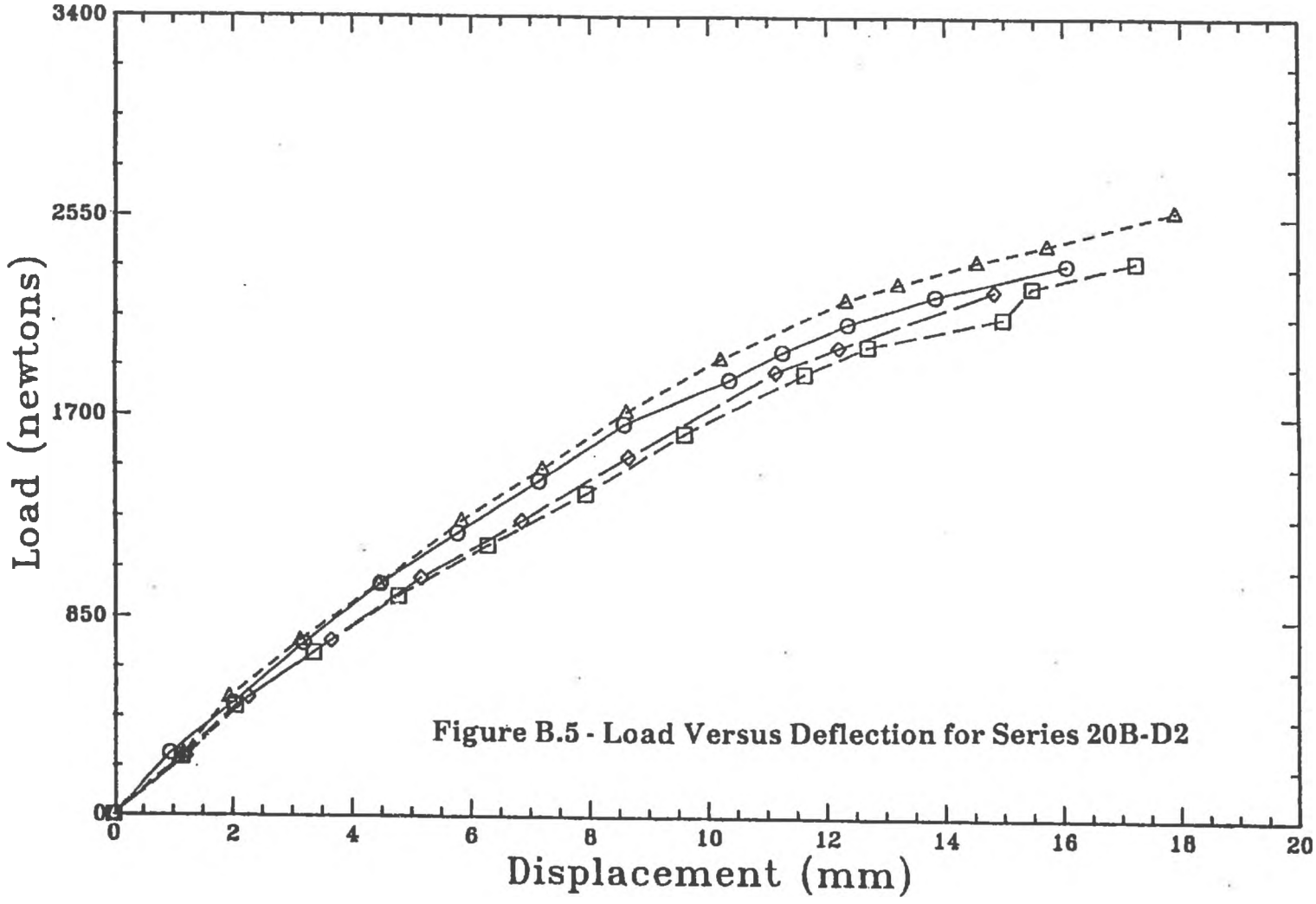

Figure B.5 - Load Versus Deflection for Series 20B-D2

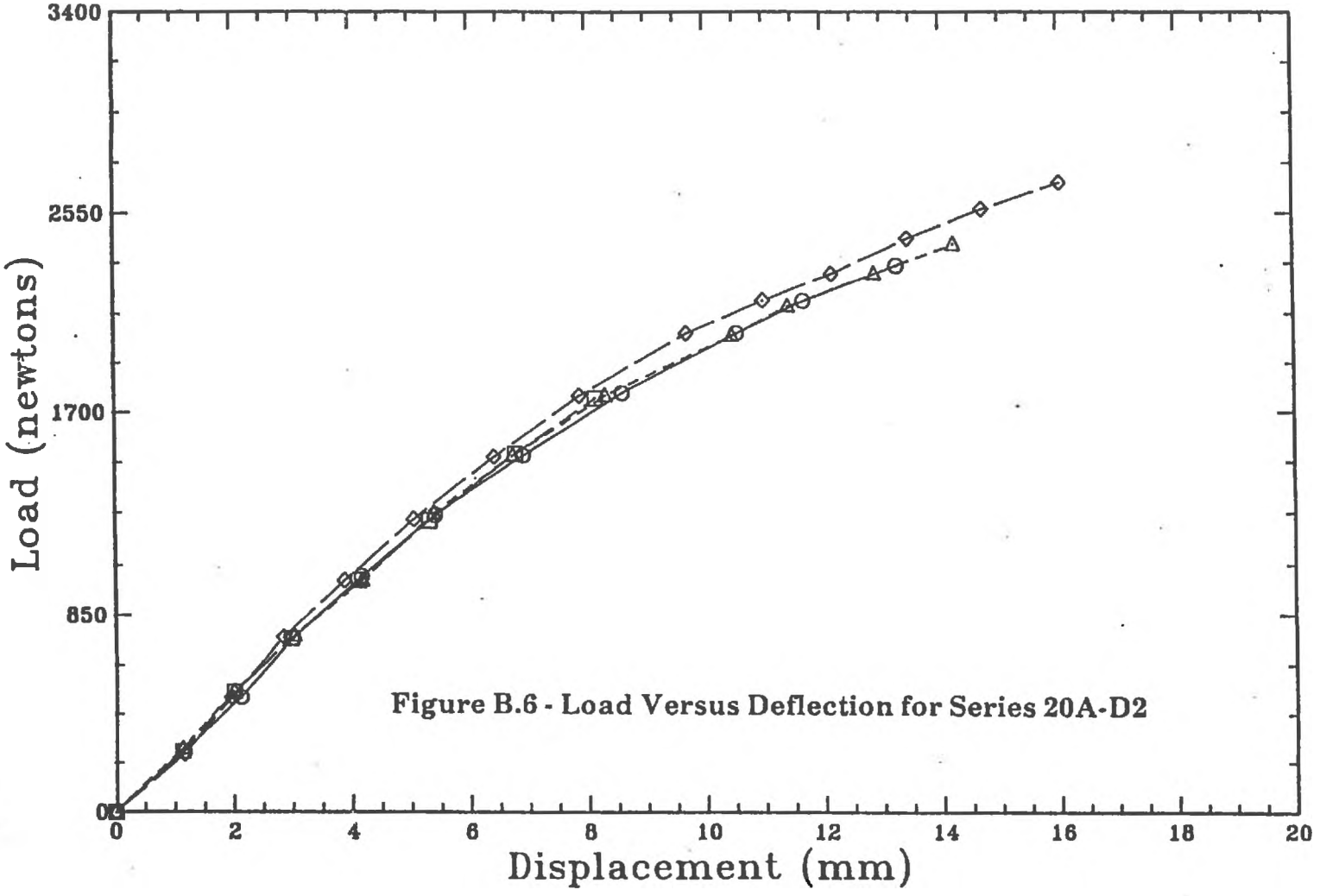

Figure B.6 - Load Versus Deflection for Series 20A-D2

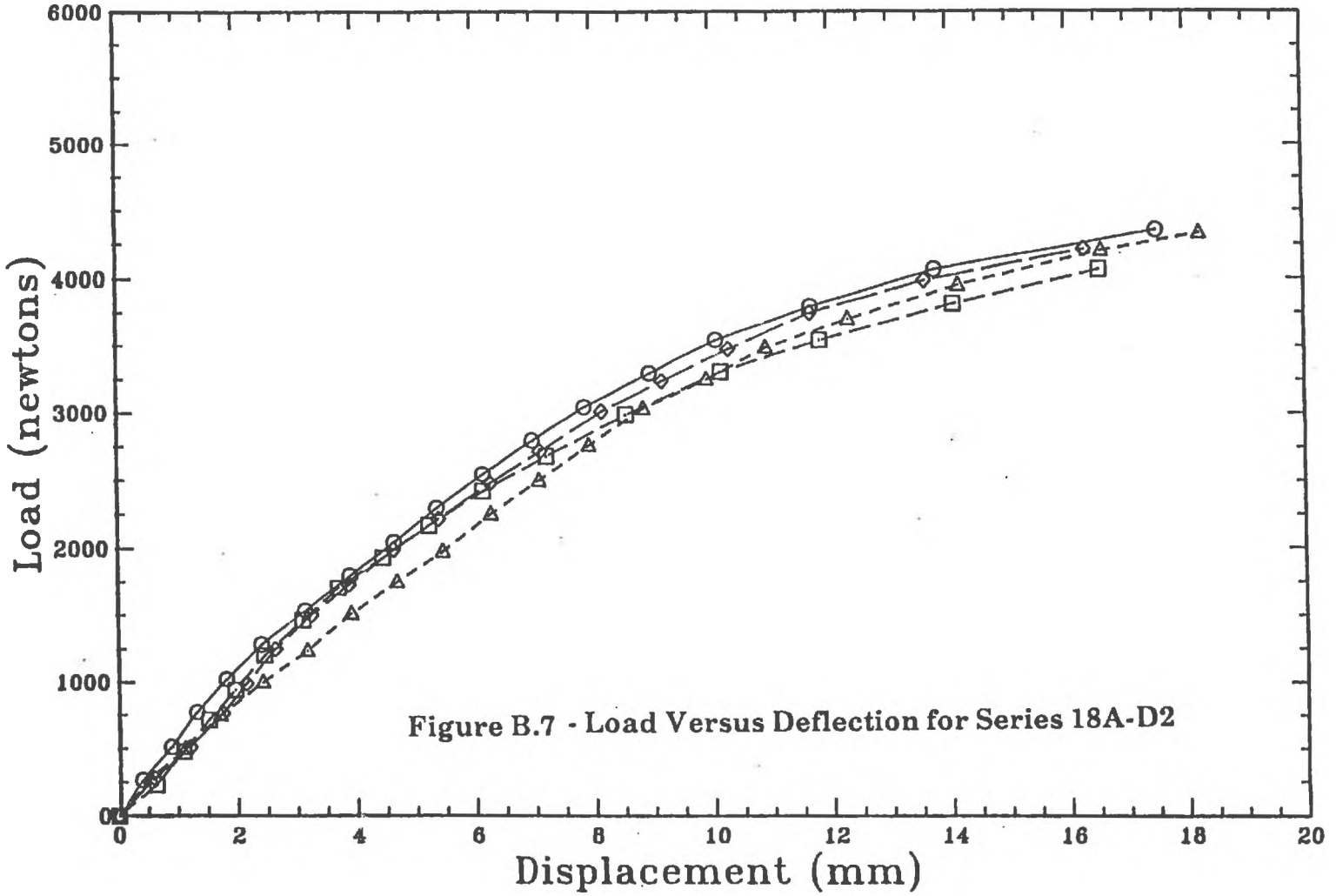

Figure B.7 - Load Versus Deflection for Series 18A-D2

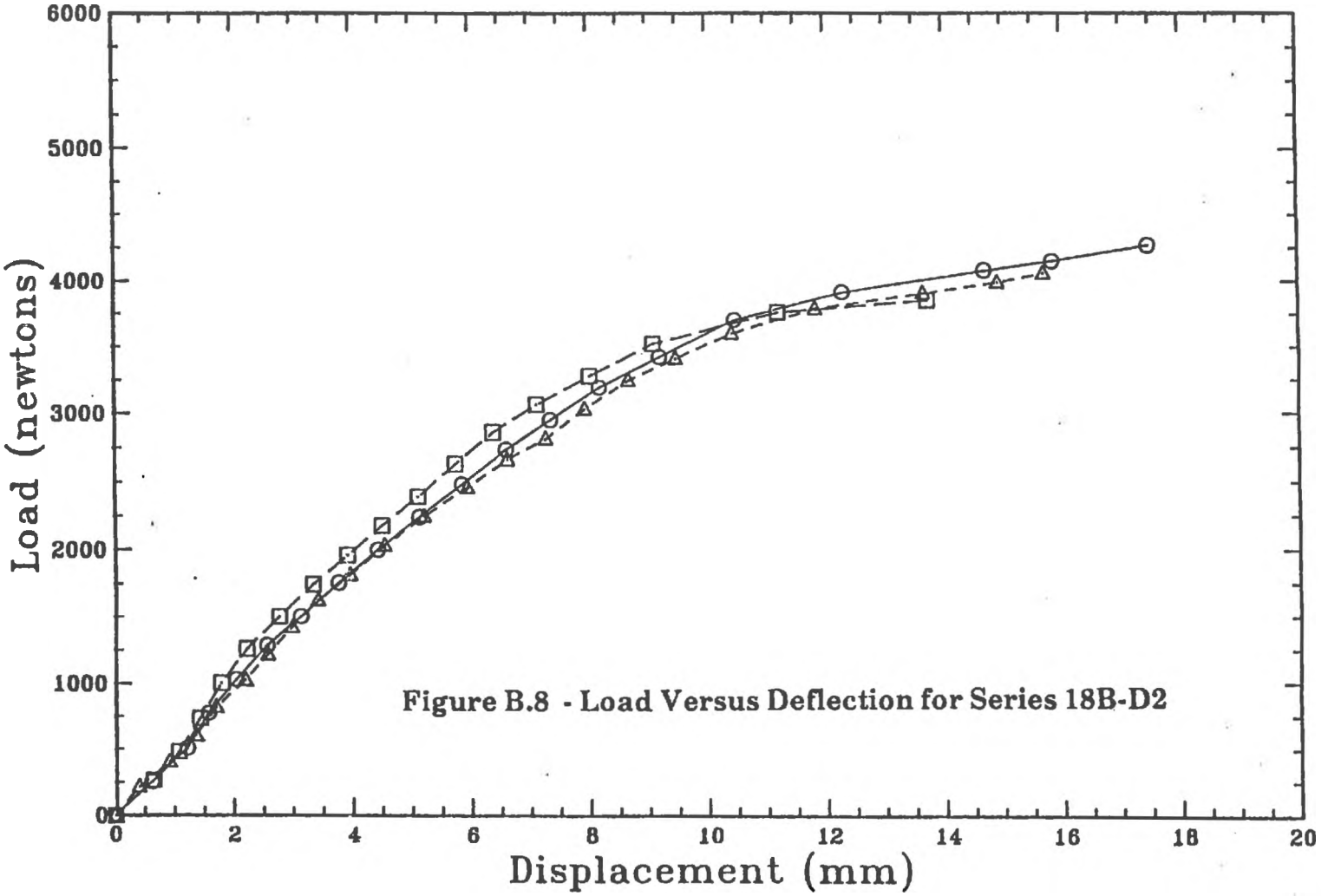

Figure B.8 - Load Versus Deflection for Series 18B-D2

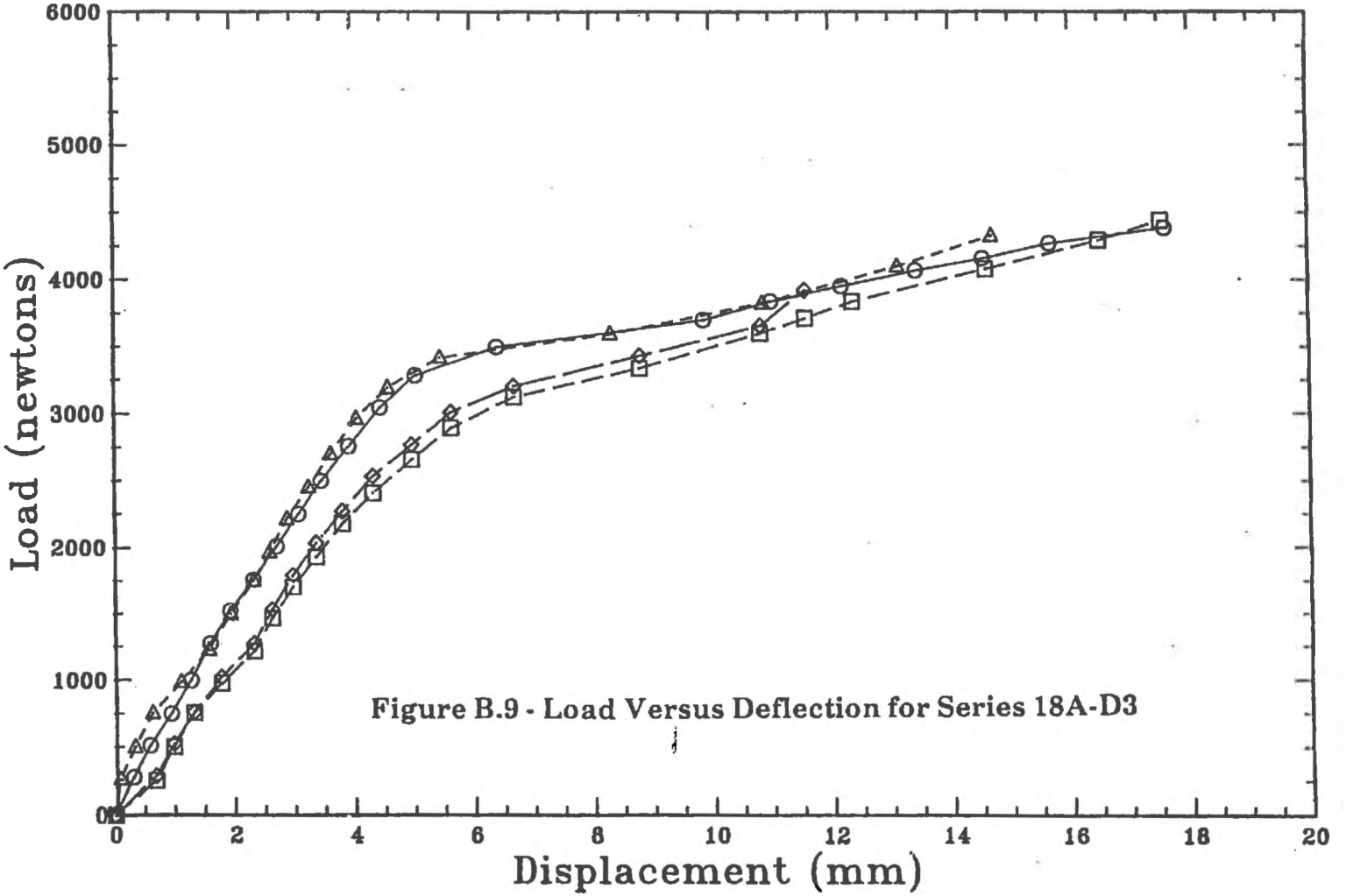

Figure B.9 - Load Versus Deflection for Series 18A-D3

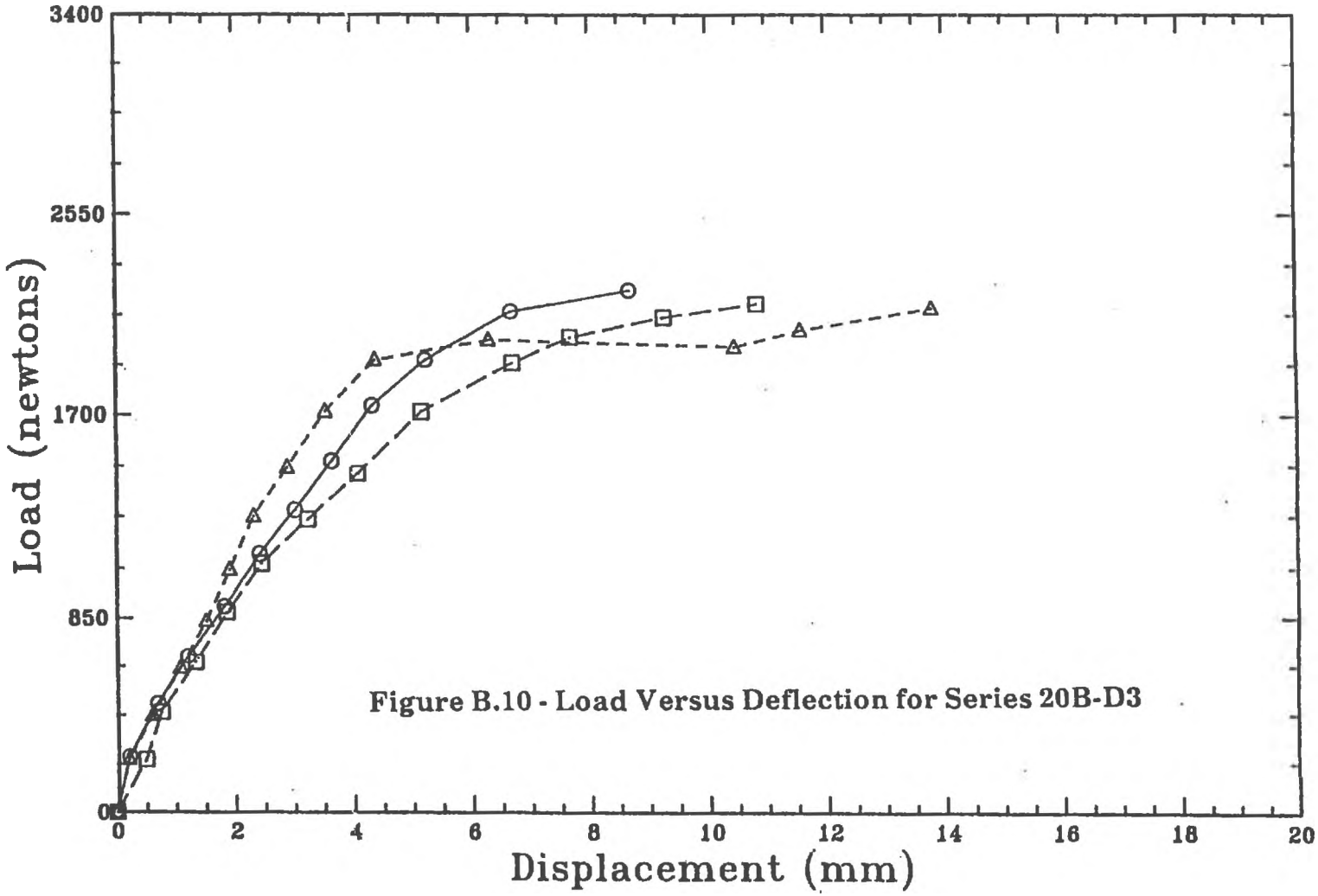

Figure B.10 - Load Versus Deflection for Series 20B-D3

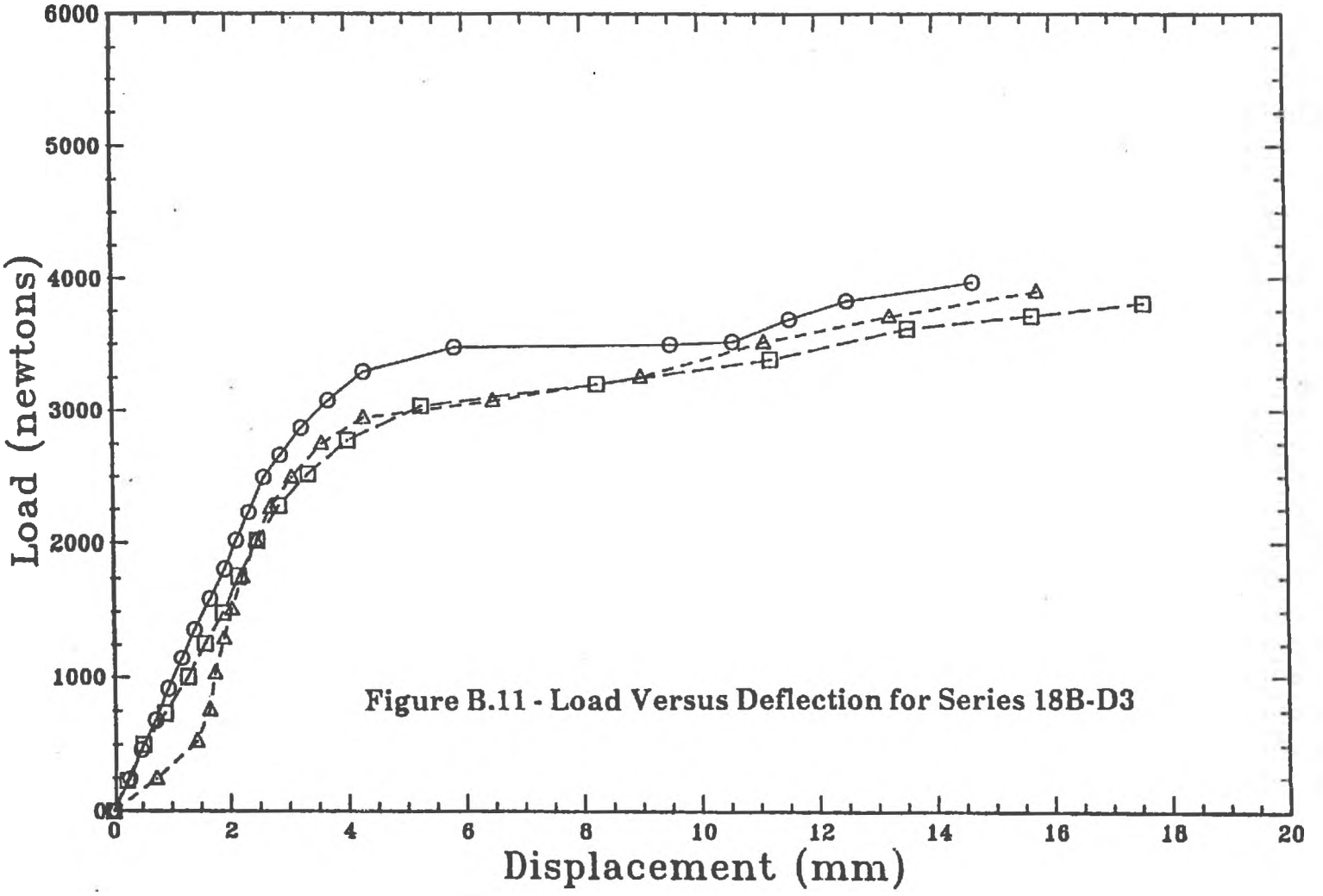

Figure B.11 - Load Versus Deflection for Series 18B-D3

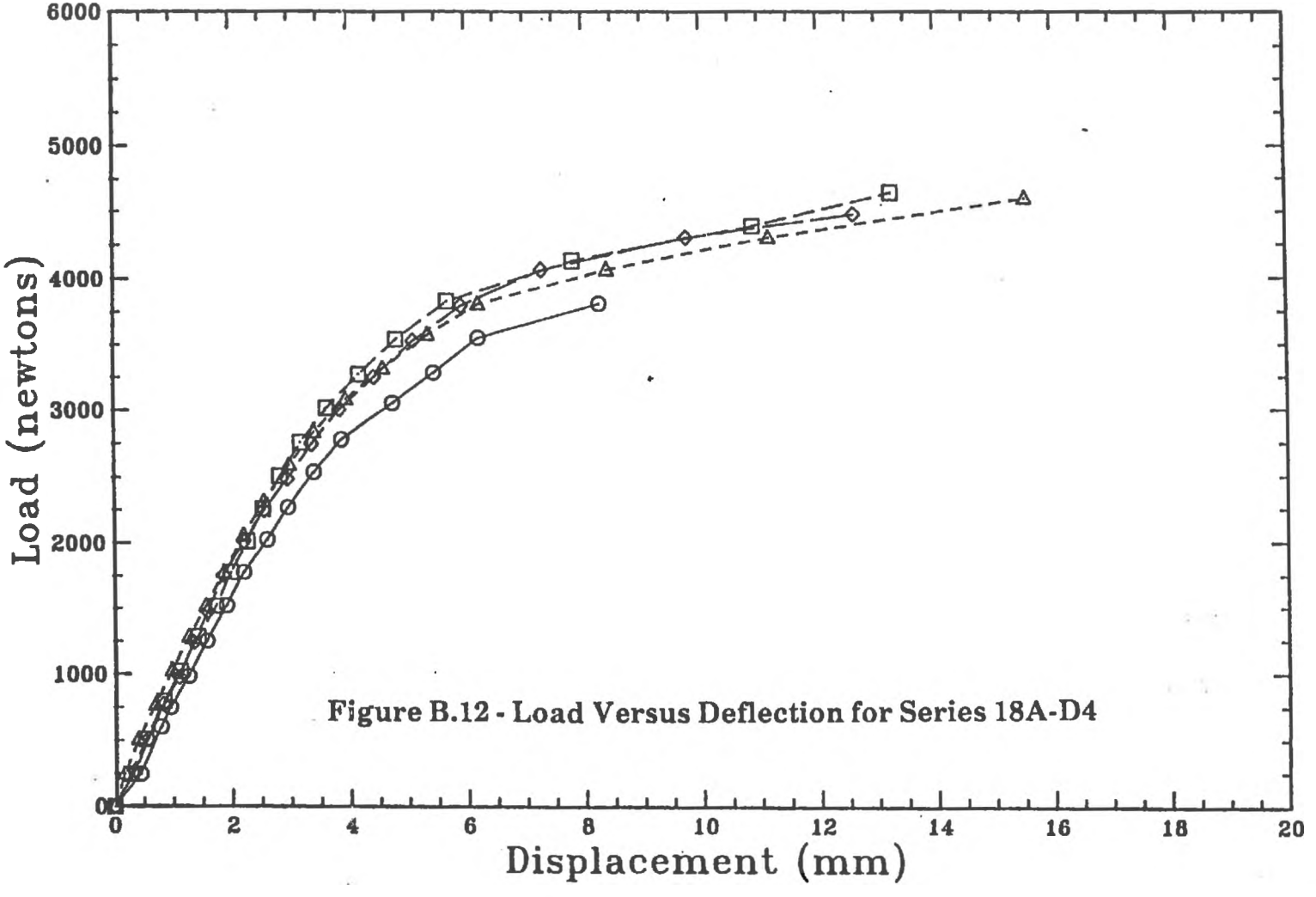

Figure B.12 - Load Versus Deflection for Series 18A-D4

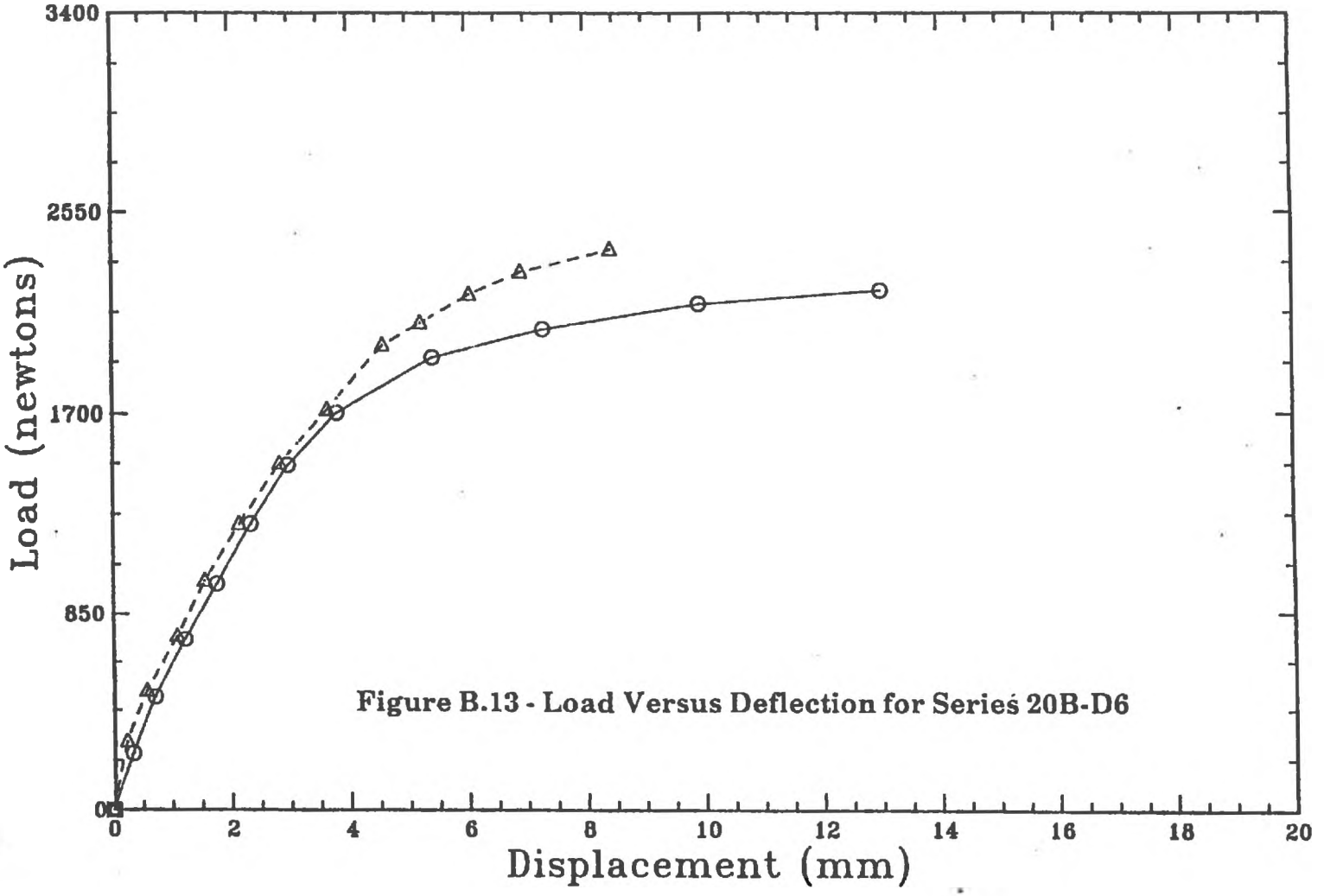

Figure B.13 - Load Versus Deflection for Series 20B-D6

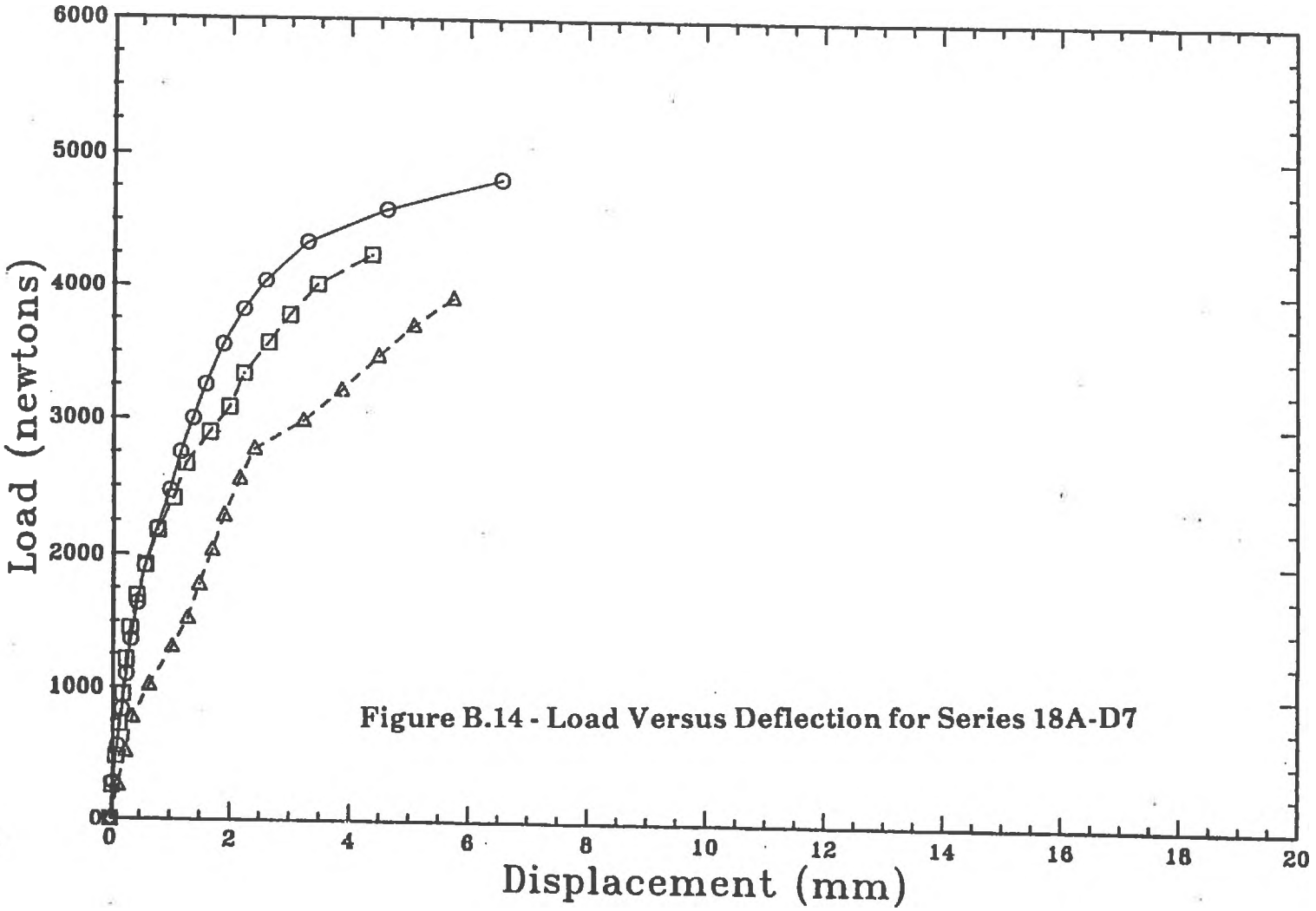

Figure B.14 - Load Versus Deflection for Series 18A-D7

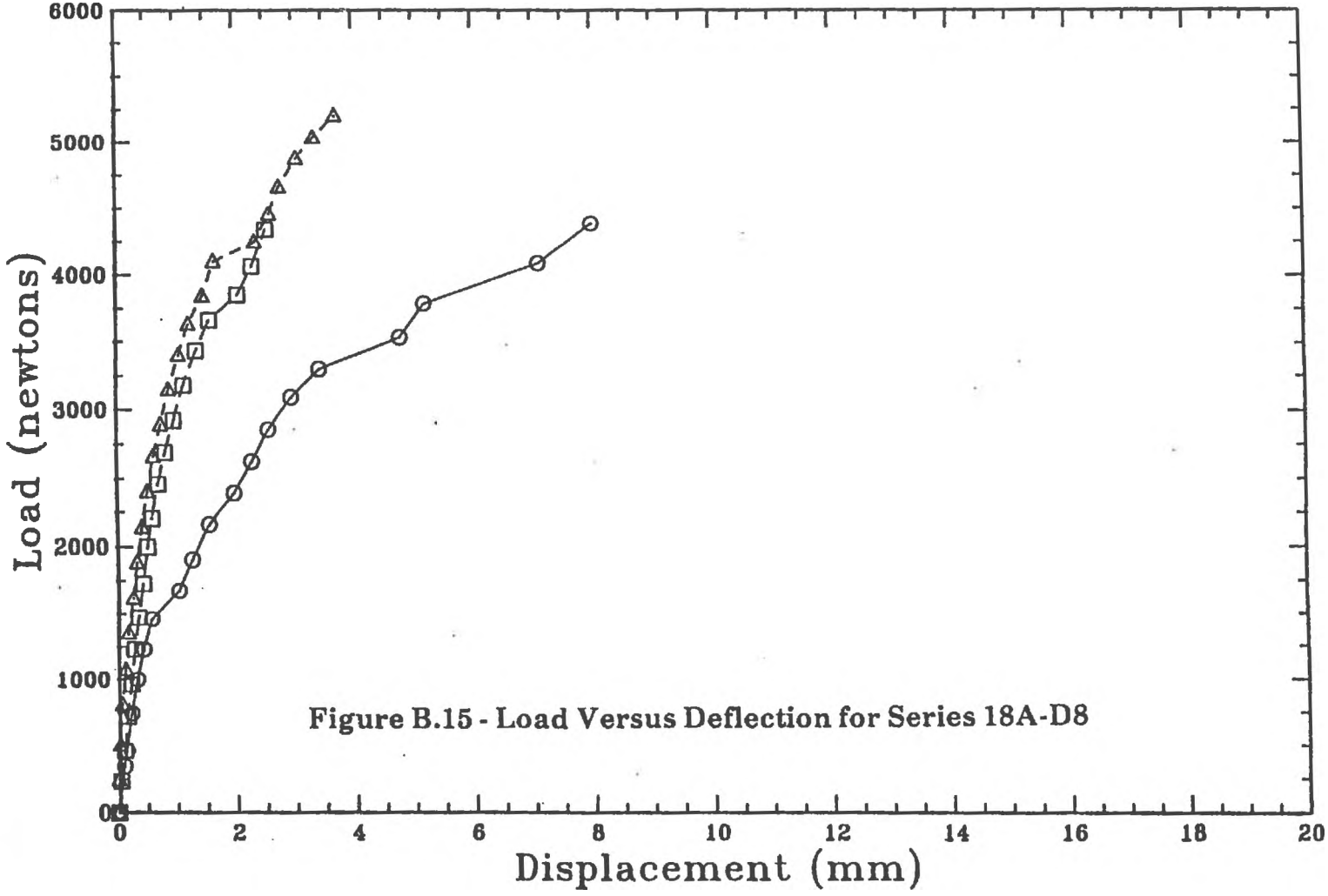

Figure B.15 - Load Versus Deflection for Series 18A-D8

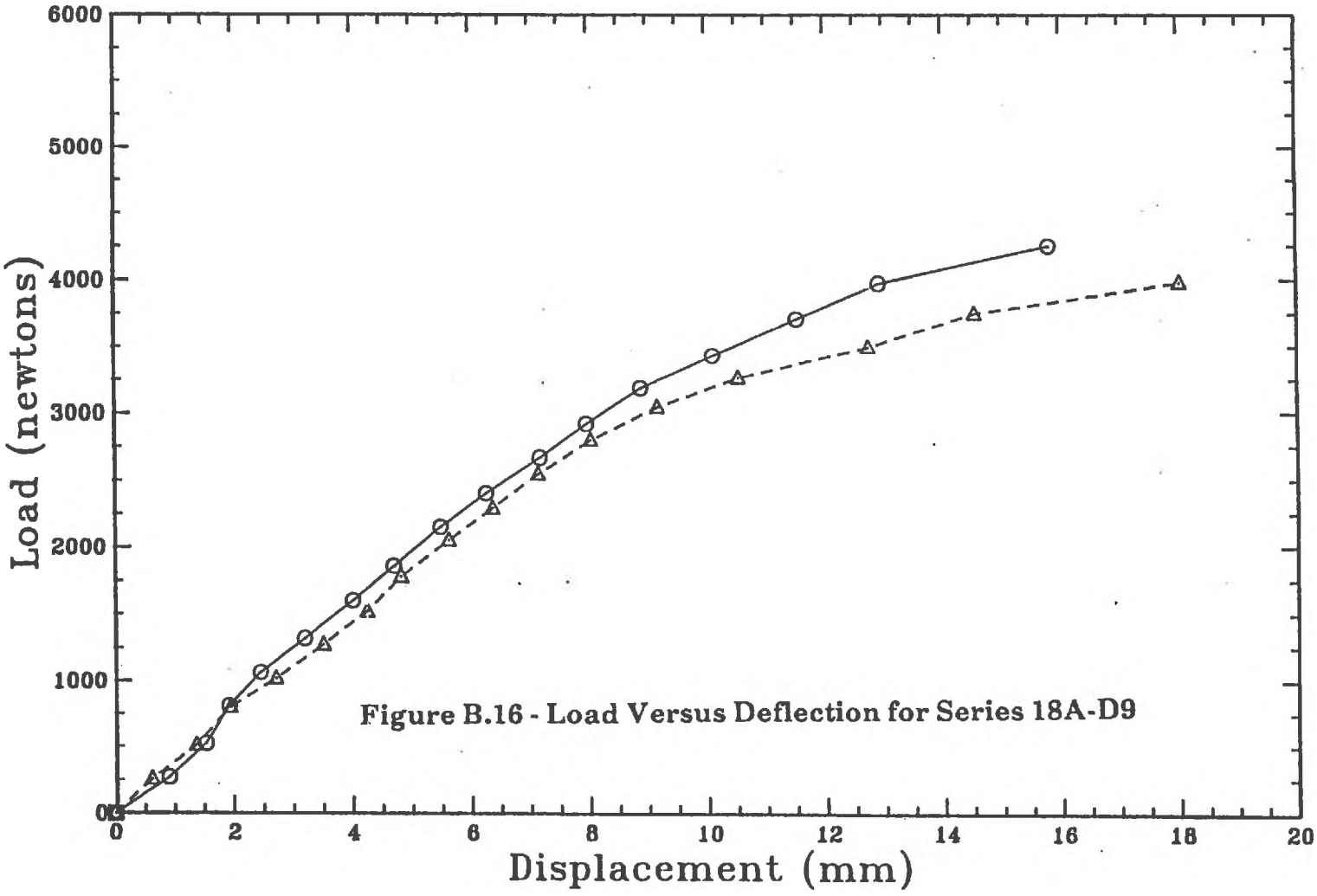

Figure B.16 - Load Versus Deflection for Series 18A-D9

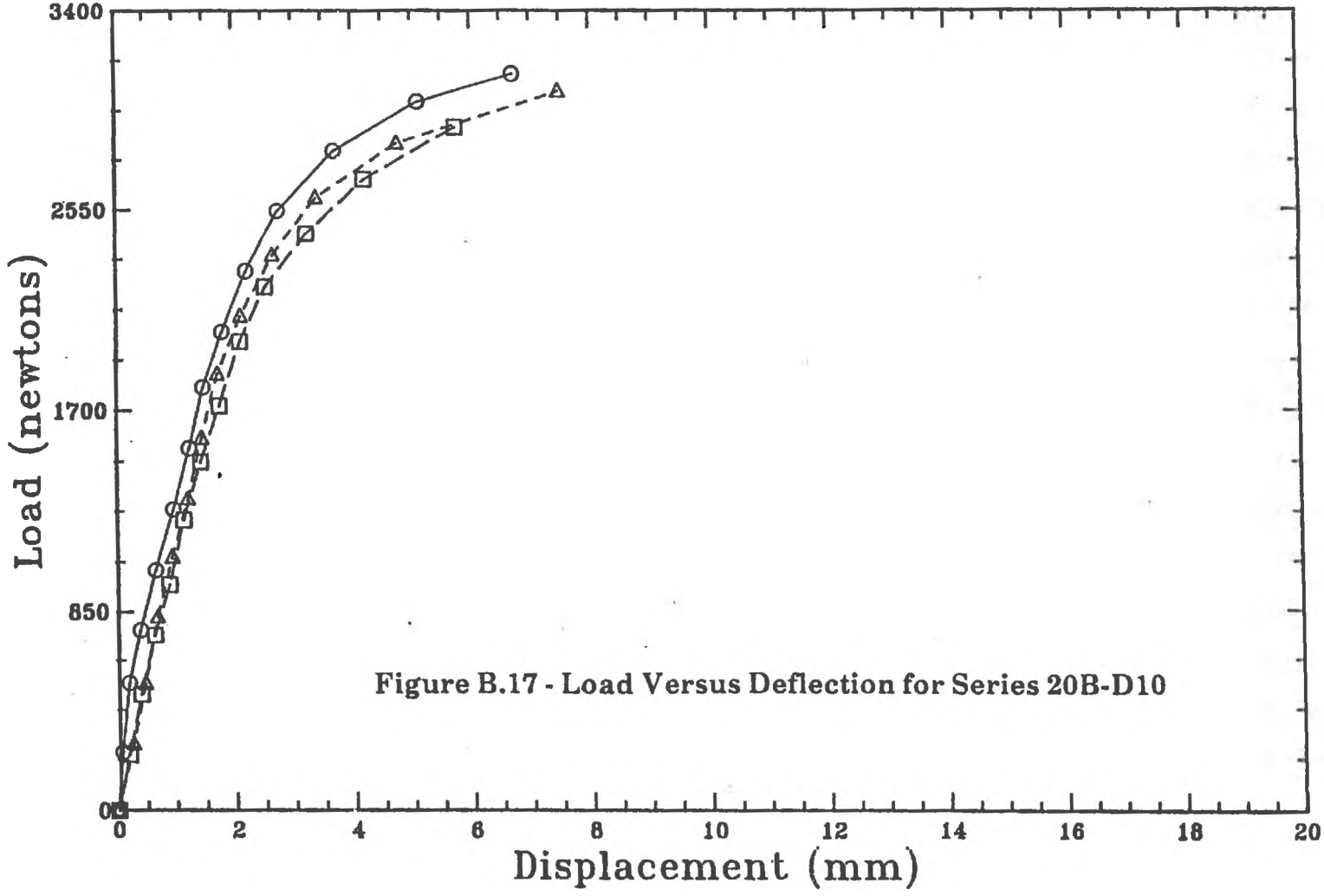

Figure B.17 - Load Versus Deflection for Series 20B-D10

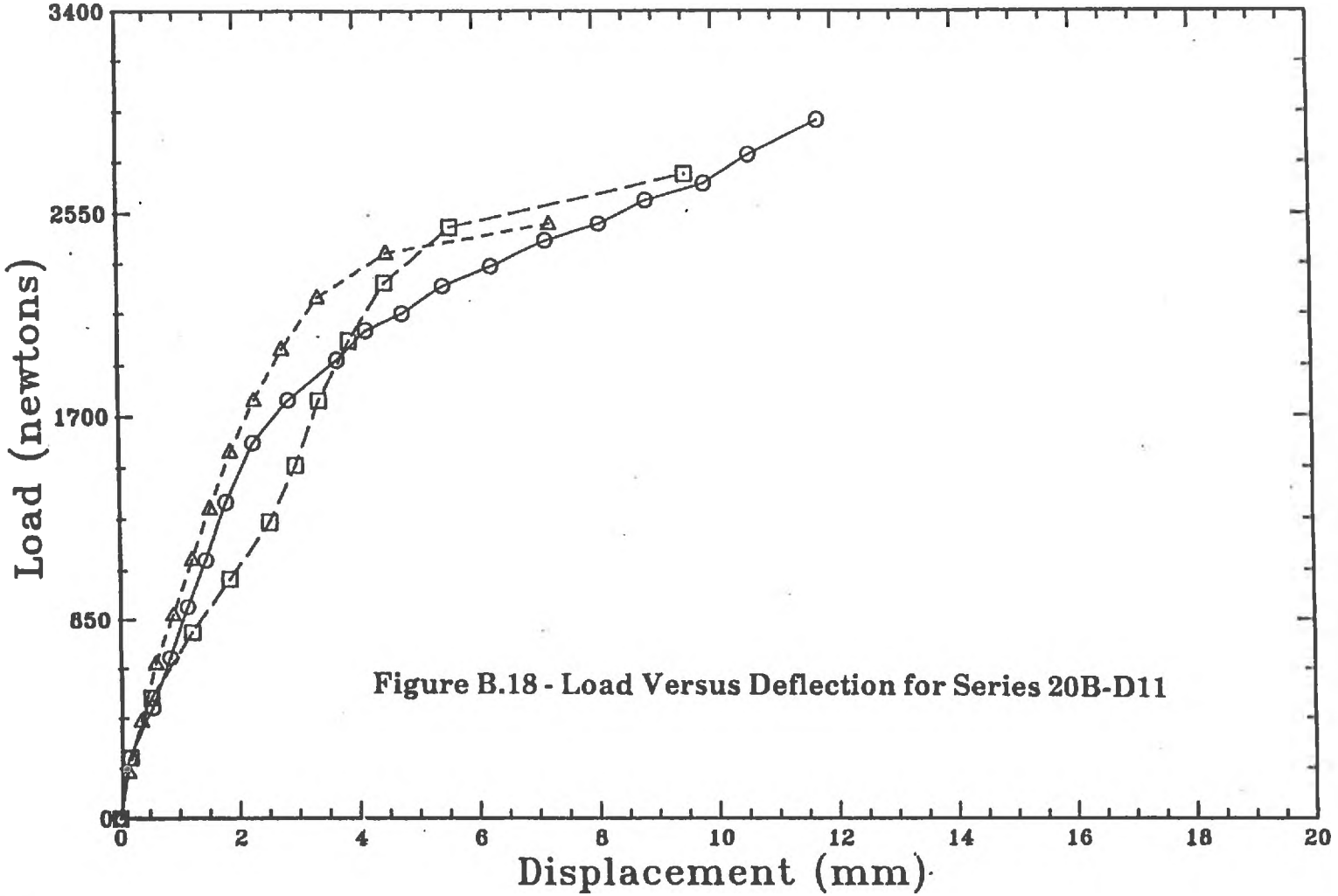

Figure B.18 - Load Versus Deflection for Series 20B-D11

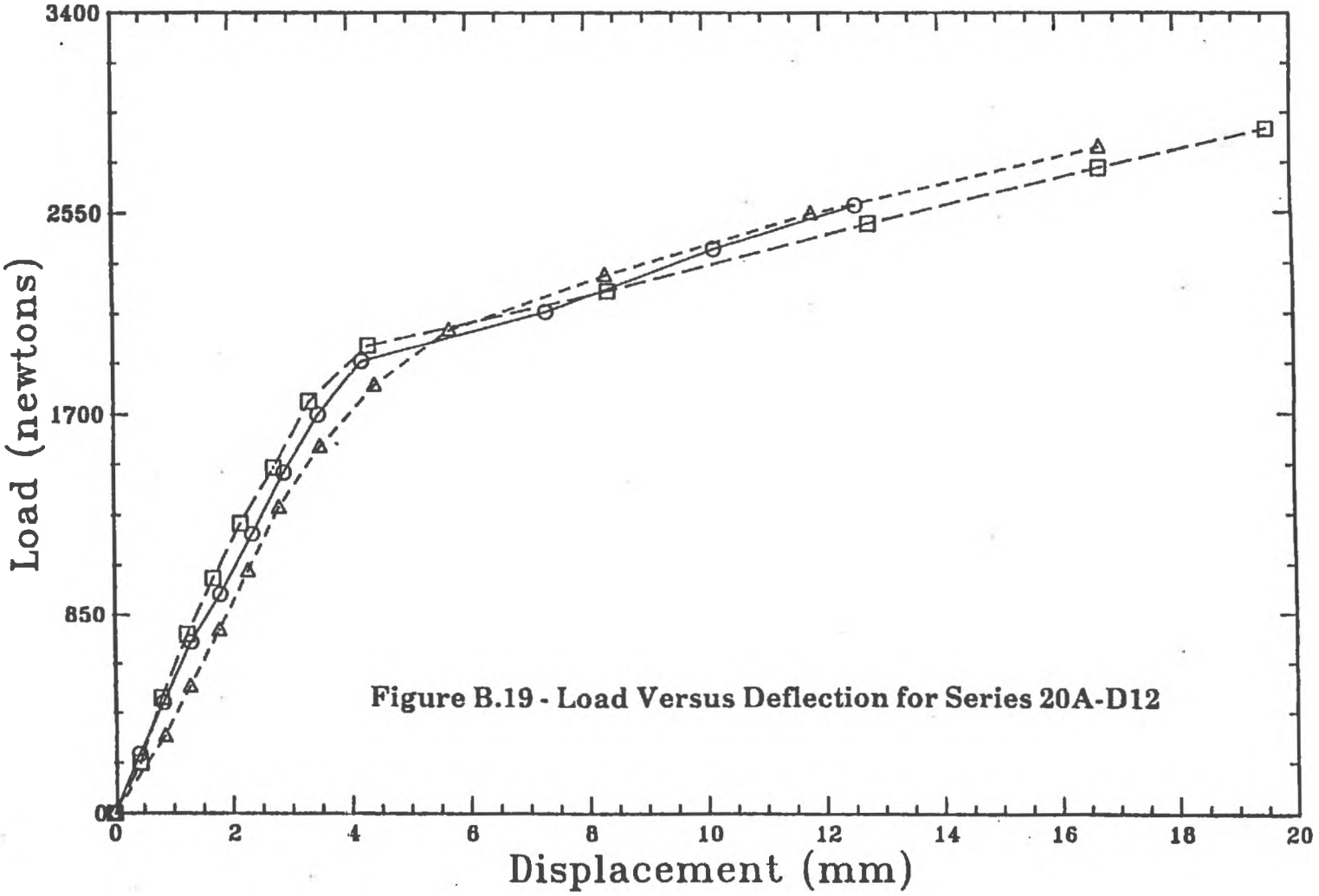

Figure B.19 - Load Versus Deflection for Series 20A-D12

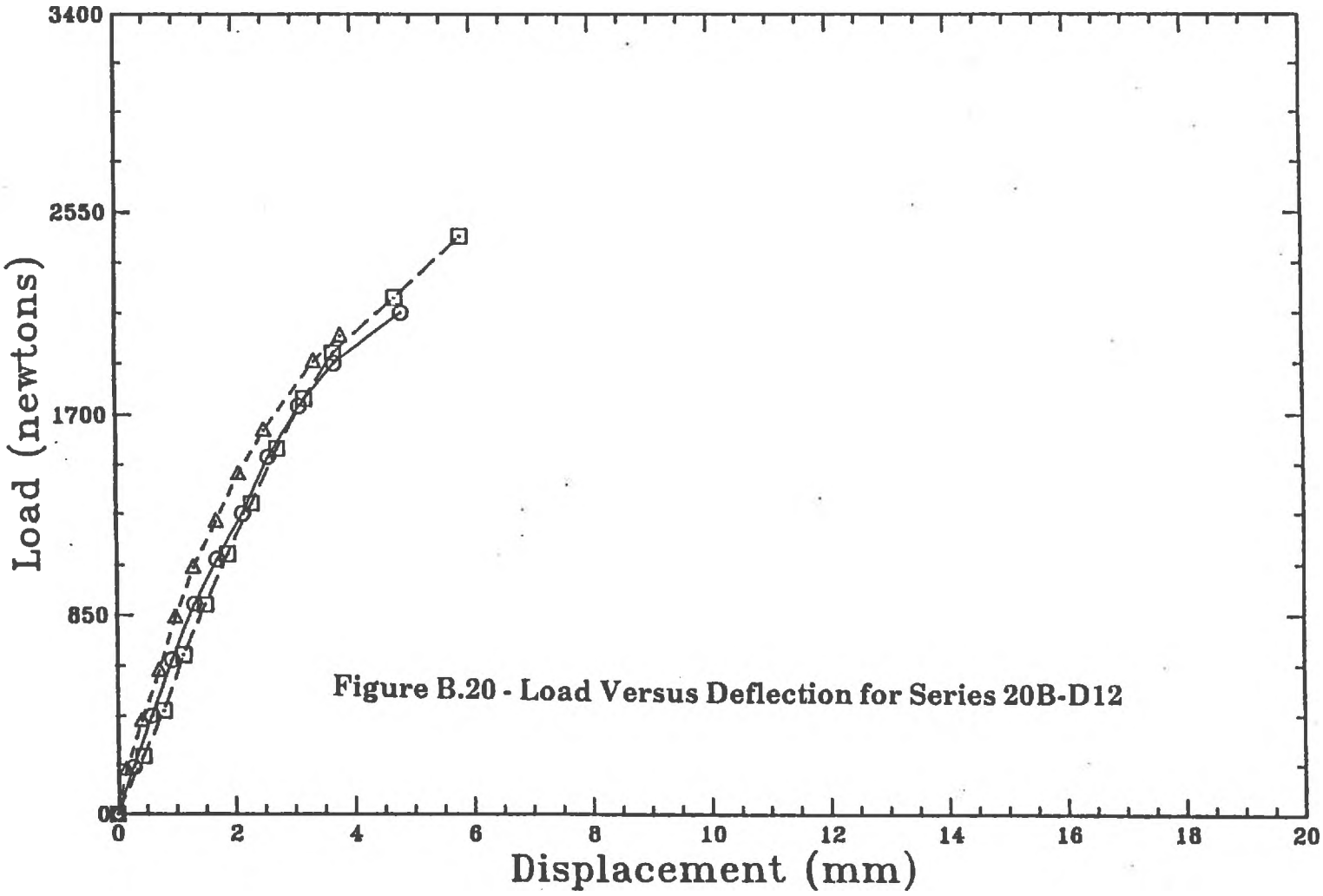

Figure B.20 - Load Versus Deflection for Series 20B-D12

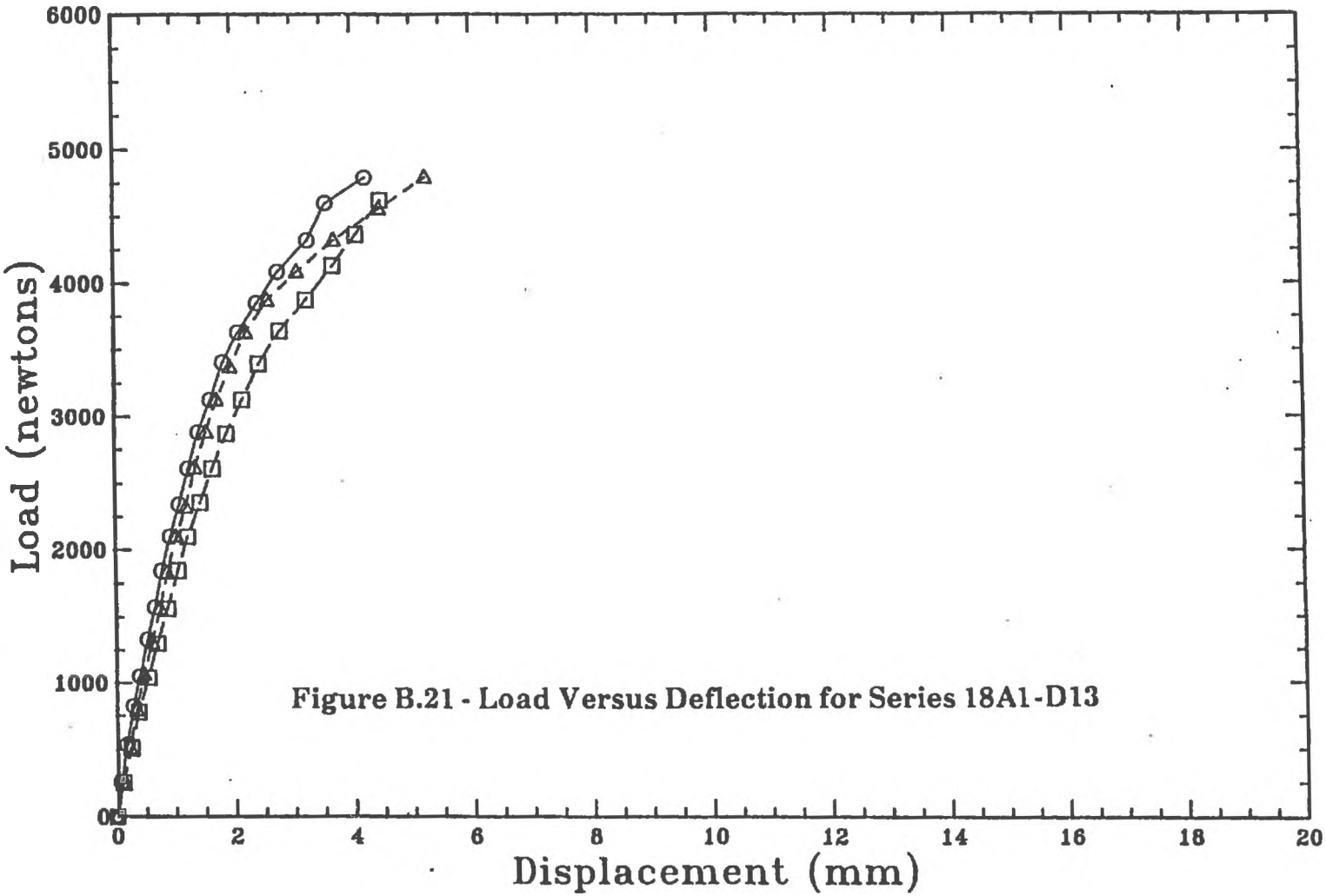

Figure B.21 - Load Versus Deflection for Series 18A1-D13

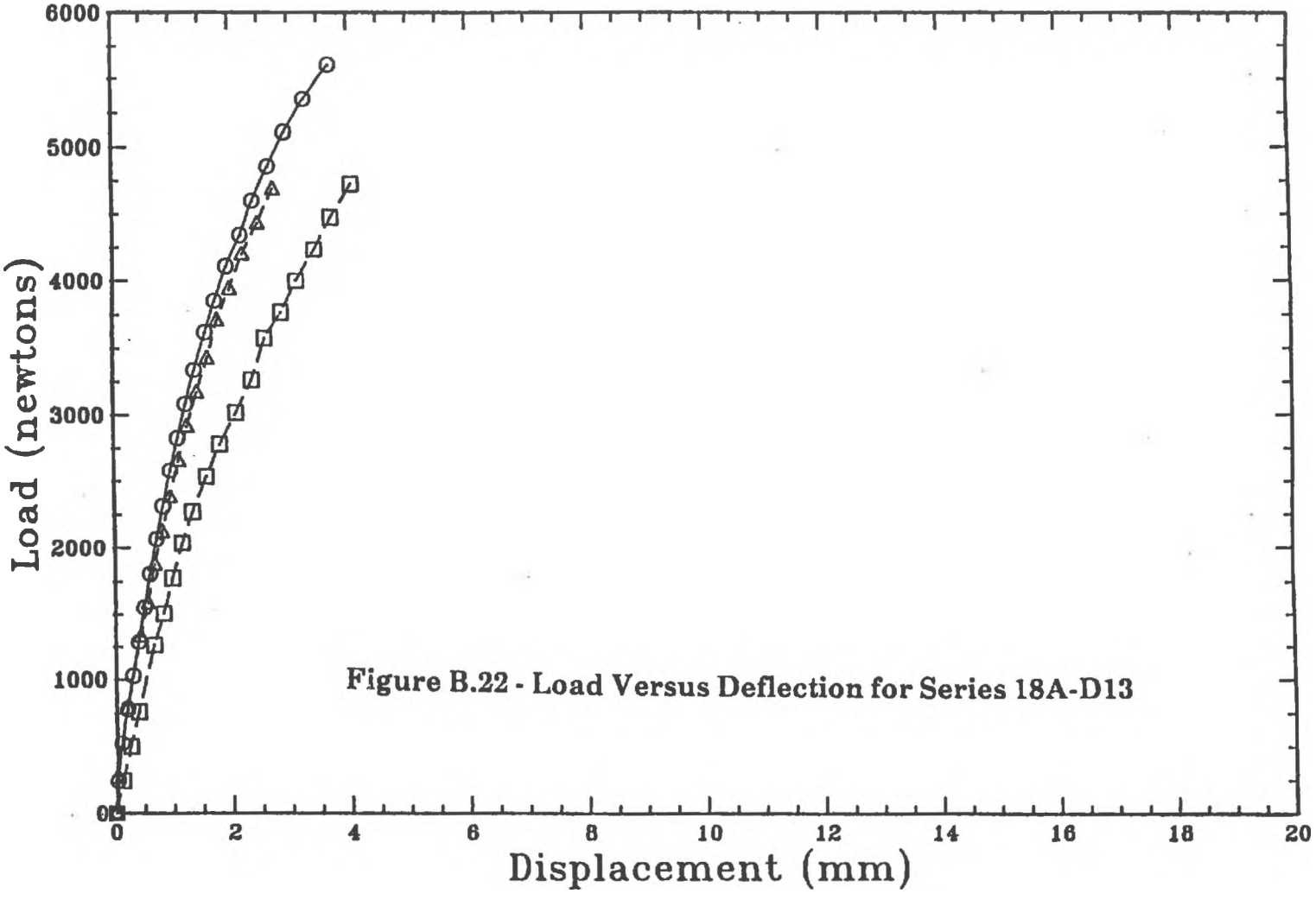

Figure B.22 - Load Versus Deflection for Series 18A-D13

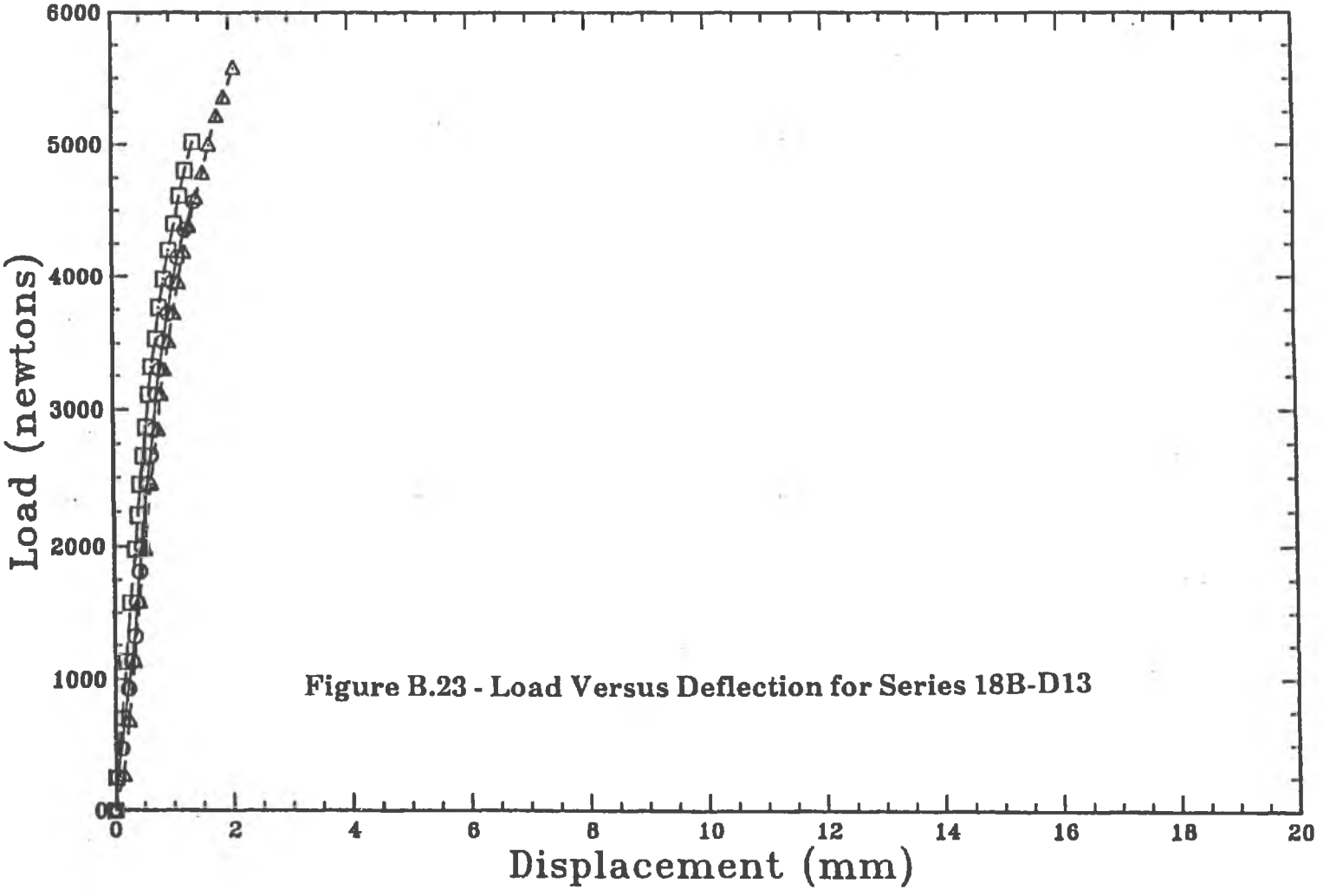

Figure B.23 - Load Versus Deflection for Series 18B-D13

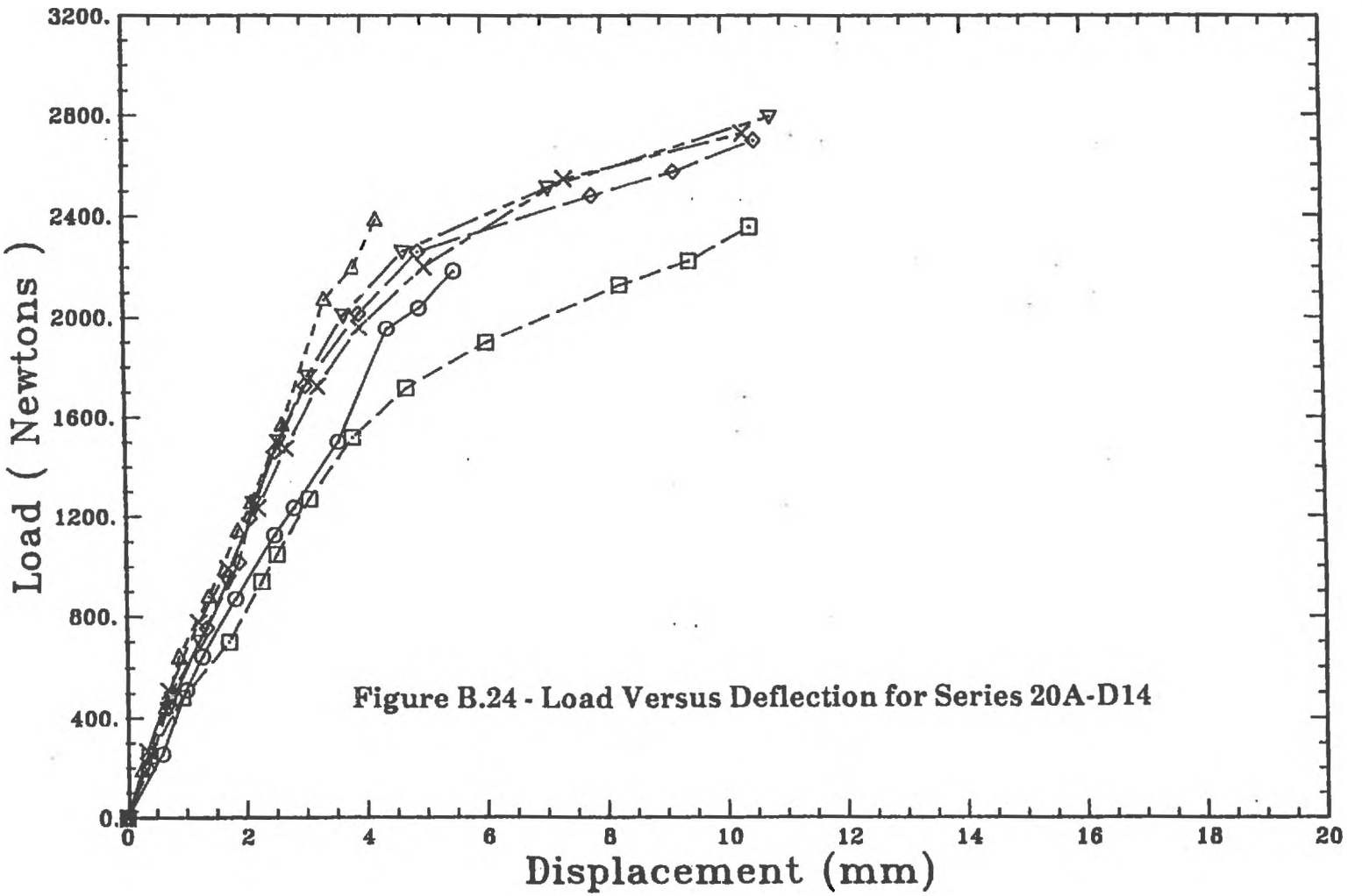

Figure B.24 - Load Versus Deflection for Series 20A-D14